DEVELOPMENT OF A HYBRID NEURAL NETWORK SYSTEM FOR PREDICTION AND OPTIMIZATION OF PROCESS IN CRYOGENIC MACHINING OF 316 SERIES STAINLESS STEEL

Thesis

Submitted in partial fulfilment of the requirements for the

degree of

DOCTOR OF PHILOSOPHY

by

KARTHIK RAO M C

DEPARTMENT OF MECHANICAL ENGINEERING

NATIONAL INSTITUTE OF TECHNOLOGY KARNATAKA,

SURATHKAL, MANGALORE -575025

JAN, 2022

Dedicated to

My Parents, Sister, Wife,

In-Laws and Gurus

DECLARATION

By the Ph. D. Research Scholar

I hereby declare that the Research Thesis entitled **" DEVELOPMENT OF A HYBRID NEURAL NETWORK SYSTEM FOR PREDICTION AND OPTIMIZATION OF PROCESS IN CRYOGENIC MACHINING OF 316 SERIES STAINLESS STEEL"** which is being submitted to **National Institute of Technology Karnataka, Surathkal** in partial fulfillment of the requirements of award of the degree **Doctor of Philosophy** in **Department of Mechanical Engineering** *is a bonafide report of the research work carried out by me*. The material contained in this Research Thesis has not been submitted to any University or Institution for the award of any degree.

Register Number : **155078ME15P06**

Name of the Research Scholar : **Karthik Rao M C**

Signature of the Research Scholar :

Department of Mechanical Engineering

Place: NITK- Surathkal

Date: 05/01/2022

CERTIFICATE

This is to certify that the Research Thesis entitled **"DEVELOPMENT OF A HYBRID NEURAL NETWORK SYSTEM FOR PREDICTION AND OPTIMIZATION OF PROCESS IN CRYOGENIC MACHINING OF 316 SERIES STAINLESS STEEL"** submitted by **Mr. KARTHIK RAO M C (Reg. No. 155078ME15P06)** as the record of the research work carried out by him, is accepted as the Research Thesis submission in partial fulfillment of the requirements for the award of the degree of **Doctor of Philosophy.**

Prof. Shrikantha S. Rao   **Dr. Mervin A Herbert**

Research Guide   Research Guide

Date:05/01/2022   Date: 05/01/2022

Chairman DRPC

Date:

ACKNOWLEDGEMENT

KARTHIK RAO M C

ABSTRACT

The high cutting temperature developed during machining at high cutting velocity and feed rate affects the ability to achieve high productivity and quality. It also causes dimensional deviation, premature failure of cutting tools, impairs the surface integrity of the product by inducing tensile residual stresses, and induces surface and subsurface micro cracks in addition to rapid oxidation and corrosion. Unlike conventional coolants which generally cause environmental and health problems to the machine operators, Cryogenic machining using LN_2 is an environmentally safe coolant which can achieve desirable control of cutting temperature and improve the machining performance. Many researchers have tried different cryogenic cooling methods such as cryogenic pre-cooling the workpiece, indirect cryogenic cooling or cryogenic tool back cooling and cryogenic jet cooling by micro-nozzles on the cutting tool edges or faces, tool–chip and tool–work interfaces. In the present research work, cryogenic cooling system was developed for supplying LN_2 at tool-chip interface during milling process. The machining study was conducted on SS316 of work material under dry, wet and cryogenic machining environments with the following work – tool combination i.e. SS316 steel Physical Vapour Deposition - TiAlN coated. The performance of the milling study involves three different cooling approaches. They were: (i) Dry machining (ii) Wet machining (iii) Cryogenic machining. In cryogenic environments, the LN2 was supplied at the tool – chip interface under constant pressure of three bar, using nozzle. The experimental results of cutting temperature, cutting force, surface roughness under cryogenic cooling were compared with those of dry and wet machining. With artificial neural network, prediction of responses of milling process are carried out using 4 different error back propagation algorithms such as (Gradient Descent, Scaled Conjugate Gradient Descent, Levenberg Marquart and Bayesian regularization or Bayesian Neural Network) models. Later, predicted results were compared between the conventional and non-conventional techniques and best suitable back propagation was identified for the current study. The validity of the models was established. The artificial neural network model formulated for cutting temperature cutting force, surface roughness and tool wear are found to predict the corresponding responses quite accurately. Support vector regression and machine learning techniques were applied for prediction using

Regression- Epsilon Method by using various kernel functions (Linear, Polynomial, Sigmoid, and Radial Basis Function). The best kernel function suitable was identified. Later on, incorporation of support vector machine to optimization (Particle Swarm Optimization was introduced in order to build the novel hybrid model).

Keywords: Cryogenic, Dry, Wet, LN$_2$, Artificial Neural Network, Back Propagation Algorithm, Gradient Descent, Scaled Conjugate Gradient Descent, Levenberg Marquart, Bayesian Neural Network, Support Vector Regression, Support Vector Machine, Particle Swarm Optimization.

CONTENTS

cutting

List of Figures

List of Tables

NOMENCLATURE

Ra   : Surface Roughness

FX   : Cutting Force

SEM   : Scanning Electron Microscope

EDAX   : Energy Dispersive X-Ray Analysis

OA   : Orthogonal Array

DOE   : Design of Experiments

RSM   : Response Surface Methodology

CCRD   : Central composite rotatable design

CNC   :   Computer Numerical Control

ANOVA   : Analysis of Variance

ANOM   : Analysis of Mean

SS   : Sequential sum of squares

SG   : Servo Guide

Adj. SS   : Adjusted Sum Of Squares

MSE   : Mean Square Error

F   : F-Ratio Value

P   : Percentage of Contribution

EA   : Evolutionary Algorithm

PSO   : Particle Swarm Optimization

ANN   : Artificial Neural Networks

BPNN   : Back Propagation Neural Network

SVR   : Support Vector Regression

SVM   : Support Vector Machine

RBF   : Radial Basis Function

BPA   : Back Propagation Algorithms

BR   : Bayesian regularization

BNN   : Bayesian Neural Network

GD   : Gradient descent

SCGD   : Scaled Conjugate Gradient Descent

LM   : Levenberg Marquart

LN$_2$: Liquid Nitrogen

RSM   : Response Surface Methodology

CT   : Cutting Temperature

CHAPTER 1

INTRODUCTION

1.1 IMPORTANCE OF MACHINING

Machining is a major part of metal working that plays an important role in metal cutting and forming. In machining, the machine tools especially cutting tools play an important role in effective metal cutting. This is because of their roles in producing different shapes and forms. The importance of machining in modern automated manufacturing systems has, in fact, increased due to the significant increase in the production time and the need to offset the high capital investment. The need for improving the technological performance of machining operations, as assessed by the cutting temperature, cutting force, tool life and surface finish has long been recognized, to increase the economic performance of the machining operations.

1.2 MILLING PROCESS

Milling is one of the common high-production machining methods. It is accomplished with a cutting tool called a milling cutter. A milling cutter is a multiple edge tool, which is a revolving body with cutting elements called teeth, arranged on the circumferential surface, or on the end faces or both. The primary cutting motion in milling is rotation, which is imparted to the cutter. The feed motion is usually imparted in a straight line to either the cutter or the workpiece. Milling is typically used to produce parts that are not axially symmetric and have many product features, such as holes, slots, pockets and even three dimensional surface contours. The milled surfaces are largely used to mate with other parts in die, aerospace, automotive, and machinery design as well as in manufacturing industries (Lee and Lin 2000).

1.3 HEAT GENERATION IN METAL CUTTING

During metal cutting, the energy dissipated gets converted into heat. Consequently, high temperatures are generated in the region of the tool cutting edge, and this temperature has a controlling influence on the rate of wear of the cutting tool, and on the friction between the chip and the tool. Long bottom (2005) described that during the machining process, a considerable amount of the machining energy is transformed into heat through plastic deformation of the workpiece surface, the friction of the chip on the tool face, and the friction between the tool and the workpiece. Figure 1.1 shows the heat generation zones in the metal cutting process.
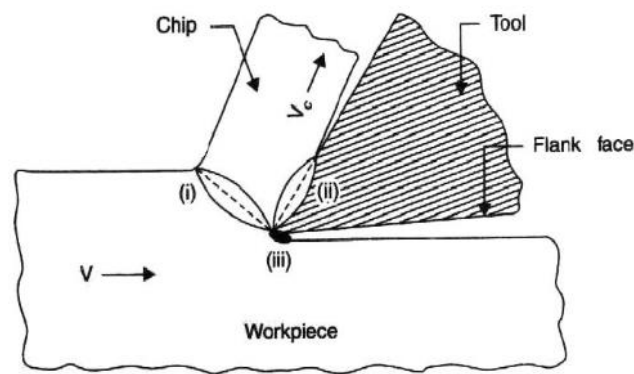
Figure 1.1: Heat generation zone in metal cutting

There are three main sources of heat generation during the process of metal cutting.

1. Heat is produced in the primary shear zone as the workpiece is subjected to large irreversible plastic deformation.

2. Heat is produced by friction and shear on the tool rake face, or secondary shear zone. Thus, there exists both sticking and sliding friction. The combined effect of shear and friction action produces heat.

3. Heat is also produced at the tool – work interface, where the tool flank runs along the workpiece surface, and generates heat through friction.

The cutting temperature is a decisive factor for other machinability indices such as the cutting force, surface finish and tool wear. It was reported that approximately 80% of

the generated heat is dissipated by the chip, about 18% by the tool and the rest by the work surface (HMT 2006).

The heat generations in intermittent machining operations like milling differ significantly from the heat generations in continuous cutting operations, such as turning. In milling operations, the tool is subjected to cyclic heating and cooling, when the tool enters and exits the workpiece material. This leads to a phenomenon known as thermal fatigue (Wang et al 1996). Generally, thermal fatigue plays a significant role in shortening the tool life for tungsten carbide tools during the milling operation, where the cutter teeth gets heated intermittently at the corners, through contact with the workpiece. This causes cracks to develop in the tool and ultimately leads to thermal fracturing of the tool (Wang et al 1996).

The temperatures attained in metal cutting are important, only so far as they affect the thermally activated mass transport phenomenon at the work – tool interface contacts. These may involve interfacial diffusion and alloy formation or self-diffusion, resulting in creep and/or softening of the tool material. The mutual diffusion of materials at the chip-tool contact is a significant cause for the formation of crater wear. Crater wear is essentially an exponential function of the average chip – tool interface temperature, provided the temperature is sufficient to cause interfacial diffusion (Kuppuswamy 1996).

Kitagawa and Maekawa (1990) and Mazurkiewicz et al (1989) have reported that the temperature of the cutting tool in machining plays an important role in thermal distortion, and the dimensional accuracy of the machined part, as well as tool life. Brown and Hinds (1985) have reported that the high temperature at the cutting zone results in dimensional deviations, fast oxidation and corrosion, thermal residual stresses and micro cracks on the workpiece.

1.4 VARIABLES AFFECTING CUTTING TEMPERATURE

1.4.1 Workpiece and Tool Material

The mechanical properties of the workpiece material, particularly the tensile strength and hardness, have a considerable influence on the cutting temperature. Generally, as more energy is required for chip formation, more heat is generated, resulting in a corresponding increase in the cutting temperature. In addition, the thermal properties of the workpiece material also influence the rise in temperature. The higher the thermal conductivity, the lower is the rise in temperature. The performance of a cutting tool is dependent on the form stability of the cutting edge, which in turn is mostly dependent on the hardness and thermal conductivity of the tool – work materials (Sreejith and Ngoi 2000)

1.4.2 Cutting Conditions

In a given combination of the work and tool material, the cutting temperature depends upon the cutting speed, feed and depth of cut, and to a limited extent, the cutting fluids. Among these factors, cutting speed has a predominant effect. The mean temperature is proportional to the cutting speed and feed as follows: Mean Temperature α V^a f^b , where a and b are constants depending on the tool and workpiece materials, V is the cutting speed and f is the feed of the tool (Kalpakjian and Schmid 2000, Shaw 2005 and Thomas Childs et al 1999).

1.4.3 Cutting Fluid

One of the important functions of the cutting fluid is to conduct the heat away from the tool and workpiece interface and avoid heat accumulation and temperature build-up in the vicinity of the active cutting edge. The fluid would be carried away by the outward flowing chip more rapidly than it could be forced between the tool and the chip. The effectiveness of the cutting fluid in lowering the tool temperature decreases with an increase in cutting speeds, and at higher speeds the fluids become completely ineffective in reducing the temperature. A flood of cutting fluid directed over the back of the chip loses its effectiveness at higher cutting speeds (Kovacevic et al 1995).

1.4.4 Tool Geometry

The geometry of cutting tool has a significant effect on machining performance. Among various parameters of tool geometry, radial rake angle is one of the most important parameters, which determines the tool and chip contact area and hence affects the power consumption. A negative rake tool requires more energy input, since the tool contact area is correspondingly increased. In addition, owing to a more massive tool point, the heat flow into the shank is more effective and the temperature level is maintained. With an increase in the approach angle, the cutting temperature increases, since, for the same feed and depth of cut, the chip thickness increases. The nose radius of the tool has an influence on the total heat generation and its distribution. A large nose radius raises the cutting temperature, but at the same time it promotes the heat flow, as the contact area is also increased for a given combination of work and tool material (HMT 2006).

1.5 CONVENTIONAL COOLANTS

Historically, cutting fluids have been used extensively for the last 200 years. Cutting fluids are widely utilized to improve the process of machining operations such as turning, drilling, boring, grinding, and milling. The most common metal working fluids used today are either oil-based fluids including straight oils and soluble oils or chemical fluids including synthetics and semi-synthetics. The primary function of the cutting fluid is temperature control through cooling and lubrication. Cooling and lubrication are critical in decreasing tool wear, extending the tool life and achieving the desired dimensional accuracy and surface finish. A secondary function of the cutting fluid is to flush away chips and metal fines from the tool/workpiece interface, to prevent a finished surface from becoming marred, and also to reduce the occurrence of a built-up edge. However, a conventional coolant fails to penetrate into the chip – tool interface, and hence the coolant cannot remove the heat effectively, due to the bulk chip-tool contact under high cutting velocity and feed, where the temperature is the maximum (Shaw et al 1951, Merchant 1958, Cassin and Boothroyed 1965 and Kitagawa et al 1997).

Furthermore, the presence of extreme pressure additives in the cutting fluids is also one of the reasons that prevent the cutting fluid to penetrate into the tool – chip interface. Conventional cutting fluids pose serious health and environment hazards. People exposed to cutting fluids may have health problem when these fluids contacts the skin, inhale mists or vapour, or even swallow mists particles. Due to their toxicity, they may cause health problems, like dermatitis, problems in the respiratory and digestive systems and even cancer. Recent studies have reported increased rates of respiratory effects, including pneumonia, asthma, chronic bronchitis and impaired pulmonary function (Ameille et al 1995, Eisen et al 1997, Greaves 1997).

According to some extensive assessments of current and past coolant exposures in relation to cancer mortality, an elevated risk of pancreatic cancer was also reported for all workers exposed to synthetics (Bardin et al 1997, Ely et al 1970). Improper disposal of these cutting fluids may even cause serious environmental problems, such as water pollution and soil contamination. Strict regulations and their enforcement against using cutting fluids has therefore, been tightened. Thus, the waste disposal and post handling of the cutting fluids and other related costs have increased substantially with tougher environmental laws. Companies and organizations are being forced to implement strategies to reduce the usage of cutting fluids in their machining operations.

Further, extra floor space and additional systems are required for pumping, storage, filtration and recycling of the conventional coolants (Howes et al 1991, Byrne and Scholta 1993, Klocke and Eisenblatter, 1997, Sreejith and Ngoi 2000, Sutherland et al 2000 and Dhar et al 2002a). Sokovic and Mijanovic (2001) have reported that on the shop floor, the operators may be affected by the bad effects of cutting fluids, such as skin and breathing problems. Chen et al (2000) and Barry and Byrne (2002) have stated that the cooling lubricant causes an increase both in the worker's health and social problems, related to their use (working environment), and correct disposal (ecological aspect). This, in turn, means an increase in the costs for the manufacturing companies. Therefore, there is a need to look for new coolant application techniques. Cryogenic cooling is an effective cooling technique that does not pollute the environment, and hence, it is becoming very popular. Besides pollution control, the

industries also reasonably derive economic viability through technological benefits, in terms of product quality, tool life and saving in power consumption by using the cryogenic cooling technique.

1.6 CRYOGENIC COOLING

Cryogenics are defined as working at very low temperatures, below -150°C (123K).Various gases such as nitrogen, helium, oxygen, hydrogen, and neon can be utilized. In cryogenics, the normal boiling point of such gases lies below -180°C (93K). Cryogenic cooling has wider applications in industries, such as manufacturing, automotive, aerospace, electronics, food processing, and health, for cooling purposes.

Liquid nitrogen is the most commonly used element in cryogenics. At atmospheric pressure, molecular nitrogen condenses (liquefies) at -196°C and freezes at - 210°C; it is the most abundant gas, and composes about four-fifths (78.03%) by volume of the atmosphere. The LN_2 in a cryogenic machining system quickly evaporates and goes back into the atmosphere, leaving no residue to contaminate the part, chips, machine tool, or operator, thus eliminating disposal costs. It is a colourless, odourless, tasteless, non-toxic and non-flammable gas. These characteristics of liquid nitrogen have made it a preferred coolant (Yakup and Muammer 2008).

Cryogenic cooling is a process which reduces the cutting temperature in the metal cutting process, by applying cryogenic fluids as the coolants. When liquid nitrogen is used as a coolant, it is environmentally safe (Kumar and Choudhury 2008) and requires no disposal facilities. To economize the cryogenic machining process, liquid nitrogen consumption must be minimized by applying it judiciously to the cutting area. Cryogenic cooling provides improved tool life, lesser cutting force, better surface finish, better chip breaking and chip handling, better dimensional accuracy, higher productivity and lower production cost.

1.7 OUTLINE OF THE THESIS

This thesis aims to address the various problems discussed in the above sections. The various stages of the investigations were carried out and these investigations were divided into 8 chapters. The summary of discussions carried out chapter wise are detailed below.

Chapter 1: This chapter presents the historical background and an introduction to the milling process, the heat generation zones in the metal cutting process, the effect of the temperature rise in the metal cutting process, and the drawbacks in the conventional cooling approaches. It also deals with the challenges faced and motivation for the need of cryogenic cooling in metal cutting operations. The objectives, scope and overall methodology of the experimental work have been outlined.

Chapter 2: This chapter presents a comprehensive survey of the literature on the machining of different materials using various cooling approaches. The recent literature, the drawbacks of conventional cooling, different cryogenic cooling approaches and machining studies conducted on various work materials under cryogenic cooling is reviewed. The recently developed cryogenic cooling approaches are also discussed elaborately. Even the conventional and non-conventional prediction and optimization techniques along with their drawbacks have been illustrated. Apart from this, the chapter also makes a critical review of the current knowledge in the field of machining learning technique. Summary of literature review, problem statement, objectives of the study, scope and plan of work also have been outlined in this chapter.

Chapter 3: In this chapter, the experimental methods and cutting conditions in the milling studies on SS316 steel using the carbide cutting tool are discussed. The details about the workpiece materials, cutting tool insert and tool holder are presented in this chapter. The instruments used to measure the cutting temperature, cutting force, surface roughness, tool wear, chip shape and chip morphology are presented. The

construction and working principle of the developed cryogenic cooling setup is also presented.

Chapter 4: This chapter explains the experimental work carried out to investigate and evaluate the performance in the milling of SS316 steel under dry, wet and cryogenic cooling conditions. The experimental results of the cutting temperature, cutting force and surface roughness along with the pertinent discussions are presented. In the summary, the influence of LN2 cooling in the milling of the SS316 is compared with dry and wet machining. This chapter even deal with the performance evaluation in terms of the tool wear, chip shape and chip morphologies in the milling of SS316 under dry, wet and cryogenic cooling conditions.

Chapter 5: The chapter illustrates the formulation of prediction model (both conventional and non-conventional techniques, i.e RSM and ANN) for the selection of major influencing factors affecting the responses, to develop mathematical model (response equation) for analysis and prediction of cutting parameters, for development of single response prediction model using RSM, development of multi objective prediction using ANN. It highlights the incorporation of 4 different back propagation algorithms to perform prediction and to identify the best suitable back propagation algorithm for the present study. Later the confirmation test (validation) was performed by conducting the experiments.

Chapter 6: Discusses the formulation of optimization models to identify the optimum parameters of the desired responses.

- Development of multi objective optimization models (Desirability approach and particle swarm optimization approach).
- Confirmation experimental verification was performed for optimized process combinations.

The chapter also addresses the performance of PSO model with corresponding statistical methods.

Chapter 7: This chapter elucidates on the concept of machine learning (Support Vector Machine) The SVM is applied for 2 sections 1) Prediction 2) Optimization. The prediction section is carried out using Support vector regression (SVR) technique via regression (epsilon) method using 4 different kernel function using "R Studio" platform. The comparison among the 4 incorporated kernel functions (linear, polynomial, radial basis, sigmoidal) is compared by attained R^2 correlation coefficient and mean square error (MSE). This chapter illustrates the integration of best attained kernel function (radial basis function-(RBF)) from prediction part to optimization section. Now the hybrid optimization method i.e. PSO-RBF-SVM method is introduced and the "MATLAB" platform is utilized to carry out the optimization.

Chapter 8: Presents the overall summary of the investigations carried out in the milling of SS316 and the conclusions drawn. It also includes suggestions for further study in this area.

CHAPTER 2

LITERATURE SURVEY

2.1 CONVENTIONAL COOLANTS IN METAL CUTTING

In today's competitive manufacturing environment, the enhancement of productiveness with multiplied product excellent and decreased cost, as properly as the maximization of the earnings decides the sustainability of a manufacturing organisation. The foremost troubles in attaining excessive productiveness and first-class are brought on by way of the excessive reducing temperature developed at some stage in machining, at excessive slicing speed and feed rates, in particular when the work material is challenging to machine. In general, the circumstance of the reducing tools performs a extensive position in accomplishing constant quality, and additionally in controlling the ordinary fee of manufacturing.

The above targets can be finished by way of lowering the excessive reducing temperature in the reducing zone. Such excessive temperature adversely impacts the device life, dimensional accuracy and surface integrity of the product. Increased cutting force, immoderate device wear, negative surface finish, bad dimensional stability, etc. are temperature-dependent facet effects; they are additionally interdependent and are the principal worries in the metallic reducing enterprise (Boothroyd 1985). The excessive reducing temperature can be decreased and sustainable excessive productiveness with suitable product nice performed through most fulfilling choice of the machining parameters, and perfect slicing fluid application, and with the aid of the use of warmth resistant tools. In industries, the excessive reducing temperature and its harmful outcomes are usually tried to be controlled, through making use of soluble oil as a traditional coolant. These fluids act each as coolants to limit the device temperature, and additionally as lubricant (Suresh et al 2009). According to (Klocke and Eisenblatter 1997), the flood kind reducing fluid is usually adopted to limit the cutting temperature, and lubricate the sliding surface at some stage in machining.

The literature survey is divided in to following sections:

❖ Introduction to conventional coolants in metal cutting

❖ Types of conventional cooling approaches

❖ Application of coolants

❖ Problems in conventional cooling

❖ Cryogenic Machining

❖ Study of different cryogenic cooling approaches in metal cutting

❖ Recent studies on cryogenic cooling

❖ Prediction Technique

❖ Optimization Technique

❖ Machine Learning – Support Vector Machine (SVM)

❖ Summary on prediction, optimization & Machine learning technique

❖ Research Gap

❖ Need for the present study

❖ Scope of the present study

❖ Objectives of the present study

2.2 TYPES OF CONVENTIONAL COOLING APPROACHES

All the machining procedures produce warmness and friction, which will doubtlessly injury the cutting equipment as nicely as the surface end of the product. To limit the friction, switch the warmness and put off the chips away from the reducing zone, normally, reducing fluids are used. Heat technology in machining entails two essential processes; first of all the technology of warmness at some point of the plastic

deformation of the work material through the tool, and secondly, friction in the course of the motion of the chips between the workpiece and the cutting tool.

2.2.1 Dry Machining

Dry slicing is practiced by way of positive industries, the place coolant is no longer used for the metal reducing processes. It is ecologically desirable. The benefits of dry machining include: non-pollution of the surroundings (or water); no residue on the swarf, which will be mirrored in decreased disposal and cleansing costs; no risk to health; no accidents to the pores and skin and hypersensitivity free. Moreover, it affords price discount in machining (Sreejith and Ngoi 2000). The removing of the use of reducing fluids, if possible, can be a good sized incentive. The costs related with the use of reducing fluids are estimated to be many instances greater than the labour and overhead expenses (Sreejith and Ngoi 2000). Hence, the implementation of dry machining will decrease the manufacturing costs.

Many metal-cutting tactics have been developed and multiplied primarily based on the availability of the coolants. It is properly acknowledged that coolants enhance the device life and device overall performance to a larger extent. In dry machining, there will be extra friction and adhesion between the device and the work piece, considering they will be subjected to excessive temperatures. This will end result in extended device wear, and hence, discount in device life. Higher machining temperatures will produce ribbon-like chips, and this will have an effect on the shape and dimensional accuracy of the machined surface (Paul et al 2001). However, dry cutting additionally has some high quality effects, such as discount in thermal shock, and hence, elevated device existence in an interrupted-cutting environment.

2.2.2 Application of Flood/Wet Cooling

This cooling method is the most broadly used in the machining industry. It presents the machining operation with a properly degree of lubrication, cooling and chip removal. Generally, soluble oil is used in the reducing quarter via flooding. The features of slicing fluids are (DE Chiffre 1988):

1. Increased device life
2. Improved surface finish
3. Improved tolerance
4. Reduction in the cutting force
5. Reduction in the vibration

The lubricant additionally enables the breaking of the chips, and can play an necessary position in the prevention and reduction of corrosion (Da Silvia and Wallbank 1998). Klocke and Eisenblatter (1997) have mentioned that no matter the excessive value of cool ants, the most frequent cooling technique in machining nevertheless consists of flooding the reducing region with a massive volume of the coolant. The utility of a copious quantity of reducing fluid for the duration of intermittent reducing may want to enlarge the massive fluctuation of the reducing temperature. This can lead to thermal shock and provoke thermal cracks in the reducing edge, and subsequently motive device failure due to facet fracture (Shaw 2005, Elbestawi et al 1997, Vieira et al 2001). Therefore, some choice techniques have been pronounced to manage the thermal shock, and thereby enhance device existence all through the milling process.

2.2.3 Application of Minimal Quantities/Mist Coolant Lubricant

The utility of a minimal volume of lubrication consists of a combination of compressed air and oil droplets to the chip – device interface; this is known as a mist coolant. Most of the researchers evaluated the overall performance of minimal extent lubrication functions in the milling technique and observed to notably enhance the device lifestyles and surface end in contrast to the traditional flood coolant and dry machining (Lio et al 2007, Thepsonthi et al 2009). Rahman et al (2001) used minimal volume lubrication (MQL) in milling functions of ASSAB 718 HH metal and located that the cutting pressure used to be decreased for MQL as in contrast with dry reducing and flood coolant reducing conditions, mainly at low cutting pace of seventy five m/min. Researchers additionally investigated MQL functions in turning process. Dhar et al (2006) investigated the impact minimal volume lubricant on reducing temperature, device put on and product best in turning AISI 4340 steel. It was once proven that the

MQL overall performance used to be higher than dry slicing as it decreased the slicing temperature and elevated surface end and dimensional accuracy.

A find out about was once performed by way of Machado and Wallbank (1997) to consider the impact of extremely low lubricant volumes in machining. Small portions of lubricant (200-300ml/hr) in a quick flowing air movement with a strain of two bar had been used in turning of medium carbon metal AISI 1040. Results had been in contrast to the typical flood cooling technique as a benchmark with 5.2 l/min. The findings disclose that surface finish, chip thickness and pressure variant are all affected beneficially by way of the equivalent. Cutting pressure and feed pressure have been discovered decreased when the lubricant was once utilized below low reducing pace and excessive feed rate.

In any other find out about with the aid of Varadarajan (2002), a difficult turning with minimal fluid software has been carried out to evaluate the machining overall performance with dry and moist turning. A specifically formulated reducing fluid was once utilized with a excessive velocity, thin-pulsed jet at the instant reducing zones at an extraordinarily low price of two ml/min. It was once located that reducing pressure was once decrease throughout minimal utility when in contrast to dry and traditional moist turning. Penetration of the reducing fluid with Epoxy components into the interface can limit the frictional contribution to cutting force, which in flip decrease the cutting temperature, shortening of tool-chip contact size and expand of shear attitude at some stage in minimal application deliver forth higher surface integrity and expanded device life. The ordinary overall performance for the duration of minimal reducing fluid software was once determined to be top of the line to that in the course of dry turning and traditional moist turning on the groundwork of reducing force, device life, surface finish, cutting temperature and tool-chip contact length. As the minimal rate of application is as low as two ml/min a fundamental element of the fluid is evaporated. The remnants carried away by means of the work and chips are too low to reason infection of the save environment. Applying a mist coolant additionally poses serious fitness dangers consisting of eye irritation; Breathing of the mist can also additionally reason serious respiratory issues and air air pollution (Yuvan et al 2001).

2.2.4 Application of High Pressure Cooling

High-pressure cooling includes the use of an excessive strain jet of soluble oil in the slicing zone. Mazurkiewicz et al (1989) cited that a excessive strain jet of soluble oil, if utilized at the chip –tool interface, may want to limit the reducing temperature and enhance device lifestyles to some extent. By making use of a high-pressure coolant at some point of machining, the device existence and surface end are discovered to enhance considerably via reducing the warmth and slicing forces generated (Kovacevic et al (1995), Rahman et al (2000), Ezugwu et al (2007), Machado et al (1998), Sorby and Tonnessen (2006), Vosough and Svenningsson (2004), Zareena et al (2001), Diniz and Micaroni (2007), Ezugwu et al (2005) and Nandy et al (2009). Kovacevic et al (1995) have experimentally investigated the impact of excessive stress water jet cooling/lubrication in milling of titanium alloy. It was once discovered that surface great and device existence had been improved.

Senthilkumar et al (2002) carried out experimental investigation on ASSAB -718 metal for the duration of give up milling operation the usage of uncoated tungsten carbide insert and a Ti-Al-CN lined insert at a velocity of one hundred fifty m/min with feed fee of 0.05 mm/tooth and depth of reduce 0.35 mm suggests that the effectiveness of excessive strain coolant in phrases of multiplied surface finish, decreased device put on and reducing forces, and manipulate of chip shape. The device put on with excessive stress coolant is considerably higher than that with dry reduce and traditional coolant. Hence, this reduces the friction at the device – work interface and will increase the surface finish. Due to the use of excessive strain coolant, the elimination of the warmth from the slicing zone, the cyclic thermal shock does now not take place, and subsequently a decrease cutting pressure probably to occur. However, the cooling with excessive strain coolant does no longer meet enterprise standards. When the coolant strain was once extended from 15 to 20.3 MPa, the device life reduced swiftly due to immoderate notch put on stated by means of Ezugwu et al (2005).

2.2.5 Application of Chilled Air Cooling

In the cold compressed air environment, a Vortex air gun with a nozzle is used to direct bloodless air generated with the aid of the air gun to the device – chip interface. With the purposes of chilled air cooling in the course of machining, the device life and surface end are improved. Rahman et al (2003) studied the performance of chilled air cooling in quit milling on ASSAB 718 mildew metal and located that the expanded device life and surface finish, and decreased reducing forces have been found as in contrast with dry and conventional coolant cutting.

Su et al (2006) studied the impact of dry, flood coolant, nitrogen oil mist, compressed cold nitrogen fuel (0°C and -10° C), and compressed cold nitrogen gasoline and oil mist cutting prerequisites on device lifestyles in the course of excessive velocity quit milling of Ti-6Al-4V. It used to be discovered that the device lifestyles beneath compressed cold nitrogen gasoline and oil mist cooling stipulations have elevated 2.69 instances in contrast to dry cutting and 1.93 times over nitrogen oil mist. It was once additionally said that the device existence used to be much less when the usage of a flood coolant due to the fact of the impact of mechanical and thermal impact, which motives thermal cracks on the cutting edge.

Su et al (2007) performed an experimental investigation on device wear, surface finish, and chip form on excessive velocity milling of AISI D2 bloodless work device metal below dry cutting, minimal extent lubrication, air cooling, and air cooling with minimal volume lubrication conditions. It was once located that the software of air cooling with minimal volume lubrication strategies resulted longer device existence in contrast to dry and minimal volume lubrication.

Yalcin et al (2009) carried out give up milling on AISI 1050 metal beneath dry, fluid and air cooling reducing conditions. The experimental outcomes confirmed that the surface roughness values for air cooling are decrease than that of dry milling, and greater in contrast to these below fluid cooling. It was once additionally said that the

flank put on in air cooling was once nearer to that in fluid cooling, and greater in dry milling in contrast to the fluid and cool air cooling systems.

Lincoln et al (2008) carried out give up milling of AISI H13 and AISI D2 steels with TiAlN lined and PCBN tools, underneath dry, compressed, and bloodless air cooling systems. The consequences indicated that the bloodless air cooling structures supplied higher effects in contrast with dry and compressed air cooling conditions. It used to be mentioned that the reducing temperature used to be greater in the machining of AISI D2 metal in contrast to AISI H13 steel.Kim (2001) carried out an scan in measuring the reducing temperature of ball-end milling of hardened steel, for distinct cooling circumstance by using the usage of a K-type thermocouple, implanted in a gap of the work piece. The reducing temperatures had been about 790 ℃, 350 ℃, 540℃ and 450 ℃ in dry, moist and compressed chilled air at –9 ℃ to -35 ℃ respectively. The reducing surroundings for compressed chilled air at –9 ℃ furnished the pleasant device lifestyles amongst all the cooling conditions. In the case of the moist condition, due to the cooling traits of the reducing fluid, the device suffers serious thermal fatigue, and the device put on swiftly will increase in contrast to dry condition.

2.3 PROBLEMS IN CONVENTIONAL COOLING

Kramar et al (2010) have said that traditional cooling is no longer environment friendly sufficient to forestall severe thermal loading in the reducing zone. Nandy et al (2009) mentioned that traditional cooling techniques fail to conduct efficaciously the warmth generated in the reducing zone, which is accountable for the shorter device life. Shaw et al (1951), Merchant (1958) and Cassin and Boothroyed (1965) have said that the conventionally utilized coolants, even with severe stress additives, fail to furnish the perfect manage of the reducing temperature, as they can't penetrate into the chip – device interface predominantly, due to the plastic contact between the device and chip, specifically at excessive reducing speed.

Choudhury and El-Baradie (1998) and Rahman et al (1997) stated that traditional cooling structures resolve the trouble partially, however create lots of technical and environmental problems, such as, the requirement of extra structures for storage,

pumping, filtering, recycling and cooling; water and soil air pollution on disposal; fitness issues to the operators when they come into direct contact with the reducing fluids; and environmental issues when the reducing fluids dissociate as they come into contact with the warm surface at excessive temperatures.

Tsai and Hocheng (1998) and Krabacher and Merchant (1951) have pronounced that the value of cutting-fluid-disposal is turning into higher, as the environmental rules are turning into tougher. Sokovic and Mijanovic (2001) referred to that on the keep surface; the operators can also be affected by means of the terrible consequences of the reducing fluids, such as pores and skin and respiratory problems.

Due to the issues in the traditional cooling system, it is indispensable to use an environmentally suited coolant in the manufacturing industries. For this purpose, liquid nitrogen as a cryogenic coolant has been explored due to the fact that Nineteen Fifties in the steel cutting enterprise (Yakup and Muammer 2008).

2.4 CRYOGENIC MACHINING

The utility of cryogenic coolants in machining started out in the year 1950s. Cryogenic machining was once first investigated round the year 1953 through E.W. Bartley, who used sub-zero cooled CO_2 as the coolant (Chattopadhyay et al 1985). Hollis (1961) has studied the impact of cryogenic cooling on the put on system of carbide tipped equipment at some point of the machining of titanium. Liquid carbon dioxide was once furnished to the base of the carbide via a capillary tube carried in the device shank, so as to furnish a low ambient temperature, and elevated temperature gradient through the go area of the tip. It used to be located that the proximity of the low temperature warmness sinks retarded crater wear, as the welding and plucking motion was once appreciably reduced.

Researchers at Grumman Aircraft Engineering Corporation mentioned protected and profitable tool-life enhancement when the usage of LN_2 to cool high-speed metal cease mills (Machinery 1965). The cryogenic method is different; in that the temperature at the cutting area is decreased to a very low vary (Cassin and Boothroyed 1965). It has

been pronounced that the temperature dependant put on is additionally decreased extensively in cryogenic machining.

Uehara and Kumagai (1968) made an preliminary effort toward reading basically the results of cryo-machining. A collection of machining experiments have been carried out on special sorts of workpiece the usage of LN_2 as a coolant. Decrease in measurement of build-up edges used to be located ensuing in accelerated surface roughness. Experiments confirmed that the slicing overall performance for the duration of cryogenic machining well-known shows complicated inclinations that rely upon the mixtures of reducing and cooling stipulations and additionally the kind of workpiece and device used. Uehara and Kumagai (1969a) have pronounced that cryogenic cooling distinctly decreased the cutting pressure and temperature, and expanded device lifestyles and surface integrity in non-stop as nicely as interrupted machining.

Jainbajranglal and Chatopadhyay (1984) furnished the LN_2 onto the tool-workpiece interface by using nozzles. The impact of LN_2 on turning and grinding of low carbon steels was once in contrast with traditional soluble oil. During cryogenic turning, the expanded surface end and device life had been discovered in contrast to the traditional turning. Reduction in reducing forces was once found due to partial transformation of shear deformation of the chip into brittle fracture and discount in stagnation tendency of chip fabric and formation of constructed up edge. During cryogenic grinding, big minimize in each temperature and pressure had been located and offers smoother machined surfaces free from micro cracks when in contrast with traditional grinding. Machining of carbon metal the use of LN_2 decreases the reducing forces and device put on and improves surface integrity.

Li et al (1989) have studied the cryogenic ultra-precision machining of ferrous metals with natural diamond tools. It used to be stated that when the ferrous metals have been machined with natural diamond, a device underneath cryogenic cooling conditions, device put on was once managed effectively, which potential that the opportunity of the diffusion and adhesion was once reduced. Evans (1991) investigated the impact of cryogenic cooling on device put on mechanisms like adhesion and formation of build-

up edges, abrasion, micro chipping, fracture and fatigue and tribo-thermal and tribo-chemical wears in the turning of ferrous materials. Specially designed cooling device has been developed that cools the device shank clamped onto the specific cause device holder designed to decrease the warmness flux from the device with the rear of the device shank immersed in LN_2 reservoir. An extraordinary chuck was once additionally designed thru which LN_2 was once furnished the usage of stationary grant tube that hits the front face of the reservoir thereby throwing out the coolant centrifugally besides stopping the spindle whilst the chuck is in operation. The outcomes confirmed diminished tool wear and significant surface finish.

Paul and Chattopadhyay (1995, 1996a, 1996b) have investigated the impact of cryogenic cooling by way of LN_2 jet in the grinding of exclusive steels like mild, excessive carbon, cold die, warm die and excessive pace steels. The consequences that have been bought through experiments with appreciate to forces, unique energy, grinding quarter temperature, and surface residual stress the usage of cryogenic coolant and have been in contrast it with dry grinding and with traditional emulsion cooling. Cryogenic cooling is superior, with which in contrast to different coolants in controlling the temperature, residual stresses and grinding forces. With Cryo cooling, substantial discount in grinding area temperature has been located in particular for ductile material main to higher surface traits of ground surface and much less wheel loading and wheel wear.

Hong and Zhao (1999) studied the important features of cryogenic cooling in the steel reducing process. It was once pronounced that liquid nitrogen as a coolant eliminated the warmness efficaciously from the reducing zone, reducing the reducing forces and editing the frictional characteristics at the chip – device interfaces. Ghosh et al (2003) investigated the impact of cryogenic cooling on the machining of 52100 bearing steel, A2 device metal and WC-Co rolls with 35 Alumina ceramic, PCBN and PCD tools. Significant device life enhancements in the cryogenic machining of such challenging ferrous substances had been attributed to greater efficient warmth elimination from the cutting insert, and a diminishment in the thermal softening of the cutting equipment at a greater temperature.

2.5 STUDY OF DIFFERENT CRYOGENIC COOLING APPROACHES IN METAL CUTTING

2.5.1 Liquid Nitrogen Circulation System

Wang et al (1996a) made an effort to maintain the tool temperatures at a lower range by circulating liquid nitrogen using copper tubes, as shown in Figure 2.1.
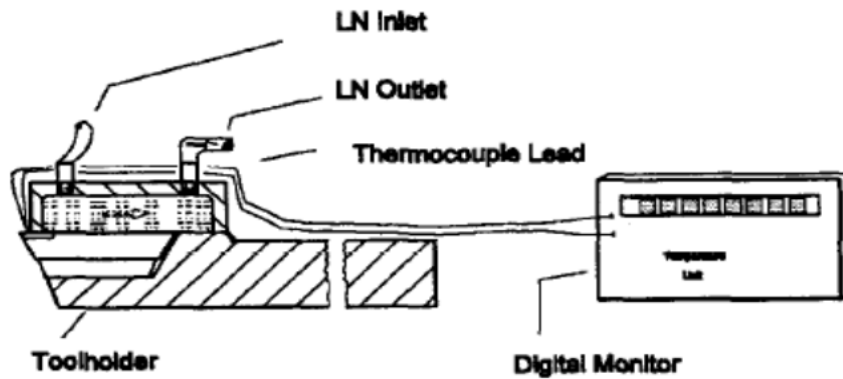
Figure 2.1: Liquid nitrogen circulation system developed by Wang et al (1996a)

Wang et al (1996a) performed experiments on machining superior ceramic composite like response bonded silicon nitride 'Si3N4' (RBSN) with a LN_2 cooled Poly Crystalline Boron Nitride device (PCBN). A liquid nitrogen circulation device used to be designed to maintain the tool temperatures at a decrease range. The surface roughness of the workpiece machined with liquid nitrogen cooling used to be an awful lot higher than the surface roughness of the workpiece machined except liquid nitrogen cooling.

Wang and Rajurkar (1997) investigated the impact of cryogenic cooling on device put on mechanism in the turning response bonded silicon nitride with CBN cutting device inserts. It used to be located that the tool life used to be improved due to cooling with the aid of liquid nitrogen. Wang and Rajurkar (2000) labored on the cryogenic machining of hard-to-cut materials. The cryogenic cooling machine presents higher cooling impact on the kind of insert used, in contrast to these used in traditional

coolants. Therefore the temperature impact in the reducing region was once minimized via keeping the greater warm power and warm hardness of the device and decreasing the device wear. There used to be an extend in the device life up to 5 folds when LN_2 coolant was once used as an alternative than the traditional coolant. The floor roughness of all the substances machined with liquid nitrogen cooling was once observed to be tons higher than the substances machined barring liquid nitrogen for the equal size of cutting.

Wang et al (2002) studied the impact of cryogenic cooling on cutting forces, device life and workpiece surface end in the course of machining of tantalum. The outcomes confirmed that, cryogenic machining supplied higher floor finish, longer device life, and decrease cutting forces in contrast with traditional machining. The discount of device put on in cryogenic cooling more desirable machining counselled a tremendous machinability as in contrast to traditional machining. There was once a sharp make bigger in temperature in the cutting region making the device – workpiece location purple warm and the formation of constructed up edges when the LN_2 coolant used to be now not used. It used to be additionally proven that the cryogenic cooling – more advantageous machining is an environment friendly approach for machining tantalum, when a carbide tool insert is used.

2.5.2 Cryogenic Chip Cooling System

In this approach of cryogenic cooling, the liquid nitrogen used to be furnished to the chip and device rake face, rather of flooding the entire cutting zone, in order to enhance the chip braking when the chip is cryogenically cooled. Figure 2.2 indicates the schematic layout of the liquid nitrogen jet that covers the chip and the device rake face. Figure 2.2 Cryogenic chip cooling developed with the aid of Hong et al (1999) Hong et al (1999) investigated the impact of cryogenic cooling on the machining of low carbon metal AISI 1008 ductile material, and suggested a considerable enchancment in chip breaking. The cooling setup was once designed such that the cryogen is impinged to the chip faces alternatively of flooding the entire cutting zone, which optimizes the coolant consumption to a giant extent. Hong and Ding (2001a) developed a secure strategy of the micro-manipulation of cutting temperatures in machining AISI / SAE

1008 low carbon steel. It was once stated that in chip breaking, the micro-temperature manipulation by using cryogenically cooling the chip, is an enhancement over pre-cooling the workpiece, especially at a greater cutting speed. Furthermore, the chip cooling strategy decreased the bad aspect impact of expanded shear power in the shear zone, which happens at some point of workpiece pre-cooling.

2.5.3 Cryogenic Dual-Nozzle Cooling System

Researchers tried in the previous to introduce appropriate cryogenic cooling approaches, which is low-budget and realistic adequate to substitute traditional machining, that grant minimum wastage of the cryogenic coolant. This can solely be completed through finding the nozzle at appropriate function that lets in a perfect quantity of the coolant to be impinged on the preferred role at work – device interfaces. . In this method, the nozzle system supplies liquid nitrogen through well-controlled and targeted jets to the device rake face, the flank face, or concurrently to both. Hong (2001) developed a new in your price range and realistic strategy to cryogenic machining method for machining of low and excessive carbon steels, and titanium alloys. The graph implementation of the cryogenic dual-nozzle cooling machine is proven in Figure 2.2 and Figure 2.3. In this method, the micro nozzle jetting to the slicing factor domestically minimizes the LN_2 consumption. This method minimizes the quantity of liquid nitrogen consumption to stages at which nitrogen fees much less than the traditional reducing fluid. It used to be mentioned that cryogenic cooling reduces device wear, and will increase device existence up to 5 times, thereby permitting for high-speed cutting, enhancing productiveness and decreasing the common manufacturing cost. In addition, this method reduces the frictional forces, improves chip breaking, eliminates the build-up edge, and improves surface quality.
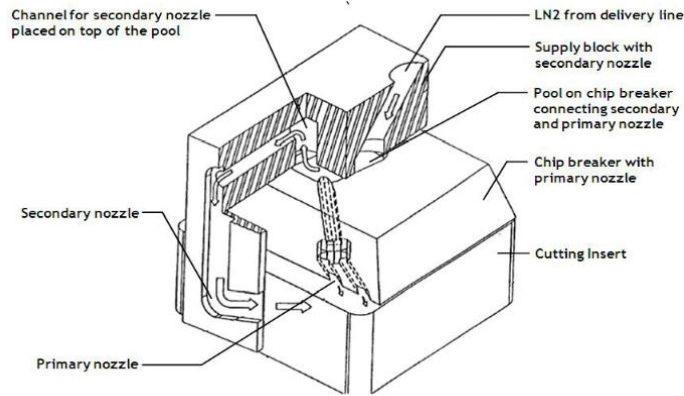
Figure 2.2: The design implementation of the cryogenic dual-nozzle system - Both the primary and auxiliary nozzles are used to supply LN$_2$
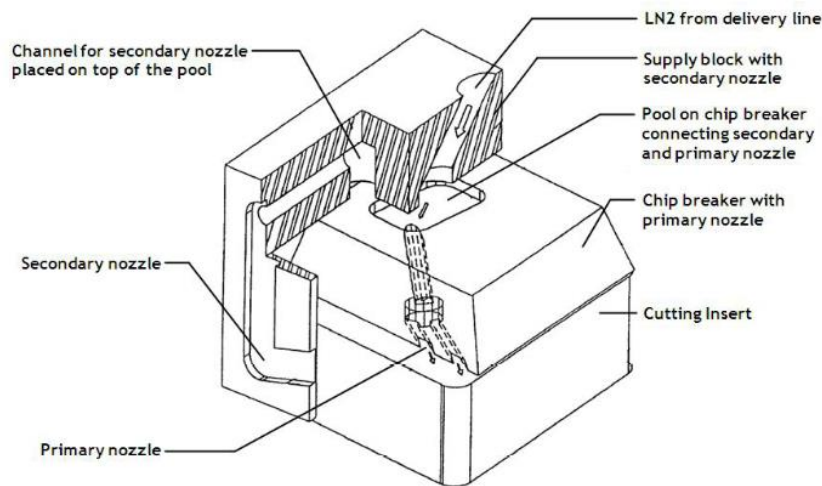
Figure 2.3: The design implementation of the cryogenic dual-nozzle system - Only the primary nozzle is used (Hong et al 2001)

Hong et al (2001) discovered the most wonderful cryogenic cooling method that yields the longest device life whilst preserving the minimum utilization of LN$_2$. It is additionally recommended that the cutting equipment shall be cooled however now not the workpiece material. In order to get most fulfilling cooling the cutting fluid should be utilized immediately to, and solely to, the tip of the cutting device the place the material is being reduce and warmness is being generated preserving the flow rate proportional to the warmness generated. A micro nozzle is placed between the device face and chip breaker which can be a new most economical business cutting device assembly and designed with convenience. During the machining the LN$_2$ absorbs the

heat, evaporates quickly, and types a fluid cushion between the chip and device face that features as lubricant as a result lowering the coefficient of friction and secondary deformation.

Hong et al (2001a) have studied the impact of cryogenic cooling on friction and cutting forces in the turning of the Ti-6Al-4V alloy. The experimental effects of the cutting pressure measurements indicated that the cold strengthening of the titanium fabric expanded the cutting pressure in cryogenic machining, decrease the friction decreasing the feed force. It was once said that the friction coefficient on the chip – device interface was once significantly decreased in cryogenic machining. Increased shear perspective and lowered thickness of the secondary deformation area in cryogenic cooling have been additionally reported.

Hong and Ding (2001) added a modern and least expensive approach of cryogenic cooling that directs the LN_2 through micro jets to the flank, the rake or both, close to the reducing aspect in the machining of the Ti-6Al-4V alloy. A small quantity of liquid nitrogen utilized regionally to the cutting part is choicest to emulsion cutting, in decreasing the reducing temperature. Liquid nitrogen utilized in shut proximity to the device cutting edge, can considerably limit the device temperature, relying on the goal location. They additionally studied the impact of more than a few cryogenic cooling strategies in the turning of the Ti-6Al-4V alloy. The software of liquid nitrogen to a chamber between the device insert and shim to freeze the device lower back face, is proven in Figure 2.4. In cryogenic workpiece pre-cooling, freezing the workpiece in advance of the device slicing edge, prior to and for the duration of the reducing cycle, is illustrated in Figure 2.5. The twin – nozzle device for localized liquid nitrogen furnish to the rake and flank surfaces is proven in Figure 2.6.

The Cutting temperature underneath cryogenic machining used to be in contrast with these underneath traditional dry cutting and emulsion coolant machining. The effects exhibit the order of effectiveness of the cooling procedures to be from worst to high-quality have been dry cutting, cryogenic device returned cooling, emulsion cooling, pre - cooling the workpiece, cryogenic flank cooling, cryogenic rake cooling and

simultaneous rake and flank cooling. It used to be additionally suggested that the cooling impact of the LN$_2$ is maximized, when it is injected as shut as feasible to the cutting side so that warmth era area can be correctly cooled.
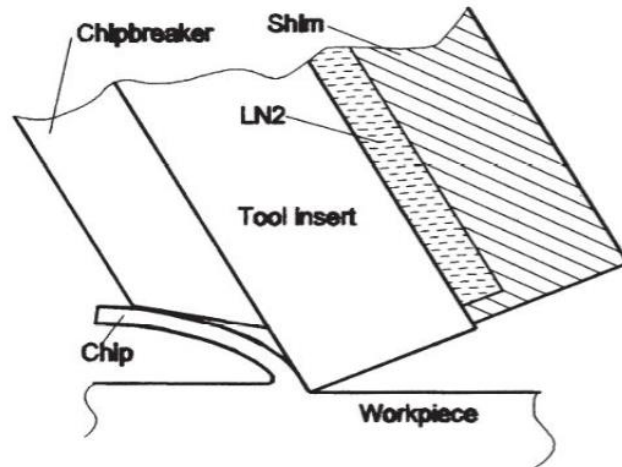
Figure 2.4: Cryogenic cooling on the tool back side (Hong and Ding 2001)
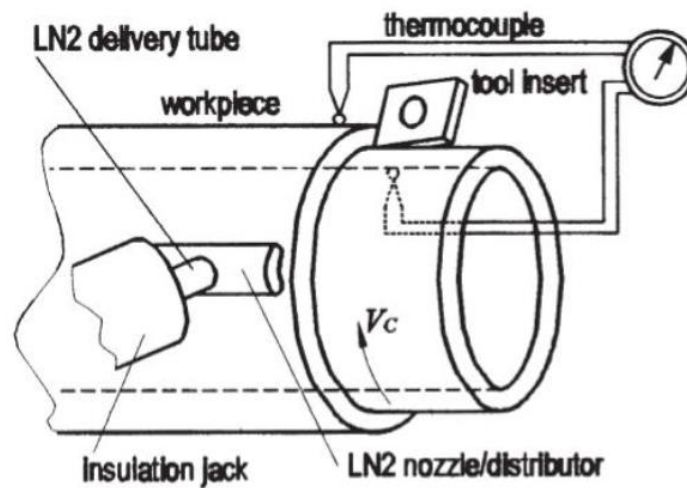
Figure 2.5: Cryogenic workpiece pre-cooling (Hong and Ding 2001)
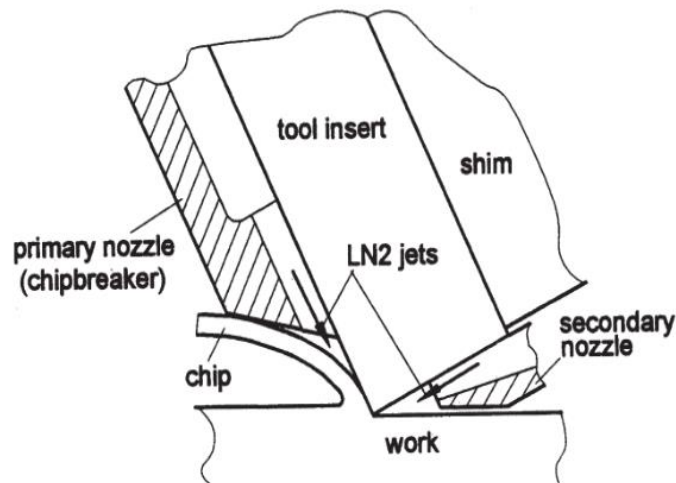
Figure 2.6: Cryogenic dual-nozzle cooling (Hong and Ding 2001)

Hong et al (2002) measured the everyday and frictional forces by means of immediately simulating the pure frictional behaviour of the device – chip interface in cryogenic cutting. A particularly designed LN_2 nozzle used to be used to follow excessive stress LN_2 jets via an obstruction kind chip breaker with the aid of properly managed jets to the device – chip interface, meant to reap each cooling and lubrication outcomes with low-priced LN_2 consumption. Proper software of LN_2 to the contacting surfaces can decrease frictional coefficients by using decreasing the interface temperature and enhancing the contact sample that adjustments sticking contact to in simple terms sliding contact main to decreased superb shear strength. It additionally enhances the hardness of the device face in the course of slicing with the aid of preserving the floor integrity of the more difficult part, minimizing inclinations of growing friction. The lubrication impact of LN_2 can be carried out through aggregate of more than a few temperature established results and micro scale hydrostatic effects.

2.5.4 Cryogenic Main and Auxiliary Cutting Edge Cooling System

In this cryogenic cooling method, the two liquid nitrogen jets from especially designed nozzles have been utilized nearly alongside the predominant and auxiliary slicing edges. Dhar et al (2000) investigated the outcomes of cryogenic cooling by using LN_2 jets on machinability traits in turning of undeniable carbon steels C-40 via carbide inserts below extraordinary slicing speeds and feeds. The liquid nitrogen jets have been

provided at the slicing area alongside the important and auxiliary cutting side at a strain of two bar. The cryogenic cooling reduces the cutting forces, device wear, and dimensional deviation and improves the chip formation and surface finish; it affords the advantages frequently thru discount in cutting temperature and beneficial trade in chip – device interaction. The gain of cryogenic cooling is appreciably influenced by using the device geometry, device and work cloth characteristics, and the ranges of the machining approaches parameters.

Paul et al (2001) studied the function of cryogenic cooling through LN_2 jet on device put on and surface end in simple turning of AISI 1060 metal at unique velocity and feed mixtures for two exceptional cutting inserts. The effectiveness of cryogenic cooling was once in contrast with these below dry and traditional cooling. The consequences confirmed that dry machining metal purpose most device put on and floor roughness whilst moist machining didn't exhibit any considerable improvement. But cryogenic machining the usage of LN_2 supplied decreased device wear, multiplied device existence and floor finish. The really helpful consequences of cooling might also make contributions to superb lubrication, retention of device hardness and beneficial chip – device and work – device interaction.

Dhar et al (2002) studied cryogenic machining of two sorts of steels AISI-1040 and AISI-4320 the use of carbide inserts and pronounced that the cooling with the aid of LN_2 jets can appreciably limit the cutting forces at some stage in machining besides affecting the working environment. It additionally offers advantages often through decreasing the reducing temperature, which helps in enhancing the chip – device interplay and keeps sharpness of the cutting edges. In machining steels by means of carbide inserts cryogenic cooling is predicted to be extra really helpful in end turning of excessive electricity steels, which are generally finished at low feed and cutting velocities.

Dhar et al (2002a) have studied the function of cryogenic cooling via a liquid nitrogen jet in the common chip – device interface temperature, device wear, dimensional accuracy and surface end in the turning of the AISI 4140 steel. Cryogenic cooling

enabled a considerable discount in the reducing region temperature, and favorable chip-tool and work-tool interactions. Cryogenic cooling furnished a discount in flank wear, and an enhancement in device existence was once said over dry machining. It used to be additionally mentioned that the surface end and dimensional accuracy extensively extended underneath cryogenic cooling. Dhar et al (2002b) have carried out experimental investigations on the function of cryogenic cooling by using liquid nitrogen jet on device put on and product excellent in the simple turning of AISI 1040 and E 4340C steels at industrial velocity – feed combinations, through two sorts of carbide inserts of special geometry. The encouraging consequences consist of a massive discount in the device put on rate, dimensional inaccuracy and floor roughness with the aid of cryogenic cooling application, in general due to the fact of beneficial cutting area temperature and a alternate in chip – device and work – device interactions.

Dhar and Kamruzzaman (2007) studied the impact of cryogenic cooling on the reducing temperature, device wear, floor roughness and dimensional deviation in the turning of AISI 4037 metal at industrial pace – feed combinations by using covered carbide insert, and in contrast the effectiveness of cryogenic cooling with dry and moist machining. The outcomes indicated great advantage in the cryogenic cooling on device life, surface end and dimensional deviation. This might also be attributed normally due to the discount in the cutting area temperature and the favorable exchange in the chip-tool interaction. Further, it was once stated that machining with soluble oil cooling failed to grant any extensive enhancement in device life; as a substitute the surface end deteriorated.

2.5.5 Modified Cutting Tool Insert System

In this cryogenic cooling method, the well-known cutting device insert used to be modified to provide liquid nitrogen at the reducing zone. Dhananchezian and Kumar (2011) investigated the impact of cryogenic cooling with a modified cutting device inserts on cutting temperature, cutting force, workpiece surface end and device put on throughout the machining of Ti-6Al-4V alloy. The consequences have been in contrast with traditional moist machining. A sizable advantage of cryogenic cooling on device

lifestyles and surface end was once reported. It used to be additionally pronounced that the utility of liquid nitrogen reduces reducing pressure due to successfully controlling the cutting temperature, preserving the power and hardness of the device material, discount in device put on and much less adhesion between device – chip and device – work interfaces.

Dhananchezian and Kumar (2011a) have studied the position of cryogenic cooling on cutting temperature, reducing force, workpiece surface end and device put on in the turning of AISI 304 stainless metal with a modified PVD TiAlN covered carbide device inserts. The effectiveness of cryogenic cooling was once in contrast with traditional cooling. The outcomes confirmed that cryogenic cooling the usage of LN_2 furnished reduced cutting temperature, reducing force, floor roughness and device put on in contrast with traditional cooling. The recommended outcomes of cryogenic cooling can be contributed that the superb lubrication, retention of device hardness and manage of temperature structured wear mechanisms.

2.5.6 Hybrid Machining System

The hybrid machining strategy combines ordinary turning with cryogenically stronger machining and plasma more suitable machining. Wang et al (2003) labored on the hybrid machining of the Inconel 718. It is stated that the hybrid machining of the Inconel 718 the usage of WG-300 ceramic device inserts, produced higher surface finish, longer device life, and decrease cutting forces in contrast with traditional machining.

2.5.7 Cryogenic Rake and Flank Surface Cooling System

In this cryogenic cooling method, liquid nitrogen jets have been impinged on the device rake and flank surfaces, the usage of a particularly designed nozzle. Venugopal et al (2007) studied the impact of cryogenic cooling on the increase and nature of device put on in the turning of the Ti-6Al-4V alloy bars with microcrystalline uncoated carbide inserts. The impact of cryogenic cooling with liquid nitrogen jets enabled a tremendous discount in the device wear, each on the crater and flank surfaces in the turning of the Ti-6Al-4V alloy. It used to be additionally mentioned that there was once extensive

enhancement in device life with the aid of a discount in adhesion – dissolution – diffusion device wear via the suitable manage of machining temperature at the reducing zone.

Venugopal et al (2007a) have investigated the device put on and device existence of uncoated carbide reducing device inserts in the machining of the Ti-6Al-4V alloy beneath dry, moist and cryogenic cooling environments. The prices of boom of all the device put on parameters, namely, the common flank wear, most flank wear, common nostril put on and part depression, have been much less in cryogenic cooling. A sizable enhancement in device existence used to be received underneath cryogenic cooling as in contrast to dry and moist machining.

2.6 RECENT STUDIES ON CRYOGENIC COOLING

Hong (2006) investigated the lubrication mechanism of liquid nitrogen in the reducing process. It was once discovered that the injection of liquid nitrogen into the contact sector created a lubricating film. The take a look at outcomes confirmed that the liquid nitrogen jet used to be very advantageous in lowering friction. Liquid nitrogen injection varieties a physical barrier or hydrodynamic impact between two bodies which is constantly fine in decreasing the friction force.

Stanford et al (2008) carried out an experimental investigation in the turning of BS 970-080A15 (En 32b) undeniable carbon slight steel below quite a number cutting environments. The following slicing environments had been evaluated: i) Flood coolant ii) Compressed air blast iii) Dry cutting iv) Ambient temperature nitrogen fuel surroundings v) Cold nitrogen gasoline and vi) Liquid nitrogen gasoline environment. The outcomes indicated that uncoated tooling used in nitrogen cutting environments even as cutting En 32b simple carbon slight steel, can grant a 55% discount in the crater put on and 30% discount in the flank put on over different environments.

Kumar and Choudhury (2008) studied the impact of cryogenic cooling on device put on and the excessive frequency dynamic cutting forces generated at some stage in the excessive speed machining of stainless steel. Liquid nitrogen was once provided to the

device tip the usage of a specifically designed nozzle. It used to be located from the experimental consequences that cryogenic cooling used to be fantastic in bringing down the slicing temperatures which accounted for the tremendous discount of the flank wear. The cutting pressure in cryogenic machining was once found to be much less than that of dry cutting, however the reduction in the cutting pressure is much less than anticipated. About 37.89% discount in the flank put on has been found with cryogenic machining over dry cutting. Cryogenic machining is a viable reply for excessive pace eco-friendly machining.

Yakup and Muammer (2008) reviewed the use of liquid nitrogen as a coolant and investigated in element the phrases of utility strategies in material elimination operations, and their outcomes on reducing device and workpiece fabric properties, reducing temperature, device put on and device life, surface roughness and dimensional deviation, friction and cutting forces. It used to be said that cryogenic cooling has resulted as one of the most beneficial approach for steel reducing operations due to its functionality of producing massive enchancment in device existence and surface end via the discount in device put on by means of a ideal manipulate of machining temperature at the reducing zone.

The traditional technique of cooling the usage of fluid is worried in manufacturing industries to resolve the trouble of extra warmness era at the steel cutting area (Natasha et al 2014). Regardless, the approach of flood cooling is no longer environment friendly in the discount of extra warmth generated at reducing location (Virginia et al 2014) and regular cooling fluids is combo pollution sources a couple of wellbeing, environmental troubles and extra relocation fee (Domenico et al 2012, Yamina et al 2020). Similarly, it is resolved that, the associated charges to cutting fluids are 30% of over-all gathering charges (Shalina et al 2020). But a couple of environmentally perceptive controls confined the endeavours in a similar way as use and alternate of general cutting fluids in view of prosperity, dangerous and everyday tainting impact (Shalina et al 2019). Cryogenic treatment in machining would be one of the alternative approaches. Accordingly, in this learn about cryogenic sprinkle cooling device is used, this entails spraying of the Liquid nitrogen (LN_2) at $-$ 1960C at the tool-workpiece interface. LN_2

liberally diminishes the temperatures at the tool-chip interface and makes an awful lot decrease grinding coefficient (Yongquan et al 2021). (Marco et al 2017) Illustrated low device put on and surface roughness price in cryogenic treatment in machining in contrast to dry machining in the midst of machining of titanium amalgam. (Ali et al 2016) Demonstrated that CO_2 yielded better device put on diverged from the moist machining for AISI 1045 steel. (Sudhansu et al 2015) outlined higher surface end cost in cryogenic machining stood out from the dry machining in the midst of machining of AISI 52100 steel. (Wit et al 2010) Observed decrease device put on and lessened floor roughness in cryogenic situation contrasted with minimal extent lubrication (MQL) machining stipulations on account of the astonishing reduction of the cutting temperatures. Accordingly, cryogenic machining grows the productiveness and nature of the issue in the machining of gamma titanium aluminides regarded in another way in relation to the subsequent wet, MQL machining. (Dhananchezian et al 2011) Completed monetary associated and everyday examination in the milling of AISI 304 and deduced that cryogenic method is greater beneficial and assist to accomplish greater one-of-a-kind gain stood out from emulsion cooling, besides prosperity and organic concerns. Table 2.1 summarized the impact of flood cooling surroundings on milling overall performance traits whilst machining of a number hard to cut. Table 2.2 summarizes the literature reachable on GRA, TOPSIS and RSM optimization strategies in milling of a number of substances beneath exceptional machining environments.

From the literature, it used to be determined that cryogenic spray cooling/cryogenic exterior jet cooling technique has many blessings like much less coolant consumption, no undesirable cooling area, decreased cooling electricity wastage; localized cooling at the machining sector reasons discount of cutting region temperatures. In the literature, many researchers have employed this approach to computing device extraordinary sorts of challenging to reduce substances and determined higher overall performance traits when in contrast to dry, moist and MQL machining conditions. Hence, the current learn about focuses on the exterior cryogenic cooling technique with LN_2 as coolant. From the literature, it used to be additionally determined that technique of provider of LN_2 at the machining sector notably influences the milling overall performance traits greatly. In the present day work, a low fee exterior cryogenic jet cooling setup has been

developed to spray the LN_2 between the tool-workpiece interfaces. To the author's understanding fewer records is on hand on machining of AISI 316 (SS316) beneath cryogenic condition. There is no change observed in the micro structure of AISI 304 stainless steel before and after cryogenic treatment for 10 min. (Muammer nalbant et al., 2010). From the literature, it can be surveyed that cryogenic cooling improves the device life, accomplishes higher surface end with in the midst of machining of hard to reduce material, paying heed to many functions of intrigue it over cools the surface, expands the hardness of the machined surface. The motive of the current examination is to reflect on consideration on the impact of LN_2 as the coolant on cutting temperature and surface roughness in the coping with of SS316 over the moist (coolant) machining

It is integral to decide the finest reducing stipulations and improvement of correlation fashions between the enter procedure parameters and output responses to enhance the productiveness with low manufacturing cost. In the literature, no try has been made on prediction and optimization of milling system whilst machining of SS316 underneath the cryogenic cooling environments. In cryogenic machining, the residual stress will form. However, the quantification of residual stresses depends on the cutting parameters levels at which machining operations are done. Based on literature, compressive type residual stress forms during cryogenic machining which are favourable to the machining operation (Jani Kenda et al., 2011)

Table 2.1: Contributions of earlier researchers on difficult to cut materials during milling with flood cooling method.

S.No.	Author (year)	Material	Milling Performance Characteristics										
			T	V_b	F_c	CM	μ	R_a	ST	H_v	PT	R	WL
1	Kumar and Choudhury (2008)	SS 202		√	√								
2	Hong and Ding (2001)	AISI 1008	√	√	√	√	√						
3	Hong et al. (2002)	Ti-6Al-4V, AISI 1018					√						
4	Hong et al. (2001)	Ti-6Al-4V			√		√						
5	Jun (2005)	Ti-6Al-4V, AISI I018					√	√					
6	Khan and Ahmed (2008)	AISI 304		√									
7	Khan et al. (2010)	AISI 304		√				√					
8	Dhananchezian et al. (2011)	AISI 304	√	√	√			√					
9	Dhananchezian and Kumar (2010;2011)	Ti- 6Al-4V, Al 6061-T6 alloy	√	√	√			√					
10	Jerold and Kumar (2011;2012;2013)	AISI 316, Ti-6Al-4V, AISI 1045	√	√	√	√		√					
11	Venugopal et al. (2007a;2007b)	Ti-6Al-4V alloy		√									
12	Bermingham et al. (2011)	Ti–6Al–4V alloy		√	√	√							
13	Paul et al. (2001)	AISI 1060		√				√					
14	Paul and Chattopadhyay (2006)	AISI1040, AISI1060, AISI E4340C, AISI 4140, AISI 4320	√	√	√	√							
15	MacHai and Biermann (2011)	Ti–10V–2Fe–3Al		√	√	√							
16	Yap et al. (2013)	Ti54			√		√	√					
17	Klocke et al. (2013)	γ-TiAl		√	√	√		√					
18	Raza et al. (2014)	Ti-6Al-4V alloy		√				√					
19	Kaynak (2014)	Inconel 718	√	√	√	√							
20	Bordin et al. (2015)	AM Ti-6Al-4V alloy		√			√	√					
21	Bordin et al. (2016)	AM Ti-6Al-4V alloy		√		√		√					
22	Sartori et al. (2017)	AM Ti-6Al-4V alloy		√									
23	Pereira et al. (2016)	AISI 304		√	√			√	√	√			
24	Chetan et al. (2015)	Nimonic 90 alloy		√		√		√					
25	Hong et al. (1999)	AISI 1008	√			√							
26	Dhar and Kamruzzaman (2007)	AISI 4037	√	√				√					
27	Dhar et al. (2001)	AISI 1040 and E4340C steels	√	√				√					
28	Schoop et al. (2015)	porous tungsten material		√				√					
29	Yap et al. (2013)	Ti-5Al-4V-0.6Mo-0.4Fe			√		√	√					
30	Sun et al. (2015)	Ti-4Al-6V	√	√	√								
31	Gupta et al. (2015)	AISI 1040	√	√	√			√					
32	Dinesh et al. (2016)	ZK60 magnesium alloy	√	√	√		√	√		√			
33	Umbrello et al. (2012)	AISI 52100						√		√	√	√	√
34	Rotella et al. (2013)	Ti-4Al-6V						√		√	√		
35	Schoop et al. (2016)	porous tungsten	√		√	√		√					
36	Kaynak (2014)	Inconel 718	√	√		√		√	√				
37	Dinesh et al. (2015)	ZK60 magnesium alloy	√		√				√				
38	Kaynak et al. (2014)	AISI 304L						√	√				
39	Kaynak et al. (2014)	NiTi								√	√		√
40	Bruschi et al. (2016)	Ti-6Al-4V alloy		√				√		√		√	
41	Pusavec et al. (2011)	Inconel 718						√		√	√	√	
42	Pu et al. (2012)	AZ31B Mg alloy						√		√	√	√	√
43	Kenda et al., (2011)	Inconel 718						√		√	√	√	√

Where: Ra = Surface roughness; T = Cutting temperature; F = Cutting force; TW = Tool wear; CM = Chip morphology; μ = Coefficient of friction; R = Residual stresses; PT = Phase transformation;   ST = Surface Topography; HV = Micro-hardness; WL = White layer thickness.

Table 2.2 (a): Literature report available on optimization and techniques during milling of different materials under environments.

S.No.	Author (s) and year	Material	Machining environment	Optimization technique used	Milling Performance Characteristics				
					V_b	R_a	F	MRR	P
1	Sahoo and Pradhan (2013)	Al/SiCp MMC	Dry	Taguchi	√	√			
2	Negrete (2013)	AISI 6061 T6 material	Dry	Taguchi		√			√
3	Philip Selvaraj et al. (2014)	duplex steel	Dry	Taguchi	√	√	√		
4	Senthilkumar et al. (2016)	Hardened alloy steel	Dry	Taguchi	√	√			
5	Dureja et al. (2014)	AISI D3 steel	Dry	Taguchi	√	√			
6	Sarikaya and Gullu (2014)	AISI 1050 steel	MQL	Taguchi		√			
7	Debnath et al. (2016)	mild steel	MQL	Taguchi	√	√			
8	Manivel and Gandhinathan (2016)	Austempered ductile iron (grade 3)	Dry	Taguchi	√	√			
9	Gupta et al. (2015)	EN24 alloy steel	Dry, Wet, Cryogenic	Taguchi	√				
10	Thakur et al. (2010)	Inconel 718	MQL	Taguchi	√		√		
11	Asiltürk and Akkuş (2011)	AISI 4140	Dry	Taguchi		√			
12	Fetecau and Stan (2012)	Polytetrafluoroethylene composite material	Dry	Taguchi		√	√		
13	Davim (2003)	A356/20SiCp/T6 type MMC	Dry	Taguchi		√	√		√
14	Singh and Kumar (2006)	EN24	Dry	Taguchi			√		
15	Kirby et al. (2006)	6061-T6	Dry	Taguchi		√			
16	Hwang and Lee (2010)	AISI 1045	Wet, MQL	Taguchi		√	√		
17	Sarıkaya et al. (2016)	Hayness 25	Dry, MQL	Taguchi	√	√			
18	Gaitonde et al. (2008)	brass	MQL	Taguchi		√	√		
19	Lin (2015)	S45C steel	Dry	GRA	√	√	√		
20	Tzeng et al. (2008)	SKD11 tool steel	Dry	GRA		√			
21	Sarikaya and Gullu (2015)	Hayness 25	MQL	GRA	√	√			
22	Ranganathan and Senthilvelan (2011)	SS 316	TAM	GRA	√	√		√	
23	Ramanujam et al. (2011)	A356/10/SiCp MMC	Dry	GRA		√			√
24	Goel et al. (2015)	mono-crystalline germanium material	Dry	GRA		√			
25	Senthilkumar et al. (2014)	hardened alloy steels	Dry	GRA	√	√		√	
26	Abhang and Hameedullah (2011)	EN-31 steel	Dry	GRA		√			
27	Singh et al. (2011)	GFRP composite	Dry	TOPSIS		√			
28	Ramesh et al.(2016)	AZ91D	Dry	TOPSIS	√	√			
29	Aggarwal et al. (2008)	AISI P-20 tool steel	Dry, wet, Cryogenic	RSM					√
30	Gupta et al. (2015;2016)	Titanium (grade 2)	MQL	RSM	√	√	√		
31	Makadia and Nanavati (2013)	AISI 410 steel	Dry	RSM		√			
32	Asiltürk et al. (2016)	Co28Cr6Mo ASTM F 1537 steel	Dry	RSM		√			
33	Bouacha et al. (2010;2014)	AISI 52100 steel	Dry	RSM	√	√	√	√	
34	Mandal et al. (2011)	EN 24	Dry	RSM	√				
35	Mandal et al. (2012;2013)	AISI 4340 steel	Dry	RSM		√	√		
36	Bhushan (2013)	7075 Al alloy+ 15 % SiC MMC	Dry	RSM	√				√
37	Palanikumar (2008)	Glass fiber reinforced plastic (GFRP)	Dry	RSM		√			
38	Seeman et al. (2010)	20% SiCp -LM25 Al MMC	Dry	RSM	√	√			
39	Aouici et al. (2011)	AISI H11	Dry	RSM	√	√			
40	Palanikumar and Karthikeyan (2006)	LM25 Al+SiC MMC	Dry	RSM		√			
41	Chauhan and Dass (2012)	Titanium (grade 5)	Dry	RSM		√	√		
42	Priyadarshi and Sharma (2015)	Al-6061-SiC-Gr MMC	Dry	RSM		√	√		

Where : Vb = Tool wear; Ra = surface roughness; F = cutting forces; MRR = Material Removal Rate; P = Power.

2.7 PREDICTION, OPTIMIZATION AND ANALYSIS TECHNIQUE

The most critical point in solving engineering problems is modelling and analysis of the correlation between input and output variables. In general, there are two crucial modelling techniques used. They are known as analytical and empirical models.

2.7.1 PREDICTION - NEURAL NETWORK MODEL

Artificial Neural Network (ANN) used in deciphering several problems like process control and automation, signal/image processing, prediction of breakdown/malfunctioning of the system and production process optimization (Pradeep A. 2012, Gweon 1999, Yousif et al. 2008, Zurada et al. 1997). The motivation behind the recognition and implementation of ANN is due to its success in solving the nonlinear problems which have no relationship between input and output parameters (Ming Zhou 2002, Farahnakian et al 2011,Shalina et al 2019).

Based on the architecture, ANN`s are classified as single layer feed-forward network, Multilayer feed-forward neural network and Recurrent neural network (Rajasekaran and Vijayalakshmi 2011).

2.7.2 Classification Framework

Classification technique is based on the inductive learning principle that analyzes and finds the patterns from the database. If the nature of an environment is dynamic, then the model must be adaptive i.e. it should be able to learn and map efficiently. Limère et al. (2004) presented a model for firm growth with decision tree induction principle. It gives interesting results and fits the model to economic data like growth competence and resources, growth potential and growth ambitions. Hoi et al. (2006) developed a novel framework of learning the unified kernel machines for both labeled and unlabeled data. This framework includes semi supervised learning, supervised learning and active learning. Also, a spectral kernel is proposed, where it classifies the given labeled data and unlabeled data efficiently.

Xu et al. (2008) proposed a reproducing kernel Hilbert space framework for information theoretic learning. The framework uses the symmetric nonnegative definite kernel

function i.e. cross-information potential. Though this framework gives better result than the previous RKHS frameworks, still there is an issue to choose an appropriate kernel function for a particular domain. Shilton and Palaniswami (2008) defined a unified approach to support vector machines. This unified approach is formulated for binary classification and later on extended to one-class classification and regression.

Kumar et al. (2012) explored a binary classification framework for two stage multiple kernel learning. The distinct advantage of this binary classification framework is that it is easier to leverage research in binary classification and to develop scalable and robust kernel based algorithms. Takeda et al. (2012) proposed a unified robust classification model that optimizes the existing classification models like SVM, minimax probability machine and fisher discriminant analysis. It provides several benefits like well-defined theoretical results, extends the existing techniques and clarifies relationships among existing models.

Yee and Haykin (1993) viewed the pattern classification as an ill-posed problem, it is a prerequisite to develop a unified theoretical framework that classifies and solves the ill posed problems. Recent literature on classification framework has reported better results for binary class datasets alone. For multiclass datasets, there is a lack in accuracy and robustness. So, developing an efficient classification framework for multiclass datasets is still an open research problem.

2.7.3 Data Selection

Data selection is a primary task in data mining that selects the calibrated data from the storage repositories or data warehouses. Then the selected datasets can be analyzed using two different strategies. They are inductive approach and deductive approach. In inductive approach, the experimental results are used to integrate the results and findings within some theoretical context whereas in deductive approach it starts with a theory and implements the observed data.

Ramakrishnan and Ullman (1995) reviewed the results with deductive databases and presented a summary of different projects that support rule based learning algorithms. Greco et al. (2001) combined deductive and inductive tools for data analysis process.

A system is developed to integrate the deductive analysis tools and data mining tools that manipulate the given datasets easily. It can also be used for large projects whose objective is to bind the information from different sources.

LaLoudouana et al. (2003) discussed the dataset selection for SVM with extensive practical applications. Here, a new principle for selecting the datasets is constructed and demonstrated with different algorithms. Tax and Duin (2004) described about support vector data description to make a robust classifier for real time applications. Van der Walt and Barnard (2006) studied the relationship between distribution of data and classification performance. From the results, it is stated that certain properties of the data can influence the classifier performance.

Schadewitz and Jachna (2007) compared the inductive and deductive research methodologies that analyze the qualitative data to identify, design and articulate the patterns. The deductive analysis helped to achieve a persistent description, structure and format for pattern design. From the investigation of data selection and its approaches, it is construed that the deductive analysis technique helps in formulating a new set of hypothesis to solve many real time problems.

2.7.4 Data Normalization

Data normalization is a preprocessing technique to transform the given data into a desired range. It improves the data quality and makes them fit for use by reducing the discrepancies in the given dataset. Data is usually normalized to remove inconsistency and to create a desirable data structure. Since the datasets are taken from the machine learning repository that contains some noise and redundant data, it is required to do normalization before classification process.

Zhang et al. (2003) projected the need for data preprocessing techniques. Data collected in the storage devices and repositories may provide low quality data due to some disturbances like noise and ambiguity. So, it is suggested to clean the data before it is used for classification or prediction. Kotsiantis et al. (2006) discussed the importance of data preprocessing techniques in supervised learning algorithm. It is stated that the

instances can be formatted and represented clearly using the data preprocessing techniques.

Jayalakshmi and Santhakumaran (2009) investigated the statistical normalization techniques like z-score, min-max and median. These normalization techniques enhance the reliability and accuracy of a classifier model. Yusof and Mustaffa (2011) compared the min-max, z-score and decimal scaling using the dengue outbreak database. These normalization techniques are used with both least square SVM and Neural Network. But, the least square SVM predicts better in comparison with the Neural Network technique.

Rathod and Momin (2012) evaluated the performance of outlier detection with normalized dataset. Preprocessing techniques like min-max, z-score and decimal scaling are implemented in outlier detection to refine the results. Chandrasekhar et al. (2011) studied the different preprocessing and clustering techniques to avoid the redundant and missing values in gene expression data. These methods augment the performance and quality of clusters in random gene datasets using silhouette measurements.

2.7.5 Data Imputation

Missing data is a major problem in data mining that diminishes the quality of data. This substantial issue can be often found in statistical data analyses. And, the improper treatment of missing data will deform the data analysis or generate biased results. So, it is necessary to replace an incomplete observation with complete information and improve the precision of the interpretation and prediction.

Efficient data imputation techniques that are used in literature are Bayesian Principal Component Analysis (BPCA), Regularization Expectation Maximization (Reg. EM), K Nearest Neighbor (KNN), Weighted K Nearest Neighbor (Wt. KNN), Local Least Squares (LLS) and Iterated Local Least Squares (It. LLS). Kim et al. (2004) discussed the imputation techniques like least square imputation, BPCA, KNN and Wt. KNN to estimate microarray gene expression data. In gene expression data, LLS imputation outperforms the other imputation methods.

Iacus and Porro (2006) discussed about the handling of missing data values using random recursive partitioning. The performance of random recursive partitioning has recorded higher accuracy when dealing with categorical attributes or in the presence of missing data. Yang et al. (2009) developed a novel imputation technique for gene expression data based on KNN and dynamic time warping. Since imputation techniques lead to computational complexity, the parameters in the techniques should be tuned appropriately.

Ghoneim et al. (2011) focused on the impact of different missing value imputation techniques where it is reflected in the classification accuracy. Techniques like singular value decomposition, Wt. KNN, KNN and zero replacement are compared. Weighted KNN method provides accurate estimation for missing value in gene expression data that belongs to the same small tight expression cluster. Also, the classifier performance is slightly affected by the imputation techniques and makes it as robust one.

Suthar et al. (2012) surveyed the different imputation techniques that are used to remove missing values in a given dataset. The merits and demerits of different imputation techniques are also presented. Magnani (2004) reported missing value techniques that deal with the knowledge discovery process. It helps in building a strong classifier model for a given dataset. Recent works have elaborated the importance of imputation techniques and its impacts on different datasets. So, before applying the data mining techniques, it is necessary to check whether the given dataset is error free. If there is any noisy or missing value, an appropriate preprocessing technique should be applied to remove the noisy and missing data.

2.7.6 Data Validation

Giannakopoulos et al. (1999) compared the performance of neural and semi neural algorithms designed for Independent Component Analysis (ICA) using Statlog datasets. A criterion was developed to select the useful basis vector of ICA and to measure the goodness of the results. King et al. (1995) evaluated the results of diverse classification algorithms with real time datasets that are taken from Statlog project. It is shown that there is no single best method that improves the accuracy of given datasets.

Rohwer and Morciniec (1995) tested twenty three classification algorithms on a tuple recognition system with eleven real time data sets and their performances are compared and depicted. Lastly, the empirical results proved that n-tuple method yields poor accuracy for certain data sets. Michie et al. (1999) compared and evaluated a range of classification techniques using Statlog project datasets. As a result, the comparative trials of different learning methods in large-scale commercial and industrial problems are represented.

Bay et al. (2001) explained the need for data collection organizations and repositories like UCI Machine Learning repository, European Statlog dataset and Reuters dataset. This helps to develop a data analysis tool that combines techniques from different field such as computer science, statistics and mathematics to extract significant knowledge from data.

Fedorova et al. (2012) investigated plug-in martingales that are used to test the exchangeability of data. The performance of the testing method was experimented with benchmark datasets and validated using real time data sets,taken from Statlog project database. From the discussion, it is deduced that the European Statlog repository contains the standard real time datasets. It can also be used for validating the newly formulated hypothesis or constraints.

2.8 OPTIMIZATION - PARTICLE SWARM OPTIMIZATION (PSO)

Aote et al. (2013) presented a detailed work on PSO along with its limitations. Bratton and Kennedy (2007) defined a standard PSO algorithm with the recent developments that helped to improve the performance on standard measures to extend original PSO. The defined standard PSO formed ~~as~~ a baseline for performance testing of improvements to the technique as well as to represent PSO to wider optimization community. Sousa et al. (2004) presented the use of PSO as a new tool for optimization, PSO performed in two stages, and in the first stage three different PSO algorithms were implemented and tested against a Genetic Algorithm and Tree Induction Algorithm (J48). In the second stage the best classifier variants improved in terms of attribute type support and temporal complexity.

Nouaouria et al. (2013) identified and discussed two data-related problems that may affect Particle Swarm Classification (PSC) efficiency: high-dimensional datasets, mixed-attribute data and presented solutions for each of these problems including recent improvements by a PSC algorithm. Hsieh et al. (2014) proposed a class of Hyper-Rectangular Composite Neural Networks (HRCNNs) of which synaptic weights can be interpreted as a set of crisp If-Then rules; however, a trained HRCNN may result in some ineffective If-Then rules which can only justify very few positive examples (i.e., poor generalization) so, a PSO had been proposed based on Fuzzy Hyper-Rectangular Composite Neural Network (PFHRCNN) to trim the rules.

Panahi et al. (2013) presented the new classifier system features an experience-evaluation mechanism that would allow the classifiers "success rates" to contribute to their rise or decline in terms of performance parameters. A high success rate would promote the classifier's chance to survive and to reproduce where as a low success rate would render the classifier vulnerable to deletion. Using multiple data mining and control case studies, Success Rate Extended Classifier System (SRXCS) outperformed Extended Classifier System (XCS) fairly noticeably. The proposed improvement reduced the computational cost of the training process and resulted in fewer, more general classifiers in the final rule set without using the traditional rule reduction techniques.

Chen et al. (2012) developed a new pruning algorithm , which had adopted Scoring Based on Associations(SBA) algorithm. The proposed algorithm aimed at improving the accuracy of associative classification for class imbalance problem. Eberhart and Kennedy (1995) presented optimization of non linear functions using PSO. Shi and Eberhart (1998) introduced a new parameter called inertia weight, into particle swarm optimizer to demonstrate the impact of this parameter on the performance of PSO. Esmin (2007) proposed the generation method of fuzzy rule by learning from examples using PSO method. Holden and Frietas (2007) proposed several modifications to the original PSO/ACO algorithm for the discovery of classification rules and evaluated the new version of the PSO/ACO (i.e., PSO/ACO2) algorithm with two different rule quality functions to illustrate the choice of rule quality measure greatly effects the end performance of PSO/ACO2.

Pan and Yang (2010) depicted a survey on transfer learning, which covered the recent advancement in transfer learning for classification, regression and clustering problems. The relationship between transfer learning and other machine learning techniques were elucidated. Simon et al. (2015) expounded association rule set summarization techniques to examine the risk of diabetic mellitus. Similar examination of the techniques on applicability, weakness and rule performance were made. Tripoliti et al. (2012) proposed an enhanced random forest algorithm for automated disease diagnosis.

Liu et al. (2014) developed a PSO based simultaneous learning frame work for clustering and classification. The proposed framework constitutes automatic cluster algorithm, finding optimal cluster centre, and classification of test data. According to Liu et al (2011) the problem of pruning redundant rules had been addressed by an efficient post processing method. Permana and Hashim (2010) designed Fuzzy Particle Swarm Optimization (FPSO) to enhance the speed of convergence and performance of fuzzy system. Mangat (2010) designed a Swarm Intelligent (SI) techniques namely the PSO, Combined ACO/PSO and ACO/PSO with precision fitness for rule discovery in medical domain and their performance measures were compared.

This chapter surveys the state of the art techniques which have been reviewed to develop the overall classification framework of this research work.

Table 2.2(b): Papers referred on PSO techniques.

SL. NO	Authors	Input Parameters	Operation	Output Parameters	Remarks/ Conclusion
1	Farahnakian et al. (2011)	Cutting speed, feed depth of cut	End milling	Cutting forces and surface roughness	A very good training capacity of the proposed PSONN algorithm
2	Yang et al.(2011a)	Number of passes, depth of cut in each pass, speed, and	Multi-face milling	Production cost	The proposed schemes may be a promising tool for the optimization of machining process parameters.
3	Yang et al.(2011b)	Number of passes, depth of cut in each pass, speed, and feed	Multi-pass face milling	Production cost	The F-MOPSO does not have any difficulty in achieving well-spread Pareto optimal solutions with good convergence to true Pareto optimal
4	Razfar et al.(2010)	Cutting speed, feed, depth of cut, engagement	Face milling	Surface roughness	A good agreement is observed between the values predicted by the PSONNOS algorithm and experimental
5	Rao and Pawar (2010b)	Number of passes, depth of cut, cutting speed and	Multi-pass milling	Production time	The results are compared with the previously published results obtained by using other optimization techniques.
6	Escamilla et al. (2009)	Speed, feed and depth of cut	End milling	Surface roughness	PSO optimization it can be successfully applied to multiobjective optimization of titanium's machining
7	Prakasvudhisarn et al. (2009)	Speed, feed and depth of cut	CNC end milling	Surface roughness	Both techniques can achieve the desired surface roughness and also maximize productivity
8	Li et al. (2008)	Spindle speed, feed rate	Milling	Cutting force, tool-life, surface roughness and cutting	PSO in optimizing process parameters can converge quickly to a consistent combination of spindle speed and feed

9	Zhao et al. (2008)	Spindle speed and feed rate.	Milling	Cutting forces	The machining process with constant cutting force can be achieved via process parameters optimization based on
10	Zuperl et al. (2007)	Cutting speeds and feed rates	Milling	Cutting forces	Compared with GA and SA the proposed algorithm can improve the quality of the solution while speeding up the
11	Huang et al. (2007)	Spindle, Feed rate, width	End milling	Tool wear	Tool wear
12	Rashmi et al. (2016)	Spindle speed, Feed rate and Depth of cut	Face Milling	Cutting force, surface roughness and power consumption	Compared with RSM, Desirability approach and the proposed PSO algorithm attained the effective results. PSO optimization it can be successfully applied to multiobjective optimization of AA6061-
13	Z.G. Wang et al.	Cutting speed (m/min) Feed rate (mm/rev)	multi-pass milling.	Four typical runs at different depth of cut	PGSA is shown to be more suitable and efficient for optimizing the cutting parameters for milling operation
14	S.Bharathi Raja et al. (2010)	Cutting speed (rev/min),Feed (mm/min),	Face Milling	Desired Surface Roughness in minimum machining	It has been found that the predicted roughness using PSO is in good agreement with the actual roughness.
15	F. Cus et al. (2008)	Cutting Speed and Fee Rate	End Milling	Optimum Cutting Speed and Feed Rate and Cutting	The simulation results show that compared with genetic algorithms (GA) and simulated annealing (SA), the proposed
16	F. Cus et al. (2003)	Cutting Speed and Fee Rate	End Milling	Surface Roughness and MRR	PSO is proved to be an efficient optimization algorithm. The experimental results show that the MRR is

17	Prakasvud hisarn et al. (2009)	Cutting speed, Feed Rate, Depth of cut	End Milling	Surface Roughness	SVMs and PSO techniques were implemented. The cooperation between both techniques can achieve the desired
18	Tandon, V et al. (2008)	Cutting Speed and Fee Rate	End Milling	Optimum Cutting Speed and Feed Rate and Cutting Force	ANN was implemented to predict cutting force and PSO to identify optimum speed and feed rate. Machining time reductions of up to 35% are observed. In addition,
19	R. Venkata Rao et al. (2010b)	Number of passes, depth of cut for each pass, cutting speed, and feed.	Milling	Minimization of Production Time	ABC, PSO and SA are implemented. The comparison between these 3 techniques have been made and concluded that ABC and PSO perform better
20	M.Chandr asekaran et al. (2010)	N/A	Milling, Turning, Grinding.	Machining Performance prediction and optimization	Discussed the overall history of the application of soft computing technique in machining performance prediction

2.9 MACHINE LEARNING - SVM APPLICATION FOR CONVENTIONAL MACHINING OPERATIONS

The prediction of machining performances such as surface roughness, cutting force and tool life need a proper optimization of the process since it is the challenging part in machining. Instead, it has been recognized that cutting condition such as cutting speed, feed rate and depth of cut should be selected to optimize the economics of machining process [13]. Hsueh and Yang [14] proposed a new diagnosis technique for tool breakage in face milling using SVM. The process parameters involved in this research are depth of cut, feed per tooth, spindle speed and cutting diameter. The considered kernel functions are linear, polynomial and radial basis function (RBF). Researchers used the feature of spindle displacement signals into the kernel-based SVM decision function to monitor tool breakage. The proposed technique is confirmed highly

sensitive, robust and reliable Least-square SVM (LS-SVM) was considered to predict the surface roughness of milling aluminium alloy [15]. The model is developed to analyse the effect of process parameter such as spindle speed, feed rate, spindle acceleration, depth of cut, rake angle and tool diameter for surface roughness. Training and testing pattern vector have been recognized before LS-SVM training. RBF was selected as a kernel training function due to the high regression precision. The training parameters were determined by 5- fold cross validation procedures. LS-SVM has given a reasonable accuracy and gives 8 % average error. Caydas and Ekici [16] applied SVM to developed prediction models for surface roughness in turning process of AISI 304 austenitic stainless steel. The considered process parameters are cutting speed, feed rate and depth of cut while RBF as a kernel function. Three different SVM models were developed. Namely, LS-SVM, spider SVM and SVM-KM. Spider SVM gave the best prediction model for surface roughness.Wang et al [17] applied LS-SVM for prediction model of surface roughness for grinding machining operation. Linear, polynomial, Gauss RBF and sigmoid function are considered as the kernel function. Result shows that LS-SVM was outperformed the RBF-NN in terms of minimum surface roughness value.

Dong et al [18] introduced a novel model based on LS-SVM for prediction of surface roughness machining operation. 54 groups of data about surface roughness and four kinds of parameters were selected to analyze the prediction model. The prediction of surface roughness in milling operation is done by changing different parameters such as spindle speed, desired rate, cutting depth and milling blade number. Hence, the results are recorded to analyze the relation between machining parameters and surface roughness of work piece. In the training process, RBF was selected as a kernel function. From the experiment, the proposed prediction model is validated in theory and experimental, and it has shown that the model can describe the influence of spindle speed, desired rate and cutting depth to the surface roughness of work piece by milling.

Table 2.2 (C): Papers referred on SVM techniques.

SL. NO	Authors & Year	Machining Type/ Material/Tool	Operation Parameters (Input)	Output Parameters	Purpose of SVM	Conclusion
1	Jingchao, Anhai Li, Rufeng Zhang **August 2020**	Milling Hardened Steel (HRC52)	Spindle Speed, Feed Rate , Sampling Data 50KHz	Cutting Force, Tool Wear	Multifractal detrended fluctuation analysis (MFDFA) –SVM Tool Condition Monitoring	MFDFA – SVM identify various tool condition stages accurately up to 95.6%
2	Qinghua Gu, Yinxin Chang, Xinhong Li, Zhaozhao Chang **July 2020**	End Milling	Spindle Speed, Feed Rate , DOC	Tool Wear Surface Roughness	Radius margin Based SVM-Fruit Fly Optimization (FOA-F-SVM)	FOA-F-SVM reduce the computational cost & achieve greater classification accuracy
3	Erhua Wang, Peng Yan, Jie Liu **June 2020**	End Milling Steel 300M	Spindle Speed, Axial DOC, Radial DOC, Feed Rate	Surface Roughness	Hybrid Chatter Detection Method (HCDM) SVM- PSO – Feature Selection	Model Recognize stable, transition and Chatter States accurately.
4	Dong-Dong, Wei-Min Zhang, Yuan-Shi Li, Feng Xue, Jurgen Fleischer **April 2020**	Milling Process	Spindle Speed, Feed Rate , DOC, Sampling Data	Cutting Force, Tool Wear	Chatter Detection in 2 cases Time domain and frequency domain. Multi –SVM can be used to conclude optimized parameters	Multi - SVM model 96.6% Accuracy achieved.

5	Meng Hu Weiwei Ming **Oct 2019**	Milling Ti-6Al-4V	Spindle Speed, Time and Frequency Domain Signals	Tool Wear	V-SVM applied for training & Prediction tool monitoring V-SVM for classification of cutting edge(Intact, Chipped, Broken)	V_SVM achieved prediction accuracy of 98.9% in tool wear monitoring
6	Ali Yeganefar, Seyed Ali Niknam, Reza Asadi **April 2019**	Slot Milling AA 7075-T6	Cutting Speed, Feed Per Tooth, DOC	Surface Roughness, Cutting Force	SVM,ANN, Regression methods utilized to predict & Optimize Surface Roughness & Cutting Force	ANN-NSGA outperformed compared to SVR & regression approaches in prediction. Pareto-Optimal & Desirability function utilized in decision making
7	Yun Chen, Huaizhong Li, Xiubing Jing, Liang Hou, Xiangjian Bu **Jan 2019**	Micro Milling Steel 104	Spindle Speed, Axial Doc, Feed Rate	Surface Roughness	Intelligent Chatter Detection based on Image feature STFT & SVM	STFT model performed Better compared to time domain and CWT image features classification
8	Shixu Sun, Xiaofeng Hu, Weili Cai, Jin Zhong **Jan 2019**	Milling	Spindle Speed, DOC, Feed Rate	Tool Wear , Surface Roughness	Tool Breakage Detection (Milling Cutter Inserts) through Acoustic Emission technique	SVM Model was proposed for insert breakage detection for offline and online phase.
9	Muzaffer Ay, Sebastian Stemmler, Dirk Abel, Max Schwenzer, Fritz Klocke **June 2018**	Milling	Feed Rate	Input & Output signals	SVM was used for Nonlinear dynamic behaviour online identification. Blackbox & Greybox model describe dynamic	SVM, LS-SVM generate blackbox & Greybox model Blackbox model – 0.0196 & Greybox model 0.0252 relative error. Blackbox model required more time to adapt to the varying training data.

					behaviour with low relative error.	
10	Dongdong Kong, Yongjie Chen, Ning Li Shenglin Tan **Jan 2016**	Ball End milling	Spindle Speed, Feed Rate, DOC	Cutting Force Flank Wear	V-SVR for predicting tool wear. Sensitive Signals(tool wear) are selected using principal component analysis (KPCA)	KPCA-VSVR effective in predicting tool wear in small samples
11	Garcia-Nieto, Garcia Gonzalo, Vilan Vilan, Segade Robleda **Dec 2015**	Milling Cast Iron	Spindle Speed, Feed Rate, DOC	Flank Wear	SVM tool wear prediction	SVM-PSO predicts flank wear, Improves generalization capability.
12	Chen Zhang, Haiyan Zhang **Jan 2015**	Ball End Milling	Spindle Speed, DOC, Feed Rate	Tool Wear	LS_SVM Modelling & Prediction of Tool wear	LS-SVM is more accurate in prediction compared to ANN
13	Guofeng Wang, Yinwei Yang, Qinglu Xie, Yanchao Zhang **Mar 2014**	Milling	Spindle Speed, DOC, Feed Rate	Tool Wear	SVM,RVM classifiers used to recognize multi stages of tool wear status during milling process	SVM, Relevance Vector Machine (RVM) comparison study depicted RVM is effective, RVM has strong generalization capability and RVM yields fewer relevance vectors.
14	Bulent Kaya, Cuneyt Oysu, Huseyin M Ertunc,Hasan Ocak **Nov 2012**	Milling Inconel 718	Spindle Speed, DOC, Feed Rate	Tool Wear	SVM-GA Classification (decision) stages prediction such as workable, sharp, close to dull, dull states	Classification rates for the tool condition monitoring system before and after inclusion of the genetic algorithm step were determined as 89% and 100% respectively.
15	Kadirgama, Noor, Rahman **June 2012**	End Milling AA6061-T6	Cutting Speed, Feed Rate,	Surface Roughness	Potential Support Vector Machine (PSVM)	Perform effective with error (2%-9%) predicting surface roughness

					Optimization of surface roughness	
16	Huang, Xinghui Li, Gan **Jan 2010**	Ball Nose End milling	Spindle Speed, DOC, Feed Rate	Cutting Force, Flank Wear, Surface Roughness	SVM developed for tool wear classification and to provide decision by constructing the hyper plane.	SVM (classification Problem) formulated Regression Problem to estimate Tool Wear
17	B. Lela, Bajic, Jozic **March 2009**	Milling Steel St 52-3	Spindle Speed, DOC, Feed Rate	Surface Roughness	RA,BNN & SVM depict the prediction relative error <8%	BNN is best suitable for predicting Surface roughness 6.1% error.
18	Yao-Wen Hsueh, Chan- Yun Yang **Jan 2008**	Face Milling Cast Iron	Spindle Speed, DOC, Feed Rate	Cutting Force, Tool Wear	SVM to classify cutting force signal feature.	Prediction of Tool breakage (TO find milling cutter with or without tool breakage)
19	Yao-Wen Hsueh, Chan- Yun Yang **Jan 2008**	Aluminium 7075	Spindle Speed, DOC, Feed Rate	Cutting Force, Tool Wear	SVM to classify spindle displacement feature.	on-line intelligent sensor tool breakage system proposed
20	Dongfeng Shi , Nabil N. Gindy **Jan 2007**	High Speed steel6667 HRC		Tool Wear	LS-SVM & Principal Component Analysis (PCA)	An online tool wear monitoring system has been developed based on platform of PXI and LabVIEW. Good Agreement between LS-SVM and actual tool wear measured by optical scan microscope.
21	Sohyung Cho, Shihab Asfour , Arzu Onar, Nandita Kaundinya **June 2005**	Milling	Spindle Speed, DOC, Feed Rate,	Cutting Force Tool Wear	Tool Breakage Detection. SVM to identify process abnormalities. SVM to initiate corrective actions in milling process	SVM model will reduce machine down time, production cost SVM is effective compared to Multiple Variable Regression Model (MVR).

2.9.1 SVM Application for Modern Machining Operations

Modern machining used chemical, thermal or electrical process to remove material in machining process. Zhang et al [19] applied SVM with multi-objective to develop a hybrid model for processing parameters optimization in micro-EDM. Researchers assigned discharge peak current, pulse duration, pulse-off time, capacitance, electrode rotating speed and servo reference speed as process parameters. All these parameters influence processing time (PT) and electrode wear (EW) in quite different ways. PT and EW are important input objectives. Since these parameters influence the output objectives in quite an opposite way, it is not easy to find an optimized combination of these processing parameters which make both PT and EW minimum. Thus, researchers adopted SVM to establish a micro-EDM process model based on the orthogonal test. Orthogonal test is designed to provide input and output data for training and testing SVM model. Gaussian function is used as a kernel function for this model. Zhang and Sui [20] proposed a condition monitoring method for rolling element bearings based on auto-regressive (AR) model and SVM in EDM machining.

The SVM model improved the traditional classification of the defect effectively such as local minimization problem, the choice of NN structure and overfitting problems. SVM obtained such a good results in the bearing condition monitoring of mechanical components. Process parameter that used in this model includes motor loads, frequency, outer diameter, inner diameter, thickness and pitch diameter. SVM model was compared with NN and RBF-NN and the correct classification rates are 91 % and 93% respectively. While the correct classification rate of the proposed method is 95%. Sugumaran et al [21] developed fault diagnostics of roller bearing using neighbourhood score multiclass SVM in EDM machining. Roller bearing is one of the most widely used rotary elements in a rotary machine. RBF is used as a kernel function. This research used kernel based neighbourhood score multiclass SVM for classification and decision tree for addressing the future selection process. The study on using a multi-class SVM showed the effectiveness in diagnosing the fault conditions of the bearing. A review of application of SVM in machining modelling has been presented.

From the review, we found that SVM was widely used for modelling of machining performances such as surface roughness, tool wear, tool breakage and fault diagnosis for both conventional and modern machining. SVM also is a multi-objective modelling tool that can meet the requirements of the machining operation for finding sets of solutions based on combination with suitable variable.

Table 2.3: Comparison of traditional and machine learning algorithms in machining.

Author and Year	Research Objective	Classification Algorithm	Kernels	Techniques	Results
Sohyung Cho, Shihab Asfour Arzu Onar Nandita Kaundinya (2004)	An intelligent tool breakage detection system to provide the ability to recognize process abnormalities and initiate corrective action during a manufacturing process, specifically in a milling process.	Kernel Based Learning	Linear Polynomial	SVR - MVR (Mulitple Variable Regression)	Proposed model (SVR) performs well with a tight threshold value for tool breakage determination.

Dongfeng Shi, Nabil N. Gindy (2007)	Predictive model by combination of least squares support vector machines (LS-SVM) and principal component analysis (PCA) technique.	Kernel, Statistical Based Learning	RBF	PCA, LS-SVM	Least Square Support Vector Machine (LS-SVM) based tool wear prediction model is constructed. A good agreement can be found between predicted tool wear constructed by LS-SVM and actual tool wear measured by optical scan microscope in broaching process.
Yao-Wen Hsueh, Chan-Yun Yang (2008)	A support vector machine (SVM) to classify the feature of the cutting force signal for the prediction of tool breakage in face milling.	Kernel Based Learning	Linear	SVM	A support vector machine (SVM) to monitor the patterns of the milling cutting force with and without tool breakage has been established. A real-time tool breakage diagnosis can be successfully implemented with the on-line intelligent sensor system.
Yao-Wen Hsueh, Chan-Yun Yang (2008)	Introduces a new diagnosis technique for tool breakage in face milling using a support vector machine (SVM).	Kernel Based Learning	Linear	SVM	Spindle displacement signals were processed by a support vector machine (SVM) to monitor tool breakage in face-milling operations.
Lela, Bajic, Jozic (2009)	To examines the influence of cutting speed, feed, and depth of cut on surface roughness in face milling process.	Kernel Based learning	RBF	BNN- SVR	The study shows that when the training dataset is relatively small (as in the study), both BNN and SVR modeling methodologies are comparable with RA methodology.
K. Kadirgama,· M. M. Noor,· M. M. Rahman (2012)	Optimization of the surface roughness when milling aluminium alloys (AA6061-T6) with carbide coated inserts.	Kernel, Statistical Based Learning	Linear	Response Surface Method (RSM), Support Vector Machine (PSVM)	PSVM has been found to be the most successful technique to predict the surface roughness with respect to various combinations of four cutting parameters (cutting speed, federate, axial depth and radial depth). (Error 2-9%)

Guofeng Wang, Yinwei Yang, Qinglu Xie, Yanchao Zhang (2014)	A tool wear monitoring system based on relevance vector machine (RVM) classifier is constructed to realize multi categories classification of tool wear status during milling process.	Kernel Based Learning	Gaussian	SVM-RVM	The comparison of SVM with RVM shows that the RVM can get more accurate results under different number of small training samples. Moreover, the speed of classification is faster than SVM. This method casts some new lights on the industrial environment of the tool condition monitoring.
Bulent Kaya, Cuneyt Oysu, Huseyin Ertunc and Hasan Ocak (2014)	Cutting forces, torque, three axis accelerometer and acoustic emission signals were analyzed and used for the development of an online tool condition monitoring system	Kernel, Statistical Based Learning	Tree Kernel	Binary Decision Tree SVM-GA	Various time domain and statistical features extracted from these signals were used to train support vector machine models in a binary decision tree, which was used to predict the condition of the cutting tool. The genetic algorithm was employed for reducing the dimensionality of the feature set by selecting the features that correlates best with the tool condition. The classification rates for the tool condition monitoring system before and after inclusion of the genetic algorithm step were determined as 89% and 100%, respectively.

Gangadhar, Hemantha kumar, Narendranath, Sugumaran (2014)	To study the tool wear state in early stage with help of monitoring system.	Statistical Based learning	J48 Algorithm	Decision Tree	J48 Algorithm was used to understand and accuracy as of 89.3%.
Garcia Nieto, Garcia Gonzalo, Vilan, Segade Robleda (2015)	To build a new practical hybrid regression model to predict the milling tool wear in a regular cut as well as entry cut and exit cut of a milling tool.	Kernel Based learning	RBF	PSO - SVM	Milling tool flank wear can be accurately modeled using a hybrid PSO–SVM-based model

Table 2.4: Comparison of traditional and machine learning algorithms.

Author and Year	Research Objective	Classification Algorithm	Kernels	Techniques	Results
Himaanshu, Amit K Agrawal, Tarun Pruthi, Chandra Shekhar, Rama Chellappa. (2002)	Comparative study of linear and kernel based methods for face recognition	Kernel, Instance based learning	Linear, Polynomial, Gaussian, RBF	SVM,PCA, Kernel PCA, LDA, KDA, Nearest Neighbor(NN)	SVM gives better performance than Nearest Neighbor
Dell Zhang, Wee Sun Lee (2003)	Automatic question classification through machine learning approaches	Kernel, Logic, Instance and Statistical based learning	Tree kernel	SVM, NN, Naive Bayes, Decision Tree, Sparse Network of Winnows	SVM works better while compared to other machine learning methods
Jin-Hyuk Hong, Jun-Ki Min, UngKeun Cho, SungBae Cho. (2007)	Effectively apply SVMs to multi-class fingerprint Classification systems	Kernel and Statistical based learning	Linear, Polynomial Gaussian Sigmoid	Multiclass SVM, Naive Bayes	Integrated Naive Bayes(NB) and SVM give good accuracy than SVMs, NB
H.Z.M Shafri, Ramle. (2009)	New approach to classify SPOT 5 satellite image	Kernel and Logic based learning	Linear, Polynomial RBF, Sigmoid	SVM, Decision trees	SVM with RBF gives the highest accuracy than Decision tree

Hongjun Jia, AleixM.Martinez. (2009)	Defines a criteria which minimizes the probability of overlap in Hyperplane	Kernel based learning	Linear	Partial SVM, simple nearest neighbor	Partial SVM obtains higher recognition rate than other algorithms
Qisong Chen, Xiaowei Chen, Yun Wu (2010)	KPCA to SVM for feature extraction	Kernel and Perceptron based learning	RBF	PSO-SVM, KPCA-SVM, Least Square SVM, Neural Network	LS-SVM with KPCA and PSO is proposed for the power load forecasting
Kunlun Li, Xuerong Luo, Ming Jin. (2010)	Novel SVM KNN classification based on Semi-supervised learning is proposed	Kernel and Instance based learning	RBF kernel	SVM - KNearest neighbor	SVM-KNN classifier improves the accuracy of classifier model
Durgesh K. Srivastava, Lekha Bhambhu. (2010)	A novel SVM based learning method for classification	Kernel and Instance based learning	linear, RBF Polynomial, Sigmoid	Rule Based, Rule Based With Discretization, KNN, Local Transfer Function, SVM	SVM outperforms other methods but choice of kernel function is critical
Piotr Nazarko. (2011)	Pattern classification in the damage detection system	Kernel, Logic and Perceptron based learning	Linear, Polynomial RBF, MLP, Quadratic	Binary decision tree (BDT), Auto associative neural network ,SVM	SVM exhibit more efficiency in comparison to ANNs , novelty index
Shelly Gupta, Dharminder, Anand Sharma. (2011)	Performance analysis of Classification techniques using the healthcare datasets	Kernel, Logic, Instance, Perceptron and Statistical based learning	Predefined kernels in Machine learning Tools	SVM,NNRBFN	SVM shows the most promising results than the Other

S. Anto, Dr.S. Chandramathi. (2011)	Supervised classification approaches are reviewed with the medical field data	Kernel, Rule, Logic, Instance, Perceptron & Statistical based learning	Nonlinear kernel	SVM, Decision Trees, Naive , Bayes Neural Network (NN)	SVMs perform better with medical field in comparison with all other methods and next NN works better
Milan Kumari, Sunila Godara. (2011)	Develop a Model to take effective decision in medical domain	Kernel, Logic & perceptron based learning	Nonlinear kernel	RIPPER, Decision Tree, ANN (MLP), SVM	SVM turned out to be best classifier model for prediction

Table 2.5: Comparison of performance metrics of different learning algorithms - (**** stars represent the best and * star the worst performance).

Metrics	Decision Trees	Neural Networks	Naive Bayes	KNN	SVM	Rule Learners
Accuracy	**	***	*	**	****	**
Learning Speed	***	*	****	****	*	**
Classification Speed	****	****	****	*	****	****
Tolerance to missing	***	*	****	*	***	**
Tolerance to	***	*	**	**	****	**
Tolerance to	**	**	*	**	***	**
Highly	**	***	***	***	**	***
Dealing with	****	***	***	***	***	***
Tolerance to noise	**	**	***	*	***	*
Tolerance to	**	*	***	***	***	**
Incremental	**	***	****	****	**	*
Interpretation	****	*	****	**	****	****
Model Parameter	***	*	***	***	****	***

2.10 SURVEY ON PREDICTION - NEURAL NETWORKS V/S STATISTICAL TECHNIQUES

As a forecasting tool, ANN can be compared to Autoregressive moving Average (ARMA) class of models. ARMA methods, since ages have been used to model time series. In general, similarities do exist between the ANN and statistical techniques. An FFNN can be termed as a form of non-liner regression (Ripley 1996, Potzinger et al. 2000). A multiple linear regression scheme, a standard statistical tool, can be thought of as a simple ANN node. For example, for a linear equation of the type, $y = w_0 + w_1x_1 + w_2x_2 + \ldots\ldots\ldots + w_nx_n$, the x_i can be taken to represent the inputs to the node, wi can be taken as the corresponding weights and w0 can be the threshold function.

The ANNs have been rigorously compared with statistical methods for applications pertaining to classification and prediction (Ripley 1994). Effectiveness of ANN in time series forecasting have been examined. Lapedes and Farber (1988) have shown that in two time series prediction problems, neural networks are clearly superior to statistical methods.

Sharada and Patil (1994) analysed 75 different time series problems and inferred that the ANN and Box-Jekins forecasting system performed equally. Interestingly, it has been observed that the memory of a time series has some bearing on the performance. ANN performs slightly better than Box-Jekins model for time series with short memory while reverse is true for time series with long memory.

A lot of study has been done on artificial neural networks and the regression methods to determine the suitability of these models for pattern mappings (Kim et al. 1993, Patuwo et al. 1993, Subramanian et al. 1993, Yoon et al. 1993 and Potts 2000).

2.11 SURVEY ON OPTIMIZATION (CONVENTIONAL V/S NON-CONVENTIONAL TECHNIQUES)

Baskar et al. (2005) implemented various operations research techniques such as GA, Tabu search (TS) algorithm, ACO and PSO for optimizing machining parameters of multi-milling operation. The authors concluded that PSO algorithm always yields best result when compared to other algorithms and handbook recommendations. Wong et al.(2004) presented a hybrid of SA and GA optimization technique to select the optimal machining parameter for multi-pass milling operations. This approach used the strengths of SA and GA and overcame their weakness. It is evident from the results that this hybrid approach was more effective than conventional methods. Indrajit Mukherjee et al. (2006) appraised the application potential of several modelling such as statistical regression technique, ANN, Response Surface Methodology (RSM) etc., and optimization techniques such as SA, GA and TS algorithm in metal cutting processes. Ramon et al. (2006) used GA for optimizing cutting parameters and made a remark on the advantages of multi-objective optimization approach over single objective function. An application sample was developed and its results were analysed for different machining conditions. Tansel et al. (2006) proposed Genetically Optimized Neural Network System (GONNS) for the selection of optimal cutting condition in machining. Optimal operating conditions were calculated to obtain the best possible compromise between roughness of machined surface and the duration. Baskar et al. (2006) developed GA, Hill Climbing Algorithm (HCA) and Memetic Algorithm (MA) to find optimum cutting parameters for multi-tool milling operations like face milling, corner milling, pocket milling and slot milling. Significant improvement was observed in using these techniques when compared to handbook recommendations and method of feasible direction.

Franci Cus et al. (2003) proposed ANN to optimize cutting parameters for machining operation. The objective was to increase the productivity and reduce the production cost. Raid Al-Aomar et al. (2006) used GA to determine near optimal settings to both machining

and production process parameters so that the overall per order production cost is minimized. The experimental results and the sensitivity analysis showed the robustness of the proposed GA. Suresh et al. (2002) dealt with the study and development of surface roughness prediction model for machining mild steel using RSM. GA was used to give minimum and maximum values of surface roughness and their respective optimal machining conditions.

Zarei et al. (2009) presented a Harmony Search (HS) algorithm to determine optimum cutting parameter for multi-pass face milling. GA was used to solve the same problem. Comparison of results revealed that the HS algorithm could obtain optimum solution with higher accuracy when compared to GA. Venkata Rao et al. (2010) applied Artificial Bee Colony (ABC), PSO and SA algorithm for parameter optimization of a multi pass milling process. Minimization of production time was the objective considered subjected to various constraints. The accuracy and quick convergence to global optimum solution of ABC and PSO were very high as compared to SA algorithm.

Yusup et al. (2012a) have incorporated Genetic Algorithm (GA) to find the optimal cutting conditions for acquiring better surface finish in milling process and concluded that good surface finish can be obtained at high speed, high rake angle and low feed rate. Benardos et al. (2002) have included the ANN technique in the study to predict surface roughness value. The authors concluded that the mean error of 1.86% obtained by using ANN seemed to be consistent throughout the range of values. In their research, Ab. Rashid et al. (2009), presented the development of mathematical model for surface roughness prediction for the milling process in order to evaluate the fitness of machining parameters namely spindle speed, feed rate and depth of cut.

2.12 SUMMARY ON USAGE OF CRYOGENIC (LN$_2$)

The review of the literature suggests that cryogenic cooling provides several benefits in machining. Based on the existing literature studies, it has been concluded that cryogenic cooling is a different approach, in which the temperature at the cutting zone is reduced substantially to a very low range (Mirghani et al 2007). It was also concluded from recent works that, cryogenic cooling is a possible answer for high speed eco-friendly machining (Kumar and Choudhury 2008). Cryogenic cooling is an environment friendly clean technology for achieving the desirable control of cutting temperature and enhancement of tool life.

A recent work dealt with the experimental investigation of cryogenic cooling by liquid nitrogen in the machining of tool steels. The substantial benefits of cryogenic cooling on cutting temperature, cutting force, surface roughness, tool wear, chip shape and chip morphology were reported. However, more work is needed to explore the potential advantage of cryogenic cooling. In the existing cryogenic cooling methods, many researchers have attempted to supply the liquid nitrogen on the workpiece pre-cooling, tool back cooling, main and auxiliary cutting edges and tool rake and flank face. It has been seen that a lot of research has been done in the past, to improve the machinability of the difficult-to-cut materials, using the cryogenic cooling technique. Machining processes, like turning and grinding has been widely investigated under cryogenic machining conditions compared to that of milling. In the present study, the milling of the SS316, steel using cryogenic cooling LN$_2$ as coolant has been investigated, for different cutting speeds and feed rates to evaluate the machining performance.

2.13 SECTION SUMMARY ON SVM

From a review of the literature, it is established that a lot of research is still going on different classification algorithms to reduce the error rate and improve the accuracy. Here, the review relates to supervised machine learning methods like Artificial Neural Networks, Decision Trees, Rule Based and Support Vector Machines. The review of literature has driven the focus of the research work in the direction of Support Vector Machines which gives more regularization, generalization and approximation. As discussed in the previous section, selection of kernel function and its parameter in SVM is a critical issue that determines the performance of the classifier. In the forthcoming chapters, the adopted kernel based classifier is discussed in detail and an admissible kernel function for SVM is formulated.

2.14 RESEARCH GAP

A review of the literature suggests that the extremely low temperature of LN_2 cooling provides significant benefits in machining without polluting the environment. Most of the cryogenic cooling applications using LN_2 in machining studies have been examined in turning and grinding processes. There are only few research work carried out in milling operations under cryogenic cooling. In general, the cryogenic cooling approaches in metal cutting may be classified into four groups, according to the applications of the researchers: cryogenic pre-cooling the work piece by repulsing or an enclosed bath, cryogenic chip cooling, indirect cryogenic cooling or cryogenic tool back cooling or conductive remote cooling, and cryogenic jet cooling by the injection of cryogen to the cutting zone by general flooding, or to the cutting tool edges or faces, tool–chip and tool–work interfaces by micro – nozzles (Yildiz et al. 2008). The other few research gap are stated below:

- Work has been done on the concept of cryogenic cooling with liquid nitrogen in end milling process.

- The percentage of work carried on cryogenic concept in turning process is higher compared to milling process.

- From the literature it can be observed that fetching and validation of cutting force has been done using direct approach.

- It can be derived from the literature that more concentration is towards the microstructural study and mechanical properties.

- Very limited focus towards the incorporation of soft computing techniques in cryogenic machining methods.

- Limited work has been noticed on the concept of cryogenic cooling and supplying liquid nitrogen at the tool – work interfaces in the face milling process.

- Investigation on the effects of cryogenic cooling on the cutting temperature, cutting force, surface roughness and chip morphology in milling of SS 316 with PVD TiAlN coated carbide tool.

- Prediction using various back propagation algorithms(BPA), identifying best BPA to utilize it in machine learning prediction.

- Incorporating machine learning concept for prediction (using various kernel functions) and optimization (Hybrid technique – PSO-RBF-SVM) in milling process.

2.15 NEED FOR THE PRESENT STUDY

The challenge of modern machining industries is mainly focused on the achievement of high quality, in terms of work piece dimensional accuracy, surface finish, high production rate, less wear on the cutting tools, economy of machining in terms of cost saving, and increase of the performance of the product with reduced environmental impact. In all machining operations, tool wear is a natural phenomenon that eventually leads to tool failure.

The growing demands for higher productivity in machining need the use of high cutting velocity and feed rates, which will increase the cutting temperature and cause tool wear and tool fracture. Such a high cutting temperature, not only reduces tool life but also impairs the product quality, particularly, when the workpiece is quite strong, hard and heat resistant (Dhar et al 2002b). Conventional cooling methods are not only ineffective, but also spoil the working environment by producing harmful gases and smoke. Kitagawa et al (1997) reported that in the high speed machining of Inconel and titanium alloys, cutting fluids failed to reduce the cutting temperature and improve tool life effectively. High cutting temperature is one of the main reasons for rapid tool wear, and hence, the poor machinability of titanium alloys (Venugopal et al 2007).

Dhar and Kamruzzaman (2007) reported that the machining of steel inherently generates high cutting temperature, which not only reduces tool life but also impairs product quality. Chip breaking is the major criterion in advanced automated industries. Machining of ductile materials in the automated machines is more complicated, because of the formation of continuous chips. In order to minimize the negative effects of the conventional cutting fluids, a new alternative coolant such as the use of cryogenics as a coolant and lubricant is now gaining increasing acceptance in the metal cutting industries. Cryogenic cooling has been attempted in the machining of steels (Dhar et al 2002, 2002a, and 2002b, Uhera and Kumagai, 1969 and 1970) with substantial technological benefits. The favorable role of cryogenic cooling in chip breaking, cutting temperature, cutting force and tool wear in the turning of steels was reported (Dhar et al 2000, 2000a and 2000b).

In this research work, cryogenic cooling system was developed for reducing the cutting zone temperature in the milling process. In this system, the LN_2 is applied to cool the cutting zone, particularly tool-chip interface by using nozzle. LN_2 can easily penetrate into the tool-chip interface to reduce the cutting temperature.

2.16 SCOPE OF THE PRESENT STUDY

The following are the scope of the present work:

➢ Designing the experimental layout using L_{31} orthogonal array.

➢ Conducting experiments for measuring process output variables while milling of SS316 (TiAlN coated carbide tool) using cryogenic technique.

➢ Evaluating the influence of process parameters (spindle speed, feed rate, depth of cut, coolant type) on process output variables (cutting temperature, cutting force, surface roughness and tool wear) during milling by integrating design of experiment (DOE), response surface methodology (RSM) and analysis of variance (ANOVA) techniques.

➢ Generation of RSM and artificial neural network (ANN) model for correlating the predicted results of milling process output variables with experimental results of milling process output variables.

➢ Generation of desirability factor approach (DFA) and particle swarm optimization (PSO) model for optimizing the results of milling process output variables.

➢ Generation and Integration of machine learning technique – support vector machine (SVM) model for prediction and optimizing the results of milling process output variables.

2.17 OBJECTIVES OF THE PRESENT WORK

The present work investigates the influence of cryogenic cooling by liquid nitrogen in the machining of SS316 steel by carbide cutting tools under different cutting conditions, and compares the effectiveness of cryogenic cooling with that of dry and wet machining. The following objectives have been identified, as part of this study:

1. To study the effect of cryogenic milling process parameters on cutting temperature, cutting forces, surface roughness, tool wear, chip morphology and to compare the results with dry and wet machining.

2. Evaluation of the effects of process parameters on process output variables, while milling of SS316 coated TiAlN tool, through the integration of Analysis of Variance (ANOVA) and Response Surface Methodology (RSM).

3. To predict and optimize the process parameters for achieving better milling performance characteristics using the statistical and soft computing techniques.

4. Development of a suitable hybrid intelligent method for the prediction and optimization of milling (SS316) parameters.

CHAPTER 3

EXPERIMENTAL CONDITIONS AND PROCEDURE

This study was undertaken to perform milling operations on AISI 316 (SS316) using carbide cutting tool inserts under various spindle speed-feed rate-depth of cut combinations. The cutting environments evaluated in the milling process were: Dry machining, Conventional cooling (Wet) and Cryogenic cooling (LN2). A cryogenic cooling setup was developed and utilized for supplying liquid nitrogen at the cutting zone. In the present work, the cutting temperature, cutting force, surface roughness, tool wear, chip shape and chip morphology are considered, for studying the effect of cryogenic cooling. The influence of cryogenic cooling using liquid nitrogen was compared to that of dry and wet machining. This chapter explains experimental procedure, workpiece materials, cutting tool materials and the equipment being used.

3.1 WORK MATERIAL - AISI 316 STAINLESS STEEL (SS316)

Stainless steel is most notable for their corrosion resistance which increases with chromium content. Materials having a hardness of over 45 HRC (Rockwell hardness C scale), can be classified as difficult-to-machine materials (Becze and Elbestawi 2002, Poulachon and Moisan, 2000). In this research work CNC Spark DTC-12 was utilized to carry out cryogenic milling experiments on SS316 stainless steel (100mm x 40mm x 30). Table 3.1 illustrate the experimental conditions, respectively, utilized in the current work. The chemical composition of the material is represented in Table 3.2. Figure 3.1 depicts the microstructure along with the EDS spectra of the work material.

Table 3.1: Experimental design matrices of RSM model.

Runs	Spindle Speed (rpm)	Feed rate (mm/min)	Depth of cut (mm)	Coolant type
1	-1	-1	-1	-1
2	1	-1	-1	-1
3	-1	1	-1	-1
4	1	1	-1	-1
5	-1	-1	1	-1
6	1	-1	1	-1
7	-1	1	1	-1
8	1	1	1	-1
9	-1	-1	-1	1
10	1	-1	-1	1
11	-1	1	-1	1
12	1	1	-1	1
13	-1	-1	1	1
14	1	-1	1	1
15	-1	1	1	1
16	1	1	1	1
17	-1	0	0	0
18	1	0	0	0
19	0	-1	0	0
20	0	1	0	0
21	0	0	-1	0
22	0	0	1	0
23	0	0	0	-1
24	0	0	0	1
25	0	0	0	0
26	0	0	0	0
27	0	0	0	0
28	0	0	0	0
29	0	0	0	0
30	0	0	0	0
31	0	0	0	0

Table 3.2: Composition ranges for 316 grade of stainless steel.

Grade	C	Mn	Si	P	S	Cr	Mo	Ni	N
316	0.08	2.0	0.75	0.045	0.03	18.0	3.00	14.0	0.1
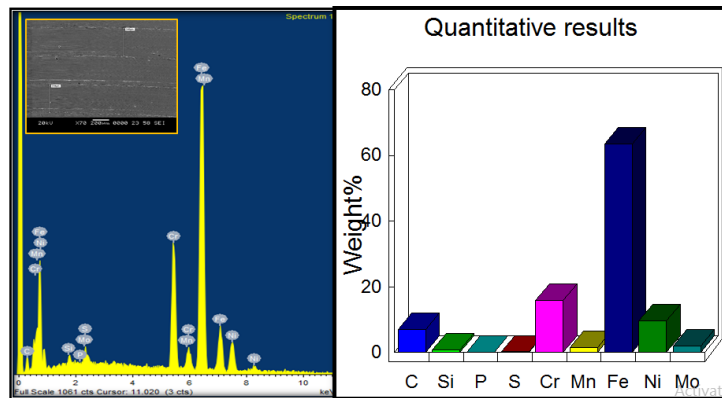
Figure 3.1: SEM image of EDS spectra of SS316

3.1.1 Methodology

In this research work, the milling experiments were carried out on the SS316 under dry, wet and LN_2 machining environments. The methodology used in the milling of the SS316 is shown in Figure 3.2(a) and the photographic view of the present investigation is depicted in Figure 3.2(b).
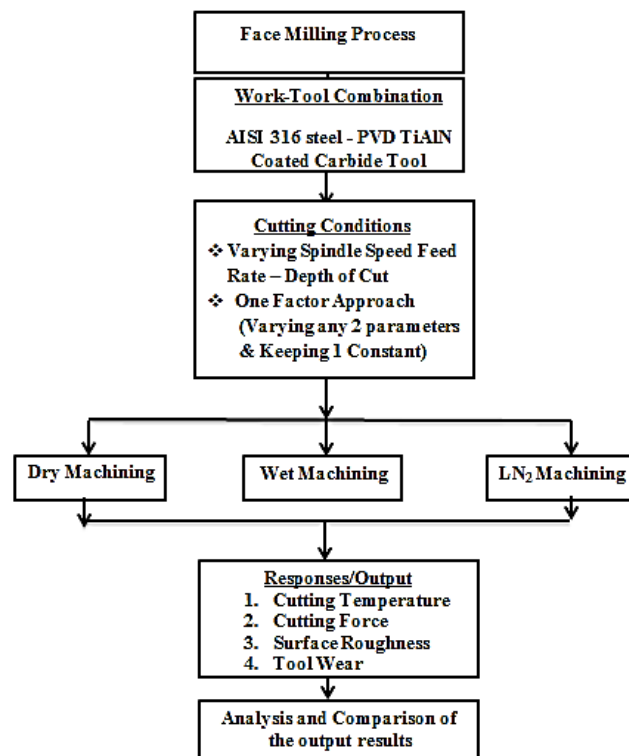
Figure 3.2(a): Methodology for the milling of the SS316 steel
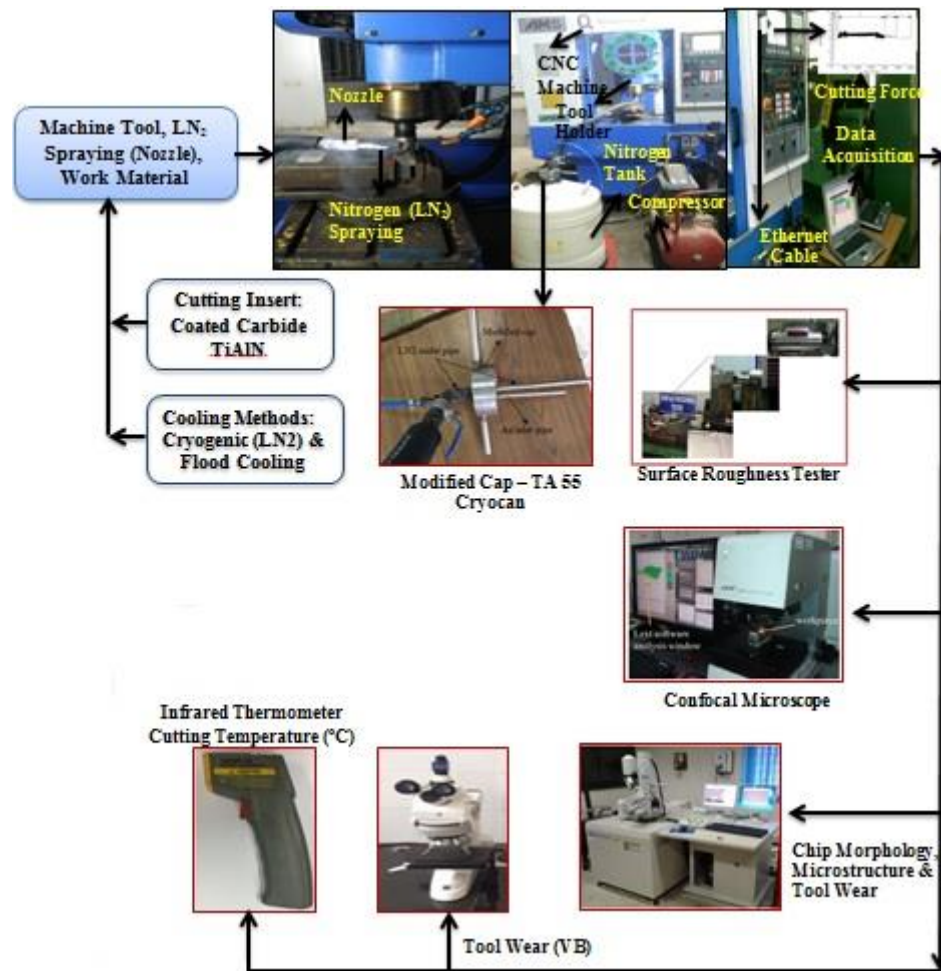
Figure 3.2(b): Photographic view of the present investigation

3.2 EXPERIMENTAL SETUP AND PROCEDURE

The work part SS316 was primarily milled on CNC machine using coated carbide tool in three distinct machining environment (dry, flood and LN_2). The machining experiments have been carried out on a CNC Milling Machine (Spark DTC 250) as shown in Figure 3.3. It is having drum type tool changer. The maximum number of tools that can be accommodated in this machine is 12. Proximate sensors are provided to sense the tool position. The movement of the axis are achieved by the servo motor. The effects of spindle speed and cooling approach were studied and compared with dry machining. The experiments were carried out at three spindle speeds i.e. 1000, 2000 and 3000rpm, feed rate of 350, 450, 550 mm/min and depth of cut of 0.5,1,1.5mm. A total flow of the current work is depicted in Figure 3.4. The cutting force were calculated via indirect approach via fetching data through Ethernet cable (Provided by

– FANUC) (data acquisition). In indirect fetching method of cutting force, first fetch the esteems in terms of current values and later using the referral current graphs and substituting the values in the formulas we obtain the cutting force values. The machining temperature at tool-chip interface was measured using the infrared thermometer. A roughness tester (surtronic) was used to measure the surface of the work part. The surface value was recorded at four different positions and the average esteem was taken. Wear on the flank and rake faces of the inserts were measured with help of an optical microscope and further analysed using SEM for each trial. Tool wear was recorded at three different locations and the average value was considered for the study. SEM and energy dispersive spectroscopy (EDS) was used to investigate the microstructure and chip morphology.

Figure 3.3(a): Experimental setup CNC vertical milling machine (Spark DTC 250)

3.2.1 Flow of Work
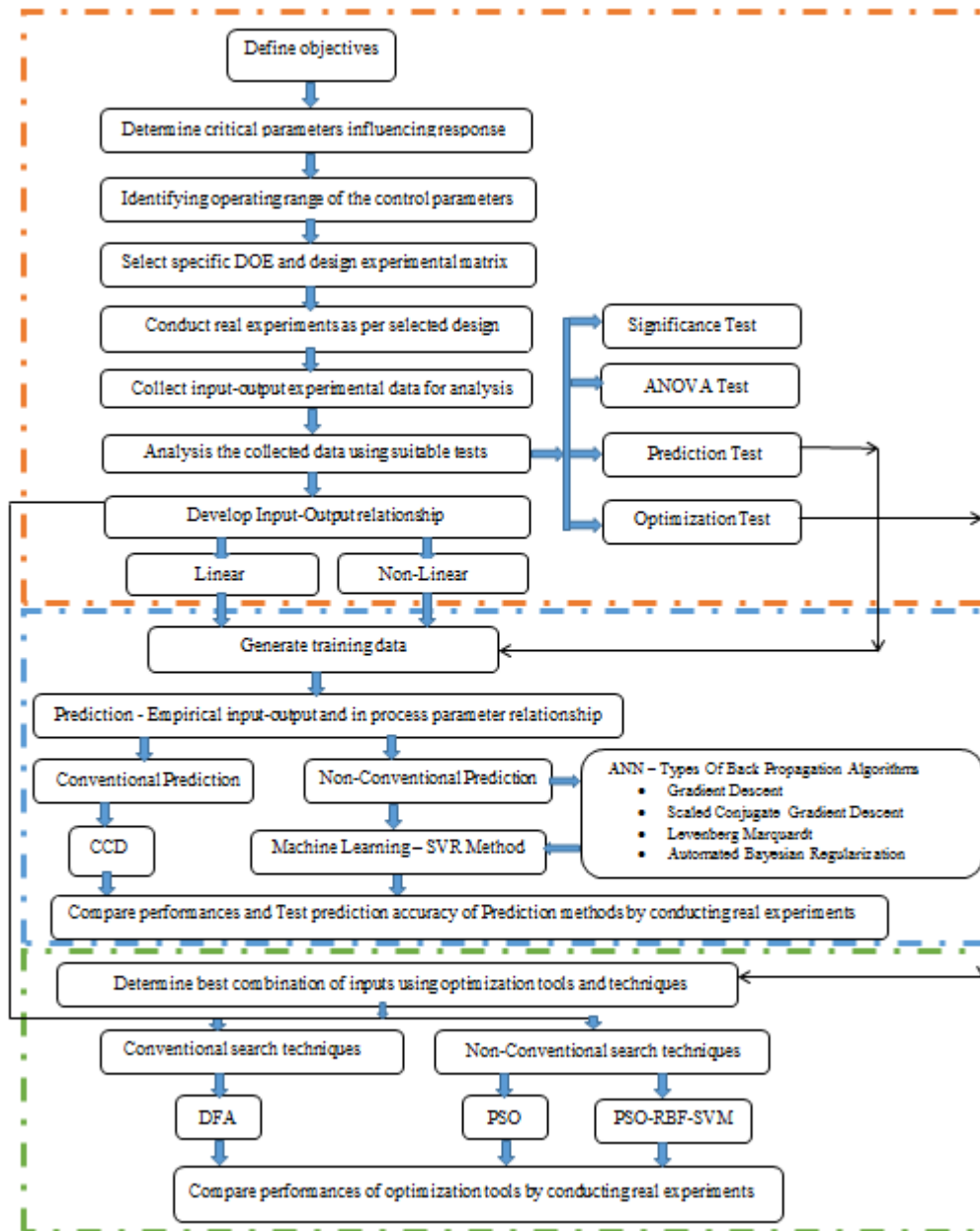
Figure 3.4: Approach pragmatic for modelling and optimization

3.3 PARAMETERS AND THEIR LEVELS

The process parameters and their levels for milling operation considered in the study are shown in Table.3.3 for L31 Design of Experiment (DOE) (orthogonal array experiments). The parameter ranges were set based on the trial experiments and cutting tool specifications.

As the degrees of freedom should be always less than number of experiments to be conducted as per the orthogonal array rule (Design of Experiment). In the current work there are 4 inputs with 3 Levels and the lack of fit observed in L9 and L27. So the L31 was opted for the current study with number of center point minimum replication 7, corner point 16 and axial (star) point 8.

Table 3.3: The machining parameters and their levels.

Machining Parameters	Units	Notation	Operating Levels		
		Coded	Low(-1)	Middle(0)	High(+1)
Spindle Speed	(rpm)	S	1000	2000	3000
Feed Rate	(mm/min)	F	350	450	550
Depth of Cut	(mm)	D	0.5	1	1.5
Coolant type		CT	-1(Dry)	0(Wet)	1(LN$_2$)

3.4 RESPONSE SURFACE METHODOLOGY

Response surface methodology (RSM) is a collection of both statistical and mathematical techniques utilized for modeling, analysis and design of experiments, in which a response of interest is influenced by several variables and the objective, is to optimize this response. This technique is helpful for modeling and analysis of parameters, in which response of interest is affected by several variables and the purpose is to optimize this response. In this study, RSM based central composite rotatable design experiments of all possible combination of levels of the spindle speed, feed rate and depth of cut were investigated. It is a dynamic and foremost important tool of design of experiment, wherein the relationship between responses of a process with its input decision variables is mapped to achieve the objective of maximization or minimization of the response properties (Raymond & Douglas 2002).

The multiplicative model for the predicted surface roughness (response surface) in end milling in terms of the independent variable investigated can be expressed as,

$$R_a = C_o \, V_o^k \, f_z^1 \, a^m \tag{3.1}$$

Where Ra is the predicted surface roughness (µm), V_o is the cutting speed (m/min), f_z is the feed per tooth (mm/tooth), and a is the axial depth of cut (mm). C_o, k, l, and m are model parameters to be estimated from experimental results. To determine the constants and exponents, this mathematical model can be linearized by employing a logarithmic transformation and equation (3.1) can be re-expressed as,

$$\ln R_a = \ln C + k \ln V + l \ln f_z + m \ln a \tag{3.2}$$

The linear model of equation (3.2) is,

$$y = \beta_0 x_0 + \beta_1 x_1 + \beta_2 x_2 + \beta_3 x_3 \tag{3.3}$$

Where y is the true response of surface roughness on a logarithmic scale $x_0 = 1$ (dummy variable), x_1, x_2, x_3 are logarithmic transformations of speed, feed, and depth of cut, respectively, while β_0, β_1, β_2, and β_3 are the parameters to be estimated. Equation (3.3) can be expressed as,

$$\widehat{y_1} = y - \varepsilon = b_0 x_0 + b_1 x_1 + b_2 x_2 + b_3 x_3 \tag{3.4}$$

Where $\widehat{y_1}$ is the estimated response and y the measured surface roughness on a logarithmic scale, ε the experimental error and the b values are estimates of the β parameters.

The second-order model can be extended from the first-order model's equation as: $\widehat{y_2} = y - \varepsilon = b_0 x_0 + b_1 x_1 + b_2 x_2 + b_3 x_3 + b_{11} x^2{}_1 + b_{22} x^2{}_2 + b_{33} x^2{}_3 + b_{12} x_1 x_2 + b_{23} x_2 x_3 + b_{13} x_1 x_3 \tag{3.5}$

Where $\widehat{y_2}$ is the estimated response based on the second order model.

It is also called multiple regressions. In this, three-way interaction is carried out.

3.5 MEASUREMENT OF PERFORMANCE CHARACTERSTICS

In the present study, the considered responses are cutting temperature, cutting force, surface roughness and tool wear. So, the upcoming section deals with the measurement of the response characteristics through various devices.

3.5.1 Cutting Force: Indirect Method of Measuring the Cutting Forces

Measuring the cutting forces during machining is a very complicated task. The direct method of measuring the cutting force is having a lot of disadvantages like cost, mounting of sensors, constrains of cutting parameters and machine, and cutting condition. Therefore indirect method of measuring cutting forces is used. There are several techniques used to measure the cutting forces in indirect method. One technique is to tap the current signals of the feed servo motor from the MCU as shown in Figure 3.5. The current drawn by each axis is measured with and without cutting. The current drawn by the servomotor is nothing but the force required to move the table from the initial stage to the cutting stage. The current drawn during without cutting includes contributing factors like the friction force, preload torque, weight of the table and component, motor inertia, disturbance in the electrical and mechanical system. The current drawn during cutting includes these effects and cutting force required to remove the material during cutting. The difference between instantaneous cutting force with cutting and without cutting. That is without cutting refers to the tool was in the air and the program was executed (the current drawn by each axis measured), whereas with cutting refers to the method where the tool is engaged with the material by a specified depth of cut (current drawn by the servo motor is measured). The torque can be calculated by multiplying the current with torque constant.

Torque of the motor T_m, = current drawn by the motor * RMS Torque constant.   (3.6)

Each motor has its own torque constant which is specified in the motor specification table. We have
$$T_{m=\frac{FL\pi\eta}{1000}}$$
(3.7)

Where F= cutting force in N, L = lead in mm, η = efficiency of power transmission.
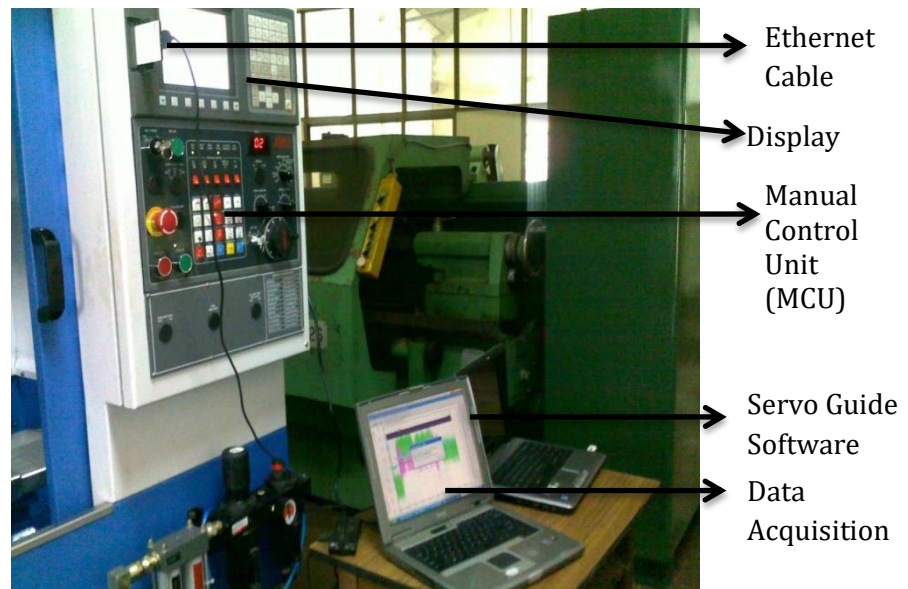
Figure 3.5: Data acquiring from SERVOGUIDE software

3.5.2 Surface Roughness Measurement

The surface roughness was measured by using 'MITUTOYO SURFTEST SJ-301 surface roughness tester as shown in Figure 3.6 (a) and Figure 3.6 (b) shows the pictorial view of surface roughness tester measuring surface roughness on the workpiece SS316. The roughness tester uses a differential inductance method as direct technique. The tester consists of a hard needle shape stylus made of diamond. The stylus includes a tip radius of 2 µm and applies a force of 0.75 mN with a stylus speed of 0.25 mm/s to measure the surface roughness. Basically, the surface roughness (Ra) was measured at three different locations. Further on, the average was calculated and the average was considered as the response. While carrying out the measurement, the cut off length and evaluation length was fixed as 0.8 mm and 4mm, respectively. The Ra and Rz values of SS316 machined surface were directly fetched using roughness tester.
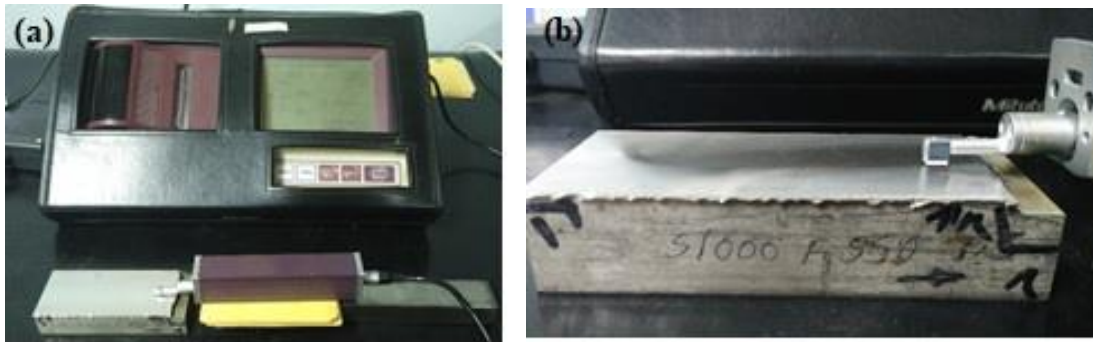
Figure 3.6: (a) Surface roughness tester MITUTOYO SURFTEST SJ-301 (b) Surface roughness tester measuring surface roughness on the workpiece SS316

3.5.3 Surface Topography

The topography of the SS316 machined surface was examined using a 3D laser microscope by using Olympus LEST OLS4000 laser confocal microscope available at CMTI, Bangalore as shown in Figure 3.7. The microscope uses a laser scanning to measure the surface profile of the machined components. The microscope can measure surface texture more accurately due to low laser spot diameter of 0.4 µm
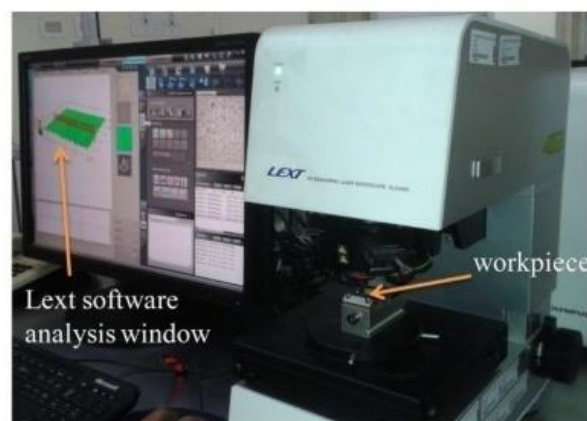
Figure 3.7: Laser optical confocal microscope

3.5.4 Scanning Electron Microscope

Scanning electron microscope with Energy dispersive X—ray spectroscopy (EDS) from JEOL as shown in Figure 3.8 was used to study the tool wear, chip morphology and surface morphology SEM was utilized. The scanning electron microscopy instrument had a resolution of at 30 KV. The specimens were loaded properly in the sequence. SEM images at different magnifications were taken.   Along with

microstructures EDS analysis was carried out for the specimen to know the elemental composition present in the alloy. Figure 3.9 depicts the Rapid-I Machine Vision System Images Depicting progression of crater wear.

Figure 3.8: Scanning electron microscopy

Figure 3.9: Rapid- I machine vision system images depicting progression of crater wear

3.5.5 X-ray diffraction (XRD) analysis

The X-ray diffraction analysis were carried out using BRUKER D8 ADVANCE machine it is used to measure the phases present in the hot machined specimens with different temperatures as shown in Figure 3.10. In XRD software, the inputs are as

follows: starting angle of scan of 20º, end angle scan of 100º, step size of 0.1 seconds and targeted CuKα. After fetching the XRD patterns, the patterns were analyzed using the software PCPDFWIN to determine the phases present in the machined specimen.

Figure 3.10: X-Ray diffraction

3.6 OPTIMIZATION OF PARAMETERS

3.6.1 Parametric Optimization Using Desirability Function

Desirability Function approach is a multiple-response optimization method. This approach was first introduced in 1980 by Suich and Deringer. The method finds operating conditions "targeted" which are the most desirable response value. The general approach is first converting each response x1 into an individual desirability function d_i that varies over the range $0 \leq d_i \leq 1$ (Deringer and Suich 1980, Baji et al.2010). The desirability functions are categorized into three sectors based on the response characteristics.

1. If the target for the response is a maximum value / "Higher is better".

$$
\begin{array}{l}
r_i \le r_{i*} \\
r_{i*} < r_i < r_i{}' \\
r_i \ge r_i{}'
\end{array}
\qquad
\left\{
\begin{array}{c}
0 \\
\left[\dfrac{r_i - r_{i*}}{r_i{}' - r_{i*}}\right]^a \\
1
\end{array}
\right.
$$

2. If the target for the response is a minimum value / "Lower is better".

$$
\begin{array}{l}
r_i \le r_i{}'' \\
r_i{}'' < r_i < r_i{}^* \\
r_i \ge r_i{}^*
\end{array}
\qquad
\left\{
\begin{array}{c}
1 \\
\left[\dfrac{r_{i*} - r_i}{r_{i*} - r_i{}''}\right]^b \\
0
\end{array}
\right.
$$

3. If the target for the response is between lower and higher value / "Nominal is better".

$$
\begin{array}{l}
r_{i*} < r_i < O_i \\
O_i < r_i < r_i{}^* \\
r_i > r_i{}^* \text{ or } r_{i*} > r_i
\end{array}
\qquad
\left\{
\begin{array}{c}
\left[\dfrac{r_i - r_{i*}}{O_i - r_{i*}}\right] \\
\left[\dfrac{r_i - r_{i*}}{O_i - r_{i*}}\right]^c \\
0
\end{array}
\right.
$$

Where: O_i is the objective value, c and a describe the exponential parameters which verify the shape of the desirability function.

3.6.2 Optimal Machining Parameters: Particle Swarm Optimization (PSO)

The optimal process parameters are achieved by employing the PSO and desirability approach. The PSO was implemented using MATLAB and the Desirability approach was carried out using Minitab software. The working conditions for the PSO model are illustrated in the algorithm. The projected model and the parameters that play a vital role in obtaining finer convergence characteristics of PSO are discussed in (Optimization Chapter 6). If the number of parameters increases, the learning rate increases in turn the number of iteration increases in the search space. The outcome leads to probability of getting global optimum solution and leading the convergence to be accomplished in a smaller number of iterations. Therefore there is a boundary on maximum velocity to be attained by the particles.

The above criterion indicates the abandoned increase in velocity of particles, so it is necessary to make the search algorithm to be limited boundary range. The direction of

the velocity gets altered in opposite direction if the velocity of the particles surpasses ahead of the specified range. This results in converging quickly towards its global optimum solution.

A) Proposed Methodology: PSO

Based on the literature survey, the PSO technique yields good result as compared to the rest of the techniques. So the PSO technique is incorporated in this present study. PSO is stochastic optimization technique which is a population based optimization technique, PSO technique was implemented (Eberhart et al.in 1995). The PSO technique was implemented by taking an inspiration of birds flocking. In the PSO algorithm the particles are estimated by the fitness function to be optimized and have velocities for the particles. The PSO has two important values which are termed as pbest and gbest. The pbest value is the best solution achieved so far among the particle, gbest value is the best solution obtained so far in the population. Once these two values i.e pbest and gbest are acquired, the particles are upgraded with their velocity and positions using the equation (3.8). PSO incorporates various parameters such as number of particles, range of particles, global vs local values, dimension of particles, learning factor. The information mechanism sharing in PSO is entirely diverse as compared to the rest of the techniques. The information sharing in PSO is one way sharing mechanism. In PSO, the gbest has the right to share the information with others. As the evolution glances only for the best solution, all the particles present intend to converge towards the best solution as quickly as possible in most of the cases. The PSO algorithm mainly consists of three different factors as follows: 1) Social 2) Cognitive 3) Inertia (Eberhart et al.in 1995, Munish et al.2015). All these three constraints concentrate mainly on accelerating the particle towards the best position. The best position is the one which is so far followed by all the neighbouring swarm; this position is considered to be the global best (gbest) position. The Cognitive constraint concentrates on accelerating the individual particle towards its best position (pbest), the position (pbest) which is accomplished by the individual particles so far. The inertia constraint plays a vital role in maintaining the stability between the gbest and pbest investigation competence among the search space. If the fitness values of gbest and pbest values are

compared among each other, if the pbest value is found to be better than the gbest value, then the value of the gbest changes

The equations (3.8 - 3.10) are incorporated to vary the position of the individual particles to reach global optimum solution in search space.

$$v_i^{r+1} = w.v_i^r + c1.Q1.(pbest_i - y_i^r) + c2.Q2.(gbest - y_i^r) \qquad (3.8)$$

Where v_i^r = ' i^{th}' particle momentum at 'r^{th}' iteration; w = inertia weight; c1,c2=learning factors which varies in the range of 1 to 4; Q1,Q2= random numbers between 0 to 1; $pbest_i$= $pbest$ location of ' i^{th}' particle or $pbest$ value is the best solution achieved so far among the particle; $gbest$=$gbest$ location of swarm; y_i^r = $[y_{i1}^r, y_{i2}^r, y_{i3}^r, \ldots \ldots \ldots \ldots . y_{iN}^r]$, "$i^{th}$" particle current position at "r^{th}" iteration in N-dimensional search space or $gbest$ value is the best solution obtained so far in the population.

After calculating the momentum, the next position of the rth particle is calculated as follows:

$$y_i^{r+1} = y_i^r + v_i^{r+1} \qquad (3.9)$$

Inertia weight can be determined by using the equation (3.10) or the Inertia weight can be chosen to be any random value. This determined inertia weight can be substituted in equation (3.9)

$$W = w_{max} - \frac{[(W_{\max} - W_{min}) * iter_{curr}]}{iter_{total}} \qquad (3.10)$$

Where W_{max} = maximum inertia weight; W_{min} = minimum inertia weight; $iter_{curr}$= current iteration; $iter_{total}$=total number of iteration.

B) PSO OPTIMIZATION OF PROCESS PARAMETERS

PSO coding structure is to be defined and the initial population is distinct. The computation with particle swarm with particle swam intelligent operators is used to evaluate fitness with respect to the objective function. General flow chart of PSO algorithm is shown in Figure 3.11.

Terminologies used in PSO algorithm:

- **Particle:** Individual in the group of swarms. A potential solution is represented each swarm in the problem.
- **Swarm:** Population of the algorithm.
- **Personal best (pbest):** Personal best position of a given particle, so far. That is, the position of the particle that has provided the greatest success, pbest in equation (3.8) represents best position (pbest) individual until iteration k.
- **Global best (gbest):** Position of the best particle of the entire swarm, gbest in equation (3.8) represents best position of the group until iteration k.
- **Leader:** Particle that is used to guide another particle towards better regions of the search space.
- **Velocity (vector):** This vector drives the optimization process, that is, it determines the direction in which a particle needs to "fly" (move), in order to improve its current position.
- **Inertia weight (w):** It is employed to control the impact of the previous history of velocities on the current velocity of a given particle and denoted by w.
- **Learning factor:** Represents the attraction that a particle has towards either its own success or that of its neighbours. Two learning factors used: C1 and C2, where C1 is the cognitive learning factor and it represents the attraction that a particle has towards its own success and C2 is the social learning factor and represents the attraction that a particle has toward the success of its neighbours. Both, C1 and C2 are constants (Malghan et al. 2016, Gonzalez et al. 2012).

C) PSO Algorithm   : (Malghan 2016, Eberhart et al.in 1995)

1. Initialize the population of n particles randomly.
2. For each particle, the fitness value is calculated.
3. If the obtained fitness value of the particle is better than the best fitness value (P_{best}) in history, than the present value is assigned as new best fitness value (new P_{best}).
4. Choose the particle with the best fitness value of all the particles which are considered so far as the global best (gbest).
5. The velocity and position of each particle need to be calculated.
6. Each particle velocities are secured to a maximum velocity. If the sum of the acceleration will cause the velocity on that dimension to surpass ahead of the specified range set by the user, then the velocity need to be limited.
7. Terminate if minimum error condition is reached or when the maximum iteration is reached else go to step 2.
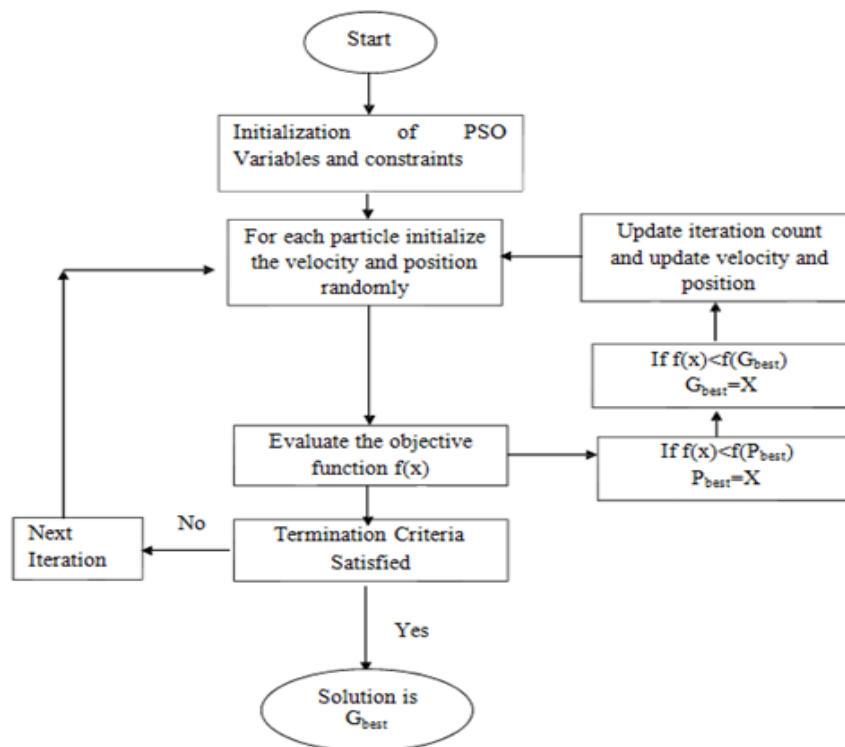
Figure 3.11: The PSO flow chart to optimize the process parameters: Cutting force, Surface roughness and Power consumption as objective functions

3.7 PREDICTION TECHNIQUE: NEURAL NETWORK (NN) MODEL

The goal of the work is to construct a neural network model in order to predict the cutting temperature, cutting force, surface roughness and tool wear during milling operation. Multilayer Perceptron (MLP) was developed for prediction. The 4 various back propagation algorithms (BPA) i.e. (Gradient descent, Scaled Conjugate Gradient Descent, Levenberg Marquart and Bayesian regularization (BR) or Bayesian Neural Network (BNN)) were incorporated in the MLP model. The following section will focus on the architecture and training methods used in the present work.

3.7.1 Architecture of Multi-Layer Perceptron (MLP) Model- ANN

The intricate and disruptive engineering problems have been effectively solved by using the MLP models. Error back propagation method has been adopted to consecutively solve this problem. In order to resolve the errors occurring during learning process various learning algorithms exist such as the Gradient Decent learning rule, Adaptive Filtering or Least Mean Square algorithm. The architecture encompasses three different types of layers namely input layer 1 (neurons -4), hidden layer 1 (neurons 6), and output layer 1 (neurons - 4). The flow of signal is named as Feed Forward Neural Network as the signal moves in a forward direction, from input layer to hidden layer and then from hidden layer to the output layer. The data being processed in the network will bypass several layers without any existence of feedback connections. Figure 3.12 shows schematic representation of input and output parameters in Multi-Layer Perceptron feed forward neural network. The neural network has to behave in a way that the set of inputs should determine anticipated result. The weights are assigned primarily in two ways. One way is to use the learning rule to learn the output pattern by providing the trained data. Another way is to assign the weights based on the prior knowledge. The back propagation algorithm for given epoch of training data executes in two different ways namely the sequential mode or batch mode. Basically the disparity among these two ways is that in sequential mode, the weights of neurons are entirely dependent on the pattern basis. While in the case of batch mode, the weights and the bias of neurons are entirely on the epoch basis. Generally, the sequential mode is widely used in back-propagation learning. Usually, the network needs to be trained in a way that it leads to

minimal error. The error is calculated based on the difference between the desired error and actual error. Basically there are two methods to specify the error, either by specifying the number of epochs or by specifying the error value. The variation among these two ways is that if number of epochs is specified, then the training data will execute until it reaches the specified epoch number; later on the testing of the data is carried out. In epoch specification, the training data will run up to the specified number of epoch and once it reaches the specified value; the testing of the data is carried out. In the other way, the training will iterate till the specified value of error is reached. In the present study, Multi-Layer Feed Forward Neural Network (MLFFNN) architecture is adopted for training and predicting the mechanical properties of the SS316 steel material. The input parameters are spindle speed, feed rate, and depth of cut. The predicted response parameters are cutting temperature (CT), cutting force (FX), surface roughness (Ra) and tool wear (TW).
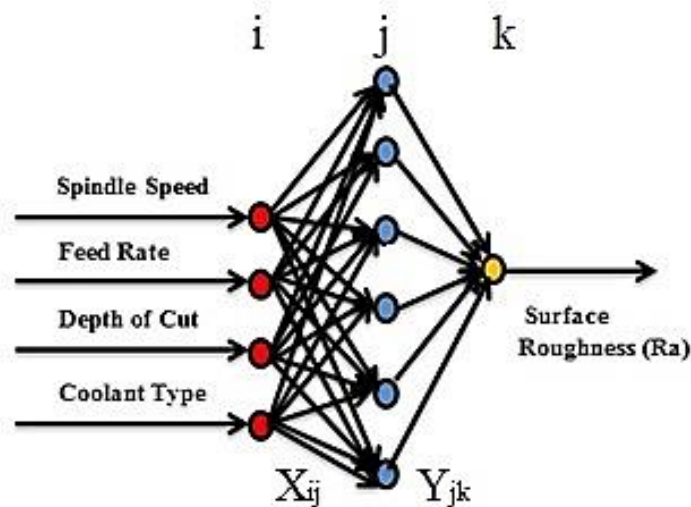
Figure 3.12: Structure of neural network with input and output parameters in multi-layer perceptron feed forward neural network

Table 3.4: Information on prediction & optimization.

Parameters	Prediction	Parameters	Optimization
Definition	Predicting is making claims about something that will happen, often based on information from past and from current state.	**Definition**	Optimization is the technique to obtain best results for the given problems under given constraints. The purpose of optimization is to achieve the "best" design relative to a set of prioritized criteria or constraints.
Advantage	The advantage includes automatic learning of dependencies only from measured data without any need to add further information (such as type of dependency like with the regression).	**Advantage**	Optimization is the technique to obtain best results for the given problems under given constraints. An investigation is done here to compare and arrive at the best optimization technique from among Desirability Approach and PSO.
Training	The neural network is trained from the historical data with the hope that it will discover hidden dependencies and that it will be able to use them for predicting into future	**Objective Function**	Finding an optimal solution for more than one objective functions is called multi-objective optimization (deals with more than one objective function).
Prediction Type (Criteria)	The prediction type can be classified according to various criteria. **Basic criteria are:** • Data that we have for teaching prediction and for prediction • What we want to predict - value	**Goal of optimization**	The goal of optimization is to minimize or maximize certain quantities. In mathematical models, these goals are expressed as functions of certain variables These include maximizing factors such as productivity, strength, reliability, longevity, efficiency, and utilization.

			This decision-making process is known as optimization.
Predict Value	When we want to get exact value (or more values) of a variable in future, then we are predicting value.	**Creation of objective Functions**	The response equations attained through RSM model are further utilized as fitness function in implementation of PSO algorithm.
Predict Trend	Whether the value will go up or down without considering size of the change - then we are predicting trend.	**PSO Inspired BY**	Particle Swarm Optimization Technique is said to be inspired by a swarm of birds or a group of fish. Thus, this algorithm is also called a population-based stochastic algorithm.
Advantage of NN in prediction	NN is able to learn from examples only and that after their learning is finished, they are able to catch hidden and strongly non-linear dependencies, even when there is a significant noise in the training set.	**Advantage of PSO**	Have few parameters to adjust, Converge fast, Has a own memory, Simple to implement
Disadvantage of NN in prediction	NN can learn the dependency valid in a certain period only	**Disadvantage of PSO**	End to fall into a sub- optimal state. Weak local search ability.

Table 3.5: Information on back propagation algorithms (BPA) / Training algorithms (TA).

Sl.NO/ Training Algorithms	Gradient descent	Scaled Conjugate Gradient Descent	Levenberg-Marquardt	Bayesian Regularization
1	Requiring many iterations for functions which have long, narrow valley structures	This method also avoids the information requirements associated with the evaluation, storage, and inversion of the Hessian matrix, as required by the Newton's method.	Levenberg-Marquardt algorithm is a method tailored for functions of the type sum-of-squared-error.	Bayesian regularization expands the cost function to search not only for the minimal error, but for the minimal error using the minimal weights.
2	The downhill gradient is the direction in which the loss function decreases most rapidly.

But this does not necessarily produce the fastest convergence. | In the conjugate gradient training algorithm, the search is performed along conjugate directions which produce generally faster convergence than gradient descent directions. | Very fast when training neural networks measured on that kind of errors. | To overcome the problem in interpolating noisy data, MacKay (1992) has proposed a Bayesian framework which can be directly applied to the neural network learning problem. |
| 3 | Big neural networks, with many thousand parameters | Recommended when we have very big neural networks. | Not recommended when we have big data sets and/or neural networks requires a lot of memory | Estimate the effective number of parameters actually used by the model.

The number of network weights actually needed to solve a particular problem. |

4	The reason is that this method only stores the gradient vector (size n), and it does not store the Hessian matrix (size n2).	Since it does not require the Hessian matrix,	It works without computing the exact Hessian matrix. Instead, it works with the gradient vector and the Jacobian matrix.	By using Bayesian regularization, one can avoid costly cross validation. It is particularly useful to problems that cannot, or would suffer, if a portion of the available data were reserved to a validation set. Regularization also reduces (or eliminates) the need for testing different number of hidden neurons for a problem.
5	It requires information from the gradient vector, and hence it is a first order method.	This method has proved to be more effective than gradient descent in training neural networks.	It cannot be applied to functions like cross entropy error.	A third variable, gamma, indicates the number of effective weights being used by the network, thus giving an indication on how complex the network should be.

Figure 3.13: Memory v/s Speed -Training algorithms
(https://www.neuraldesigner.com/blog/5_algo)

Table 3.4 represents the general information on prediction and optimization techniques. Table 3.5 represents the 4 different back propagation algorithms incorporated in the current study for prediction of responses. From the Figure 3.13, it can be inferred that Bayesian Regularization is better approach when compared to rest of BPA's. As discussed earlier in Table 3.5, Bayesian is best suitable for the current study due to its convergence rate, speed and storage parameters.

CHAPTER 4

RESULTS AND DISCUSSION (Part-I)

MACHINABILITY STUDY OF SS316

4.1 MILLING PERFORMANCE OF SS316 UNDER CRYOGENIC COOLING

The milling experiments were carried out on SS316 specimen's with PVD TiAlN coated carbide tools at different spindle speeds (1000,2000 and 3000 rpm), keeping feed rate (450 mm/min) and depth of cut (Doc,1mm) combinations constant under dry, wet and cryogenic machining conditions. The experimental results of cryogenic machining on the cutting temperature, cutting force, surface roughness and tool wear have been compared with those under dry and conventional coolant (wet) machining conditions

4.1.1 Cutting Force (N)

The investigation explores variation of cutting forces in different machining condition since it co-relates with the other fundamental cut characteristics such as tool wear, machining temperature, and surface quality (Kumar et al 2020, Ramesh et al 2018, Meddour et al 2014, Azlan et al 2012). Figure 4.1 (i), (ii) and (iii) portrays the variation in resultant cutting force concerning machining span (time) under dry, flood and LN_2 method of cutting with spindle speed 1000, 2000 and 3000 rpm respectively. Figure 4.1 demonstrates that the resultant cutting force shows an expanding pattern with machining condition. It may be due to the warm softening of the work material at raised temperature and higher cutting velocity.

Related article:

Captivatingly, LN_2 method of machining brought exceptional reduction of cutting power of around 43% and 16% in comparison with dry and surge cooling conditions individually. It is obvious from the Figure 4.1, that cryogenic approach offers promising diminishment in the machining power, feasible results like less instrument wear, and better surface quality. Likewise, considerable variation in the resultant cutting power was seen among surge and LN_2 cooling mode for spindle speed of 1000-3000 rpm

(i)   **(ii)**

(iii)
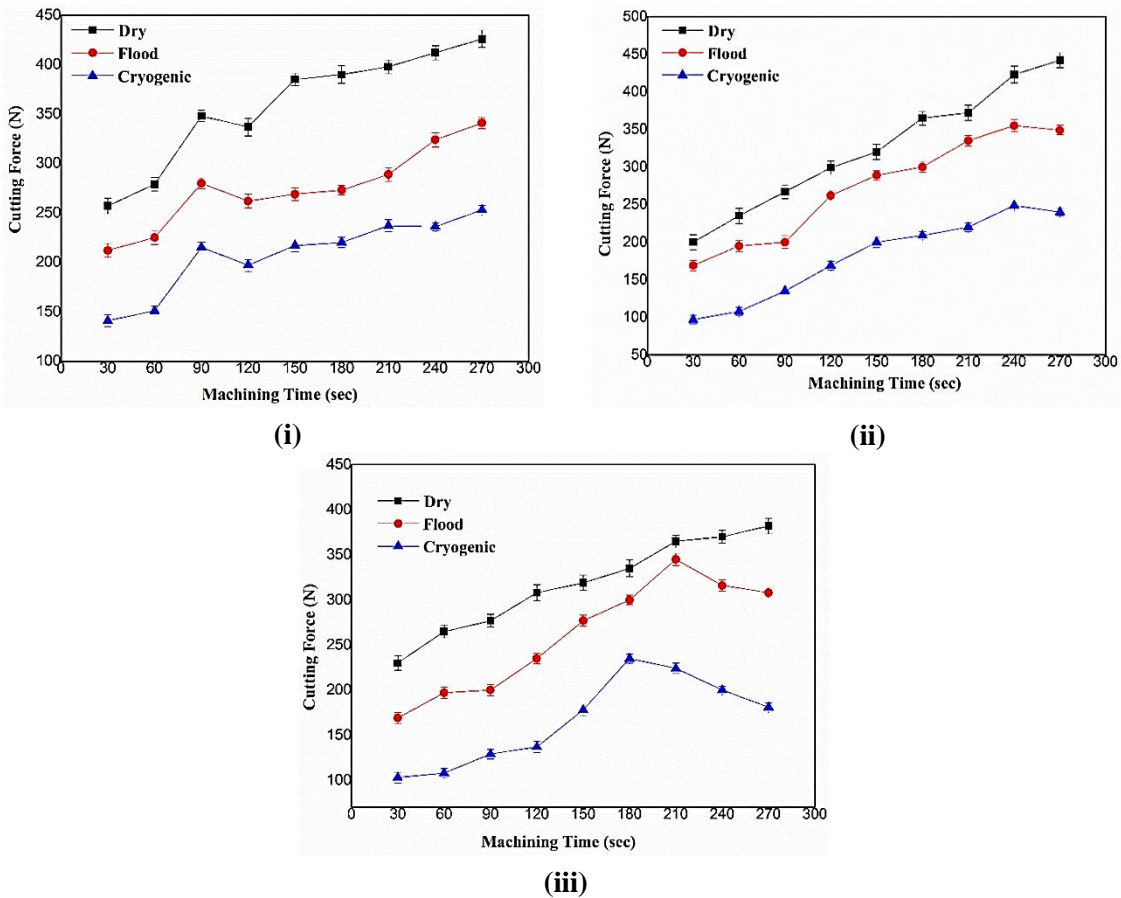
Figure 4.1: Variation of cutting force at speed of (i) 1000rpm (ii) 2000rpm (iii) 3000rpm

4.1.2 Machining Temperature (°C)

Cooling strategies in machining are adopted with an objective of diminishing the cutting temperature. These are likewise helpful in keeping the Cutting tools from extreme impairment like adhesion, diffusion and abrasion which are emphatically co-identified with machining temperature. In addition, at machining SS316 at raised temperature prompts to swift tool wear.

The disparity recorded in cutting temperature amid the examination is shown in Figure 4.2 (i), (ii) and (iii) for spindle speed 1000, 2000 and 3000rpm respectively. It is clear from the figure that, spindle speed increases linearly with cutting temperature at machining zone because of enhanced friction at device work interface. In case of LN_2, the machining temperature was relatively less in contrast with dry and flood modes for all considered scopes of spindle speeds. A remarkable diminishment in cutting temperature was seen under LN_2 condition than that of dry (around 58%) and flood (around 42%) situations. This is on the grounds that, the heat exchange happens amid LN_2 machining mode through convection and dissipation. Utilization of LN_2 superbly encourages the liquid beads to reach at device workpiece interface which offer proficient warmth exchange in this manner and gives enhanced lubrication prompting low machining temperature. This may be added to the prevalence of atomised coolant particles to enter effectively in to the cutting zone.
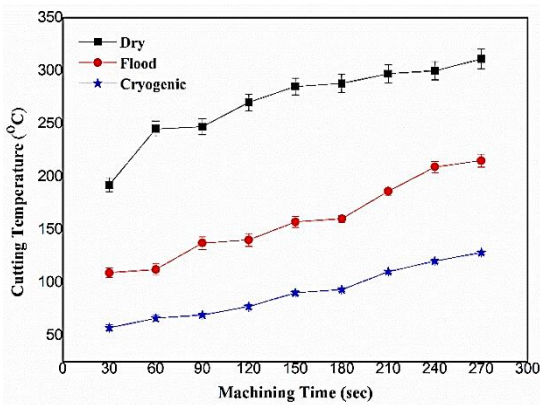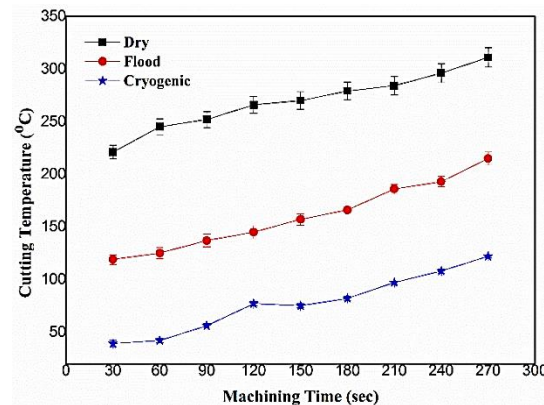
(i)   (ii)
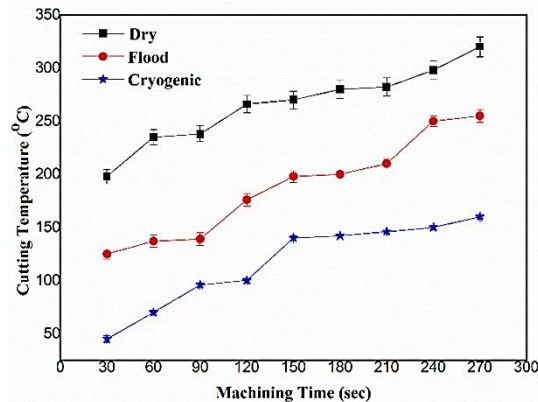
(iii)

Figure 4.2: Variation of cutting temperature at speed of (i) 1000rpm (ii) 2000rpm

(iii) 3000rpm

4.1.3   Surface Roughness (µm)

After milling, the surface roughness (Ra) values of the samples are estimated, and these attained Ra values of the work part under all the three cutting conditions are shown in Figure 4.3 (i), (ii) and (iii) for spindle speed 1000, 2000 and 3000rpm respectively. Marginally lower Ra reverences were seen at higher rates (2000 rpm and 3000rpm) when contrasted to the lower (1000 rpm). The previously mentioned figure illustrated that surface roughness diminishes with increment in spindle speed. This showed the machined surface has a tendency to become smoother for rapid regular machining. High machining temperature resulted in softening of work part (samples) which decreases the initiated cutting forces and subsequently a decent surface quality was accomplished (Patricia et al 2010, Azlan et al 2010, Suresh et al 2012). At higher spindle speed, the chips are created and split away close to the tool tip with less deformation of material which thus safeguards the surface attributes of machined part causing enhanced surface quality (Venkatesh et al 2018, Chandrasekaran et al 2010). Then again, surface unpleasantness recorded under dry and flood machining condition in comparison with LN_2. This is because of the way that, LN_2 mode offers more successful cooling and lubrication than that of dry and flood conditions. Because of which a critical diminishment in the friction could be accomplished in blend with high rate of heat exchange. Thus, surface quality

99

was good in contrast to flood machining. However, in case of dry machining, no cutting liquid was provided leading to high friction which thus added to higher surface roughness. It is evident from the Figure 4.4 and Figure 4.5 that less surface defects were found in cryogenic machining. This is ascribed to lower cutting temperatures and retaining of the tool shape provided by the LN_2 spray. In contrast, more surface defects like side flow, debris, grooves and adhered micro particles were identified in dry and wet machining conditions due to the type of tool geometry obtained in the respective machining environments (Refer Figure 4.6)

(i)

(ii)

(iii)
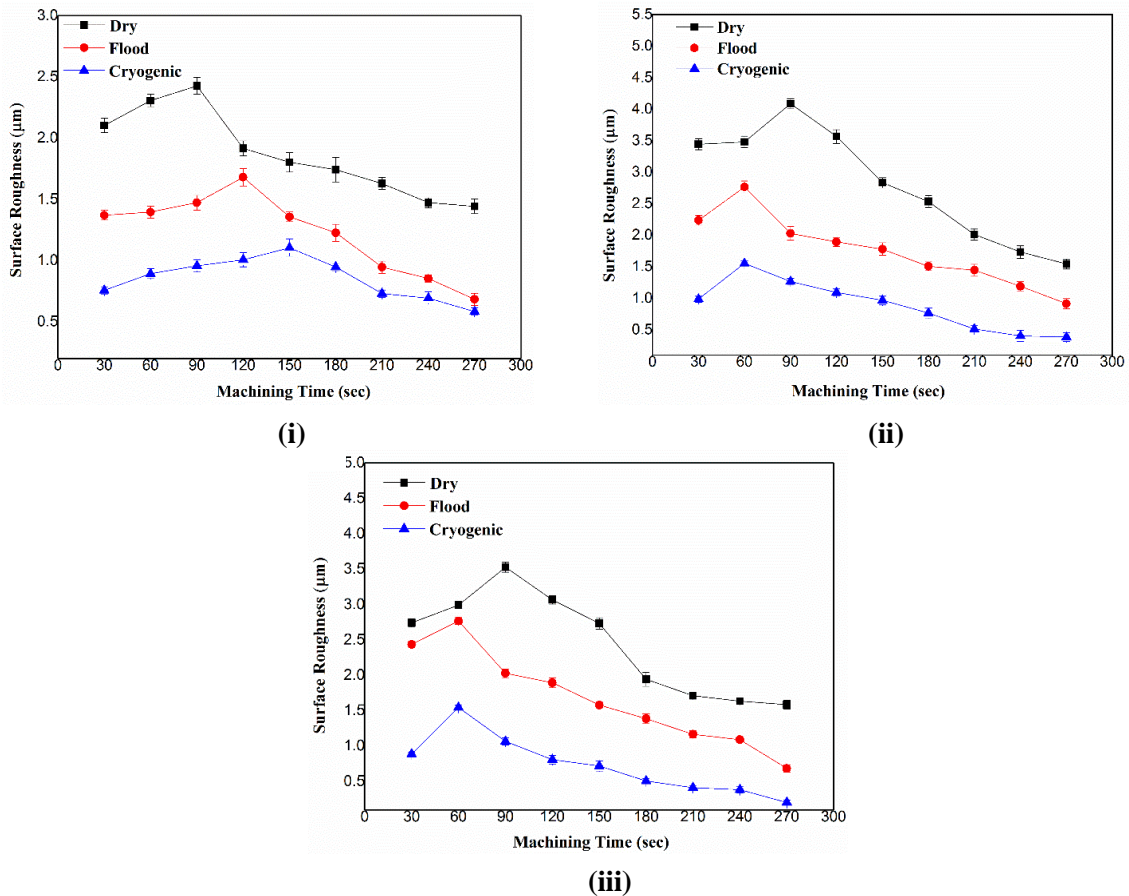
Figure 4.3: Variation of surface roughness at speed of (i) 1000rpm (ii) 2000rpm (iii)
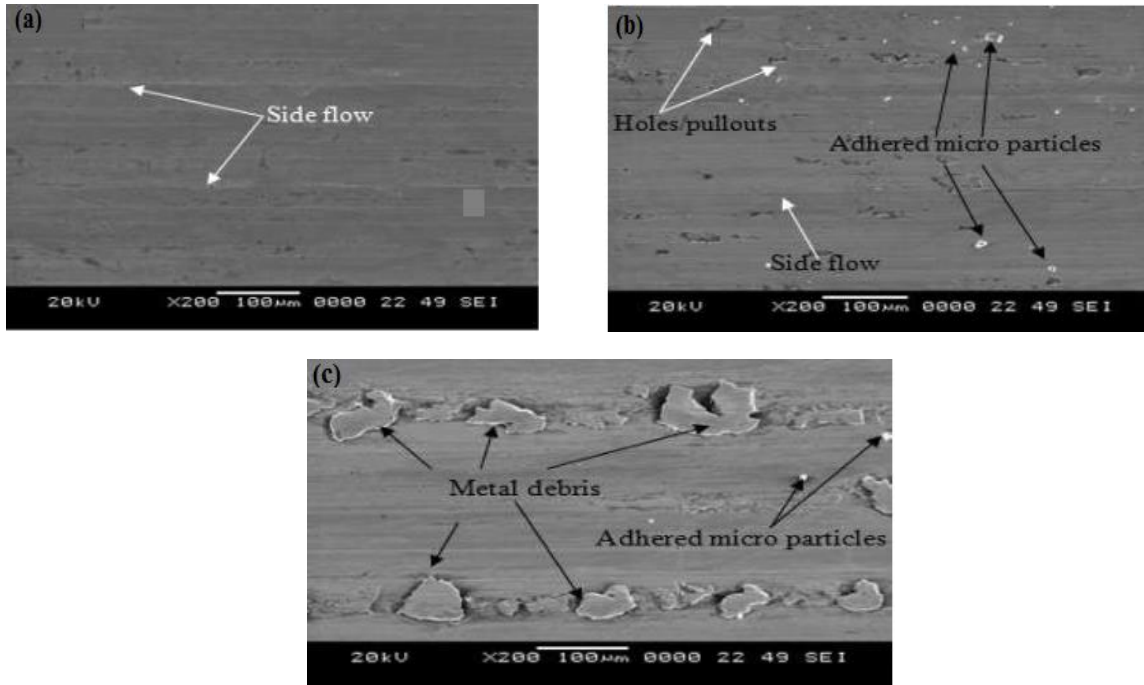
3000rpm

Figure 4.4: SEM images of machined surfaces at s = 1000 rpm, f =450 mm/min and d = 1 mm under different cooling environments (a) Cryogenic (b) Flood (wet) (c) Dry
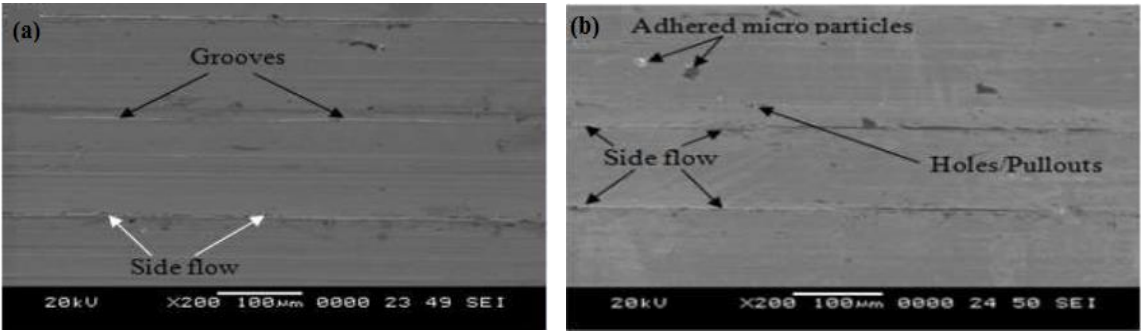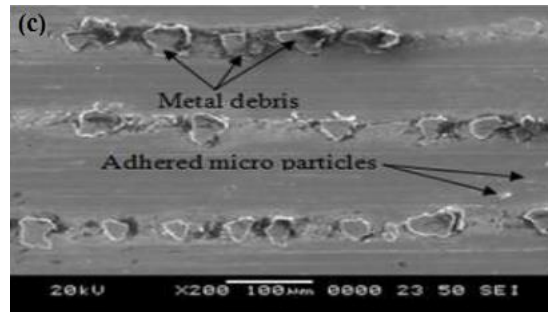
Figure 4.5: SEM images of machined surfaces at s = 3000 rpm, f =450 mm/min and d = 1 mm under different cooling environments (a) Cryogenic (b) Flood (wet) (c) Dry

4.2 Tool Wear Study of a PVD TiAlN Coated Carbide Tool in the milling of SS316 steel

4.2.1   Introduction

The temperature created at cutting zone is primarily responsible for rapid tool wear while machining SS316. High machining temperature regularly presented serious tool wear like chipping, break of the tool nose and plastic deformation. There are various wear mechanisms which can altogether influence the tool wear amid processing of SS316. The significant wear components saw in the present examination were abrasion, diffusion, plastic deformation and chipping.

Figure 4.6 shows the SEM views of the worn out tips of a PVD TiAlN coated carbide tool at cutting speeds of 1000, 2000 and 3000 rpm, constant feed rate of 450 mm/min and depth of cut 1 mm under dry, wet and LN_2 machining. In the milling of SS316 steel with a PVD TiAlN coated carbide tool, chipping and flaking were observed under all the machining environments. The chipping on the cutting edge during dry and wet machining was more serious than under LN_2 machining (Girish et al 2015, Gianni et al 2014). In the wet machining also chipping and flaking of the cutting edge was observed.

In the case of milling of SS316 steel with the cutting speeds of 1000, 2000 and 3000 rpm chipping and flaking observed in dry machining was higher than that of wet and

cryogenic cooling. The flaking was observed in dry machining due to a strong adhesion between the chip and the tool rake as a result of high cutting temperature. Compared to dry and wet machining, the chipping of the cutting edge under LN_2 cooling was lower. At the same cutting speed, less chipping and flank wear were observed in cryogenic cooling due to the control of temperature-dependant tool wear mechanisms (Branimir et al 2009, Mohanraj et al 2021). Further, with the application of LN_2 coolant, both cooling and lubricating of the tool reduces cutting temperature and cutting force resulting in decreased chipping and flaking.
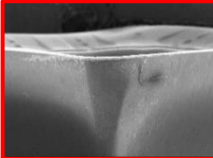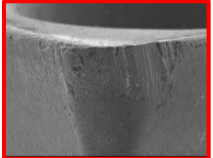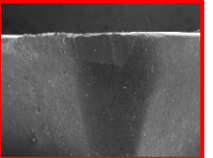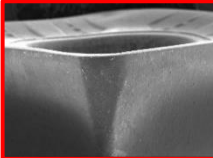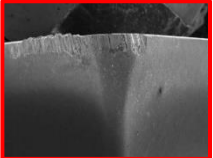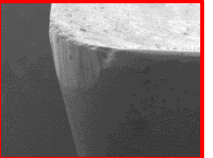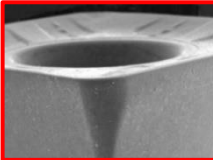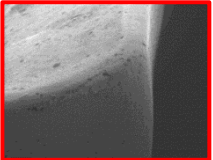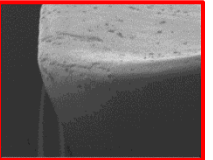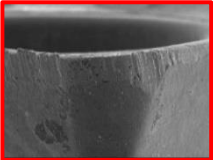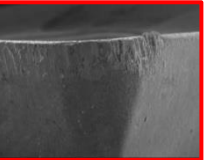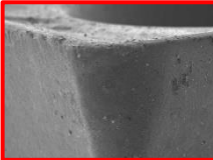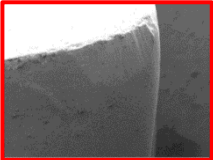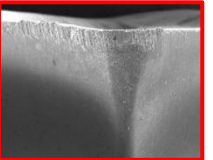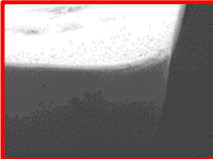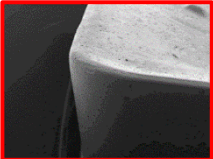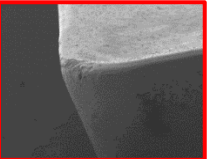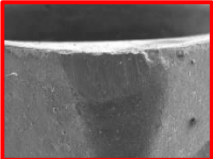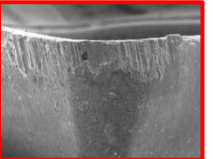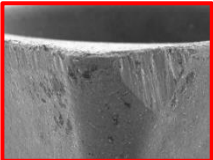
Time (Seconds)	Machining Type	30	60	90
Spindle speed: 1000 rpm Feed: 450 mm/min Doc:1 mm	Dry			
	Coolant			
	LN$_2$			
Spindle speed: 2000 rpm Feed: 450 mm/min Doc:1 mm	Dry			
	Coolant			
	LN$_2$			
Spindle speed: 3000 rpm Feed: 450 mm/min Doc:1 mm	Dry			
	Coolant			
	LN$_2$			

Figure 4.6: Optical microscopic images depicting progression of flank wear.

4.2.2 Investigation of Flank Wear (µm)

Tool wear amid processing of SS316 was described by flank and crater wear and in this way envisioned with the assistance of optical magnifying lens (microscope) and SEM imaging. Figure 4.7 demonstrates the movement of average flank wear for various machining span at the spindle speed of 1000, 2000 and 3000 rpm under dry, flood and LN_2 cutting conditions. A quick development in flank wear was seen after 60s of machining at high spindle speed (2000-3000rpm), particularly while machining under dry cutting condition. However, the prevalence of using LN_2 was all the more prominently obvious for high spindle speed persistent machining which offers better cooling in contrast to dry and flood machining prompts less wear (Solntsev 2001, Ajit et al 2011). Thus, LN_2 emerged as a reasonable option for machining SS316.

Figure 4.8 exhibits the microscopic pictures of flank wear alongside machining span under all machining conditions. High substance reactivity of SS316 prompts adhesion of the material on the tool confront which brings about the creation of built up edge (BUE). This phenomenon which is ascribed to higher friction was seen subsequent to machining span of 90s under dry and flood cutting conditions. Besides, the previously mentioned figure likewise shows that the inclination of BUE generation was more conspicuous amid dry mode when contrasted with wet mode of machining. Excellent cooling along with effective lubrication brought about critical decrease in friction and thus added to the remarkable cutting inserts performance especially under LN_2 mode even at higher spindle speed.
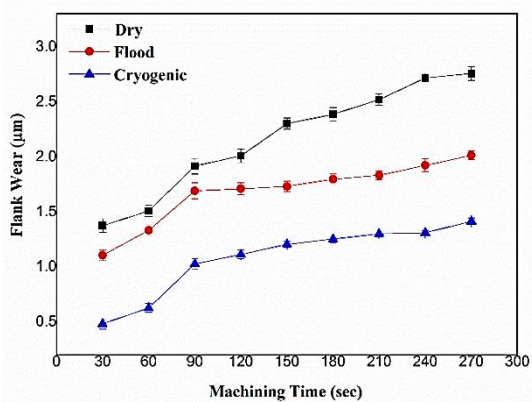
(i)
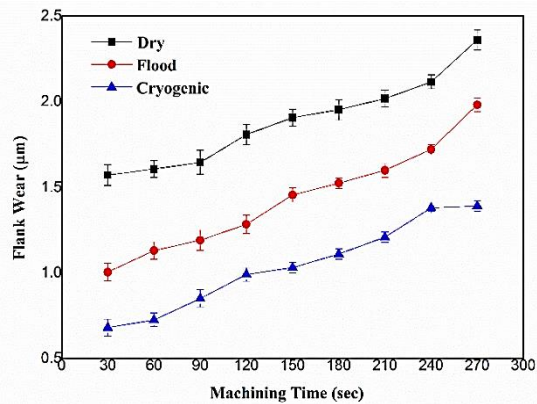
(ii)
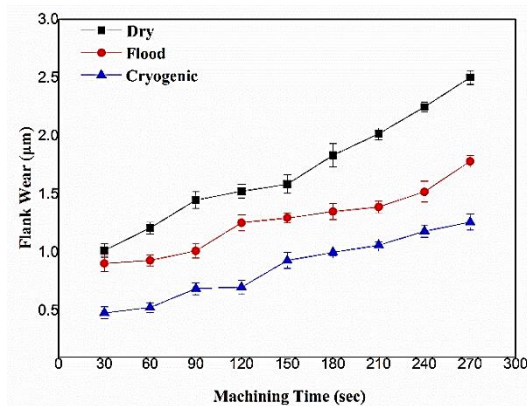
(iii)

Figure 4.7: Variation of flank wear at speed of (i) 1000rpm (ii) 2000rpm (iii) 3000rpm
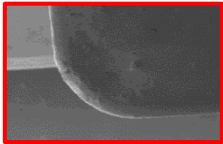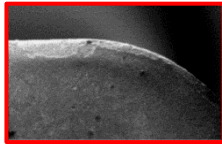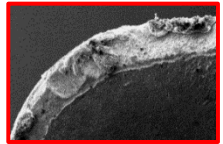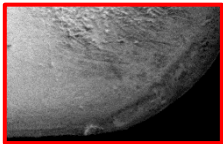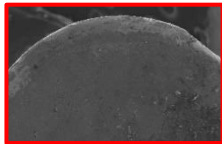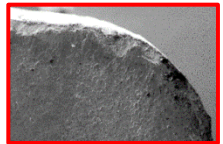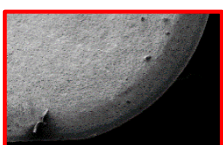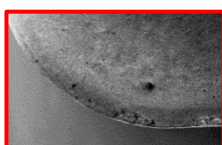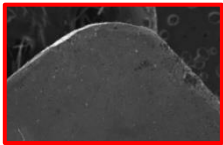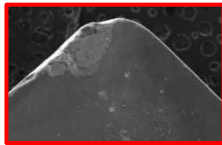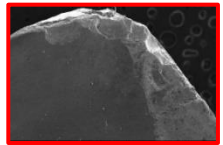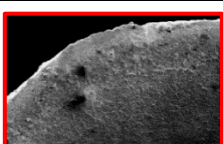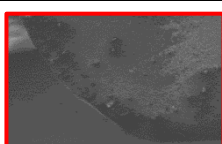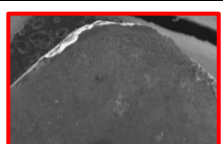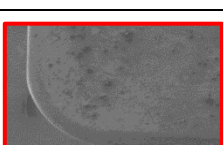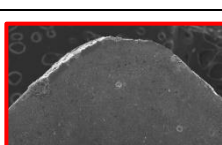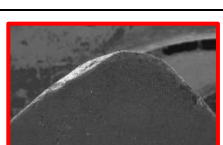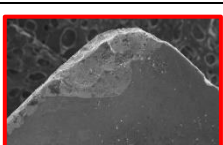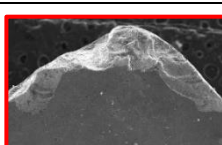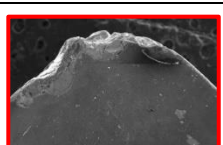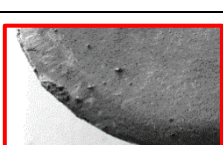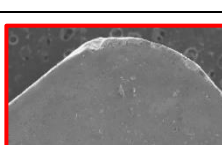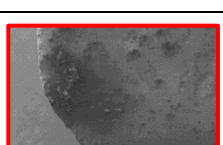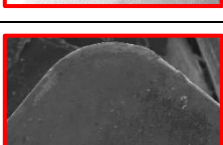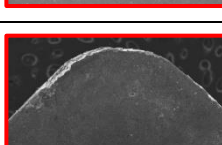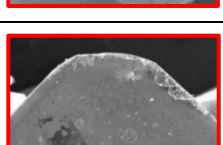
106

Time (Seconds)	Machining Type	30	60	90
Spindle speed: 1000 rpm Feed: 450 mm/min Doc:1 mm	Dry			
	Coolant			
	LN$_2$			
Spindle speed: 2000 rpm Feed: 450 mm/min Doc:1 mm	Dry			
	Coolant			
	LN$_2$			
Spindle speed: 3000 rpm Feed: 450 mm/min Doc:1 mm	Dry			
	Coolant			
	LN$_2$			

Figure 4.8: Optical microscopic images depicting progression of crater wear

4.2.3 Examination of Crater Wear

Wear on rake face of the inserts while milling of SS316 is principally represented at the contact asperities or interface region. High temperature at this area is the central point which reacts in adhesion wear and diffusion wear. Figure 4.8 and 4.9, demonstrate the rapid-I and optical microscopic pictures of rake faces for both dry and wet (flood and LN_2) machining at various spindle speed and machining duration. Greater damages are predominantly visible at rake faces under dry mode contrasted to flood and LN_2 machining (Daniel et al 2019, Uma et al 2018, Daniela et al 2014).

The main type of tool wear noticed amid this study are plastic deformation, development of BUE and built-up-layer (BUL) as portrayed in figure **4.9.** Adhesion of the work material was the most noteworthy wear under dry, flood and LN_2 machining. The previously noted Figure 4.8 demonstrates the development of BUE and BUL because of plastic distortion of the work material (Zhirafar et al 2007, Hussein et al 2018, Prashant et al 2021, Mohanraj et al 2021). Lower thermal conductivity and higher substance affinity of the work part SS316 might have contributed to this. Interestingly, a more impact of applying LN_2 procedure over dry and flood methods is evidenced from Figure 4.8. It even displays the better execution capacity of LN_2 based machining.

Dry	1000 rpm	3000 rpm
	Dry condition: Spindle Speed 1000rpm, Feedrate 450mm/min DOC 1mm	Dry condition: Spindle Speed 3000rpm, Feedrate 450mm/min DOC 1mm
Coolant	**1000 rpm**	**3000 rpm**
	Coolant condition: Spindle Speed 1000rpm, Feedrate 450mm/min DOC 1mm	Coolant condition: Spindle Speed 3000rpm, Feedrate 450mm/min DOC 1mm
LN$_2$	**1000 rpm**	**3000 rpm**
	LN$_2$ condition: Spindle Speed 1000rpm, Feedrate 450mm/min DOC 1mm	LN$_2$ condition: Spindle Speed 3000rpm, Feedrate 450mm/min DOC 1mm

Figure 4.9: Rapid- I machine vision system images depicting progression of crater wear

4.2.4 Summary (Tool Wear)

In all the work-tool combinations, the flank wear (VB) was lower in LN_2 cooling over dry and wet machining. The present method of LN_2 cooling reduced the flank wear in the range of 39 - 55% and 30 - 48.5%, respectively, over dry and wet machining, depending upon the work – tool combinations and cutting parameters. The reduction of the tool wear in LN_2 cooling leads to reduced abrasion and attrition wear, by maintaining the tool hardness with a reduction in the cutting temperature (Oppenkowski et al 2010, dhananchezian et al 2011). Moreover, the adhesion and diffusion wear were also reduced due to better penetration of the liquid nitrogen into the tool – chip and tool – work interfaces.

In wet machining, large quantities of coolant are applied at low pressure into the cutting zone, in order to remove the heat, which was not able to penetrate into tool-chip interface. This is because of the fact that the soluble oil in wet machining has a smaller effect on tool – chip interface, whereas LN_2 coolant has a higher cooling and lubrication effect to reduce tool wear. Kumar and Choudhury (2008) investigated on tool wear in machining of stainless steel with carbide inserts under dry machining and cryogenic cooling by nozzle and observed around 37.39% reduction in the flank wear with cryogenic machining over the dry machining

4.3 STUDY OF CHIP MORPHOLOGY UNDER CRYOGENIC COOLING

4.3.1 Chip Morphology on Milling of SS316

The chips that are formed during the machining operation have strong effects on the surface finish, cutting force, workpiece accuracy and tool life. Generally, chip formation is influenced by the cutting speed as well as the feed rate. Further, the chip could give information on both force and temperature experienced at the cutting zone. In this section, the chips obtained from each of the cutting conditions are analysed. Chip morphology is important because it influences:

1. The stability of the process – e.g., long chips can disturb the machine, and the environment, and they have a negative effect on the cutting process itself.
2. The environmental effect of the production – e.g. small, broken chips is far easier to handle, store, transport and recycle.

The chip formation under different metal cutting conditions can be classified into few categories. Workpiece material and cutting condition will influence the type of chips formed during machining. The surface finish and overall cutting operation are significantly influenced by chips produced. The types of chips produced during metal cutting are continuous chips, continuous chips with built up edge, discontinuous chips and serrated chips (Kalpakjian and Schmid 2003, Noordin et al 2004, Yogesh et al 2018, Ajit et a 2011)

The morphology of the top surface of the chips delivered in the wake of milling of the work part was profoundly analysed with the assistance of the SEM pictures as portrayed in Figure 4.10 (i), Figure 4.10 (ii) and Figure 4.10 (iii). Generally, SS316 is described by serrated chips which are firmly confirmed from the previously mentioned Figure 4.10 (iv) and Figure 4.10 (v). This phenomenon is fundamentally credited to shear localisation and plastic distortion of the work material amid machining (Kalpakjian and Schmid 2003, Noordin et al 2004, Yogesh et al 2021). In addition, machining SS316 at higher spindle speed (3000rpm) causes higher friction at contact asperities leading to high plastic deformation and henceforth creates more serrated chips under dry condition. Along these lines, level of serration was seen to be more under dry condition when contrasted with that of wet machining condition. This can be credited to high temperature development at cutting zone while machining the work material under dry condition. Such high machining temperature prompts a noteworthy upgrade in the plasticity of the work part. At the other cases of machining, the distortion of the workpiece material under flood and LN_2 condition was less because of lower machining zone temperature. This may be due to the side stream of chip material, as apparent from the Figure 4.10 (iii).

(a)	**(b)**	**(c)**
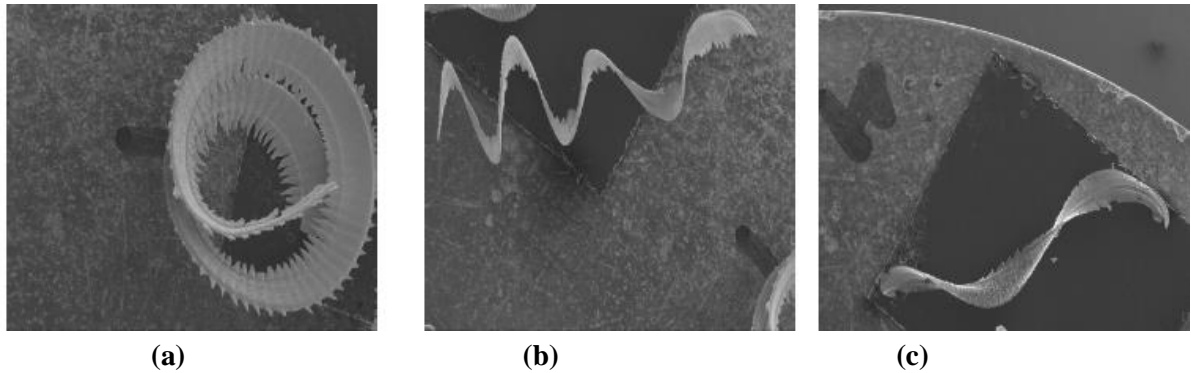
Figure 4.10 (i): SEM images of the chip shape of the SS316 steel at a spindle speed of 1000 rpm and feed rate of 450 mm/min under various machining conditions (a) Dry machining (b) Wet machining (c) LN$_2$ machining

(a)	**(b)**	**(c)**
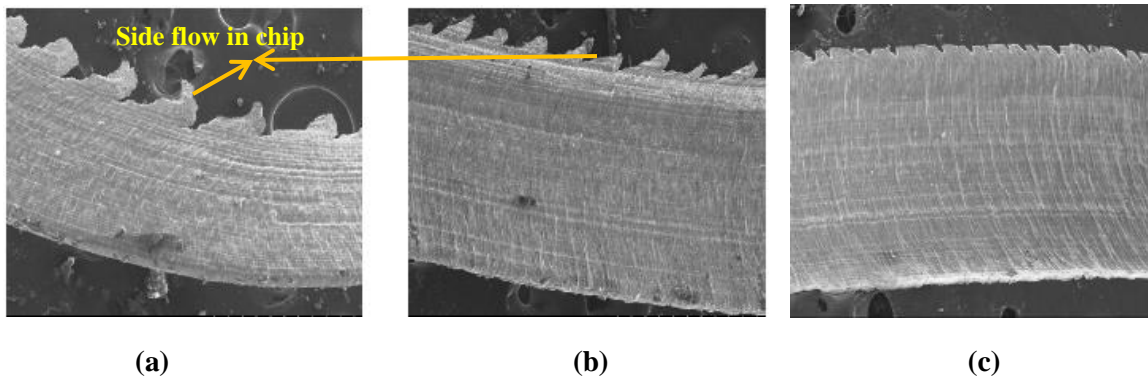
Figure 4.10 (ii) : SEM images of the chip shape of the SS316 steel at a cutting speed of 3000 rpm and feed rate of 450 mm/min under various machining conditions (a) Dry machining (b) Wet machining (c) LN$_2$ machining

Related Article

Karthik Rao M C*, Rashmi L Malghan, Arun Kumar Shettigar, Shrikantha S Rao and Mervin A Herbert, (2017). "Machinability Study of Austenitic Stainless Steel under Wet and Cryogenic Treatment in Face Milling", *Journal of Materials Science & Surface Engineering***, 5(6): 653-656, ISSN (Online): 2348-8956; 10.jmsse/2348-8956/5-6.3, NCMDMM-2017.**
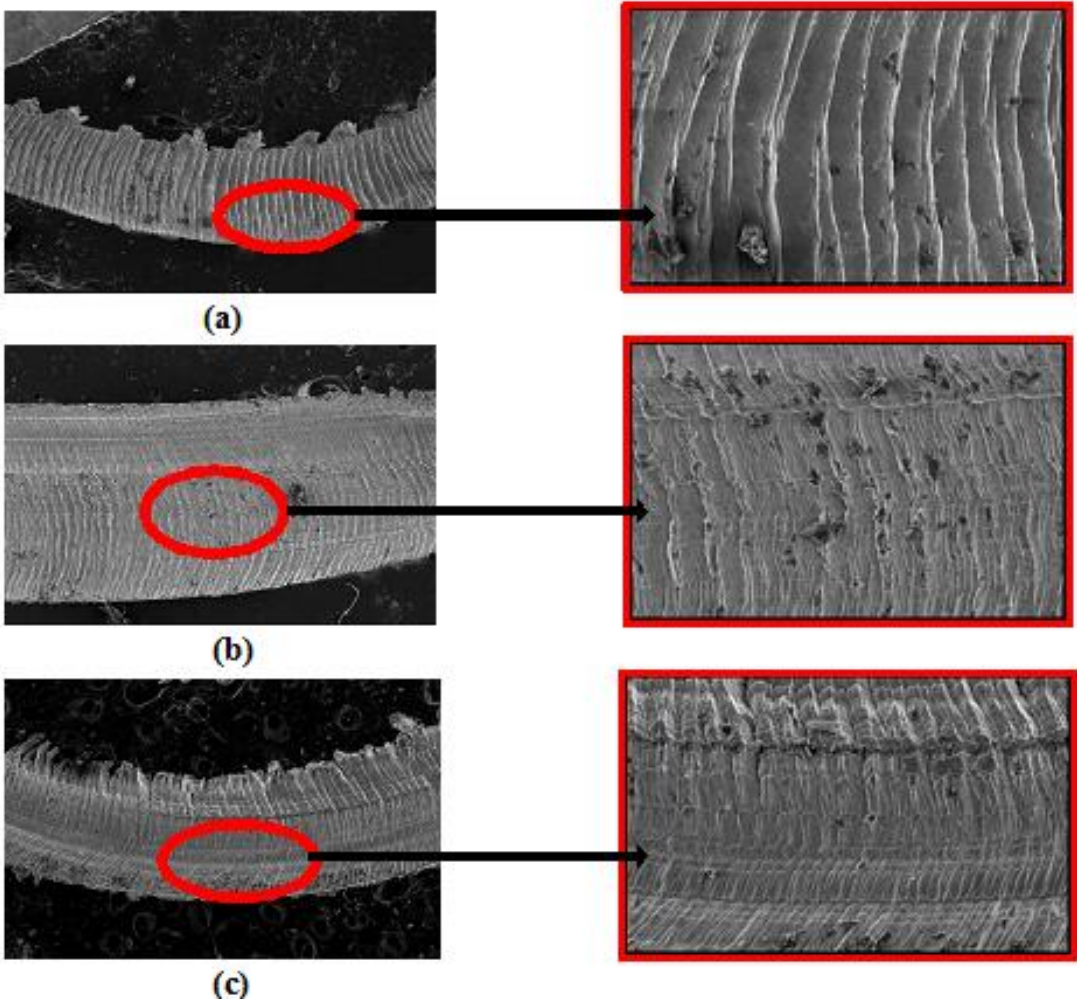
Figure 4.10 (iii): SEM images of chips produced under (a) Dry (b) Flood (c) Cryogenic conditions
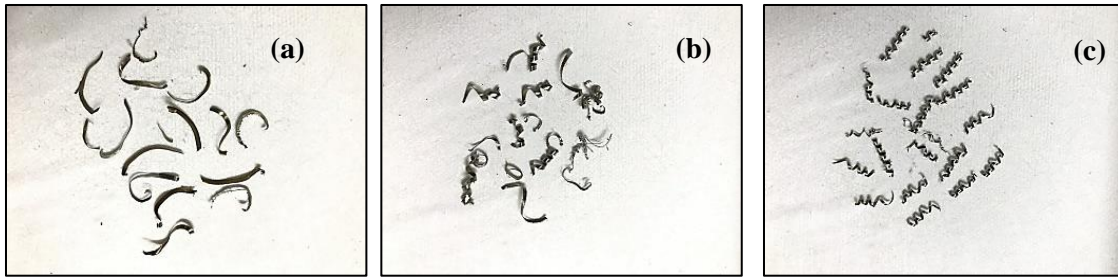
Figure 4.10 (iv): Chip forms generated at s = 1000 rpm, f = 450 mm/min and d = 1 mm under different cooling environments (a) Cryogenic (b) Wet (c) Dry.
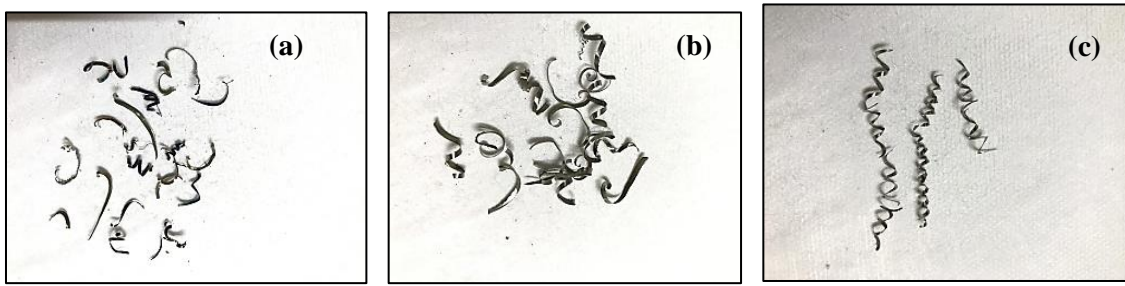
Figure 4.10 (v): Chip forms generated at s = 3000 rpm, f = 450 mm/min and d = 1 mm under different cooling environments (a) Cryogenic (b) Wet (c) Dry.

4.3.2 Summary on Chip Morphology

In all work – tool combinations the chips obtained under LN_2 cooling are smaller than those obtained under similar machining conditions than those under dry and wet machining. Further, the chips obtained in the case of dry machining were found dark blue colour due to extreme heat generated at tool – chip interface. In wet machining, the chips produced in black colour which also indicates intense heat generated at tool – chip interface. The chips produced in LN_2 machining were silver in colour indicating that chips were not burnt due to lower heat generation at tool – chip interface. Therefore, favourable chip shapes are obtained in all work materials under LN_2 machining, when compared to dry and wet machining. This may be attributed mainly to better penetration of LN_2 into the tool – chip interface, resulting in the reduction of the cutting temperature. Further, at lower temperature, the chip cannot promote curl, due to increased chip

114

hardness and lower ductility. This enhances the chip brittleness for easy chip breaking. Mirghani et al (2007) have reported that cryogenic cooling enhances the chip brittleness for easy chip breaking, when the evaporated gas is directed towards the tool cutting edge, thereby cooling the newly generated chips. The serration on chip surface obtained under dry machining is very rough indicating that the higher shearing action at tool – chip interface (Sivaiah et al 2019). The chip surface produced under wet machining also is serrated, indicating intensive shearing action at tool – chip interface. When the LN_2 coolant is used, serration on the chip surface is reduced due to lower shearing action at tool – chip interface. This is because, the penetration of LN_2 into the tool-chip interface results in the formation of a nitrogen cushion at tool – chip interface, which reduces the friction.

Related Article

Karthik Rao M C*, Rashmi L Malghan, Arun Kumar Shettigar, Mervin A Herbert and Shrikantha S Rao. (2021). "Advantages of Cryogenic Machining Technique over Without Coolant and With Coolant Machining on SS316", *Engineering Research Express***, 3,015040, https://doi.org/10.1088/2631-8695/abecd6.**

CHAPTER 5

RESULTS AND DISCUSSION (PART 2)

PROCESS MODELLING FOR PREDICTION

5.1 RSM FOR SS316

The Central Composite Design (CCD) was used to implement the response prediction using RSM. All L20 orthogonal array (OA) was utilized and 20 experiments were performed, which incorporates 8 cube points, 6 center points in cube, 6 Axial points and alpha value is 1. The range of the process parameters were set by taking into consideration the tool or insert specification and also by performing trial experiments in order to achieve the desired responses. In the present work, CCFCD is used for establishing the relationship between the empirical process parameters and the milling process output variables of SS316. The final obtained mathematical regression equations are listed in equations 5.1-5.4. The experimental data considered to perform RSM is represented in Table 5.1.

Later on the model performance was validated with the help of analysis of variance (ANOVA) (Tables 5.2- 5.5). The significance of the model is identified by this method. If the model satisfies the condition of Prob>f less than 0.0500, then the model is significant (Bement 1989, Huang et al 2007, Prakasvudhisarn et al 2009, Venkata et al 2011, Dikshit et al 2016,Malghan et al 2016, Montgomery 2017). Since, all the proposed models satisfy the condition of Prob>f is less than 0.0500, it can be concluded that all the proposed models are significant (Tandon et al 2002, Rao et al 2010, Yu et al 2015).

The adequacy of the fitted regression model was identified using the R^2 correlation coefficient, the value of R^2 need to be close to unity. For all the responses, the "Pre R-squared" are in reasonable accidence with the "Adj R-Squared" values (Rashid et al 2012, Zhang et al 2000, Raja et al 2001). The precision ratio of all the developed models (ratio >4 is desirable) shows the adequacy of incorporating the proposed model (Suresh et al 2010,Mukherjee et al 2006, Tansel et al 2014).

5.1.1 Regression Equations (RSM Approach) For Responses

The attained response equations through RSM approach are stated below:

$T = 157.752 + 15.3889*S + 16.0556*F + 3.38889*D - 104.889*CT + 2.87067*S*S - 3.12933*F*F + 0.870667*D*D + 15.3707*CT*CT - 4.50000*S*F + 1.37500*S*D + 5.37500*S*CT + 2.0*F*D - 9.25000*F*CT - 1.62500*D*CT$ **(5.1)**

$FX = 337.224 - 27.1667*S + 27.1667*F + 3.27778*D - 63.5556*CT + 14.3480*S*S - 15.6520*F*F - 5.65200*D*D - 4.15200*CT*CT - 6.31250*S*F - 0.812500*S*D + 8.93750*S*CT - 0.437500*F*D + 2.06250*F*CT + 0.562500*D*CT$ **(5.2)**

$Ra = 1.23988 - 0.193944*S + 0.137611*F + 0.0157778*D - 0.585556*CT - 0.0370733*S*S - 0.0310733*F*F + 0.0104267*D*D + 0.191427*CT*CT - .00300000*S*F + 0.00487500*S*D + 0.112250*S*CT - 0.00325000*F*D - 0.0498750*F*CT + 0.00400000*D*CT$ **(5.3)**

$FW = 0.251472 + 0.0418333*S + 0.0180000*F + 0.00350000*D - 0.0520000*CT - .0420227*S*S - 0.01252*F*F + 0.00797733*D*D - 0.0335227*CT*CT + 0.00125000*S*F - 0.00137500*S*D - 8.75000E-04*S*CT - 6.25000E-04*F*D - 0.00137500*F*CT - 0.00100000*D*CT$ **(5.4)**

Where: T = Cutting temperature, FX = Cutting Force (X-axis), Ra = Surface roughness, Fw = Flank wear. Where coolant type column indicates, -1 = Dry, 1 = LN_2 and 0 = Flood (wet) machining conditions.

Table 5.1 Experimental conditions for RSM method.

SL. No	Spindle Speed (rpm)	Feed Rate (mm/min)	Depth Of Cut (mm)	Coolant type	Cutting Temperature CT, (°C)	Cutting force Fx (N)	Surface Roughness Ra,(µm)	Flank Wear, Vb,(µm)
1	1000	350	0.5	-1	237	384	2.09	0.16
2	3000	350	0.5	-1	269	337	1.443	0.24
3	1000	550	0.5	-1	299	459	2.427	0.195
4	3000	550	0.5	-1	295	365	1.857	0.283
5	1000	350	1.5	-1	241	393	2.103	0.17
6	3000	350	1.5	-1	271	340	1.473	0.25
7	1000	550	1.5	-1	304	464	2.463	0.203
8	3000	550	1.5	-1	324	370	1.883	0.291
9	1000	350	0.5	1	35	243	0.747	0.06
10	3000	350	0.5	1	84	214	0.583	0.142
11	1000	550	0.5	1	56	309	0.957	0.09
12	3000	550	0.5	1	89	269	0.77	0.18
13	1000	350	1.5	1	39	256	0.757	0.069
14	3000	350	1.5	1	85	219	0.693	0.146
15	1000	550	1.5	1	59	315	0.996	0.102
16	3000	550	1.5	1	95	276	0.78	0.175
17	1000	450	1	0	142	382	1.397	0.168
18	3000	450	1	0	177	326	0.964	0.25
19	2000	350	1	0	139	300	1.07	0.211
20	2000	550	1	0	168	348	1.303	0.253

5.1.2 Analysis of Variance (ANOVA) Results

Table 5.2: Analysis of variance for cutting temperature (CT, ℃) of SS316 using RSM method.

Source	DF	Seq SS	Adj MS	F	P	Percentage Contribution
Regression	14	210053	15003.8	187.08	0.000	
Linear	4	205808	780.5	9.73	0.000	
Speed	1	5033	88.8	1.11	0.004	2.381
Feed	1	4356	75.2	0.94	0.347	2.061
DOC	1	272	28.8	0.36	0.557	0.128
Coolant type	1	196147	2909.7	36.28	0.000	92.812
Square	4	1822	455.5	5.68	0.005	
Speed*Speed	1	1078	14.4	0.18	0.678	0.510
Feed*Feed	1	48	25.7	0.32	0.579	0.022
DOC*DOC	1	84	1.9	0.02	0.880	0.039
Coolant type * Coolant type	1	612	611.7	7.63	0.014	0.289
Interaction	6	2423	403.9	5.04	0.004	
Speed*Feed	1	410	410.1	5.11	0.038	0.194
Speed*DOC	1	60	60.1	0.75	0.400	0.028
Speed*Coolant type	1	564	564.1	7.03	0.017	0.266
Feed*DOC	1	105	105.1	1.31	0.269	0.049
Feed*Coolant type	1	1208	1207.6	15.06	0.001	0.571
DOC*Coolant type	1	77	76.6	0.95	0.343	0.036
Residual Error	16	1283	80.2			
Lack-of-Fit	10	1228	122.8	13.29	0.002	
Pure Error	6	55	9.2			
Total	30	211336				

S = 8.95545, R-Sq = 99.39%, R-Sq(pred) = 96.82%, R-Sq(adj) = 98.86%

From the Table 5.2, it can be derived that coolant type has major contribution of 92.812 %, followed by Spindle Speed of 2.381%, Feed Rate 2.061 % and Depth of cut 0.128%, and remaining minor contribution of 2.618 % made by square and interaction terms on the CT. The attained R-Sq is 99.39%, R-Sq(pred) is 96.82% and R-Sq(adj) is 98.86% for the response CT.

Table 5.3 Analysis of variance for cutting force (FX, N) of SS316 using RSM method.

Source	DF	Seq SS	Adj MS	F	P	Percentage Contribution
Regression	14	149472	10676.6	96.99	0.000	
Linear	4	145142	1225.0	11.13	0.000	
Speed	1	21425	1.9	0.02	0.003	14.166
Feed	1	30012	1587.8	14.42	0.002	19.844
DOC	1	249	88.0	0.80	0.385	0.1646
Coolant type	1	93456	2682.8	24.37	0.000	61.796
Square	4	2561	640.2	5.82	0.004	
Speed*Speed	1	141	130.2	1.18	0.293	0.093
Feed*Feed	1	346	1046.8	9.51	0.007	0.228
DOC*DOC	1	51	43.3	0.39	0.539	0.003
Coolant type * Coolant type	1	2022	2022.4	18.37	0.001	1.337
Interaction	6	1769	294.8	2.68	0.054	
Speed*Feed	1	23	22.6	0.20	0.657	0.015
Speed*DOC	1	86	85.6	0.78	0.391	0.056
Speed*Coolant type	1	1278	1278.1	11.61	0.004	0.845
Feed*DOC	1	2	1.6	0.01	0.907	0.001
Feed*Coolant type	1	371	370.6	3.37	0.085	0.245
DOC*Coolant type	1	11	10.6	0.10	0.761	0.007
Residual Error	16	1761	110.1			
Lack-of-Fit	10	1733	173.3	37.14	0.000	
Pure Error	6	28	4.7			
Total	30	151233				

S = 5.91834, R-Sq = 99.46%, R-Sq(pred) = 96.49%, R-Sq(adj) = 98.99%

Similarly, From the Table 5.3 it can be observed that coolant type has major contribution of 61.796 %, followed by Spindle Speed of 14.166%, Feed Rate 19.844 % and Depth of cut 0.1646%, and remaining minor contribution of 4.029% made by square and interaction terms on FX. The attained R-Sq is 99.46%, R-Sq(pred) is 96.49 and R-Sq(adj) is 98.99% for the response FX

.

Table 5.4: Analysis of variance for surface roughness (Ra, μm) of SS316 using RSM method.

Source	DF	Seq SS	Adj MS	F	P	Percentage Contribution
Regression	14	7.47851	0.534179	107.91	0.000	
Linear	4	7.05665	0.047927	9.68	0.000	
Speed	1	0.72320	0.000141	0.03	0.002	9.569
Feed	1	0.34086	0.000236	0.05	0.830	4.510
DOC	1	0.00448	0.003895	0.79	0.388	0.059
Coolant type	1	5.98811	0.187811	37.94	0.000	79.231
Square	4	0.17950	0.044875	9.07	0.001	
Speed*Speed	1	0.06686	0.008562	1.73	0.207	0.884
Feed*Feed	1	0.02900	0.000129	0.03	0.874	0.383
DOC*DOC	1	0.02482	0.006120	1.24	0.283	0.328
Coolant type * Coolant type	1	0.05883	0.058828	11.88	0.003	0.778
Interaction	6	0.24235	0.040392	8.16	0.000	
Speed*Feed	1	0.00014	0.000144	0.03	0.867	0.001
Speed*DOC	1	0.00038	0.000380	0.08	0.785	0.005
Speed*Coolant type	1	0.20160	0.201601	40.72	0.000	2.667
Feed*DOC	1	0.00017	0.000169	0.03	0.856	0.002
Feed*Coolant type	1	0.03980	0.039800	8.04	0.012	0.526
DOC*Coolant type	1	0.00026	0.000256	0.05	0.823	0.003
Residual Error	16	0.07921	0.004950			
Lack-of-Fit	10	0.07611	0.007611	14.76	0.002	
Pure Error	6	0.00309	0.000516			
Total	30	7.55771				

S = 0.0395831, R-Sq = 99.67%, R-Sq(pred) = 98.36%, R-Sq(adj) = 99.38%

From the data represented in the Table 5.4 it can be seen that coolant type has major contribution of 79.231%, followed by Spindle Speed of 9.569%, Feed Rate 4.510% and Depth of cut 0.059%, and remaining minor contribution of 6.631 % is made by square and interaction terms on Ra. The attained R-Sq is 99.67%, R-Sq(pred) is 98.36 and R-Sq(adj) is 99.38% for the response Ra.

Table 5.5: Analysis of variance for flank wear VB (μm) of SS316 using RSM method.

Source	DF	Seq SS	Adj MS	F	P	Percentage Contribution
Regression	14	0.127682	0.009120	90.62	0.000	
Linear	4	0.087005	0.002250	22.36	0.000	
Speed	1	0.031500	0.004935	49.04	0.000	24.363
Feed	1	0.006612	0.001245	12.38	0.003	5.114
DOC	1	0.000221	0.000154	1.53	0.234	0.170
Coolant type	1	0.048672	0.000971	9.65	0.007	37.645
Square	4	0.040557	0.010139	100.74	0.000	
Speed*Speed	1	0.035304	0.003970	39.44	0.000	27.305
Feed*Feed	1	0.002812	0.001050	10.43	0.005	2.174
DOC*DOC	1	0.000009	0.000308	3.06	0.100	0.006
Coolant type * Coolant type	1	0.002432	0.002432	24.16	0.000	1.881
Interaction	6	0.000120	0.000020	0.20	0.972	
Speed*Feed	1	0.000025	0.000025	0.25	0.625	0.019
Speed*DOC	1	0.000030	0.000030	0.30	0.591	0.023
Speed*Coolant type	1	0.000012	0.000012	0.12	0.732	0.009
Feed*DOC	1	0.000006	0.000006	0.06	0.806	0.004
Feed*Coolant type	1	0.000030	0.000030	0.30	0.591	0.023
DOC*Coolant type	1	0.000016	0.000016	0.16	0.695	0.012
Residual Error	16	0.001610	0.000101			
Lack-of-Fit	10	0.001453	0.000145	5.53	0.024	
Pure Error	6	0.000158	0.00002			
Total	30	0.129292				

S = 0.0100321, R-Sq = 98.75%, R-Sq(pred) = 95.95%, R-Sq(adj) = 98.66%

From the Table 5.5, it can be derived that coolant type has major contribution of 37.645 %, followed by Spindle Speed of 24.363%, Feed Rate 5.114% and Depth of cut 0.170%, the square term speed * speed made contribution of 27.305% and the remaining minor contribution of 5.403 % is made by other square and interaction terms on FW. The attained R-Sq is 98.75%, R-Sq(pred) is 95.95% and R-Sq(adj) is 98.66% for the response Ra.

Thus the effect of all terms (Table 5.2-5.5) of responses is assessed by employing the significance tests. Table (5.2-5.5) depicts the attained "P" values (95% confidence level) of all terms via the CCD model (Yang et al 2011, Malghan et al 2017, Benardos et al 2002). In Table (5.2-5.5) if the terms "P" values <0.05 then these terms are considered to be significant terms else non-significant terms (Yang et al 2011b, Venkata

et al 2010, Farahnakian et al 2011). Thus the ANOVA approach gives the substantial influence of the input variables towards the responses (cutting temperature, cutting force, surface roughness and flank wear). The effect of each term is distinguished to assess sufficiency and exactitude of the model.

The experimental accumulated control-response data are applied for generation of mathematical (nonlinear) models of the responses. The attained results and the effect of input parameters on flank wear is elaborated via the surface plots. The evaluation is executed and sufficiency is tested via assistance of coefficient of correlation, ANOVA and significance test (Rao et al 2017, Baskar et al 2005, Venkata et al 2010). The response (wear) equation attained through CCD model is shown below in equation 5.4.

(a)

(b)

(c)

(d)

(e)   **(f)**
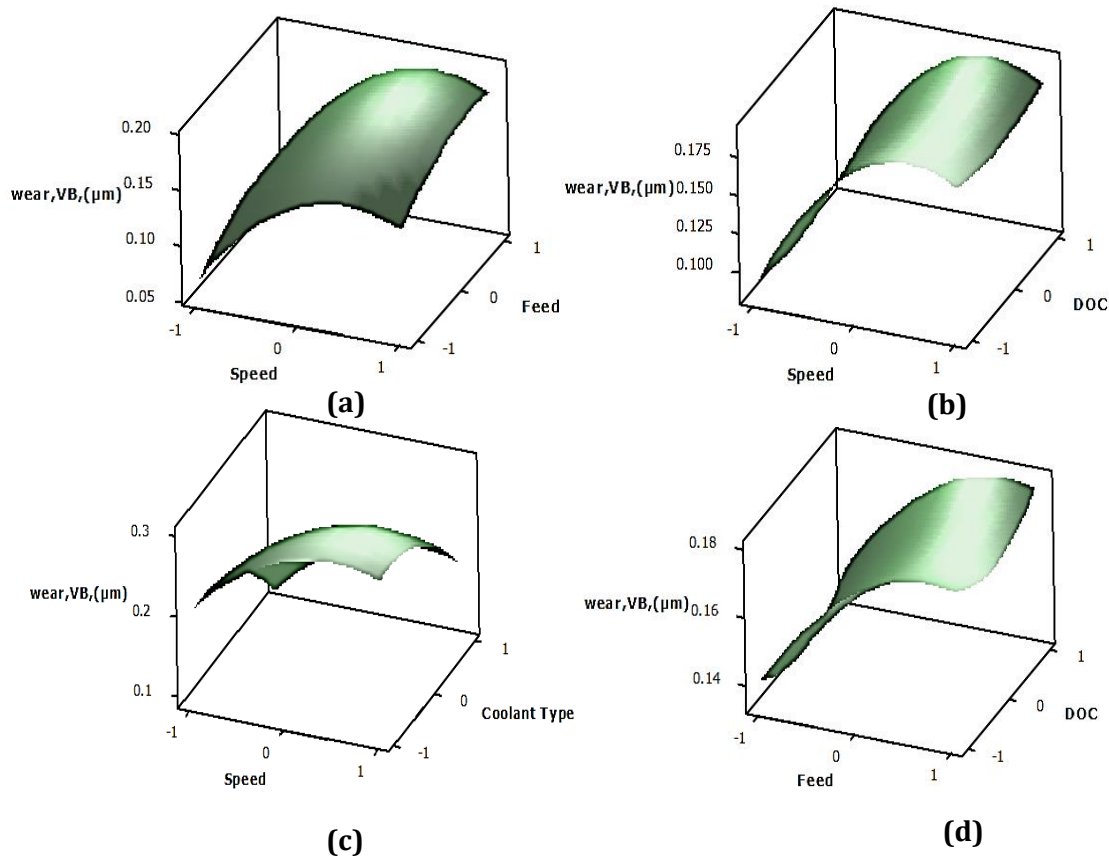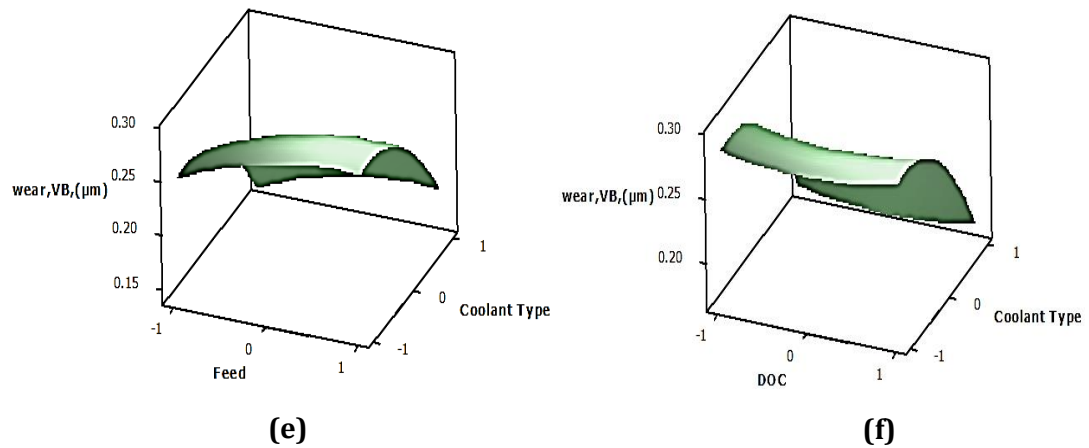
Figure 5.1: Surface plots of wear rate with (a) speed & feed (b) speed & depth of cut (c) speed & coolant type (d) feed & depth of cut (e) Feed & coolant type (f) depth of cut & coolant type

Figure 5.1 depicts the surface plots in which two variables can be simultaneously analysed while keeping rest of the parameter to its mid-value. These plots are acquired from the CCD to identify the conduct of wear variation with milling variables. The accompanying key perceptions were made to comprehend the method,

1. The response (wear) increments linearly with spindle speed and feed rate as represented in Figure 5.1(a). At higher spindle speed the contact zone between tool and the chip interface diminishes and the tool material softens due to the exposure of excess heat at the cutting edge, thus causing excess wear at the tool. Hence at higher feed rate more built up edge is caused leading to higher adhesion wear.

2. The response (wear) increases with an expansion of spindle speed and depth of cut as appeared in Figure 5.1(b). Higher depth of cut causes more friction between contacting asperities thus causing thermal softening of tool resulting in increased tool wear.

3. From the Figure 5.1(c), it can be delineated that at higher speed and using LN_2 the wear mechanism observed is only abrasion. This is due to spraying of LN_2

at cutting zone which reduces the sticking of workpiece material to cutting edge and results in less built up edge formation on tool.

4. From the Figure 5.1(d), it is observed that at higher feed rate more built up edge is caused leading to fracture of tool and formation of micro groves and more adhesion wear. Higher depth of cut leads to greater friction between tool and workpiece, subsequently causing thermal softening of tool thus resulting higher tool wear.

5. Figure 5.1(e) states that at higher feed rate by using LN_2 less adhesion wear was attained due to the less formation of built up edge on the cutting tool edge.

6. Figure 5.1(f), the significant reduction of wear rate was obveserved using LN_2. The reduction of wear rate was due to the diminishment nature of material adhesiveness and chipping at cutting edge.

Table 5.2-5.5 exhibits the ANOVA result of response attained through the CCD model. The CCD model terms such as linear and corresponding square "P" values of CCD model are found to be less than 0.05. From the Table 5.5 it can be noticed that the CCD model is observed to be adequate and fit for improving prediction of the response (wear). The generated CCD model is tested for its accuracy in predicting with the assistance of 15 test cases as shown in Table 5.2-5.5. The deviation (in terms of %) for prediction of all responses through CCD approach is demonstrated in Figure 5.2. The percent deviation varies in the range between -8.0152 to +5.3241% for CCD method in case of wet machining. The CCD design established regression equation is used to produce best milling conditions corresponding to required responses (Cus et al 2003, Zarei et al 2008, Al-Aomar et al 2018).
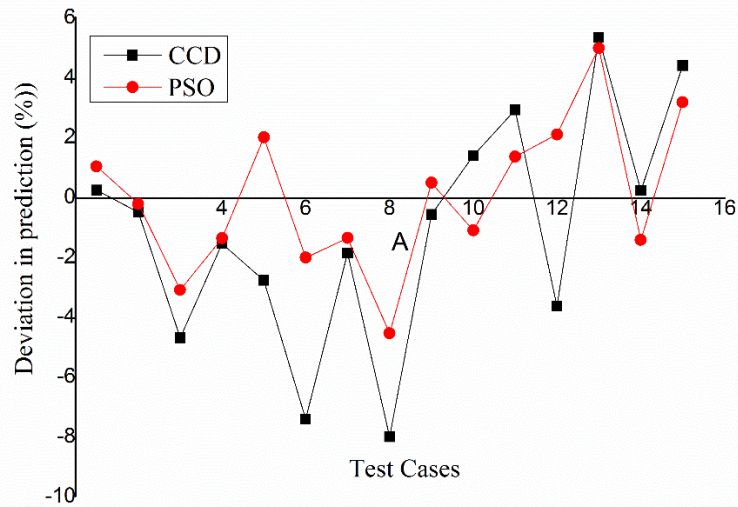
Figure 5.2: **Wear prediction deviation values (in terms of %) for fifteen test cases for LN₂ machining**

5.1.3 Comparison results of responses under wet and LN₂ machining for SS316

The Table 5.6-5.9 exhibits the ability of RSM in predicting the responses of required Cutting Temperature (CT,℃), Cutting Force (FX, N), Surface Roughness (Ra, µm) Flank Wear(VB, µm) for the given input process parameters. Table 5.6-5.9 exhibits comparison of CT, FX, Ra and VB predicted by RSM Model, with the experimentally obtained CT, FX, Ra and VB of SS316 material. From the data presented in Table 5.6 the maximum error obtained for Cutting Temperature (CT, ℃) is 14.36% at spindle speed of 1260 rpm, feed rate of 530 mm/min and depth of cut of 1.1 mm, Similarly the minimum percentage of error is 2.92 % at spindle speed of 1560 rpm, feed rate of 510 mm/min and depth of cut 1.3 mm for wet machining. The maximum error obtained in case of LN₂ machining for response Cutting Temperature (CT, ℃) is 12.31% at spindle speed of 2650 rpm, feed rate of 430 mm/min and depth of cut of 0.8 mm and the minimum percentage of error is 2.86 % at spindle speed of 1380 rpm, feed rate of 385 mm/min and depth of cut 1.1 mm. Figure 5.3 indicates the comparison between experimental and RSM predicted for the response cutting temperature (CT) under wet and LN₂ machining conditions. From the Table 5.6 it can be agreed that the RSM technique is acceptable and suitable for the prediction of experiments conducted. Also indicating that the experiments conducted are correct and suitable.

Table 5.6: Test Cases - Comparison of cutting temperature (CT, ℃) predicted by RSM with the experimentally obtained CT of SS316 for Wet and LN₂ machining.

SL. NO	Cutting Temperature (℃)								
	Experimental					Predicted		Error (%)	
	Spindle Speed (rpm)	Feed Rate (mm/min)	Depth Of Cut (mm)	Wet	LN₂	RSM Wet	RSM LN₂	Wet	LN₂
1	2110	460	1.2	163	85	148	95	9.20	11.76
2	2840	380	0.6	220	148	195	154	11.36	4.05
3	1750	365	0.8	162	68	141	75	12.96	10.29
4	1280	420	1.4	154	49	134	45	12.94	8.16
5	2007	455	0.9	193	80	200	89	3.63	11.25
6	1560	510	1.3	171	92	166	103	2.92	11.96
7	2650	430	0.8	209	130	183	146	12.44	12.31
8	1260	530	1.1	188	38	161	42	14.36	10.53
9	2315	520	0.7	192	119	169	129	11.98	8.40
10	1380	385	1.1	161	70	152	68	5.59	2.86
11	2540	490	1.2	200	126	187	142	6.50	12.70
12	1870	525	1.4	194	77	200	85	3.09	10.39
13	2740	415	0.9	213	134	196	154	7.98	12.06
14	2290	375	0.7	197	109	171	122	13.20	11.93
15	2460	520	0.4	201	121	174	135	12.43	11.57
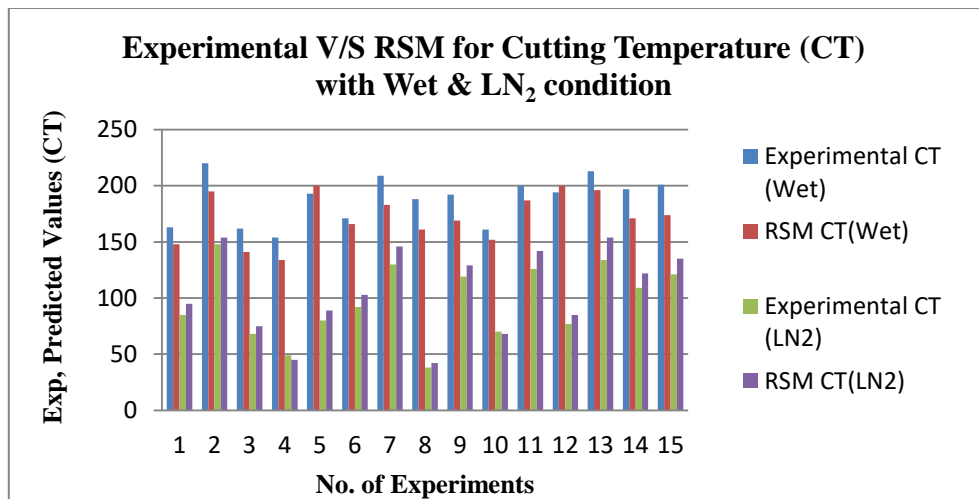
Figure 5.3: Represents the experimental v/s RSM predicted for response (CT) under wet and LN₂ machining conditions

Table 5.7: Test Cases - Comparison of cutting force (FX, N) predicted by RSM with the experimentally obtained CT of SS316 for Wet and LN₂ machining.

SL. NO	Spindle Speed (rpm)	Feed Rate (mm/min)	Depth Of Cut (mm)	Wet	LN₂	RSM Wet	RSM LN₂	Wet	LN₂
				Cutting Force (N)					
		Experimental				Predicted		Error (%)	
1	2110	460	1.2	209	118	216	127	3.35	7.63
2	2840	380	0.6	287	187	300	201	4.53	7.49
3	1750	365	0.8	193	102	201	113	4.15	10.78
4	1280	420	1.4	177	84	192	92	8.47	9.52
5	2007	455	0.9	200	113	208	124	4.00	9.73
6	1560	510	1.3	186	98	197	107	5.91	9.18
7	2650	430	0.8	256	168	284	188	10.94	10.90
8	1260	530	1.1	171	80	189	89	10.53	10.14
9	2315	520	0.7	227	136	246	151	8.37	10.23
10	1380	385	1.1	181	91	190	101	4.97	10.95
11	2540	490	1.2	245	153	272	171	11.02	10.76
12	1870	525	1.4	198	109	205	121	3.54	10.01
13	2740	415	0.9	269	177	293	193	8.92	9.04
14	2290	375	0.7	213	121	189	122	11.27	0.83
15	2460	520	0.4	238	145	256	161	7.56	11.03

Similarly, From the Table 5.7 it can be observed that, the maximum error obtained for Cutting Force (FX, N) in case of wet machining is 11.27% at spindle speed of 2290 rpm, feed rate of 375 mm/min and depth of cut of 0.7 mm. Similarly, the minimum percentage of attained error is 3.35 % at spindle speed of 2110 rpm feed rate of 460 mm/min and depth of cut 1.2 mm. The maximum error obtained in case of LN₂ machining for response Cutting Force (FX, N) **is** 11.03% at spindle speed of 2460 rpm, feed rate of 520 mm/min and depth of cut of 0.4 mm and the minimum percentage of error is 0.83 % at spindle speed of 2290 rpm, feed rate of 375 mm/min and depth of cut 0.7 mm. Figure 5.4 indicates the comparison between experimental and RSM predicted for the response cutting force (FX) under wet and LN₂ machining conditions.
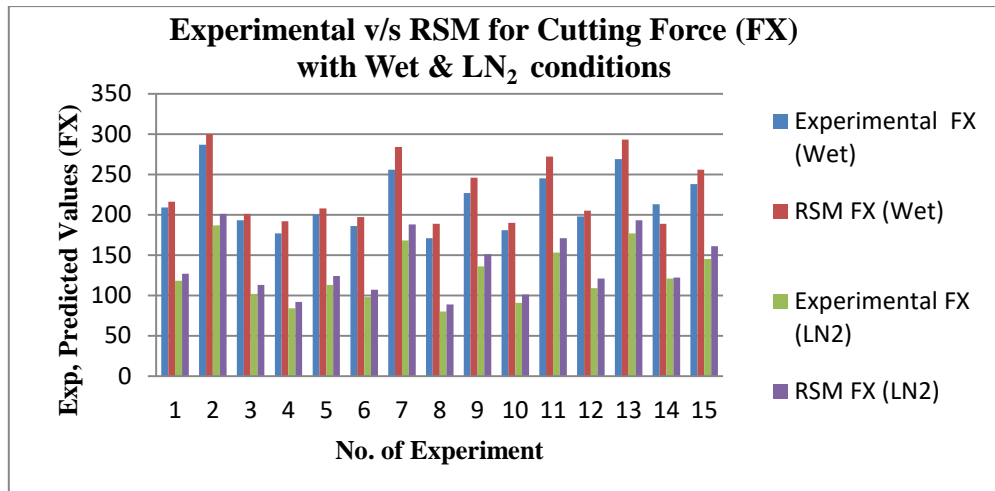
Figure 5.4: Represents the experimental v/s RSM predicted for response cutting force (FX) under wet and LN2 machining conditions.

From the data represented in Table 5.8, it can be seen that the maximum error obtained for Surface Roughness (Ra, µm) in case of wet machining is 13.09% at spindle speed of 1750 rpm, feed rate of 365 mm/min and depth of cut of 0.8 mm. Similarly, the minimum percentage of attained error is 7.18 % at spindle speed of 2007 rpm feed rate of 455 mm/min and depth of cut 0.9 mm. The maximum error obtained in case of LN_2 machining for response Cutting Force (FX, N) is 12.73 % at spindle speed of 1280 rpm, feed rate of 420 mm/min and depth of cut of 1.4 mm and the minimum percentage of error is 9.38 % at spindle speed of 1750 rpm, feed rate of 365 mm/min and depth of cut 0.8 mm. Figure 5.5 indicates the comparison between experimental and RSM predicted for the response surface roughness (Ra) under wet and LN_2 machining conditions.

Table 5.8: Test Cases - Comparison of surface roughness (Ra, μm) predicted by RSM with the experimentally obtained CT of SS316 for Wet and LN$_2$ machining.

SL. NO	Surface Roughness (Ra, μm)								
	Experimental					Predicted		Error (%)	
	Spindle Speed (rpm)	Feed Rate (mm/min)	Depth Of Cut (mm)	Wet	LN$_2$	RSM Wet	RSM LN$_2$	Wet	LN$_2$
1	2110	460	1.2	2.13	1.1	2.31	1.23	8.45	11.82
2	2840	380	0.6	2.62	1.46	2.93	1.61	11.83	10.27
3	1750	365	0.8	1.91	0.96	2.16	1.05	13.09	9.38
4	1280	420	1.4	1.73	0.55	1.91	0.62	10.40	12.73
5	2007	455	0.9	2.09	1.08	2.24	1.21	7.18	12.04
6	1560	510	1.3	1.83	0.89	2.05	0.98	12.02	10.11
7	2650	430	0.8	2.47	1.3	2.69	1.44	8.91	10.77
8	1260	530	1.1	1.71	0.42	1.85	0.47	8.19	11.90
9	2315	520	0.7	2.26	1.19	2.55	1.31	12.83	10.08
10	1380	385	1.1	1.77	0.64	1.99	0.72	12.43	12.50
11	2540	490	1.2	2.35	1.28	2.59	1.44	10.21	12.50
12	1870	525	1.4	1.99	1.01	2.18	1.12	9.55	10.89
13	2740	415	0.9	2.56	1.37	2.87	1.52	12.11	10.95
14	2290	375	0.7	2.22	1.16	2.5	1.29	12.61	11.21
15	2460	520	0.4	2.31	1.21	2.57	1.35	11.26	11.57
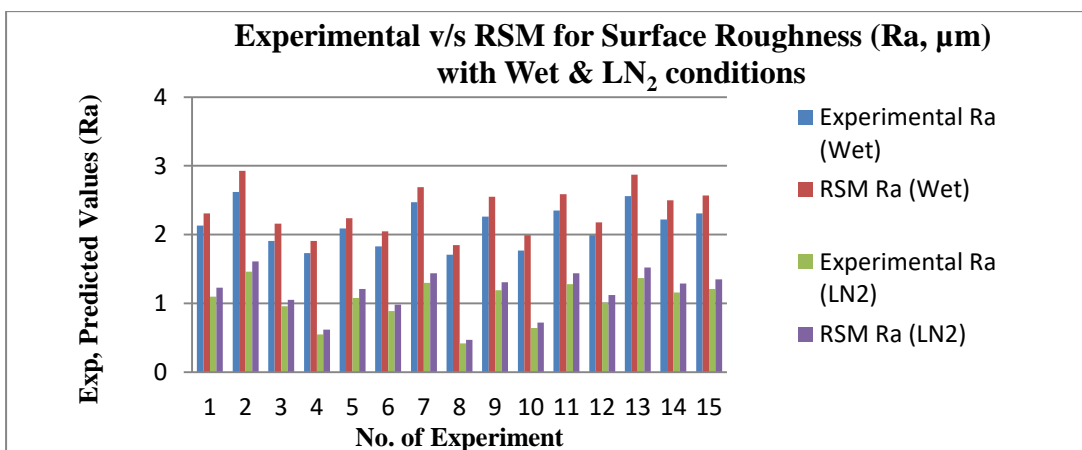
Figure 5.5: Represents the experimental v/s RSM predicted for response Surface roughness (Ra) under wet and LN$_2$ machining conditions.

Table 5.9: Test Cases - Comparison of flank-wear Rate (VB, μm) predicted by RSM with the experimentally obtained CT of SS316 for Wet and LN$_2$ machining.

SL. NO	Flank-Wear Rate (μm)								
	Experimental					Predicted		Error (%)	
	Spindle Speed (rpm)	Feed Rate (mm/min)	Depth Of Cut (mm)	Wet	LN$_2$	RSM Wet	RSM LN$_2$	Wet	LN$_2$
1	2110	460	1.2	2.29	1.51	2.56	1.63	11.79	7.95
2	2840	380	0.6	2.51	1.93	2.31	2.15	7.97	11.40
3	1750	365	0.8	1.96	0.86	2.15	0.77	9.69	10.47
4	1280	420	1.4	1.82	0.74	1.65	0.66	9.34	10.81
5	2007	455	0.9	2.22	1.49	2.06	1.64	7.21	10.07
6	1560	510	1.3	1.87	0.78	2.1	0.69	12.30	11.54
7	2650	430	0.8	1.14	0.53	1.26	0.59	10.53	11.32
8	1260	530	1.1	0.68	0.37	0.61	0.41	10.29	10.81
9	2315	520	0.7	2.16	1.43	2.31	1.57	6.94	9.79
10	1380	385	1.1	1.69	0.68	1.85	0.61	9.47	10.29
11	2540	490	1.2	2.32	1.57	2.56	1.75	10.34	11.46
12	1870	525	1.4	2.07	1.12	1.89	1.25	8.70	11.61
13	2740	415	0.9	2.69	1.99	2.92	1.77	8.55	11.06
14	2290	375	0.7	2.18	1.41	2.36	1.55	8.26	9.93
15	2460	520	0.4	2.41	1.63	2.13	1.44	11.62	11.66
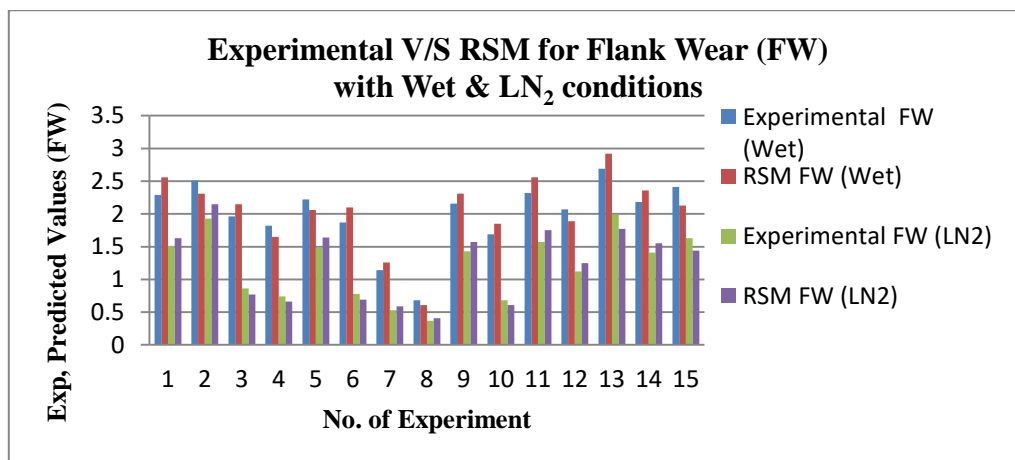
Figure 5.6: Experimental v/s RSM predicted for response Flank Wear (FW) under wet and LN$_2$ machining conditions

From Table 5.9, it can be derived that, the maximum error obtained for Surface Roughness (Ra, μm) in case of wet machining is 12.30 % at spindle speed of 1560 rpm, feed rate of 510 mm/min and depth of cut of 1.3 mm. Similarly, the minimum percentage of attained error is 6.94 % at spindle speed of 2315 rpm feed rate of 520 mm/min and depth of cut 0.7 mm. The maximum error obtained in case of LN_2 machining for response Cutting Force (FX, N) is 11.61 % at spindle speed of 1870 rpm, feed rate of 525 mm/min and depth of cut of 1.4 mm and the minimum percentage of error is 7.95 % at spindle speed of 2110 rpm, feed rate of 460 mm/min and depth of cut 1.2 mm. Figure 5.6 indicates the comparison between experimental and RSM predicted for the response Flank wear (FW) under wet and LN_2 machining conditions.

5.1.4 Summary

The effect of process parameters of SS316 on CT, FX, Ra and VB of machined components for milling in different conditions (wet and LN_2), has been investigated experimentally. The experiments were carried out as per orthogonal array (OA) in order to identify the effects of input parameters such as Spindle speed, Feed Rate and Depth of cut on the performance attributes.

- ❖ RSM modelling developed has produced quite satisfactory predictions for the Output of milling operation in different conditions (Wet and LN2), which is indicated again by the validation experiments.
- ❖ RSM modelling also helps in understanding the correctness of the conducted experiments and suitability.
- ❖ RSM technique leads in predicting the single response individually thus reducing the importance of the other responses. Hence, a multi-objective optimization is advisable   in case of more than one response.

Further, the same data is used for prediction of the responses using artificial neural network (ANN) using various back propagation algorithms. The neural network based approach has been incorporated in the study, as few literatures suggest that neural network (NN) techniques are well suited to predict the non-linear behaviour of the system.

ANN MODELLING FOR PREDICTION

5.2 ANN MODEL DEVELOPMENT TO PREDICT RESPONSES OF SS316

5.2.1 Neural Network Modelling

Neural networks are nonlinear mapping systems consisting of neurons and weighted connection links, which consist of user-defined inputs and produce an output that reflects the information stored in connections during training (Azlan et al 2018, Karkalos et al 2016). In this study, a multilayer neural network consisting of three layers, i.e., input, hidden, and output layer, was considered. In this study, several back propagation training algorithms have been tested, including gradient descent with momentum and adaptive learning method, scaled conjugate gradient descent algorithm, Levenberg–Marquardt algorithm and the Bayesian regularization. In addition, the Levenberg–Marquardt with Bayesian regularization is used to improve the generalization capability of the neural networks (Prashant et al 2021, Kuldip et al 2016). In all of those neural network models, the nonlinear *tanh* activation functions are used in the hidden layer, and input data are normalized in the range of [-1,1]. Linear activation functions are used in the output layer (Venkatesh et al 2018, Sener et al 2015). The weights and biases of the network are initialized to small random values to avoid immediate saturation in the activation functions. The data set is divided into two sets as training and test sets (Farag Abdallah et al 2019, Ireneusz et al 2017). Neural networks are trained by using training data set, and their generalization capacity is examined by using test sets. The training data were never used in test data. Matlab's neural network toolbox is used to train neural networks. Simulations with test data repeated many times with different weight and bias initializations.

5.2.2 Prediction of Cutting Temperature (CT,℃), Cutting Force (FX, N), Surface Roughness (Ra, µm) Flank Wear(VB, µm)

The responses Cutting Temperature (CT,℃), Cutting Force (FX, N), Surface Roughness (Ra, µm) Flank Wear(VB, µm) are predicted with a trained feed-forward neural network. Spindle Speed, feed rate and depth of cut are used as inputs to neural network. These neural networks are trained with 18 data sets without including 9 data

sets. Training algorithms and network architectures are selected for minimum root-mean-squared (RMS) error for best predictions using a training procedure. Selection process for the ANN architecture includes identifying first most optimum training algorithm and most optimum number of hidden layer neurons for a minimized RMS error (Girish et al 2017). Hence, the number of neurons in the hidden layer is decided by choosing the network structure that minimizes the RMS error with trial-and-error. The results of these tests are summarized in Table 3. The data used for modelling without random noise has been taken care. In the present study the noise refers to:

1) The Ethernet cable used is shielded as per the industrial ISO standard format nullifying the noise.

2) The machine used for carry out the experiment is a rigid industrial type 3-axis standard CNC machine in a good condition without any significant noise.

3) All experiments are conducted with proper operating ambient conditions.

4) No other electronic sensors are used during experiments.

5) The data being prepared for neural networks model are properly normalized.

The experimental data are found to be in normal condition without the occurrence of any abnormality.

A. Scope

In this section, it is proposed to formulate a Neural Network based approach (ANN) with incorporation of various back propagation algorithm to predict the responses of SS316 Cutting Temperature (CT,℃), Cutting Force (FX, N), Surface Roughness (Ra, µm) Flank Wear (VB, µm) with the input parameters being spindle speed, feed rate and depth of cut.

B. Data Collection

The data for training the ANN network proposed for response prediction in SS316 is collected from the experiments carried out on milling. The data are listed in Table 5.1.

C. Neural Network Training

In any FFNN application even today, the exact architecture to be used needs to be found (Reddy et al. 2005). More often than not, this is a trial and error exercise, as regards to the selection of a number of hidden layers and neurons in each of these layers. In this application, training was started with one hidden layer from 3 to 7 neurons in each hidden layer. The minimum mean squared error (MSE) was set as 0.0001. Initially, during training, the learning rate parameter and momentum factor were preferred as 0.5 each. The number of hidden neurons was fixed based on MSE and the mean error in prediction of training data. Single hidden layer was tried out to obtain the minimum MSE. It was observed that the network converges well with a single hidden layer when tried with a different number of nodes varying from 3 to 7 in the hidden layer. Here the training was started with varying learning rates from 0.1 to 0.9 in steps of 0.05. The learning rate and the momentum parameters were initially taken as 0.3 and 0.9, respectively, for training. For all patterns, p, the global error function is expressed in terms of MSE (Yagnanarayana 2008) and is given by equation 5.5

$$E = \Sigma E_P = \left(1/p\right) \Sigma\Sigma \left(b_{kp} - S_{kp}^{0}\right)^2 \qquad (5.5)$$

Where, b_{kp} is the actual output and S_{kp}^{0} is the network output for the Kth output neuron for the pth pattern.

The mean error in the output prediction is shown in equation 5.6 (Reddy et al. 2005)

$$E_{tr}(x) = 1/N \ S \ |(b_k(x) - P_k(x))| \qquad (5.6)$$

Where, $E_{tr}(x)$ is the mean error in prediction of training data set for output parameter x, N is the number of the data sets, $b_k(x)$ is the actual output and $P_k(x)$ is the predicted output. The following sigmoid function as represented in equation 5.7 was used as the activation function (Reddy et al. 2008, Mandal et al. 2009, Reddy et al. 2005, Li, Liu and Xiong 2002, Mousavi et al.2007, Haque and Sudhakar 2002).

$$F(x) = 1/ (1+\exp (-x)) \qquad (5.7)$$

5.2.3 Training of the Neural Identifier

Identification requires setting up a suitably parameterized identification model and adjustment of these parameters of the model to optimize a performance function based on the error between the outputs from the plant and the identification model (Gianni et al 2014). It is assumed that the weight matrices of the neural network proposed as the identifier exists, for which, both plant and the identifier have the same output for any specified inputs, for the same initial conditions (Yu et al 2015, Malghan et al 2015). The system under consideration is simulated at different operating conditions for a wide range of the steady state active power flow level in the tie-line flowing between the two areas to generate data for training. During training the weights and biases of the network are iteratively adjusted to minimize the network performance function. The performance function used for the neural identifier under consideration is the mean square error, MSE, given by equation 5.8.

$$V = \frac{1}{N} \sum_{q=1}^{N} \left(P_{12_q} - \hat{P}_{12_q} \right)^2 = \frac{1}{N} \sum_{q=1}^{N} (e_q)^2$$

(5.8)

Where, N is the size of the training dataset P_{12} and $\hat{P}_{12}$ are the target and predicted value of the output of the neural network when the qth input is presented and e is the error (difference between the target and predicted value) for the qth input. The performance index V in (Zhou et al 2017) is a function of weights and biases, $x = [x_1,x_2,x_3...X_n]$ and can be given by equation 5.9.

$$V(x) = \frac{1}{N} \sum_{q=1}^{N} e_q^2(x)$$

(5.9)

The performance of the neural network can be improved by modifying x till the desired level of the performance index, is achieved. This is achieved by minimizing V(x) with respect to and the gradient required for this is given by equation 5.10

$$\nabla V(x) = J^T(x) e(x)$$

(5.10)

Where, J(x) is the Jacobian matrix given by

$$J(x) = \begin{bmatrix} \dfrac{\partial e_{1(x)}}{\partial x_1} & \cdots & \dfrac{\partial e_{1(x)}}{\partial x_n} \\ \vdots & \ddots & \vdots \\ \dfrac{\partial e_{N(x)}}{\partial x_1} & \cdots & \dfrac{\partial e_{N(x)}}{\partial x_n} \end{bmatrix}$$

And *e(x)* is the error for all the inputs. The gradient in (Tandon et al 2008) is determined using backpropagation, which involves performing computations backward through the network. This gradient is then used by different algorithms to update the weights of the network. These algorithms differ in the way they use the gradient to update the weights of the network and are known as the variants of the Backpropagation algorithm. This work compares the performance of the basic implementation of the Backpropagation algorithm i.e. Gradient descent algorithm with other variants in order to investigate the potentials of these algorithms for online applications in power system identification. A brief overview of the different algorithms considered in this work is given under:

i) Gradient Descent algorithm (GD): The network weights and biases, is modified in a direction that reduces the performance function in (Jingchao et al 2020) most rapidly i.e. the negative of the gradient of the performance function (Shixu Sun et al 2019). The updated weights and biases in this algorithm are given by equation 5.11.

$$x_{k+1} = x_k - \alpha_k \nabla V_k$$

(5.11)

Where, x_k is the vector of the current weights and biases, ΔV_k is the current gradient of the performance function and α_k is the learning rate.

ii) Scaled Conjugate Gradient Descent algorithm (SCGD):
The gradient descent algorithm updates the weights and biases along the steepest descent direction but is usually associated with poor convergence rate as compared to the Conjugate Gradient Descent algorithms, which generally result in faster convergence (Dongdong et al 2016). In the Conjugate Gradient Descent algorithms, a search is made along the conjugate gradient direction to determine the step size that minimizes the performance function along that line. This time consuming line search is required during all the iterations of the weight update. However, the Scaled Conjugate Gradient Descent algorithm does not require the computationally expensive line search

and at the same time has the advantage of the Conjugate Gradient Descent algorithms (Sohyung Cho et al 2015). The step size in the conjugate direction in this case is determined using the Levenberg-Marquardt approach. The algorithm starts in the direction of the steepest descent given by the negative of the gradient as shown in equation 5.12.

$$p_o = -\nabla V_o$$
(5.12)

The updated weights and biases are then given by equation 4.13

$$x_{k+1} = x_k + \alpha_k p_k$$
(5.13)

Where, α_k is the step size determined by the Levenberg-Marquardt algorithm (Chen Zhang et al 2015). The next search direction that is conjugate to the previous search directions is determined by combining the new steepest descent direction with the previous search direction and is given by equation 5.14.

$$p_k = -\nabla V_k + \beta_k p_{k-1}$$
(5.14)

The value of β_k is as given in (Yao-Wen et al 2008), by equation 5.15

$$\beta_k = \frac{|\nabla V_{k+1}|^2 - \nabla V_{k+1} \nabla V_k}{\mu_k}$$
(5.15)

Where μ_k is given by equation 5.16

$$\mu_k = p_k{}^T \nabla V_k$$
(5.16)

iii) Levenberg-Marquardt algorithm (LM):

Since the performance index in (Ali et al 2019) is sum of squares of non-linear function, the numerical optimization techniques for non-linear least squares can be used to minimize this cost function. The Levenberg-Marquardt algorithm, which is an approximation to the Newton's method is said to be more efficient in comparison to other methods for convergence of the Backpropagation algorithm for training a moderate-sized feedforward neural network (Zhang et al 2015). As the cost function is a sum of squares of non-linear function, the Hessian matrix required for updating the

weights and biases need not be calculated and can be approximated as shown in equation 5.17.

$$H = J^T(x)J(x)$$

(5.17)

The updated weights and biases are given by equation 5.18.

$$x_{k+1} = x_k - [J^T(x)J(x) + \mu I]^{-1} J^T(x)e(x)$$

(5.18)

iv) Bayesian Regularization (BR):

Regularization as a mean of improving network generalization is used within the Levenberg-Marquardt algorithm. Regularization involves modification in the performance function. The performance function for this is the sum of the squares of the errors and it is modified to include a term that consists of the sum of squares of the network weights and biases. The modified performance function is given by equation 5.19.

$$F_{reg} = \beta SSE + \alpha SSW$$

(5.19)

Where SSE and SSW are given by equations 5.20 and 5.21

$$SSE = \sum_{q=1}^{N} e_q^2(x)$$

(5.20)

$$SSW = \sum_{j=1}^{n} w_j^2$$

(5.21)

Where, n is the total number of weights and biases, W_j in the network. The performance index in (5.19) forces the weights and biases to be small, which produces a smoother network response and avoids over fitting. The values of α and β are determined using Bayesian Regularization in an automated manner (Lela et al 2009, Gu et al 2020, Dong et al 2020).

Feed forward neural networks are well-known modelling tools for complex nonlinear problems. The aim is always to infer the function from the given data set. The data set usually consists of input vectors x and corresponding target vectors t. Neural networks parameterize the unknown function by means of parameter vector w, which leads to a

nonlinear function y(x; w) (Wang et al 2020). By inferring the parameter w, the function y(x; w) is inferred as well. This is achieved by adjusting w so as to minimize an error function (Ali et al 2019, Hu et al 2019), which is usually the sum-of-squares error (SSE). The process of adjusting w is also called learning or training. This research uses the BNN modelling approach. BNN gives a probabilistic interpretation to the network learning process. The SSE function is expressed in terms of the likelihood function representing probability of the observed data when the parameters are known (Chen et al 2019). This function is usually taken to be a separable Gaussian assuming zero-mean Gaussian noise on the target variables and the hyperparameter ß controls the variance of the noise (Muzaffer et al 2018, Yeganefar et al 2019). BNN includes regularization, and the regularizer is interpreted as prior probability distribution over the parameters. For a weight decay regularizer, prior distribution is a Gaussian where variance is governed by the hyperparameter (Yeganefar et al 2019). Once the likelihood function and a prior distribution have been determined, the Bayes' theorem can be used to find the posteriori distribution of the network weights. Having found the posteriori distribution, predictions can be made by marginalization over the parameters (Garcia et al 2015, Kong et al 2016, Jingchao et al 2020). (BNN automatically controls the network complexity, so there is no need for validation data set and cross-validation procedure.

BNN model used in this study consists of three layers and a hidden layer of six neurons. The input layer is composed of three neurons. The output layer has four neuron and a linear activation function. Among 31 datasets, 18 are used for training cycle and remaining 9 are used for testing and validation with 4 datasets. To optimize BNN weights w, the scaled conjugate gradient algorithm (Lela et al 2009) has been used. The final values of the hyper parameters have been obtained as a=2.88, ß=20.39. The R values of 0.987 and 0.984 have been obtained for training and testing, respectively. The purpose of a set of data sets (exclusive) for testing is to verify the generality of the ANN model for accurate interpolation in the given domain of the problem

Table 5.10 Statistical comparison of different training algorithms.

SL. NO	Output	Network Structure	RMS Error			
			Gradient descent w/momentum & adaptive learning	Scaled Conjugate Gradient Descent	Levenberg Marquart	Bayesian regularization
1	Surface Roughness Ra(μm)	3-5-1	9.0338	8.0692	8.9047	7.355
2	Cutting Force Fx (N)	3-5-1	5.5874	7.5351	4.7693	3.3894
3	Cutting Temperature (℃)	3-5-1	7.0313	5.6074	4.4586	4.0291
4	Flank Wear, Vb, (μm)	3-5-1	5.939	6.0197	5.5612	5.0764
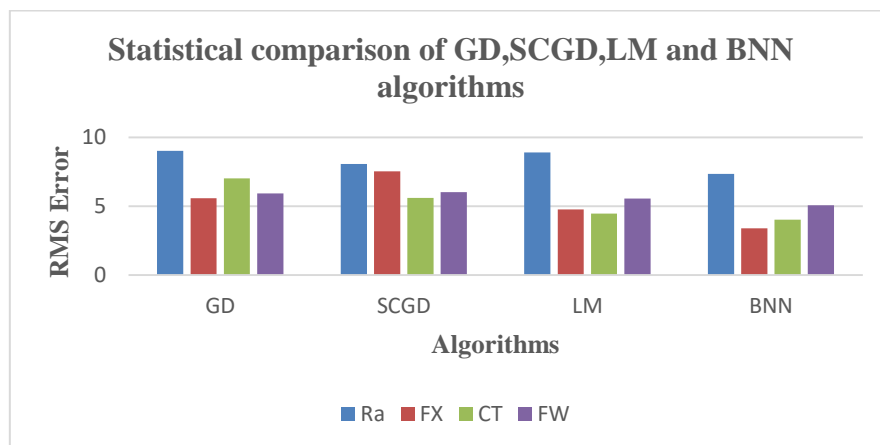
Figure 5.7: Statistical RMS error comparison between GD, SCGD, LM and BNN algorithms

5.2.4 Analysis of Results and Discussion

The validation of all models was performed with the testing data set. Relative errors obtained using RSM and BNN methodologies have been compared, and the results of testing are shown in Table 5.11-5.13. The average relative errors for RSM and BNN models are clearly indicated for responses (CT, FX, Ra, FW) in Table 5.11-5.13 for the test cases. Thus from the Table 5.10 the results attained indicate that the BNN model offers the best prediction capability compared to rest of the back propagation algorithms. So in upcoming chapter of optimization the BNN is taken in to account to

compare with Support vector regression technique. Figure 5.7 represents the statistical RMS error comparison between GD, SCGD, LM and BNN algorithms. Figure 5.8 represents the output response cutting temperature (CT) comparison between experimental, RSM and BNN. Figure 5.9 represents the output response cutting force (FX) comparison between experimental, RSM and BNN. Figure 5.10 represents the output response surface roughness (Ra) comparison between experimental, RSM and BNN. Figure 5.11 represents the output response Flank Wear (FW) comparison between experimental, RSM and BNN.

Table 5.11: Summary of the test cases results for the response: Cutting temperature (CT) for LN$_2$ condition.

Exp. NO	Experimental CT	RSM	BNN	Relative Error Obtained by RSM (%)	Relative Error Obtained by BNN (%)
1	48	53	50	10.42	4.17
2	57	62	60	8.77	5.26
3	70	77	66	10.00	5.71
4	62	58	66	6.45	6.45
5	73	79	70	8.22	4.11
6	86	93	89	8.14	3.49
7	68	74	71	8.82	4.41
8	89	96	93	7.87	4.49
9	97	104	92	7.22	5.15
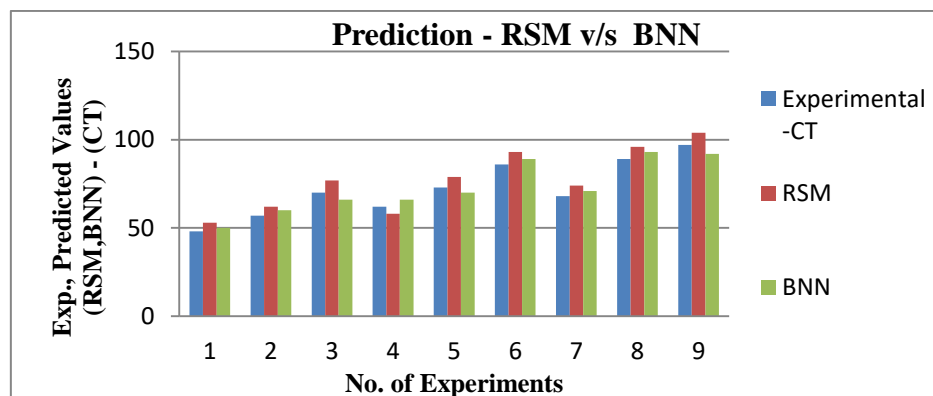
Figure 5.8: Output response cutting temperature (CT) comparison between experimental, RSM and BNN

Table 5.12: Summary of the test cases results for the response: Cutting force (FX) for LN$_2$ condition.

Exp. NO	Experimental FX	RSM	BNN	Relative Error Obtained by RSM (%)	Relative Error Obtained by BNN (%)
1	107	99	101	7.48	5.61
2	125	135	131	8.00	4.80
3	156	171	167	9.62	7.05
4	92	101	96	9.78	4.35
5	109	119	116	9.17	6.42
6	131	141	139	7.63	6.11
7	77	84	80	9.09	3.90
8	89	97	94	8.99	5.62
9	110	119	115	8.18	4.55
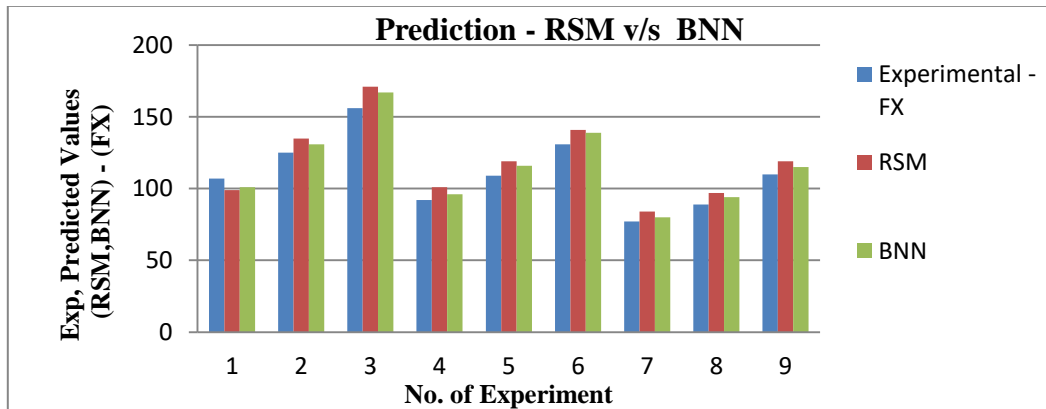
Figure 5.9: Output response cutting force (FX) comparison between experimental, RSM and BNN

Table 5.13: Summary of the test cases results for the response: Surface Roughness (Ra) for LN$_2$ condition.

Exp.NO	Experimental Ra	RSM	BNN	Relative Error Obtained by RSM (%)	Relative Error Obtained by BNN (%)
1	1.36	1.47	1.44	8.09	5.88
2	1.77	1.84	1.81	3.95	2.26
3	1.93	2.09	1.98	8.29	2.59
4	1.12	1.2	1.17	7.14	4.46
5	1.4	1.32	1.45	5.71	3.57
6	1.67	1.76	1.62	5.39	2.99
7	0.83	0.9	0.87	8.43	4.82
8	1.26	1.35	1.31	7.14	3.97
9	1.38	1.47	1.44	6.52	4.35
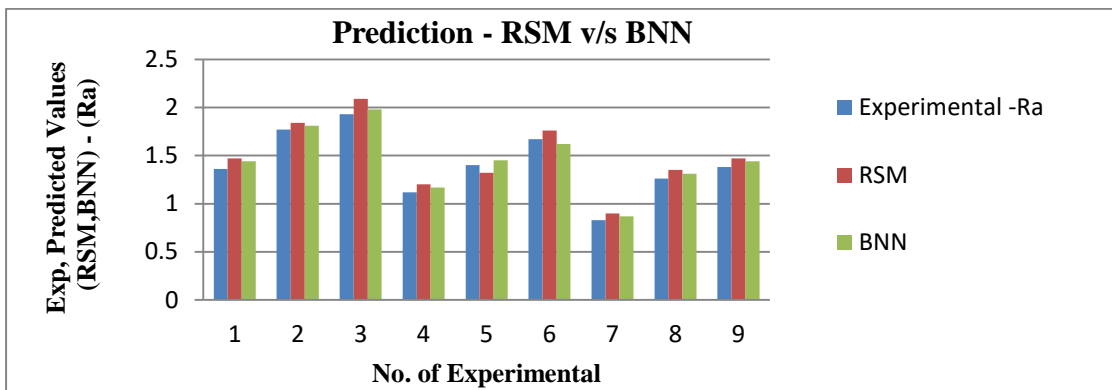
Figure 5.10: Output response surface roughness (Ra) comparison between experimental, RSM and BNN.

Table 5.14: Summary of the test cases results for the response: Flank Wear (FW) for LN$_2$ condition.

Exp.NO	Experimental FW	RSM	BNN	Relative Error Obtained by RSM (%)	Relative Error Obtained by BNN (%)
1	1.31	1.39	1.26	6.11	3.82
2	1.78	1.95	1.92	9.55	7.87
3	1.42	1.57	1.48	10.56	4.23
4	0.89	0.97	0.84	8.99	5.62
5	1.66	1.82	1.76	9.64	6.02
6	1.05	1.14	1.11	8.57	5.71
7	0.49	0.53	0.47	8.16	4.08
8	1.1	1.17	1.14	6.36	3.64
9	0.93	0.87	0.97	6.45	4.30
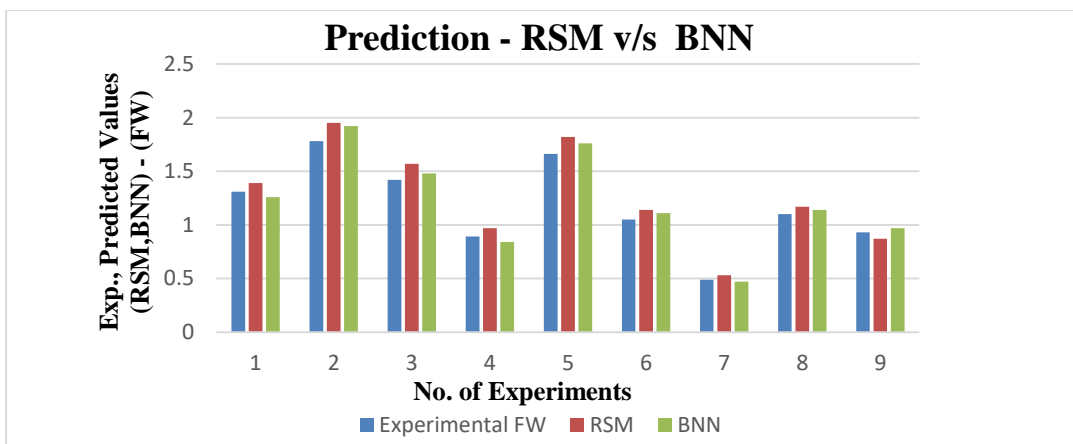
Figure 5.11: Output response flank wear (FW) comparisons between experimental, RSM and BNN

After the validation of the models, a simulation of the prediction, using the best model, was performed. The simulation was carried out by varying two cutting parameters, while the third is kept constant. Figure 5.12 shows how the surface roughness depends on the feed and depth of cut in the case when the spindle speed of 2000 (rpm) is kept constant. It can be seen that both factors influence on Ra but the feed is by far more dominant factor.

Figure 5.13 shows the influence of the spindle speed and feed on the surface roughness for the invariable depth of cut of 1 (mm). It is obvious that Ra decreases when the spindle speed increases and the feed simultaneously decreases. The feed is again, by far, a more influential factor.

The influence of the spindle speed and depth of cut on the surface roughness for the constant feed of 450 (mm/min) is shown on Figure 5.14. Both factors show the similar intensity of influence on Ra. The surface roughness decreases if the spindle speed increases.

Generally, the surface roughness decreases with the increase of spindle speed. This is usually explained relating to the type of chip formation and built-up edge generated from the machining process. At very low spindle speed, discontinuous chip formation occurs, which gives a poor surface finish. As the spindle speed increases, the chip formation becomes less discontinuous, and the surface finish improves. Further increase of spindle speed reduces the size of the built-up edge until a continuous chip is formed, and then, surface roughness approaches a steady low value.

Considering the fact that the research has been made above the spindle speed range where built-up edge appears, the increase of spindle speed leads to the decrease of surface roughness. Further increase of the spindle speed causes tool wear, and that maintains approximate constant value of surface roughness.

The feed rate is the most significant factor associated with surface roughness. When feed rate increases, surface roughness increases too. The selection of the feed rate must

be performed carefully, because apart from the strong influence on Ra, excessive feed increases cutting forces, tool deflections, tool wears, chipping, etc.

In comparison with spindle speed and feed, the depth of cut has a minor influence on surface roughness. From a geometrical point of view, depth of cut has not influence surface roughness because the height and form of the roughness profile are independent of the depth of cut. The depth of cut has indirect influence on surface roughness through the formation of the built-up edge, chip deformation, cutting force, cutting temperature, vibration, etc.
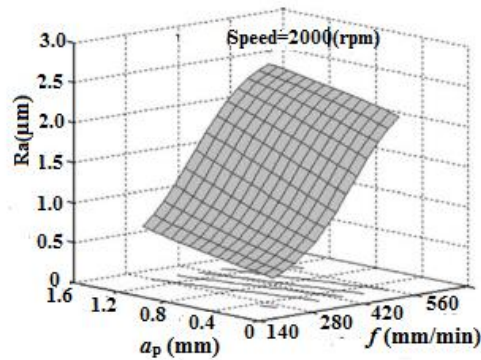
Figure 5.12: Influence of feed and depth of cut on surface roughness for constant spindle speed of 2000(rpm).
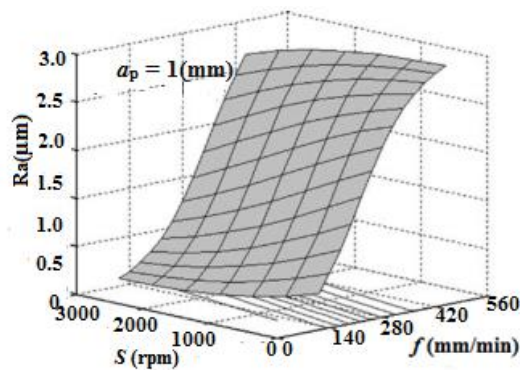
Figure 5.13: Influence of spindle speed and feed on surface roughness for constant depth of cut 1(mm).
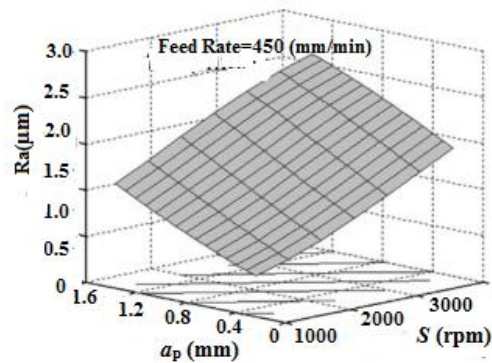
Figure 5.14: Influence of spindle speed and depth of cut on surface roughness for constant feed of 450 (mm/min).

The Gradient Descent algorithm was very slow in converging for the required value of the performance index. The time required for training the network using the BNN was the least whereas, maximum time was required for training the network using the Scaled Conjugate Gradient Descent algorithm. The training algorithm employing Levenberg-Marquardt algorithm continuously modifies its performance function and hence, takes more time as compared to the Bayesian Regularization but this time is still far less than the Scaled Conjugate Gradient Descent method. From Table 5.10, it can be established that the Bayesian Regularization is the fastest of all the training algorithms considered in this work for training a neural network.

A neural network has been proposed to predict the responses on the basis of the values of the input variables. The proposed neural network is trained using different variants of the Back propagation algorithm. Investigations in to the training performance of the different algorithms establish that the Levenberg-Marquardt algorithm is the fastest to converge. Comparison of the predictions made by the different neural networks reveal that the neural network trained using the BNN algorithm gives the most accurate predictions. The fast convergence teamed with good predictive quality makes Bayesian regularization algorithm are the most suitable choice of all the variants considered in this work for training a neural network for this application.

Table 5.15 Information on back propagation algorithms / Training algorithms.

Sl.NO/ Training Algorithms	Gradient descent	Scaled Conjugate Gradient Descent	Levenberg-Marquardt	Bayesian Regularization
1	Requiring many iterations for functions which have long, narrow valley structures	This method also avoids the information requirements associated with the evaluation, storage, and inversion of the Hessian matrix, as required by the Newton's method.	Levenberg-Marquardt algorithm is a method tailored for functions of the type sum-of-squared-error.	Bayesian regularization expands the cost function to search not only for the minimal error, but for the minimal error using the minimal weights.
2	The downhill gradient is the direction in which the loss function decreases most rapidly. But this does not necessarily produce the fastest convergence.	In the conjugate gradient training algorithm, the search is performed along conjugate directions which produce generally faster convergence than gradient descent directions.	Very fast when training neural networks measured on that kind of errors.	To overcome the problem in interpolating noisy data, MacKay (1992) has proposed a Bayesian framework which can be directly applied to the neural network learning problem.
3	Big neural networks, with many thousand parameters	Recommended when we have very big neural networks.	Not recommended when we have big data sets and/or neural networks requires a lot of memory	Estimate the effective number of parameters actually used by the model. The number of network weights actually needed to solve a particular problem.
4	The reason is that this method only stores the gradient vector (size n), and it does not store the Hessian matrix (size n2).	Since it does not require the Hessian matrix,	It works without computing the exact Hessian matrix. Instead, it works with the gradient vector and the Jacobian matrix.	By using Bayesian regularization, one can avoid costly cross validation. It is particularly useful to problems that cannot, or would suffer, if a portion of the available data were reserved to a validation set. Regularization also reduces (or eliminates) the need for testing different number of hidden neurons for a problem.
5	It requires information from the gradient vector, and hence it is a first order method.	This method has proved to be more effective than gradient descent in training neural networks.	It cannot be applied to functions like cross entropy error.	A third variable, gamma, indicates the number of effective weights being used by the network, thus giving an indication on how complex the network should be.

Table 5.15 represents the working concepts of Training Algorithms such as Gradient descent, Scaled Conjugate Gradient Descent, Levenberg-Marquardt and Bayesian Regularization. Figure 5.15 depicts the speed of training algorithms versus memory of training algorithms for Gradient descent, Scaled Conjugate Gradient Descent, Levenberg-Marquardt and Bayesian Regularization. Bayesian is best suitable for the current study due to its convergence rate, speed and storage parameters.
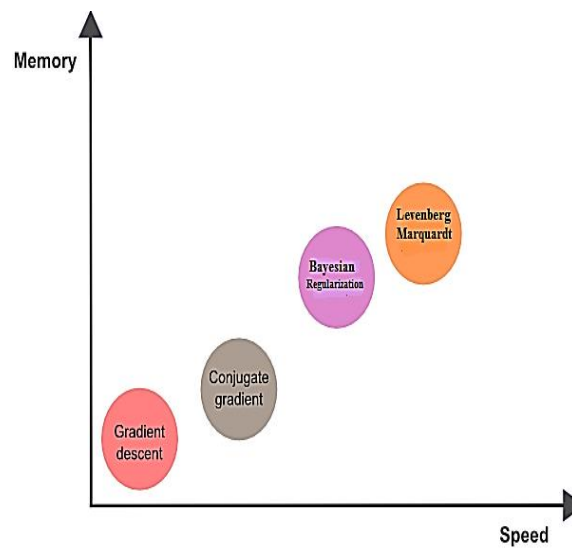
Figure 5.15: **Memory v/s Speed -Training algorithms**

Table 5.16: Test cases - Comparison of cutting temperature (CT, ºC) predicted by RSM, GD, SCGD, and LM with the experimentally obtained CT of SS316 for LN₂ machining.

Exp.No.	Experimental - CT	RSM	GD	SCGD	LM	BNN	Relative Error - CT Obtained by RSM (%)	Relative Error - CT Obtained by GD (%)	Relative Error - CT Obtained by SCGD (%)	Relative Error - CT Obtained by LM (%)	Relative Error - CT Obtained by BNN (%)
1	48	43	44	51	50	49	10.42	8.33	6.25	4.17	2.08
2	57	62	62	61	60	59	8.77	8.77	7.02	5.26	3.51
3	70	77	64	65	66	67	10.00	8.57	7.14	5.71	4.29
4	62	57	67	66	65	64	8.06	8.06	6.45	4.84	3.23
5	73	80	67	78	69	70	9.59	8.22	6.85	5.48	4.11
6	86	94	92	91	90	89	9.30	6.98	5.81	4.65	3.49
7	68	61	63	72	65	66	10.29	7.35	5.88	4.41	2.94
8	89	97	97	96	94	92	8.99	8.99	7.87	5.62	3.37
9	97	107	91	92	94	95	10.31	6.19	5.15	3.09	2.06

Table 5.17: Test Cases - Comparison of cutting force (FX, N) predicted by RSM, GD, SCGD, and LM with the experimentally obtained FX of SS316 for LN₂ machining.

Exp.No.	Experimental - Fx	RSM	GD	SCGD	LM	BNN	Relative Error - Fx Obtained by RSM (%)	Relative Error - Fx Obtained by GD (%)	Relative Error - Fx Obtained by SCGD (%)	Relative Error - Fx Obtained by LM (%)	Relative Error - Fx Obtained by BNN (%)
1	107	99	100	102	103	104	7.48	6.54	4.67	3.74	2.80
2	125	136	134	133	131	129	8.80	7.20	6.40	4.80	3.20
3	156	171	167	166	163	162	9.62	7.05	6.41	4.49	3.85
4	92	101	99	98	97	96	9.78	7.61	6.52	5.43	4.35
5	109	119	117	116	115	113	9.17	7.34	6.42	5.50	3.67
6	131	142	140	137	136	135	8.40	6.87	4.58	3.82	3.05
7	77	84	83	82	81	80	9.09	7.79	6.49	5.19	3.90
8	89	97	96	95	93	92	8.99	7.87	6.74	4.49	3.37
9	110	119	118	117	116	115	8.18	7.27	6.36	5.45	4.55
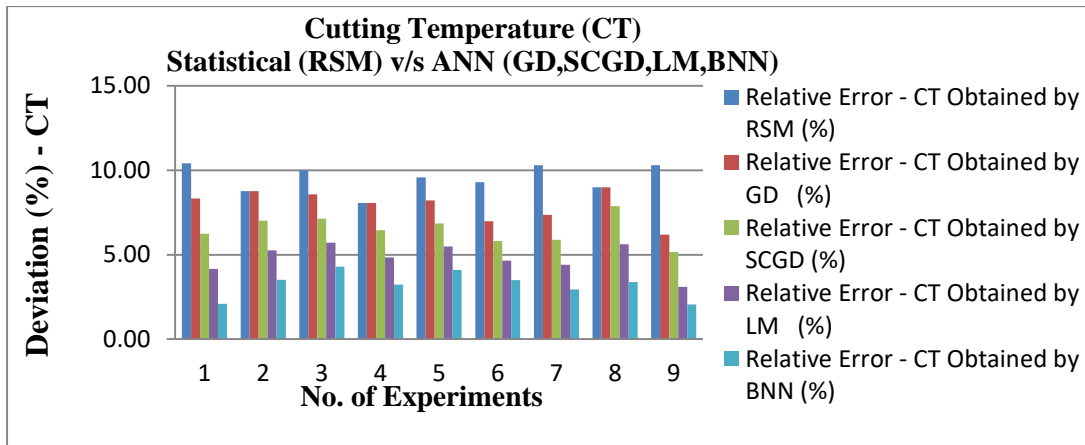
Figure 5.16: Statistical (RSM) v/s ANN (GD, SCGD, LM, BNN) for response cutting temperature (CT) under LN2 machining conditions

Table 5.16 represents the 9 Test Cases - Comparison of Cutting Temperature (CT, ºC) predicted by RSM, GD, SCGD, LM and BNN with the experimentally obtained CT of SS316 for LN_2 Machining. Figure 5.16 depicts the deviation (%) of output CT attained through the statistical (RSM) and ANN (GD, SCGD, LM and BNN) approaches for SS316 in LN_2 Machining.
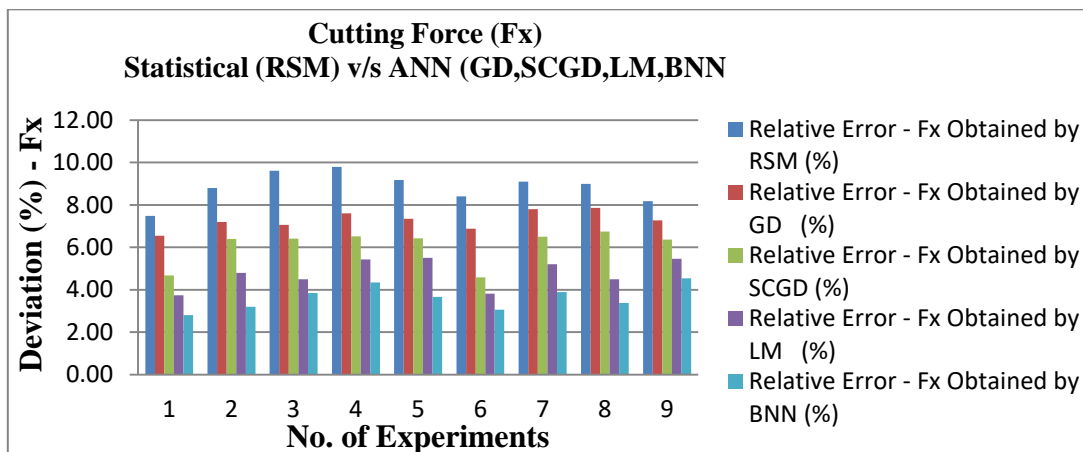
Figure 5.17: Statistical (RSM) v/s ANN (GD, SCGD, LM, BNN) for response cutting force (Fx) under LN2 machining conditions

Table 5.18: Test cases - Comparison of surface roughness (Ra, μ) predicted by RSM, GD, SCGD, LM and BNN with the experimentally obtained Ra of SS316 for LN₂ machining.

Exp. No.	Experimental - Ra	RSM	GD	SCGD	LM	BNN	Relative Error - Ra Obtained by RSM (%)	Relative Error - Ra Obtained by GD (%)	Relative Error - Ra Obtained by SCGD (%)	Relative Error - Ra Obtained by LM (%)	Relative Error - Ra Obtained by BNN (%)
1	1.36	1.47	1.45	1.43	1.42	1.41	8.09	6.62	5.15	4.41	3.68
2	1.77	1.89	1.88	1.86	1.85	1.83	6.78	6.21	5.08	4.52	3.39
3	1.93	2.09	1.8	1.82	1.83	1.85	8.29	6.74	5.70	5.18	4.15
4	1.12	1.2	1.19	1.18	1.17	1.16	7.14	6.25	5.36	4.46	3.57
5	1.4	1.29	1.5	1.49	1.48	1.45	7.86	7.14	6.43	5.71	3.57
6	1.67	1.8	1.55	1.58	1.6	1.61	7.78	7.19	5.39	4.19	3.59
7	0.83	0.9	0.89	0.88	0.87	0.86	8.43	7.23	6.02	4.82	3.61
8	1.26	1.36	1.35	1.34	1.33	1.31	7.94	7.14	6.35	5.56	3.97
9	1.38	1.49	1.48	1.47	1.46	1.44	7.97	7.25	6.52	5.80	4.35

Table 5.19: Test cases - Comparison of flank wear (VB, μm) predicted by RSM, GD, SCGD, LM and BNN with the experimentally obtained VB of SS316 for LN₂ machining.

Exp .NO	Experimental - FW	RSM	GD	SCGD	LM	BNN	Relative Error - FW Obtained by RSM (%)	Relative Error - FW Obtained by GD (%)	Relative Error - FW Obtained by SCGD (%)	Relative Error - FW Obtained by LM (%)	Relative Error - FW Obtained by BNN (%)
1	1.31	1.43	1.2	1.22	1.24	1.26	9.16	8.40	6.87	5.34	3.82
2	1.78	1.93	1.92	1.89	1.87	1.85	8.43	7.87	6.18	5.06	3.93
3	1.42	1.54	1.53	1.52	1.49	1.48	8.45	7.75	7.04	4.93	4.23
4	0.89	0.97	0.82	0.83	0.84	0.86	8.99	7.87	6.74	5.62	3.37
5	1.66	1.8	1.79	1.76	1.73	1.71	8.43	7.83	6.02	4.22	3.01
6	1.05	1.14	1.13	1.11	1.1	1.09	8.57	7.62	5.71	4.76	3.81
7	0.49	0.54	0.45	0.46	0.51	0.5	10.20	8.16	6.12	4.08	2.04
8	1.1	1.2	1.19	1.18	1.16	1.14	9.09	8.18	7.27	5.45	3.64
9	0.93	0.85	1	0.99	0.98	0.97	8.60	7.53	6.45	5.38	4.30
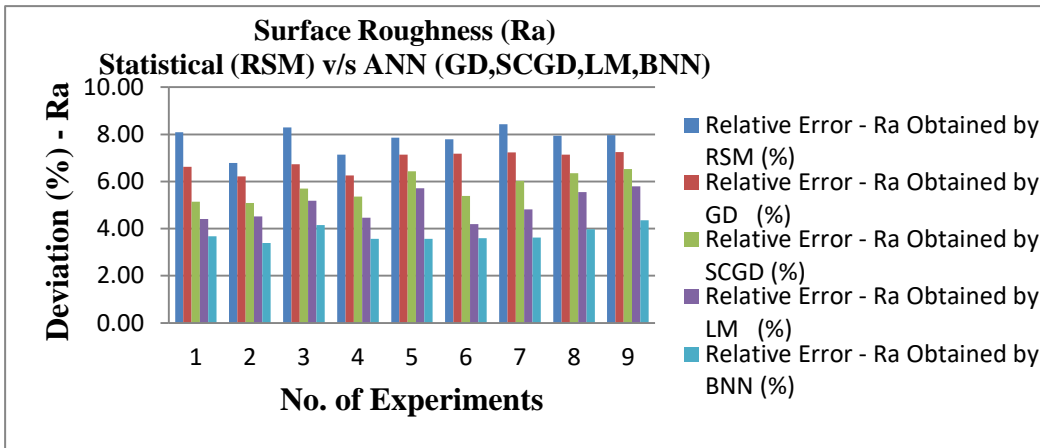
Figure 5.18: Statistical (RSM) v/s ANN (GD, SCGD, LM, BNN) for response surface roughness (Ra) under LN2 machining conditions

Table 5.18 represents the 9 Test Cases - Comparison of Surface Roughness (Ra, µm) predicted by RSM, GD, SCGD, LM and BNN with the experimentally obtained Ra of SS316 for LN$_2$ Machining. Figure 5.16 depicts the deviation (%) of output Ra attained through the statistical (RSM) and ANN (GD, SCGD, LM and BNN) approaches for SS316 in LN$_2$ Machining.
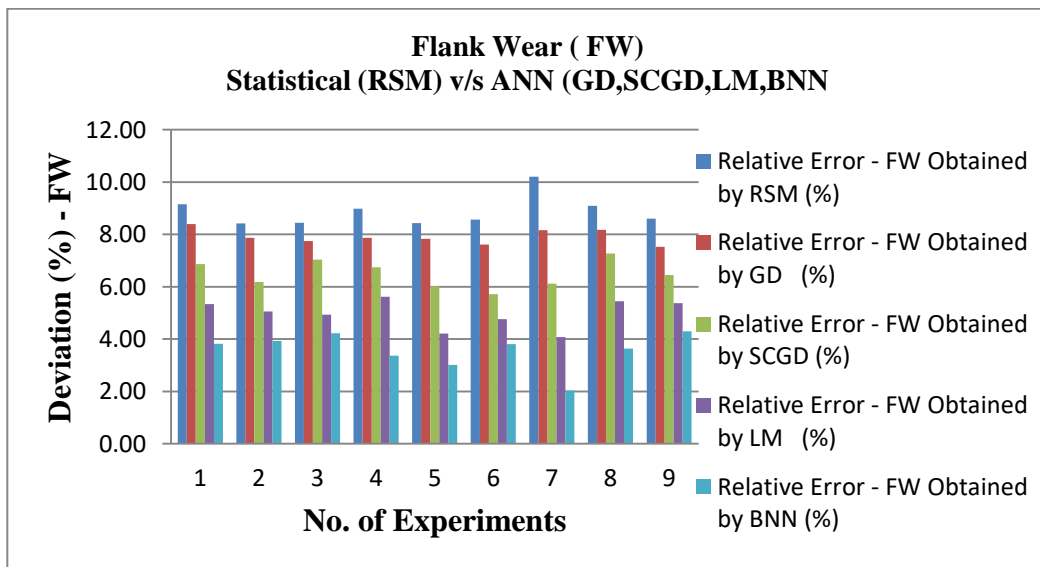
Figure 5.19: Statistical (RSM) v/s ANN (GD, SCGD, LM, BNN) for response flank wear (FW) under LN2 machining conditions

Table 5.19 represents the 9 Test Cases - Comparison of Flank Wear (FW, µm) predicted by RSM, GD, SCGD, LM and BNN with the experimentally obtained FW of SS316 for LN$_2$ Machining. Figure 5.17 depicts the deviation (%) of output FW attained through the statistical (RSM) and ANN (GD, SCGD, LM and BNN) approaches for SS316 in LN$_2$ Machining.

153

Table 5.20: Summary of relative error comparison between RSM, GD, SCGD, LM and BNN for output parameters CT, CF, Ra, and FW.

Methods	Relative error (%) CT (ºC)	Relative error (%) CF (FX)	Relative error (%) Ra (μm)	Relative error (%) FW (μm)
RSM	8.06 - 10.42	7.48 - 9.78	6.78 - 8.43	8.43 - 10.2
GD	6.19 - 8.99	6.54 - 7.87	6.21 - 7.25	7.53 - 8.4
SCGD	5.15 - 7.87	4.58 - 6.74	5.08 - 6.52	5.71 - 7.27
LM	3.09 - 5.71	3.74 - 5.5	4.19 - 5.8	4.08 - 5.62
BNN	2.06 - 4.29	2.8 - 4.55	3.39 - 4.35	2.04 - 4.3

5.2.5 Summary

1. ANN modelling developed has produced quite satisfactory predictions for the output of milling operation, ANN model has been successfully designed and validated to predict the responses namely Cutting Temperature (CT, ºC), Cutting Force (FX, N), Surface Roughness (Ra, μm) Flank Wear (VB, μm) using various network structure and different methods with the experimental data carried out on face milling of SS316 being used for training.

2. Comparison of the predictions made by the different neural networks reveal that the neural network trained using the BNN algorithm gives the most accurate predictions.

3. The fast convergence teamed with good predictive quality makes Bayesian regularization algorithm are the most suitable choice of all the variants considered in this work for training a neural network for this application.

4. The relative error attained through BNN is accurate and less as compared to rest of the back propagation algorithms i.e. (Gradient descent learning, Scaled Conjugate Gradient Descent, Levenberg-Marquart).

5. The comparative study made between the statistical techniques (RSM) and neural based approach (BNN) indicate that the error achieved in prediction using BNN model is much lesser than that of the RSM prediction. Hence, this model gives better results as compared to RSM.

The comparison study was made among all the prediction approaches by one parametric approach. The attained results through one parametric approach are summarized as follows in Table 5.20.

CHAPTER 6
RESULTS AND DISCUSSION (PART 3)
OPTIMIZATION CRYOGENIC MILLING PROCESS

6.1 INTRODUCTION

The milling process modelling and optimization strategy mentioned. The phases and methodology followed to mannequin and optimize the milling operation for the responses are illustrated in Figure 3.4. The experimental data (Table 5.1) has been accrued as per outline matrices of Central Composite Design (CCD/RSM). Further, using analysis of variance (ANOVA) the statistical sufficiency of the strategy has been evaluated. The experimental accumulated control-response data are applied for generation of mathematical (nonlinear) models of the responses. The procedure involved in the study is explained via the surface plots. The evaluation is executed and sufficiency is tested via assistance of coefficient of correlation, ANOVA and significance test. The response equations attained through RSM model are shown in equation 6.1-6.4. The accuracy of the prediction of the created model is verified with 15 test cases and the superlative one is chosen in light of the average absolute percent deviation esteem.

The chapter deals with comparison of both traditional (RSM-Desirability Factor Approach (DFA)) and non-traditional (PSO) approach

Related Article:

Karthik Rao M C, Rashmi L Malghan*, Arun Kumar Shettigar, Shrikantha S Rao and Mervin A Herbert. (2019). "An Efficient Approach to Optimize Wear Behaviour of Cryogenic Milling Process of SS316 Using Regression Analysis and Particle Swarm Techniques", *Trans Indian Inst Met,* **72(1):191–204, https://doi.org/10.1007/s12666-018-1473-y**

6.2 TRADITIONAL APPROACH (RSM)

The Central Composite Design (CCD) was used to implement the response prediction using RSM. A total of 20 experiments were performed, which incorporates of 8 cube points, 6 center points in cube, 6 axial points and alpha value is 1. The range of the process parameters were set by taking into consideration the tool or insert specification and even by performing the trial experiments in order to achieve the desired responses. In the present work, CCFCD is used for establishing the relationship between the empirical process parameters and the milling process output variables of SS316. The final obtained mathematical regression equations are listed in equations 6.1-6.4.

Later on the model performance was validated with the help of analysis of variance (ANOVA) (Tables 5.2-5.5). The significance of the model is identified by this method. If the model satisfies the condition of Prob>f is less than 0.0500, then the model is considered to be significant. All the proposed models satisfies the condition of Prob>f is less than 0.0500, Hence, it can be concluded that all the proposed models are significant. The adequacy of the fitted regression model was identified using the R^2 correlation coefficient and the value of R^2 need to be close to unity. For all the responses the "Pre R-squared" are in reasonable accordance with the "Adj R-Squared" values. The precision ratio of all the developed models (ratio >4 is desirable) shows the adequacy of incorporating the proposed model.

6.3 NON TRADITIONAL OPTIMIZATION APPROACH (EVOLUTIONARY APPROACH- PSO)

Evolution algorithms (EAs) are imitative of natural evolutionary principles to constitute search and optimization procedure. Genetic algorithm (GA) is evolutionary algorithm and was introduced by John Holland (1975). These algorithm functions are for selection of the fittest to produce better approximation to solutions.

Particle swarm optimization algorithm (PSO) is a relatively new approach in modern heuristics for optimization and it is one of the evolutionary protocol methods. PSO

was first developed by Eberhart and Kennedy (1995) for continues function optimization. There are several stochastic algorithms such as genetic algorithms, differential evolution, Tabu search, simulated annealing, ant colony optimization and particle swarm optimization. These algorithms are used to find optimal solution for different objective function. The basic concept of PSO originated from the food hunting behaviour of birds. It was found that through the intelligent swarming behaviour, flocks of birds would always suddenly change the direction, scatter and gather. Behaviour of birds is also unpredictable but always consistent as whole, with individuals keeping the most suitable distance. Every swarm of PSO is a solution in the solution space. It adjusts the fight according to its own and its companion flying experience. The goal of optimization is to minimize or maximize certain quantities such as life, mass, etc. In mathematical models, these goals are expressed as functions of certain variables. There are various methods available for solving these models towards minimization or maximization. The response equations attained through RSM model are further utilized as fitness function in implementation of PSO algorithm. The chapter deals with the implementation and comparison of both statistical and evolutionary optimization techniques and background of these optimization techniques are explained in chapter 3 (section 3.10). The foresaid optimization techniques are carried out to predict the optimum combinations of process parameters for the desired responses. For veracity, the validation experiments have been conducted.

6.4 PHASES FOLLOWED TO ATTAIN THE STATED GOALS

To satisfy the stated goals of the current work four phases have been followed and these are elaborated below:

Phase 1: Selecting milling factors and respective levels

The decision of machining factors and choice on the working levels are of central significance to persuade over the procedure and abate the imperfections. Too wider working scope of the factors will lead to infeasible elucidation on the retort surface, on the other hand excessively limit range will bring about inadequate or poor data about the process (Pereira et al 2016, Sartori et al 2017, Shalina et al 2020).

Design of experiment and RSM methods are pragmatic to contemplate and evaluate the impression of factors on responses. Accordingly, accessing available literature, doyen's recommendation and trial tests directed at the study are utilized to choose process factors and fix their working reach. Table 6.1 exemplifies the considered input factors and their respective operating ranges.

Phase2: Experiment Conduction

CCD is largely acceptable and utilized non-linear regression strategy to fit the response surface. Experiments are carried out according to CCD design matrices and are represented in Table 3.1. In the work, for the CCD model thirty-one experimental runs are carried out, these runs deliver the complete perception of point by point comprehension of all input terms over the outcomes (Chetan et al 2015, Shalina et al 2019). Further, fifteen distinctive (experiments) blend of milling variables was carried out to validate (test cases) models.

Phase 3: Development of CCD model, statistical investigation and Performance assessment. The data represented in Table 6.2 are utilized to generate a CCD model. The common type of polynomial function (second order) is signified underneath through equation (a):

$$\widehat{Z_1} = z - \varepsilon = b_0 x_0 + b_1 x_1 + b_2 x_2 + b_3 x_3 + b_4 x_4 + b_{11} x^2_1 + b_{22} x^2_2 + b_{33} x^2_3 +$$
$$b_{44} x^2_4 + b_{12} x_1 x_2 + b_{23} x_2 x_3 + b_{13} x_1 x_3 + b_{14} x_1 x_4 \quad\quad\quad \textbf{(a)}$$

The previously mentioned response surface function incorporates linear (X1, X2, X3, X4) quadratic (X12, X22, X32, X42) and two-term factor interaction (X1*X2, X1*X3, X1*X4, X2*X3, X2*X4 and X3*X4) and the error term (ε), where z is the true response on a logarithmic scale x0 = 1 (dummy variable), x1, x2, x3 are logarithmic conversions of spindle speed, feed rate, and depth of cut, respectively, while b0, b1, b2, b3 and b4 are the factors to be appraised.

The coefficients are determined firstly by means of accumulating milling (control-response) data and next are to perform the model which is constructed via regression analysis. The collected control and response data are analysed and nonlinear control-

response associations are established. The fundamental and interaction among the factors effect is analysed. The originated model is verified for its efficacy and significance by incorporating ANOVA strategy. The software tool (Minitab) was incorporated for the stated goal. Further, to overview the CCD performance the 15 test cases were adapted.

Phase 4: Optimization of Milling Process Parameters

No impeccable general prerequisites characterized yet to distinguish the best set of milling parameters. Currently there are numerous optimization tools accessible and each has distinctive constraint and focal points. The model performance for the most parts relies upon the specific issue area and process multifaceted nature. The current work compares the performance of DFA and PSO techniques to distinguish set of milling process variables that will yield preferred responses.

Phase 5: Results and Discussions

In this section, milling process modeling and optimization are discussed. The experimental data has been accrued as per outline matrices of CCD. The surface plots and the corresponding input and output relations are generated using the gathered data is utilized.

Further, using analysis of variance (ANOVA) the statistical sufficiency of the strategy has been evaluated (Yongquan et al 2020, Marco et al 2017). The accuracy of the prediction of the created model is verified with 15 test cases and the superlative one is chosen in light of the average absolute percent deviation esteem. The best ideal milling prerequisites accountable for the desired responses are resolved using DFA and PSO (Chen et al 2010). At long last, the best optimization technique is opted by evaluating the performance between conventional (DFA) and nonconventional (PSO).

Table 6.1: Experimental conditions for RSM method.

SL. No	Spindle Speed (rpm)	Feed Rate (mm/min)	Depth Of Cut (mm)	Coolant type	Cutting Temperature (℃)	Cutting force Fx (N)	Surface Roughness Ra(μm)	Flank wear, Vb,(μm)
1	1000	350	0.5	-1	237	384	2.09	0.16
2	3000	350	0.5	-1	269	337	1.443	0.24
3	1000	550	0.5	-1	299	459	2.427	0.195
4	3000	550	0.5	-1	295	365	1.857	0.283
5	1000	350	1.5	-1	241	393	2.103	0.17
6	3000	350	1.5	-1	271	340	1.473	0.25
7	1000	550	1.5	-1	304	464	2.463	0.203
8	3000	550	1.5	-1	324	370	1.883	0.291
9	1000	350	0.5	1	35	243	0.747	0.06
10	3000	350	0.5	1	84	214	0.583	0.142
11	1000	550	0.5	1	56	309	0.957	0.09
12	3000	550	0.5	1	89	269	0.77	0.18
13	1000	350	1.5	1	39	256	0.757	0.069
14	3000	350	1.5	1	85	219	0.693	0.146
15	1000	550	1.5	1	59	315	0.996	0.102
16	3000	550	1.5	1	95	276	0.78	0.175
17	1000	450	1	0	142	382	1.397	0.168
18	3000	450	1	0	177	326	0.964	0.25
19	2000	350	1	0	139	300	1.07	0.211
20	2000	550	1	0	168	348	1.303	0.253

Where: In coolant type column -1 = Dry, 1 = LN$_2$ and 0 = Flood (wet) machining conditions.

6.4.1 Regression Equations (RSM Approach) For Responses

The attained response equations through RSM approach are stated below:

T =157.752+15.3889*S+16.0556*F+3.38889*D-104.889*CT+2.87067*S*S-3.12933*F*F+ 0.870667 * D*D +15.3707*CT*CT-4.50000*S*F+1.37500*S*D+5.37500*S*CT+2.0*F*D-9.25000*F*CT-1.62500*D*CT   **(6.1)**

FX = 337.224-27.1667*S+27.1667*F+3.27778*D-63.5556*CT+14.3480*S*S-15.6520*F*F- 5.65200 *D*D-4.15200*CT*CT-6.31250*S*F-0.812500*S*D+8.93750*S*CT-0.437500*F*D +2.06250 *F*CT+0.562500*D*CT   **(6.2)**

Ra = 1.23988-0.193944*S+0.137611*F+0.0157778*D-0.585556*CT-0.0370733*S*S-0.0310733*
F*F+0.0104267*D*D+0.191427*CT*CT-0.00300000*S*F+0.00487500*S*D+0.112250*S*CT-
0.00325000*F*D-0.0498750*F*CT+0.00400000*D*CT   **(6.3)**

FW=0.251472+0.0418333*S+0.0180000*F+0.00350000*D-0.0520000*CT-0.0420227*S*S- 0.01252
*F*F+0.00797733*D*D-0.0335227*CT*CT+0.00125000*S*F-0.00137500*S*D-8.75000E-
04*S* CT-6.25000E-04*F*D-0.00137500*F*CT-0.00100000*D*CT   **(6.4)**

Where: T = Cutting temperature, FX = Cutting Force (X-axis), Ra = Surface roughness, Fw = Flank wear.

6.5 OPTIMIZATION OF MILLING PROCESS PARAMETERS

The way towards deciding the superlative result among numerous probable plausible elucidations is indicated as an optimization. The CCD strategy is one of the best method for determination of response coefficient value (i.e. R=0.9791), as its determination coefficient point out the goodness of fit of the model (Debnath et ll 2016, Gupta et al 2015 and Gupta et al 2016). The coveted responses can be identified by incorporating the empirical model (DFA) and non-traditional (PSO) optimization strategies. In process of optimization the attained model via CCD approach is used as objective function. In CCD method the regression equations are attained, with these equations the data can be generated via substituting the selected range of input parameters in the study, thus CCD is opted and used as objective function to carry out prediction and optimization.

6.5.1 Traditional Method of optimization

This method uses a deterministic inquiry technique. Where the results moment will be in the uni-directional way and thus end up in local (sub optimal) solutions. In order to decide the optimal solution the DFA is the best way as this method is widely used approach. The plots as depicted in Figure 6.1 have clarified the qualitative information about the close optimal solution. Figure 6.1 exhibits the milling optimum parameter values acquired via DFA method for milling operation.

6.5.2 Nonconventional optimization

A stated optimization technique is stochastic in its way of multi-modal search and accurately situates the close optimal outcomes (Wang et al 2020, Garcia et al 2015). The PSO enactment relies principally on algorithm factors tuning and the rate of convergence for the stated province. The PSO factors tuning and the obtained outcomes are conferred in the accompanying segment.

A. PSO: PSO is established on the idea of rummaging conduct of bird flocks. PSO is prominent in manufacturing sector due to its few factors such as fine-tuning of factors, rate of convergence and simplicity of execution trademark (characteristic). In PSO, swarm is considered as a unit which is comprised of numerous distinct results and each result is considered as a particle. Every particle possesses position and velocity vector and the search space takes place in multi-dimensional. In PSO it can be noted that, each individual movement of the particles takes place with a specific speed and progressively change their flight way in view of self-flying and particle involvement in a manifold-way search domain. The systematic study was made to reach to an optimized value of PSO factors. The estimation of optimized factors of PSO is listed underneath:

Number of factors   4

Number of Particles   80

Number of iterations   110

Learning rate   0.6

The PSO optimized factors return desired responses and the corresponding milling condition is represented in Table 6.7.

6.6 CONFIRMATION EXPERIMENTS

The superlative milling conditions that outcome in required responses are resolved utilizing both conventional and nonconventional optimization techniques. The goal function solely dependent on the regression equation created via CCD approach. The response surface may be one-way or diverse-modal in gamut space. The conventional

optimization strategy, DFA involves deterministic type of explore with specific standards. The attained optimal value of responses CT, FX, Ra and FW achieved via DFA are represented in Figure 6.1. From Figure 6.1, it is observed that the attained response values for optimal input parameters are comparatively higher than PSO method. The comparative study between the DFA and PSO approaches can be related through the achieved optimal responses and by calculating the percentage of error gained via both DFA and PSO methods. This may conceivably due to the multi-modal search domain. Optimum estimations of process parameters and their relating response esteems are exhibited in Table 6.7. The incorporated techniques are tested for its accuracy in predicting with the assistance of 15 test cases as shown in Table 6.3-6.6. Table 6.3-6.6 represent the percentage of LN_2 impact on wet machining of all responses achieved via RSM and PSO approaches. The results gained via LN_2 point towards achievement of better results as compared to that of wet machining. From Table 6.4-6.7, it can be derived that, the quantity (in terms of %) of influence of LN_2 over wet machining.

Scanning electron microscope (SEM) is ideally involved to contemplate the material surface, because of the blend of crystal and clear resolution, amplification level and field profundity depth. Flank wear is a standout amongst the most vital value to be controlled in light of the fact that the flank confront ceaselessly contacts with the machined material and eventually rises the values of cutting forces, thus it impairs the surface (Pereira et al 2016, Kaynak et al 2016, Yamina et al 2020, Ali et al 2016).

Table 6.2: Test cases for conditions (Wet machining and Cryogenic machining)

SL.NO	Experimental			Cutting Temperature		Flank-Wear Rate (µm)		Surface Roughness (µm)		Cutting Force (N)	
	S (rpm)	F (mm/min)	D (mm)	Wet	LN_2	Wet	LN_2	Wet	LN_2	Wet	LN_2
1	2110	460	1.2	163	85	2.29	1.51	2.13	1.1	209	118
2	2840	380	0.6	220	148	2.51	1.93	2.62	1.46	287	187
3	1750	365	0.8	162	68	1.96	0.86	1.91	0.96	193	102
4	1280	420	1.4	154	49	1.82	0.74	1.73	0.55	177	84
5	2007	455	0.9	193	80	2.22	1.49	2.09	1.08	200	113
6	1560	510	1.3	171	92	1.87	0.78	1.83	0.89	186	98
7	2650	430	0.8	209	130	1.14	0.53	2.47	1.3	256	168
8	1260	530	1.1	188	38	0.68	0.37	1.71	0.42	171	80
9	2315	520	0.7	192	119	2.16	1.43	2.26	1.19	227	136
10	1380	385	1.1	161	70	1.69	0.68	1.77	0.64	181	91
11	2540	490	1.2	200	126	2.32	1.57	2.35	1.28	245	153
12	1870	525	1.4	194	77	2.07	1.12	1.99	1.01	198	109
13	2740	415	0.9	213	134	2.69	1.99	2.56	1.37	269	177
14	2290	375	0.7	197	109	2.18	1.41	2.22	1.16	213	121
15	2460	520	0.4	201	121	2.41	1.63	2.31	1.21	238	145
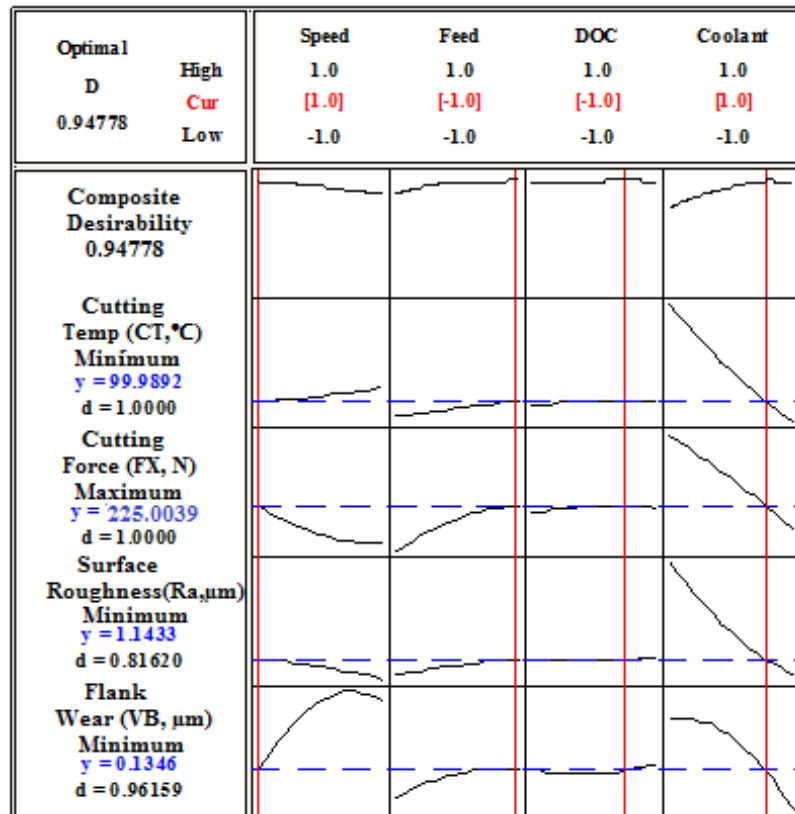
Figure 6.1: Result of CT, FX, Ra and FW using DFA technique

Table 6.3: Comparison of cutting temperature (CT, ºC) predicted by RSM and PSO, with the experimentally obtained CT of SS316 for Wet and LN$_2$ machining.

SL. NO	Cutting Temperature (ºC)									% of LN$_2$ Impact on Wet machining	
	Experimental					Prediction					
	Spindle Speed (rpm)	Feed Rate (mm/min)	Depth Of Cut (mm)	Wet	LN$_2$	PSO Wet	PSO LN$_2$	RSM Wet	RSM LN$_2$	LN$_2$ Over Wet (PSO)	LN$_2$ Over Wet (RSM)
1	2110	460	1.2	163	85	154	89	143	97	42.2	32.1
2	2840	380	0.6	220	148	209	132	195	154	36.8	21.0
3	1750	365	0.8	162	68	149	75	138	90	49.6	34.7
4	1280	420	1.4	154	49	132	54	120	45	59.0	62.5
5	2007	455	0.9	193	80	197	85	200	93	56.8	53.5
6	1560	510	1.3	171	92	185	99	166	108	46.4	34.9
7	2650	430	0.8	209	130	196	124	183	146	36.7	20.2
8	1260	530	1.1	188	38	161	29	140	49	81.9	65.0
9	2315	520	0.7	192	119	180	124	169	129	31.1	23.6
10	1380	385	1.1	161	70	159	79	152	68	50.3	55.2
11	2540	490	1.2	200	126	191	131	187	142	31.4	24.0
12	1870	525	1.4	194	77	198	70	200	85	64.6	57.5
13	2740	415	0.9	213	134	209	147	196	160	29.6	18.3
14	2290	375	0.7	197	109	189	111	156	128	41.2	17.9
15	2460	520	0.4	201	121	197	129	174	135	34.5	22.4
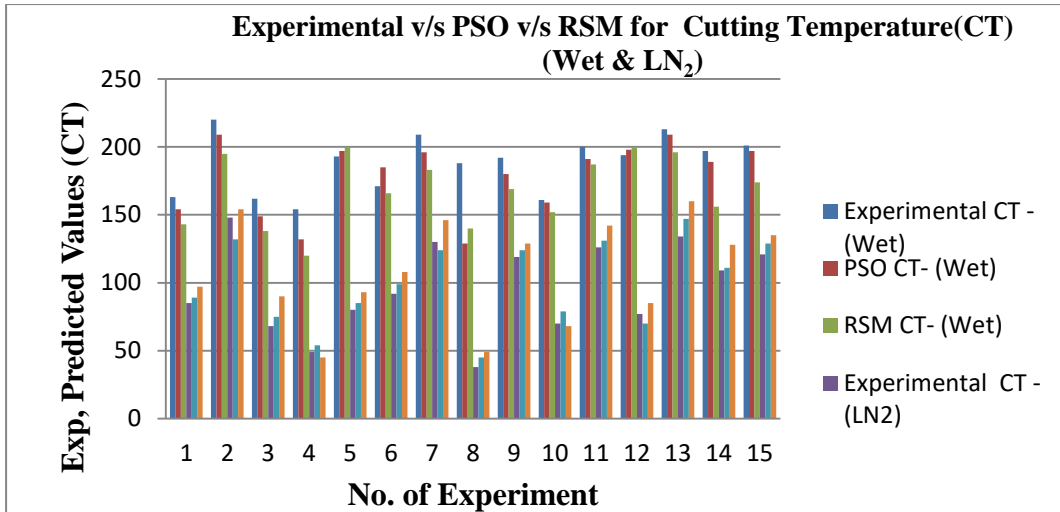
Figure 6.2: Experimental v/s PSO v/s RSM for cutting temperature (CT) for wet & LN$_2$
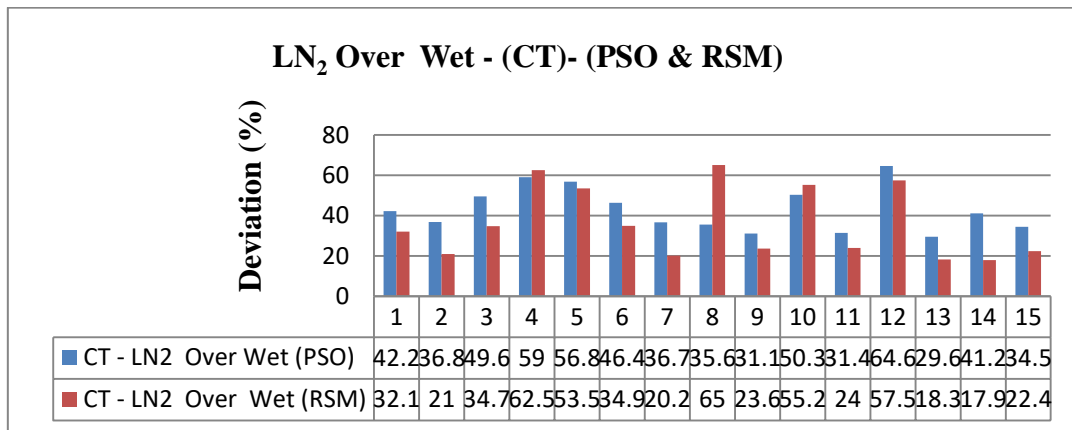
Figure 6.3: LN$_2$ influence over wet machining achieved in terms of percentage (%) for response cutting temperature (CT) achieved through PSO & RSM Methods

In Figure 6.2 the comparison between experimental, PSO and RSM has been done with respect to the output response of cutting temperature (CT) with machining condition as wet and LN$_2$.

Figure 6.3 represents the percentage of LN$_2$ impact on wet machining of all responses achieved via RSM and PSO approaches. The results gained via LN$_2$, point towards achievement of better results as compared to that of wet machining. From Figure 6.3, it can be derived that, LN2 influence over wet machining achieved in terms of percentage (%).

Table 6.4: Comparison of cutting force (FX, N) predicted by RSM and PSO, with the predicted obtained cutting force (FX) of SS316 for Wet and LN$_2$ machining.

SL. NO	Cutting Force (N)									% of LN$_2$ Impact on Wet machining	
	Experimental					Prediction					
	Spindle Speed (rpm)	Feed Rate (mm/min)	Depth Of Cut (mm)	Wet	LN$_2$	PSO Wet	PSO LN$_2$	RSM Wet	RSM LN$_2$	LN$_2$ Over Wet (PSO)	LN$_2$ Over Wet (RSM)
1	2110	460	1.2	209	118	209	118	216	127	43.5	41.2
2	2840	380	0.6	287	187	287	187	300	201	34.8	33.0
3	1750	365	0.8	193	102	193	102	201	113	47.2	43.8
4	1280	420	1.4	177	84	177	84	192	98	52.5	49.0
5	2007	455	0.9	200	113	200	113	208	124	43.5	40.4
6	1560	510	1.3	186	98	186	98	197	107	47.3	45.7
7	2650	430	0.8	256	168	256	168	284	190	34.4	33.1
8	1260	530	1.1	171	80	171	80	189	91	53.2	51.9
9	2315	520	0.7	227	136	227	136	246	165	40.1	32.9
10	1380	385	1.1	181	91	181	91	190	103	49.7	45.8
11	2540	490	1.2	245	153	245	153	272	187	37.6	31.3
12	1870	525	1.4	198	109	198	109	205	121	44.9	41.0
13	2740	415	0.9	269	177	269	177	293	193	34.2	34.1
14	2290	375	0.7	213	121	213	121	128	122	43.2	4.7
15	2460	520	0.4	238	145	238	145	256	174	39.1	32.0
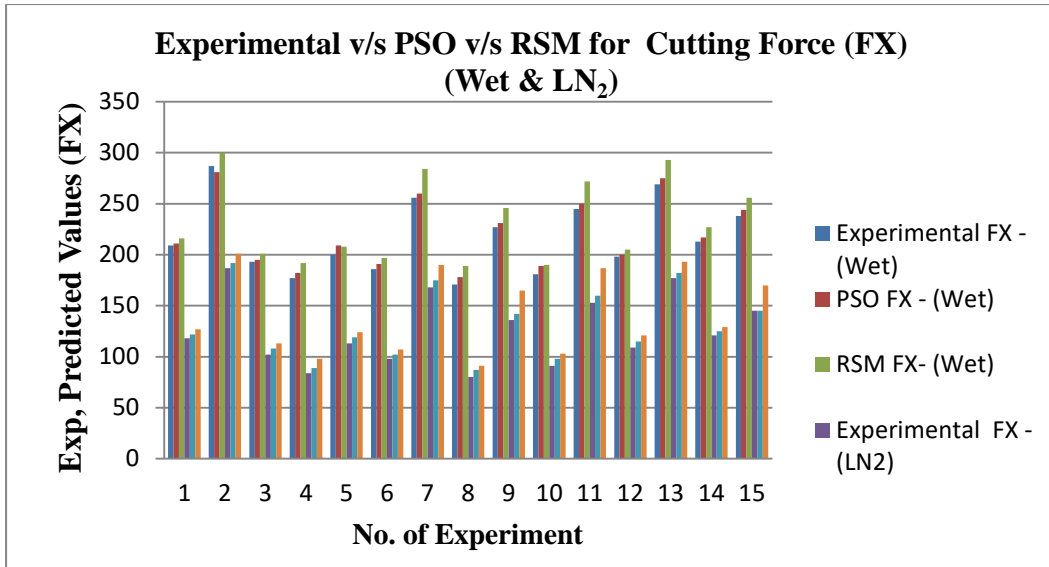
Figure 6.4: Experimental v/s PSO v/s RSM for cutting force (FX) for Wet & LN₂

	1	2	3	4	5	6	7	8	9	10	11	12	13	14	15
FX - LN2 Over Wet (PSO)	42	31	45	51	43	47	33	52	39	48	36	43	34	42	41
FX - LN2 Over Wet (RSM)	41	33	44	49	40	46	33	52	33	46	31	41	34	4.7	32
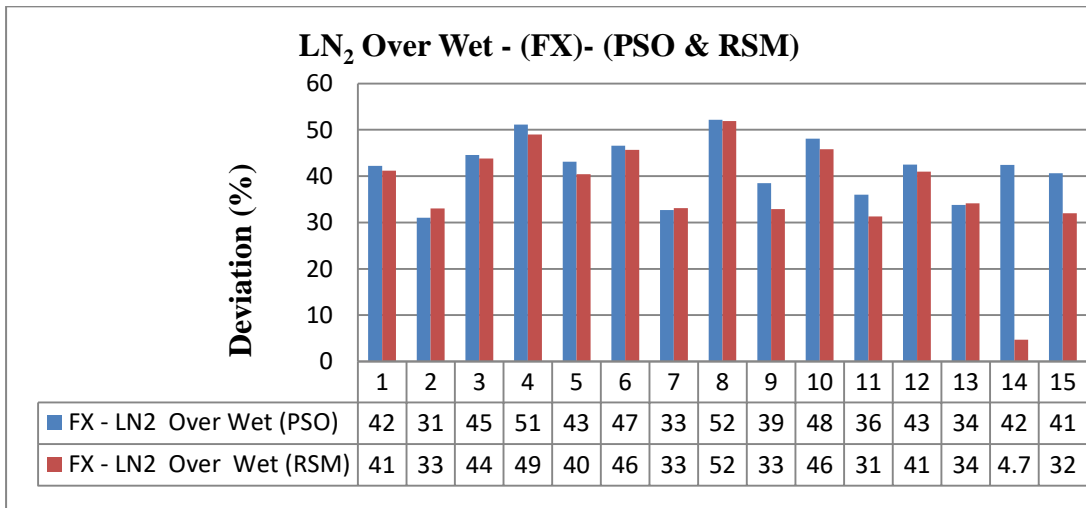
Figure 6.5: LN₂ influence over wet machining achieved in terms of percentage (%) for response Cutting Force (FX) achieved through PSO & RSM Methods

In Figure 6.4 the comparison between experimental, PSO and RSM has been done with respect to the output response of cutting force (FX) with machining condition as wet and LN₂. Figure 6.5 represents the percentage of LN₂ impact on wet machining of all responses achieved via RSM and PSO approaches. The results gained via LN₂, point towards achievement of better results as compared to that of wet machining. From Figure 6.5, it can be derived that, LN2 influence over wet machining achieved in terms of percentage (%).

Table 6.5: Comparison of surface roughness (Ra, μm) predicted by RSM and PSO, with the experimentally obtained CT of SS316 for Wet and LN$_2$ machining.

| SL. NO | Surface Roughness (μm) | | | | | | | | | % of LN$_2$ Impact on Wet machining | |
| | Experimental | | | | | Prediction | | | | | |
	Spindle Speed (rpm)	Feed Rate (mm/min)	Depth Of Cut (mm)	Wet	LN$_2$	PSO Wet	PSO LN$_2$	RSM Wet	RSM LN$_2$	LN$_2$ Over Wet (PSO)	LN$_2$ Over Wet (RSM)
1	2110	460	1.2	2.13	1.1	2.13	1.1	2.48	1.34	48.4	46.0
2	2840	380	0.6	2.62	1.46	2.62	1.46	2.93	1.69	44.3	42.3
3	1750	365	0.8	1.91	0.96	1.91	0.96	2.16	1.23	49.7	43.1
4	1280	420	1.4	1.73	0.55	1.73	0.55	2.08	0.84	68.2	59.6
5	2007	455	0.9	2.09	1.08	2.09	1.08	2.24	1.28	48.3	42.9
6	1560	510	1.3	1.83	0.89	1.83	0.89	2.13	1.20	51.4	43.7
7	2650	430	0.8	2.47	1.3	2.47	1.3	2.69	1.68	47.4	37.5
8	1260	530	1.1	1.71	0.42	1.71	0.42	2.01	0.79	75.4	60.7
9	2315	520	0.7	2.26	1.19	2.26	1.19	2.55	1.38	47.3	45.9
10	1380	385	1.1	1.77	0.64	1.77	0.64	2.10	1.02	63.8	51.4
11	2540	490	1.2	2.35	1.28	2.35	1.28	2.59	1.61	45.5	37.8
12	1870	525	1.4	1.99	1.01	1.99	1.01	2.18	1.28	49.2	41.3
13	2740	415	0.9	2.56	1.37	2.56	1.37	2.87	1.77	46.5	38.3
14	2290	375	0.7	2.22	1.16	2.22	1.16	2.50	1.32	47.7	47.2
15	2460	520	0.4	2.31	1.21	2.31	1.21	2.57	1.56	47.6	39.3
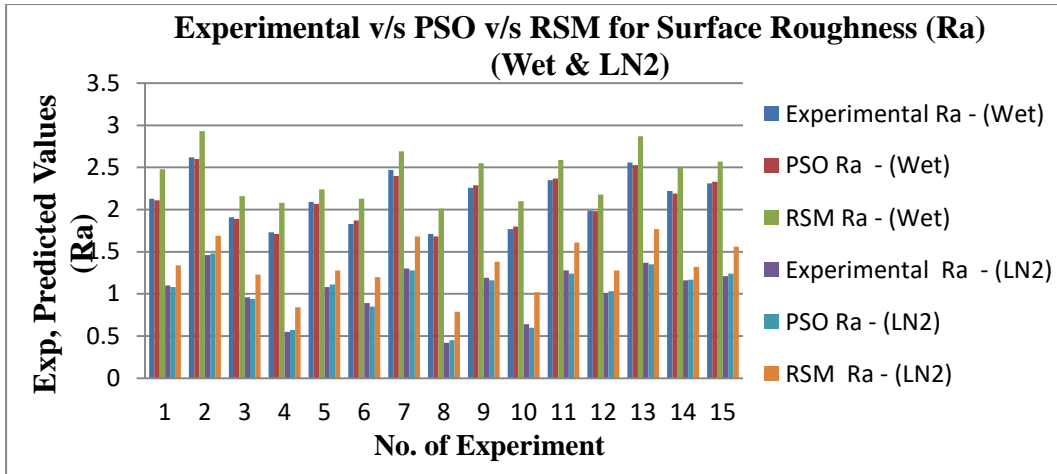
Figure 6.6: Experimental v/s PSO v/s RSM of surface roughness (Ra) for Wet & LN$_2$
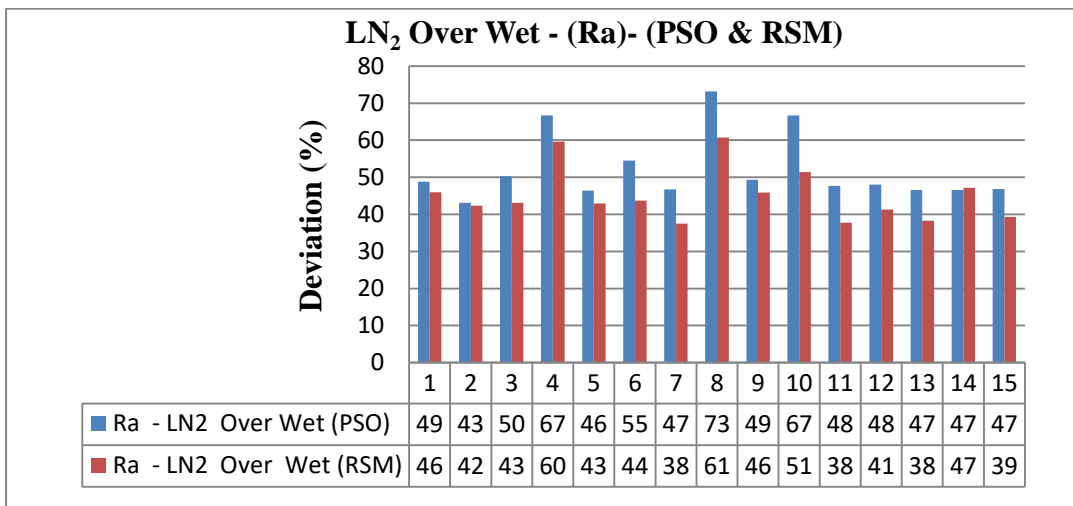
Figure 6.7: LN$_2$ influence over wet machining achieved in terms of percentage (%) for response Surface Roughness (Ra) achieved through PSO & RSM Methods.

In Figure 6.6 the comparison between experimental, PSO and RSM has been done with respect to the output response of surface roughness (Ra) with machining condition as wet and LN$_2$.

Figure 6.7 represents the percentage of LN$_2$ impact on wet machining of all responses achieved via RSM and PSO approaches. The results gained via LN$_2$, point towards achievement of better results as compared to that of wet machining. From Figure 6.7, it can be derived that, LN2 influence over wet machining achieved in terms of percentage (%).

Table 6.6: Comparison of flank-wear Rate (VB, µm) predicted by RSM and PSO, with the experimentally obtained CT of SS316 for Wet and LN$_2$ machining.

SL.NO	Flank-Wear Rate (µm)									% of LN$_2$ Impact on Wet machining	
	Experimental					Prediction					
	Spindle Speed (rpm)	Feed Rate (mm/min)	Depth Of Cut (mm)	Wet	LN$_2$	PSO Wet	PSO LN$_2$	RSM Wet	RSM LN$_2$	LN$_2$ Over Wet (PSO)	LN$_2$ Over Wet (RSM)
1	2110	460	1.2	2.29	1.51	2.32	1.44	2.65	1.83	37.9	30.9
2	2840	380	0.6	2.51	1.93	2.75	1.87	2.31	2.2	32.0	4.8
3	1750	365	0.8	1.96	0.86	1.77	0.69	2.7	1.45	61.0	46.3
4	1280	420	1.4	1.82	0.74	2.03	0.86	1.52	0.38	57.6	75.0
5	2007	455	0.9	2.22	1.49	2.26	1.32	2.06	1.74	41.5	15.5
6	1560	510	1.3	1.87	0.78	1.68	1.24	2.7	1.52	26.1	43.7
7	2650	430	0.8	1.14	0.53	1.14	0.65	1.38	0.89	42.9	35.5
8	1260	530	1.1	0.68	0.37	0.39	0.31	0.38	0.22	20.5	42.1
9	2315	520	0.7	2.16	1.43	2.44	1.21	2.19	1.77	50.4	19.2
10	1380	385	1.1	1.69	0.68	1.98	0.47	2.28	1.03	76.2	54.8
11	2540	490	1.2	2.32	1.57	2.09	1.86	2.56	1.89	11.0	26.2
12	1870	525	1.4	2.07	1.12	2.28	1.4	1.89	1.45	38.5	23.3
13	2740	415	0.9	2.69	1.99	2.43	2.06	2.78	1.37	15.2	50.7
14	2290	375	0.7	2.18	1.41	2.28	1.89	2.08	1.65	17.1	20.7
15	2460	520	0.4	2.41	1.63	2.39	1.47	2.13	1.24	38.4	41.8
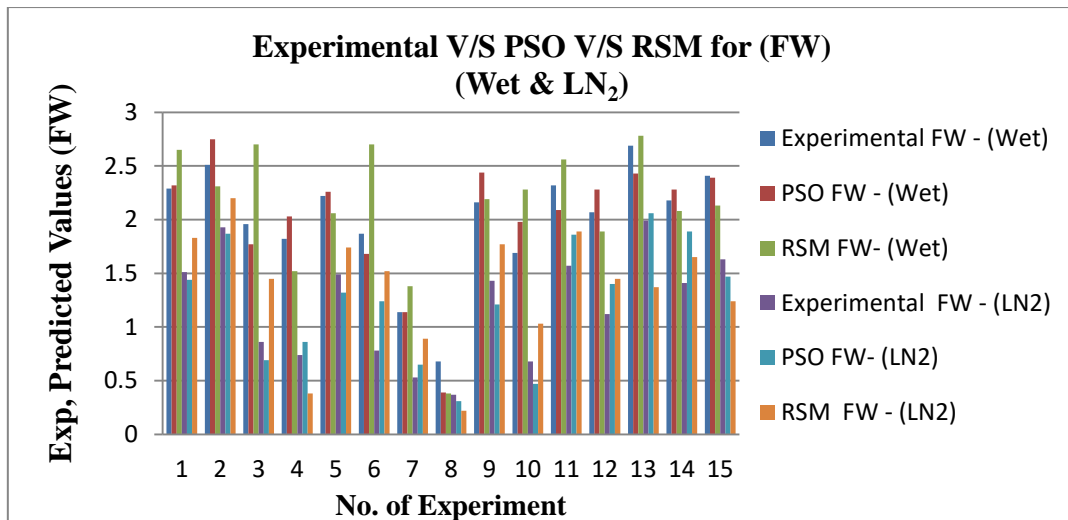
Figure 6.8: Experimental v/s PSO v/s RSM of flank wear (FW) for Wet & LN₂

	1	2	3	4	5	6	7	8	9	10	11	12	13	14	15
FW - LN2 Over Wet (PSO)	37.9	32	61	57.6	41.5	26.1	42.9	20.5	50.4	76.2	11	38.5	15.2	17.1	38.4
FW - LN2 Over Wet (RSM)	30.9	4.8	46.3	75	15.5	43.7	35.5	42.1	19.2	54.8	26.2	23.3	50.7	20.7	41.8
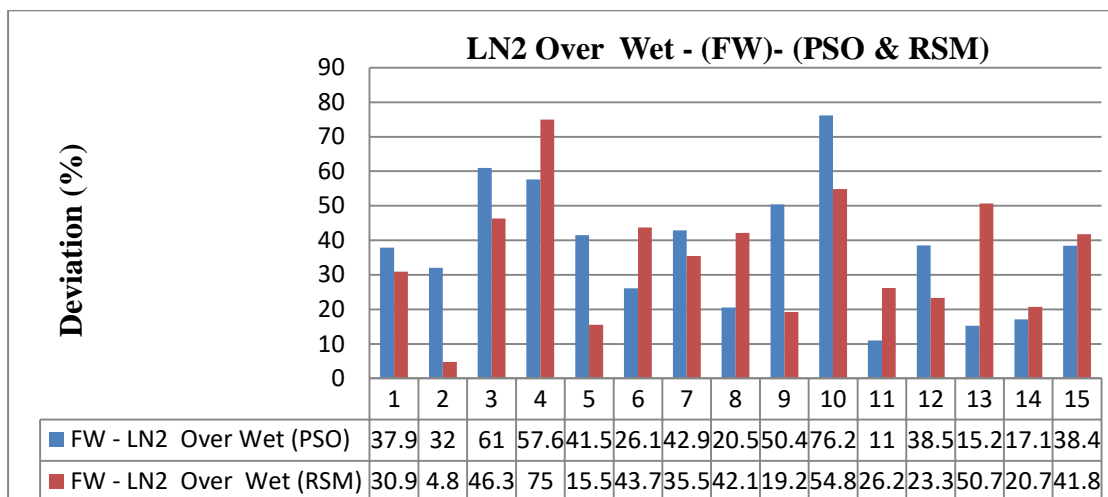
Figure 6.9: LN₂ influence over wet machining achieved in terms of percentage (%) for response flank wear (FW) achieved through PSO & RSM Methods

In Figure 6.8 the comparison between experimental, PSO and RSM has been done with respect to the output response of flank wear (FW) with machining condition as wet and LN₂.

Figure 6.9 represents the percentage of LN₂ impact on wet machining of all responses achieved via RSM and PSO approaches. The results gained via LN₂, point towards achievement of better results as compared to that of wet machining. From Figure 6.9, it can be derived that, LN2 influence over wet machining achieved in terms of percentage (%).

6.7 COMPARATIVE STUDY FOR FW – (EXPERIMENTAL V/S PSO V/S RSM) UNDER WET & LN₂ MACHINING CONDITIONS

From the Figure 6.10 it can be noticed that the flank wear increments linearly with spindle speed beneath both environmental conditions i.e. (cryogenic and wet) (Sudhansu et al 2015, Wit et al 2010, Bailey et al 1976, Natasha et al 2014). Since, the higher spindle speed produces high temperatures within very minute time. Additionally contact area diminishes amid the tool - workpiece area of interface. Thus tool material softening leads to higher tool wear, because as the cutting edge is continuously exposed to high cutting temperatures at higher spindle speed.

In LN₂ (cryogenic) condition, flank wear diminishment was observed to be 45.16 % contrasted with the wet machining. The control over the mechanism of wear (i.e abrasion and adhesion) was successful and adequate by spraying required amount of nitrogen liquid at the tool appearances of rake and flank, as the appearance of tool prompts change in wear resistance of the cutting tool and additionally decreases in the cutting zone temperature (Kaynak et al 2014, Virgina et al 2014, Domenico et al 2012 Dinesh et al 2016).

Figure 6.10 delineates the tool flank wear SEM images, with concerning the changing speed subsequently 3 minute machining in both environments (i.e. Wet and Cryogenic). The mechanisms of wear (i.e. Abrasion and adhesion) were detected on the appearance of the tool (flank face) in both conditions (i.e. wet, cryogenic). It was observed that, in case of wet condition flank wear was higher contrasted with the case of cryogenic condition. This is mainly to the fact of the temperature increment generated in wet case of machining further, leading to creation of built-up-edges (BUE) due to the robust adhesion of the chip to the tool face (rake) (Umbrello et al 2012). From Figure 6.10 it is apparent that at the cutting tool tip (flank) there is adhesion of machined material. But by spraying of liquid nitrogen (LN₂) at the zone of machining will substantially lessen the temperatures, thus reducing the adhesion and BUE formation. The outcomes signify that even at higher spindle speed; by spraying (LN₂) tool wear can be reduced. Thus machining with the LN2 will enhance

tool life and quality of product. The consequences of PSO determined optimized milling condition is in good concurrence with SEM images contrasted with CCD approach.

Study of **SEM micrographs of machined SS316**

Environment (Optimal Conditions)	
Process Parameters: 3000 (rpm) 350(mm/min) 0.5 (mm) 1 LN$_2$	
Wet (Coolant) Machining	Cryogenic (LN2) Machining
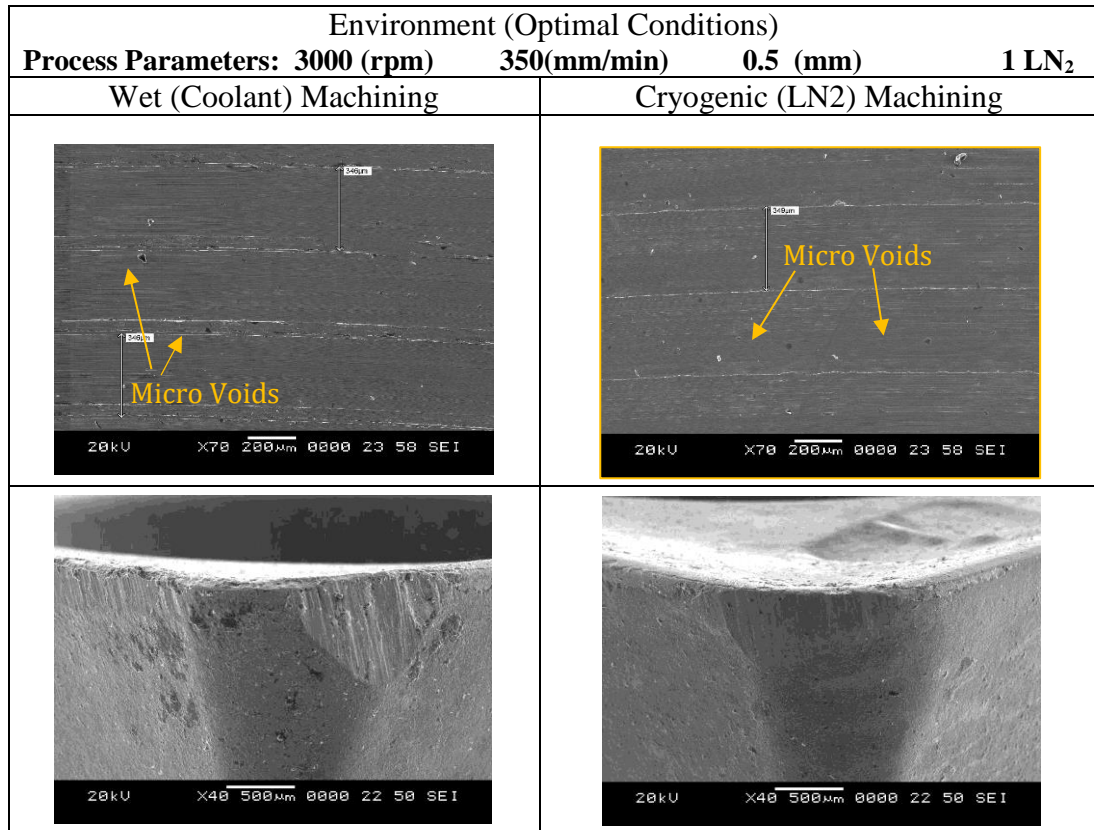
Figure 6.10: Microscopic view of milling samples of tool flank wear at different machining condition

Table 6.7: Optimized process parameters in milling.

Optimization Tool	Milling Condition							
	Spindle Speed (rpm)	Feed rate (mm/min)	Depth of cut (mm)	Coolant type	Cutting Temperature (CT, °C)	Cutting Force (Fx, N)	Surface Roughness (Ra, μm)	Flank Wear (VB, μm)
Experimen	3000	350	0.5	1	84	214	0.583	0.142
DFA	3000	350	0.5	1	99.98	225.0	1.14	0.13
PSO	3000	350	0.5	1	97	223	1.10	0.152

6.8 CONCLUSIONS

The response data are gathered for various milling conditions according to CCD outline (using regression equations of all outputs). Both conventional and nonconventional optimization strategies have been employed to decide the optimum process factors compared to desired responses. The accompanying inferences are drawn:

- It is to be noticed that, CCD model is observed to be statistically sufficient in response prediction. In order to carry out and attain the optimized values, the achieved response (regression equation) is used as a goal (objective) function.

- The desired responses and the relative milling prerequisite are resolved using traditional and non-traditional. It is fascinating to take note that non-traditional strategy (PSO) outperformed DFA in determining the best milling condition that generate required responses.

- The comparative study was carried out using RSM and PSO techniques in order to identify the best machining condition and to indicate the optimized parameters under wet and LN_2 machining condition.

- The results attained indicate that utilization of LN_2 helps in achieving better results compared to that of wet machining condition (see Table 6.3-6.6).

- The goal of the current study is to build up a relation (nonlinear) for the response and to decide the best set of process factors that brought about desired responses and further to accomplish better microstructure. In order to reach the stated purpose. The data set, modelling and various tools of optimization have been involved.

- The computational results reveal that the PSO algorithm is competitive with or superior to the other optimization algorithms for the considered problem.

- The outcomes acquired through PSO are likewise compared with the customary desirability approach and it was found that PSO gives closer values compared to the results obtained with the desirability approach.

- Since, PSO could able to obtain a global optimum solution within a reasonable execution time due to its faster convergence characteristic, the algorithms can be used on on-line systems for the selection of optimal cutting parameters.

- The method is completely generalized and problem independent, so that it can be easily generalised to other machining operations such as drilling, grinding, non-traditional machining operations, etc.

CHAPTER 7
RESULTS AND DISCUSSION (PART 4)
PART A
MACHINE LEARNING – SUPPORT VECTOR MACHINE

7.1 INTRODUCTION

The support vector machine (SVM) is firmly grounded in the framework of statistical learning theory, which characterizes the properties of learning machines enabling them to generalize well to unseen data. Traditional neural network approaches for the empirical data modelling have suffered from difficulties with generalization, producing models that may over-fit the data (Muzaffer et al 2018). The SVM learning is gaining popularity due to its many attractive features and promising empirical performance. The formulation of SVM embodies the structural risk minimization (SRM) principle, which has been shown to be superior (Garcia et al 2015) (to traditional empirical risk minimization (ERM) principle, employed by conventional neural networks. SRM minimizes an upper bound on the expected risk, as opposed to ERM that minimizes the error on the training data. Support vector regression (SVR) is a new technique, which has been successfully applied to function estimation based on the concept of SVM. SVR has advantages over traditional approaches such as neural networks for the following reasons:

➢ Good generalization performance—once it is presented with a training set, it is able to learn a rule, which can correctly classify a new object quite often.

➢ Computational efficiency—it is efficient in terms of speed and complexity.

➢ Robust in high dimensions—in general, dealing with high-dimensional data is difficult for a learning algorithm because of over-fitting. One of the major reasons for attracting much attention is that SVRs are more robust to this over-fitting than other algorithms.

In the current research the SVR is implemented in order to perform regression, Regression model can be seen from these set of packages (Kernlab, e1071).

SVR can be performed in a linear or nonlinear manner, depending on what is known as the "kernel-trick." The use of support vector kernel expansion provides us a potential avenue to represent nonlinear dynamical systems and underpin advanced analysis. Other computational models are often computationally expensive and sufficient model sparsity cannot be guaranteed. In an attempt to mitigate these drawbacks, focus is on the application of support vector regression (SVR) with hybrid kernel in nonlinear black-box systems identification.

There are three different types of SVM regression i.e SVM eps – Regression, SVM nu – Regression, Bound Constraint SVM eps – Regression. Among these 3 types SVM eps – Regression, SVM nu – Regression utilize the e1071 package and Bound Constraint SVM eps – Regression utilize kernlab package. The functions used in the regression method are SVM for SVM eps – Regression, SVM nu – Regression and KSVM function for Bound Constraint SVM eps – Regression. By taking a dataset how model can be built using SVM on the training data and do the testing of the same. Even, how to access the goodness or accuracy fit of the model.

7.2 SVM eps – REGRESSION AND SVM nu - REGRESSION

- Package e1071 with the svm function.
- Svm (y ~., data, kernel, cost, type = "eps – regression", epsilon, gamma, cost,…)
  Where : y = response variable (need to be numerical and continuous variable), dot = all other attributes are contributing to it, data = dataframe need to be specified, kernel = need to be specified (linear, polynomial, radial basis, sigmoid, cost = default, type = "eps – regression", epsilon =(default), gamma =(default), cost =(default).
- Kernel ->kernel function.
- Parameters cost, gamma and epsilon.
- Type set to "eps – regression".
- Continuous response variable y and the covariates data.

7.3 STEPS TO PERFORM SVR

1) Load the e1071 package.

2) Get the necessary data with a continuous response variable.

3) Preliminary inspection of the data (Summary).

4) Split the sample data into training set and a testing set on a random basis.

5) Estimate the SVM using the default settings (Radial basis function as the kernel with cost parameter value set equal to 1)

6) Summary function provides details of the estimated model.

7.4 COMMANDS UTILIZED TO PERFORM SVR

Step 1: Load the data

Ex: milling (<- read.csv("H:\\Training\\RDatasets\\milling.csv")

- **dim(milling)**

    [1] 150 7

    Where 150 : Indicate rows, 7 : Indicates columns

Step 2: Head(milling)

Displays the data with column names. (Identify the independent and dependent data,

Identify the response variable - Quantitative column).

- **Load package:** library(e1071)

- **Load function:** svm

- **Provide** Formula, Kernel Functions[Linear, Polynomial, Radial Basis, Sigmoid], Scale = True (default), Size (default), Type =(Select any one among these 5 types {c – Classification, nu – Classification, One – Classification (for novelty detection), eps – regression, nu – regression}), epsilon = 0.1(default), gamma (based on kernel function),Cost =1 (default)

Step 3: Basic Check-up of Data (To identify the irregularities/abnormalities/outliers in the data)

✓ Summary (milling): To identify the categorical and quantitative data values.

- ✓ Library (paych)
- ✓ Describe (milling): Identify the skewness in the data (If anything more then 0, highly skew value: Indicates the abnormalities/ outliers in the data on the higher side.
- ✓ High Skew value: logarithmic Transformation on data needs to be performed (So that response variable comes in the normal range).

Objective: The best possible output or model which is having higher level of accuracy when performed on my testing data so that it can very well roll it out in to the production cost.

Step 4: Split Data in to Training and Testing Data
- ➢ set.seed(1000)
  - o 1338*0.7
  - o [1] 936.6
- ➢ train (-sample(1:1338,937, replace = False)
  - o System picks random values without any duplications (so replace = false)
- ➢ traindata(-milling[train,]
  - o (traindata is subset of milling dataset, rows which come part of train and all columns, so (+train).
- ➢ testdata(-milling[-train,]
  - o rows which didn't come as part of the train and all columns(so –train).

Step 5: Estimate the svm using the default settings
- ➢ Type = "eps – regression"
- ➢ Kernel = "All 4 types".
- ➢ Cost, Gamma, Scale, epsilon = default values.

Kernel Functions Commands

> fitepslinear(-svm(dependent variable name., data = traindata (building the model using traindata and later testing it on testdata), type = "eps-regression", kernel = "linear")

> fitepspoly(-svm(dependent variable name., data = traindata, type = "eps-regression", kernel = "polynomial")

> fitepsradial(-svm(dependent variable name., data = traindata, type = "eps-regression", kernel = "radial")

> fitepssigmoid(-svm(dependent variable name., data = traindata, type = "eps-regression", kernel = "sigmoid").

Objective: To check whether to what extent objective is met in terms of making accurate predictions on testing data (**Theoretical way:** Whether for this data this particular model would be fit or no).

Step 6: To check each of the model:

> **fitepslinear** or **summary**(fitepslinear)

> **Parameters**

  o Svm – type = eps-regression
  o Svm – kernel= linear
  o Cost = 1
  o Gamma = 0.1111
  o Epsilon = 0.1

  Number of support vectors = 12

> **Plot (fitepslinear)**

  Similarly other models can be performed.

Step 7: Setting the Cross – Validation (To improvise the model)

> fitepslinear(-svm(dependent variable name., data = traindata, type = "eps-regression", kernel = "linear", cross = 17)

> fitepspoly(-svm(dependent variable name., data = traindata, type = "eps-regression", kernel = "polynomial", cross = 17)

> ➤ fitepsradial(-svm(dependent variable name., data = traindata, type = "eps-regression", kernel = "radial", cross = 17)

> ➤ fitepssigmoid(-svm(dependent variable name., data = traindata, type = "eps-regression", kernel = "sigmoid", cross = 17)

Cross – Validation: After Execution of Cross- Validation, It gives the 2 important things (TMSE = Total Mean Square Error for each model, R^2 = Correlation Coefficient Square) on the training data (To identify where this model is heading to).

Objective: To create the best possible model, which is giving the least possible error as well has highest possible R^2 both on training and testing data.

Step 8: Results

Table 7.1: To identify the accuracy associated with each of the model.

Dataset	Kernel Types / Models :				
		Linear	**Polynomial**	**Radial**	**Sigmoid**
Training Data	**TMSE**	44.27	40.31	30.35	79.93
	R^2	72.63	75.52	82.46	15.26
Testing Data	R^2	79.91	80.28	89.57	28.45

7.5 STEPS TO OBTAIN RESULTS

1) **Summary**(fitepslinear)

    a. **Parameters**
        i. Svm – type = eps-regression
        ii. Svm – kernel= linear
        iii. Cost = 1
        iv. Gamma = 0.1111
        v. Epsilon = 0.1

    b. **Number of support vectors = 12**
    c. 10 fold cross-validation on training data:
    d. **Total Mean Squared Error :** 44274925

e. **Squared Correlation Coefficient:** 0.7263019

f. **Mean Squared Errors:** 165510515   302226.3   33272219 354367.4……….(Errors obtained for different tried 937 combination).

From the obtained results indicated in Table (7.1) it can be infer that Radial model is doing better job. But before concluding. Prediction need to be performed on the test data to identify which model results in attaining a greater accuracy.

2) **To perform predictions (on test data) on each model: using** "predict" function.

> predepslinear(-predict(fitepslinear,testdata)
> predepspoly(-predict(fitepspoly,testdata)
> predepsradial(-predict(fitepsradial,testdata)
> predepssigmoid(-predict(fitepssigmoid,testdata)

3) **Plot**

plot(testdata$charges, predepslinear) : we obtain scatter plot (as actual values are incr4easing even the predicted looks increasing).

4) **Correlation existing between the actual data and predicted data**

> Cor(testdata$charges,predepslinear)^2
>> [1] 0.7635 : R^2 for linear model
> Cor(testdata$charges,predepspoly)^2
>> [1] 0.792296 : R^2 for linear model
> Cor(testdata$charges,predepsradial)^2
>> [1] 0.8629372 : R^2 for linear model
> Cor(testdata$charges,predepssigmoid)^2
>> [1] 0.1639803 : R^2 for linear model

Thus from the attained results of the Table (7.1) it can be inferred that radial model is reliable (86.29 % of accuracy on test data) as it does good job on both the training and testing data.

7.6 ENTIRE SVM eps – REGRESSION AND nu – REGRESSION

Steps

❖ Provides details of the type of svm, cost parameter, kernel type and associated gamma and epsilon, kernel parameter, number of support vectors, training error and cross validation error.

❖ Tune the model to obtain optimum parameters – set up the ranges for the cost and sigma and epsilon parameters (-> tune.svm)

❖ Find the best cross validation performance and store the optimal values.

❖ Estimate the optimal model using the training data and show the cross validation error

❖ Use predict method with the test data and the fitted model.

❖ Look at the scatter plot between the predicted and actual values.

❖ Also evaluate the R- Squared.

7.7 Comparison of Statistical Model (RSM), BNN, SVR and RVM for Responses

Table 7.2 (a): Summary of the test cases results for the response: Surface Roughness (Ra).

Exp. NO	Experimental Ra	RSM	BNN	SVR	Relative Error Obtained by RSM (%)	Relative Error Obtained by BNN (%)	Relative Error Obtained by SVR (%)
1	1.36	1.47	1.44	1.39	8.09	5.88	2.21
2	1.77	1.84	1.81	1.79	3.95	2.26	1.13
3	1.93	2.09	1.98	1.95	8.29	2.59	1.04
4	1.12	1.2	1.17	1.14	7.14	4.46	1.79
5	1.4	1.32	1.45	1.36	5.71	3.57	2.86
6	1.67	1.76	1.62	1.71	5.39	2.99	2.40
7	0.83	0.9	0.87	0.8	8.43	4.82	3.61
8	1.26	1.35	1.31	1.28	7.14	3.97	1.59
9	1.38	1.47	1.44	1.35	6.52	4.35	2.17
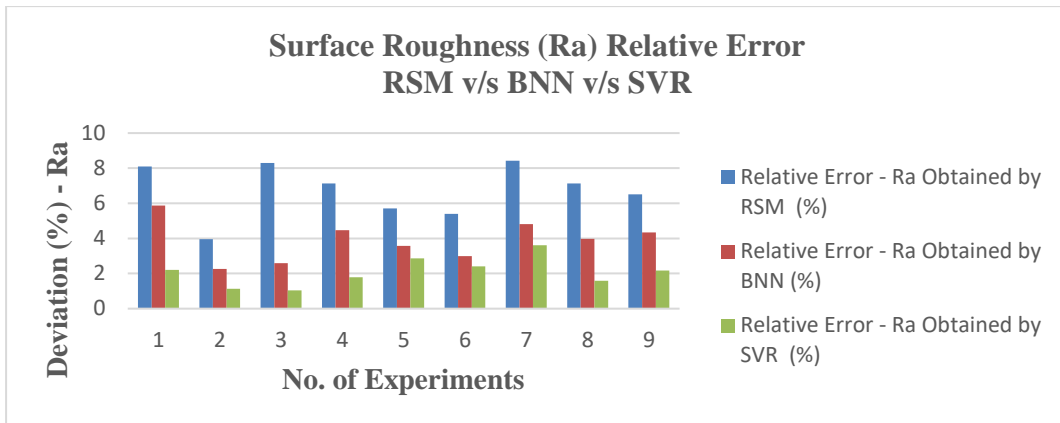
Figure 7.1: RSM v/s BNN v/s SVR predicted for response surface roughness (Ra) under wet and LN₂ machining conditions

Table 7.2 (b): Summary of the test cases results for the response: Cutting Force (FX).

Exp. NO	Experimental FX	RSM	BNN	SVR	Relative Error Obtained by RSM (%)	Relative Error Obtained by BNN (%)	Relative Error Obtained by SVR (%)
1	107	99	101	110	7.48	5.61	2.80
2	125	135	131	117	8.00	4.80	6.40
3	156	171	167	160	9.62	7.05	2.56
4	92	101	96	93	9.78	4.35	1.09
5	109	119	116	112	9.17	6.42	2.75
6	131	141	139	137	7.63	6.11	4.58
7	77	84	80	78	9.09	3.90	1.30
8	89	97	94	90	8.99	5.62	1.12
9	110	119	115	112	8.18	4.55	1.82
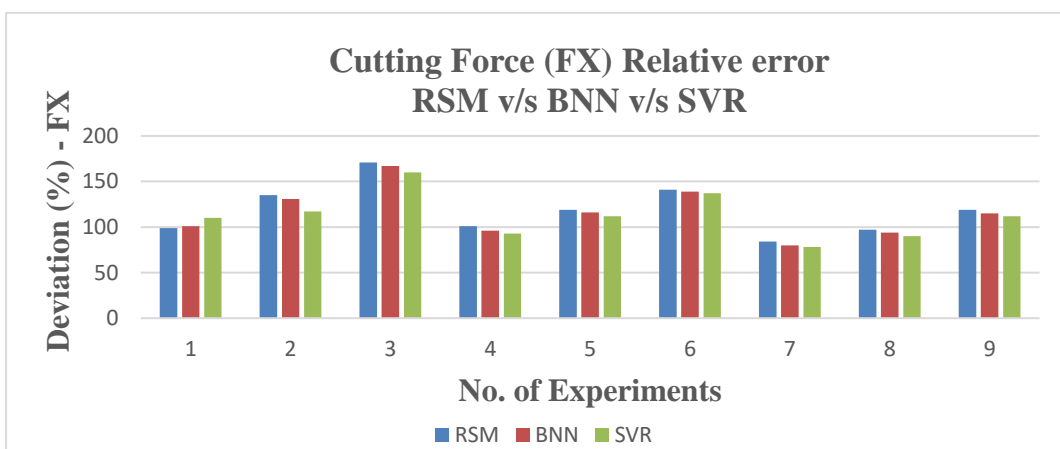
Figure 7.2: RSM v/s BNN v/s SVR predicted for response Cutting Force (FX) under wet and LN₂ machining conditions

Table 7.2 (c): Summary of the test cases results for the response: Cutting Temperature (CT).

Exp. NO	Experimental CT	RSM	BNN	SVR	Relative Error Obtained by RSM (%)	Relative Error Obtained by BNN (%)	Relative Error Obtained by SVR (%)
1	48	53	50	47	10.42	4.17	2.08
2	57	62	60	55	8.77	5.26	3.51
3	70	77	66	73	10.00	5.71	4.29
4	62	58	66	61	7.9	6.45	1.61
5	73	79	70	75	8.22	4.11	2.74
6	86	93	89	83	8.14	3.49	3.49
7	68	74	71	65	8.82	4.41	4.41
8	89	96	93	86	7.87	4.49	3.37
9	97	104	92	94	7.22	5.15	3.09
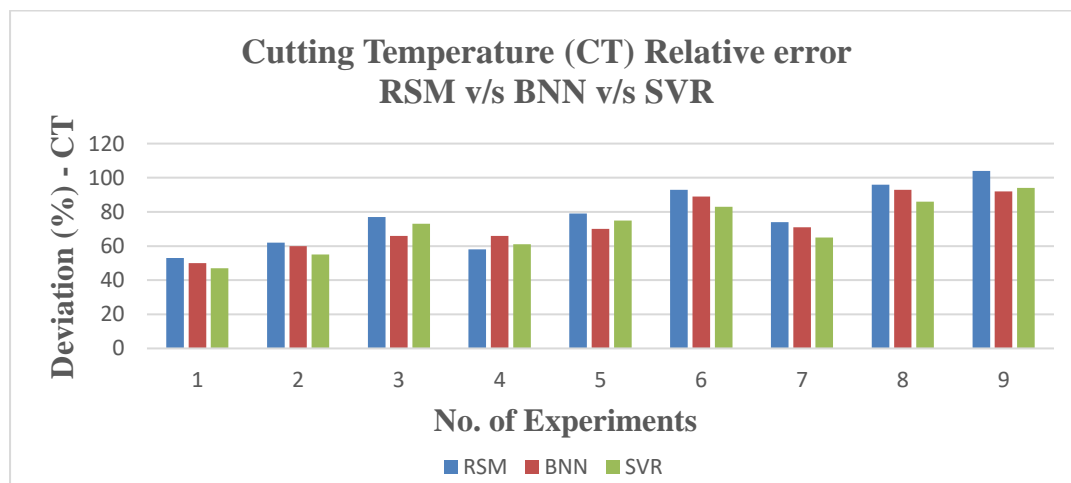
Figure 7.3: RSM v/s BNN v/s SVR predicted for response cutting temperature (CT) under wet and LN₂ machining conditions

Table 7.2 (d): Summary of the test cases results for the response: Flank Wear (FW).

Exp. NO	Experimental FW	RSM	BNN	SVR	Relative Error Obtained by RSM (%)	Relative Error Obtained by BNN (%)	Relative Error Obtained by SVR (%)
1	1.31	1.39	1.26	1.35	6.11	3.82	3.05
2	1.78	1.95	1.92	1.87	9.55	7.87	5.06
3	1.42	1.57	1.48	1.39	10.56	4.23	2.11
4	0.89	0.97	0.84	0.93	8.99	5.62	4.49
5	1.66	1.82	1.76	1.71	9.64	6.02	3.01
6	1.05	1.14	1.11	1.09	8.57	5.71	3.81
7	0.49	0.53	0.47	0.48	8.16	4.08	2.04
8	1.1	1.17	1.14	1.07	6.36	3.64	2.73
9	0.93	0.87	0.97	0.9	6.45	4.30	3.23
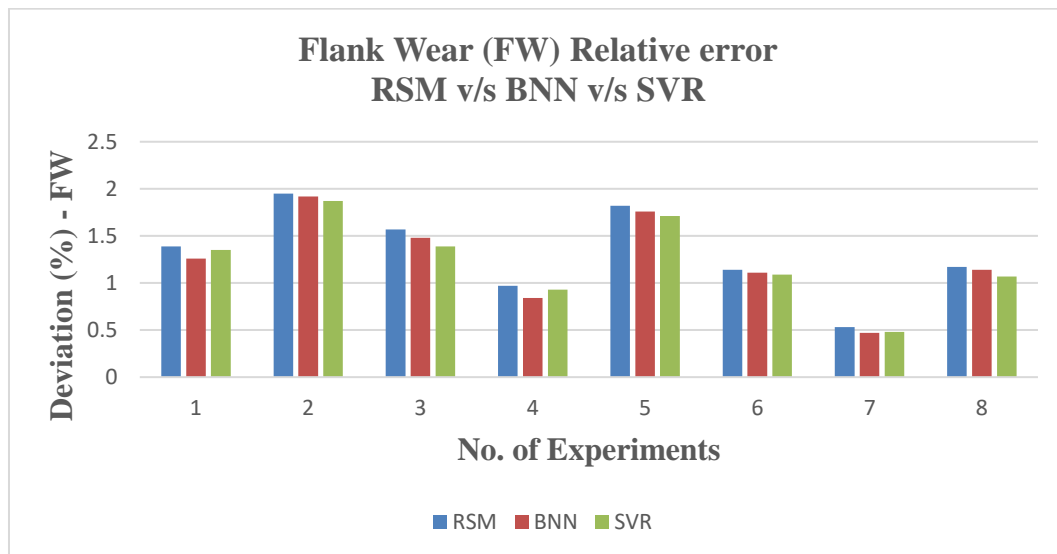
Figure 7.4: RSM v/s BNN v/s SVR predicted for response flank wear (FW) under wet and LN$_2$ machining conditions

Tables 7.2(a-d) represents the comparison results attained for responses (Ra, FX CT and FW) respectively through statistical, neural network, machine learning models. From Table 7.2(a-d) it is apparent that SVR approach yields better predicted results as compared to other prediction techniques RSM and ANN for all responses (Ra, Fx,

CT, FW) due to its features of Good generalization performance, Computational efficiency and Robust in high dimensions (M S Ahmad et al 2020). From Figures 7.1, 7.2, 7.3 and 7.4 it can be derived that radial model with cross validation utilized to carry out SVR technique helps in predicting greater desired results as compared to other prediction techniques of RSM and ANN for all responses (Ra, Fx, CT, FW respectively) due to its features of Good generalization performance, Computational efficiency and Robust in high dimensions (M S Ahmad et al 2020). After Execution of Cross- Validation (SVR), It yields main 2 things (TMSE = Total Mean Square Error for each model, R^2 = Correlation Coefficient Square) on the training data (To identify where this model is heading to). The TMSE and R^2 acts as deciding factors to choose the best technique, thus based on this from Figures 7.1-7.4 it can be concluded that SVR tends to predict best desired values of responses compared to RSM and BNN techniques.

7.8 RESULTS USING "R" PLATFORM

A)   Description of Dataset

```
Console   Terminal ×   Jobs ×
~/ ⇨
> describe(mil2)
                         vars  n    mean     sd median trimmed     mad     min     max   range  skew
Spindle.Speed..rpm.         1 20 2000.00 973.33 2000.00 2000.00 1482.60 1000.00 3000.00 2000.00  0.00
Feed.Rate*                  2 21    2.90   1.04    3.00    2.94    1.48    1.00    4.00    3.00 -0.07
Depth.Of.Cut*               3 21    2.90   1.00    3.00    2.94    1.48    1.00    4.00    3.00 -0.11
Coolant.type                4 20    0.00   0.92    0.00    0.00    1.48   -1.00    1.00    2.00  0.00
Cutting.Temperature....     5 20  170.40 100.73  155.00  169.12  134.92   35.00  324.00  289.00  0.14
Cutting.force*              6 21   11.00   6.20   11.00   11.00    7.41    1.00   21.00   20.00  0.00
Surface.Roughness.Ra.µm.    7 20    1.34   0.61    1.19    1.29    0.63    0.58    2.46    1.88  0.51
Flank.wear.Vb..µm.          8 20    0.18   0.07    0.18    0.18    0.07    0.06    0.29    0.23 -0.18
                         kurtosis    se
Spindle.Speed..rpm.         -2.00 217.64
Feed.Rate*                  -1.71   0.23
Depth.Of.Cut*               -1.54   0.22
Coolant.type                -1.87   0.21
Cutting.Temperature....     -1.65  22.52
Cutting.force*              -1.37   1.35
Surface.Roughness.Ra.µm.    -1.21   0.14
Flank.wear.Vb..µm.          -1.05   0.02
```

Figure 7.5: Description of dataset

B) Find the abnormalities in datasets

```
> summary(mil2)
 Spindle.Speed..rpm.    Feed.Rate Depth.Of.Cut  Coolant.type  Cutting.Temperature....  Cutting.force Surface.Roughness.Ra.µm. Flank.wear.Vb..µm.
 Min.   :1000     (mm/min):1    (mm):1     Min.   :-1    Min.   : 35.00         214     : 1    Min.   :0.5830          Min.   :0.0600
 1st Qu.:1000     350     :9   0.5 :8     1st Qu.:-1    1st Qu.: 84.75        219     : 1    1st Qu.:0.7775          1st Qu.:0.1450
 Median :2000     450     :2   1   :4     Median : 0    Median :155.00        243     : 1    Median :1.1865          Median :0.1775
 Mean   :2000     550     :9   1.5 :8     Mean   : 0    Mean   :170.40        256     : 1    Mean   :1.3378          Mean   :0.1819
 3rd Qu.:3000                              3rd Qu.: 1    3rd Qu.:269.50        269     : 1    3rd Qu.:1.8635          3rd Qu.:0.2425
 Max.   :3000                              Max.   : 1    Max.   :324.00        276     : 1    Max.   :2.4630          Max.   :0.2910
 NA's   :1                                 NA's    :1    NA's    :1            (Other):15    NA's    :1              NA's
> |
```

Figure 7.6: Find the abnormalities in datasets.

C) Summary of All Models

Linear Model

```
> summary(fitepslinear)

Call:
svm(formula = Cutting Temp ~ ., data = traindata, type = "eps-regression", kernel = "linear")


Parameters:
   SVM-Type:  eps-regression
 SVM-Kernel:  linear
       cost:  1
      gamma:  0.1111111
    epsilon:  0.1


Number of Support Vectors: 12
```

Figure 7.7 (a): Linear model

Polynomial Model

```
> fitepspoly

Call:
svm(formula = Cutting Temp~ ., data = traindata, type = "eps-regression", kernel = "polynomial")


Parameters:
   SVM-Type:  eps-regression
 SVM-Kernel:  polynomial
       cost:  1
     degree:  3
      gamma:  0.1111111
     coef.0:  0
    epsilon:  0.1


Number of Support Vectors: 14
```
Figure 7.7 (b): Polynomial model

Radial Model

```
> fitepsradial

Call:
svm(formula =cutting Temp ~ ., data = traindata, type = "eps-regression", kernel = "radial")


Parameters:
   SVM-Type:  eps-regression
 SVM-Kernel:  radial
       cost:  1
      gamma:  0.1111111
    epsilon:  0.1


Number of Support Vectors: 11
```

Figure 7.7 (c): Radial model

Sigmoidal Model

```
> fitepssigmoid

Call:
svm(formula = cutting Temp ~ ., data = traindata, type = "eps-regression", kernel = "sigmoid")


Parameters:
   SVM-Type:  eps-regression
 SVM-Kernel:  sigmoid
       cost:  1
      gamma:  0.1111111
     coef.0:  0
    epsilon:  0.1


Number of Support Vectors: 21
```

Figure 7.7 (d): Sigmoidal model

D)   To check accuracy of the model

```
> fitepslinear<-svm(charges~.,data = traindata, type = "eps-regression", kernel = "linear", cross = 14 )
> fitepspoly<-svm(charges~.,data = traindata, type = "eps-regression", kernel = "polynomial", cross = 14 )
> fitepsradial<-svm(charges~.,data = traindata, type = "eps-regression", kernel = "radial", cross = 14)
```

```
> summary(fitepslinear)

Call:
svm(formula = charges ~ ., data = traindata, type = "eps-regression", kernel = "linear", cross = 14 )


Parameters:
   SVM-Type:  eps-regression
 SVM-Kernel:  linear
       cost:  1
      gamma:  0.1111111
    epsilon:  0.1


Number of Support Vectors: 12


14 -fold cross-validation on training data:

Total Mean Squared Error: 44274925
Squared Correlation Coefficient: 0.7263019
Mean Squared Errors:
 185510515 302226.3 33272219 354367.4 225812.9 282191861 49540727 6366557 452393.5 32699.65 741.7093 175081.2 65137.79 17482158
```

Figure 7.7 (e): To find fitness of the model

E) Prediction for testdata

```
> predepslinear<-predict(fitepslinear,testdata)
> predepspoly<-predict(fitepspoly,testdata)
> predepsradial<-predict(fitepsradial,testdata)
> predepssigmoid<-predict(fitepssigmoid,testdata)
```

Figure 7.7 (f): To find prediction of test data of models

F) To plot scatter plot
Plot(testdata$cuttingtemperature,predepslinear) [As actual values are increasing even the predicted values are increasing]

Figure 7.7 (g): To plot scatter graph

G) To find Correlation square between actual and predicted data

```
> cor(testdata$charges,predepslinear)^2
[1] 0.799157
> cor(testdata$charges,predepspoly)^2
[1] 0.802869
> cor(testdata$charges,predepsradial)^2
[1] 0.895713
> cor(testdata$charges,predepssigmoid)^2
[1] 0.284561
```

Figure 7.7 (h): To find Correlation square between actual and predicted data
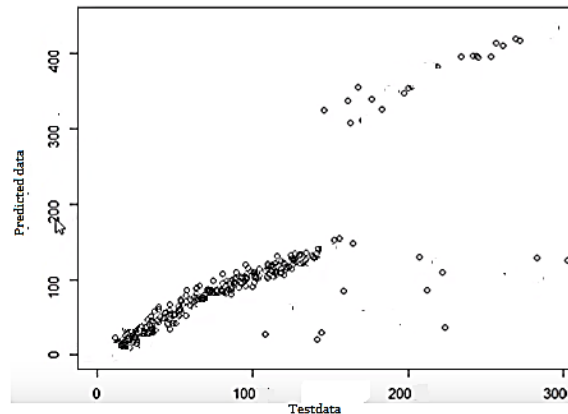
Figure 7.8: Predicted Data V/S Test Data

It is obvious that estimation accuracy of SVM depends on kernel parameters, capacity C and insensitivity region e. The value of e influences the number of support vectors used to form the regression function. If e increases, fewer support vectors are chosen, and the smoothness of the regression function increases too. The capacity C represents a trade-off cost between the empirical error and the model complexity (flatness). Figure 7.5 gives a brief idea on usage and description of dataset, Figure 7.6 represents the procedure to filter out the abnormalities present in the considered dataset. Figure 7.7 (a-d) mentions the steps carried out to identify the fitness and number of support vectors required for the models (Linear, Polynomial, Radial and Sigmoidal models) respectively to predict the desired results. Figure 7.7 (e) describes and checks the accuracy of models. Figure 7.7 (f) implies the prediction approach on test data. Figure 7.7 (g) shows the commands utilized to plot the scatter graph for both actual and predicted datasets. Similarly Figure 7.7 (h) represents and checks the Correlation square attained between actual and predicted data. SVM Programming was carried out using "R" platform.

In this research, radial basis function kernel was used. The kernel parameter s and the parameter e were determined by a leave-one-out (LOO) cross-validation procedure (Mazaffer et al 2019, Kong et al 2016).All 30 data points were used in the LOO procedure. First, the capacity C was chosen to be constant and set to 10, and e was set to 0.21. Then, the LOO procedure was performed to find s, which minimizes the mean squared error (MSE). The minimal MSE was achieved at s=1.7. Afterward, the same

procedure was repeated but now to find e, which minimizes the MSE, and in this case, s was set to 1.7. It was found that e=0.13 gives the minimal value of the MSE. In both cases, the minimal values of the MSE were found using PSO optimization algorithm (Wang et al 2020). The results of the LOO procedure in a graphical form are shown on Figure 7.8, precisely for kernel parameter (Figure 7.9a) and parameter e (Figure 7.9b). After both parameters have been found, the SVM model is ready for the learning process. The effectiveness of training of the SVM model is depicted on Figure 7.10a and its ability to predict correct values for unseen data on Figure 7.10b. The values of R very close to 1 for both training and testing indicate that the model has been very well learned and that also has the excellent generalization ability.
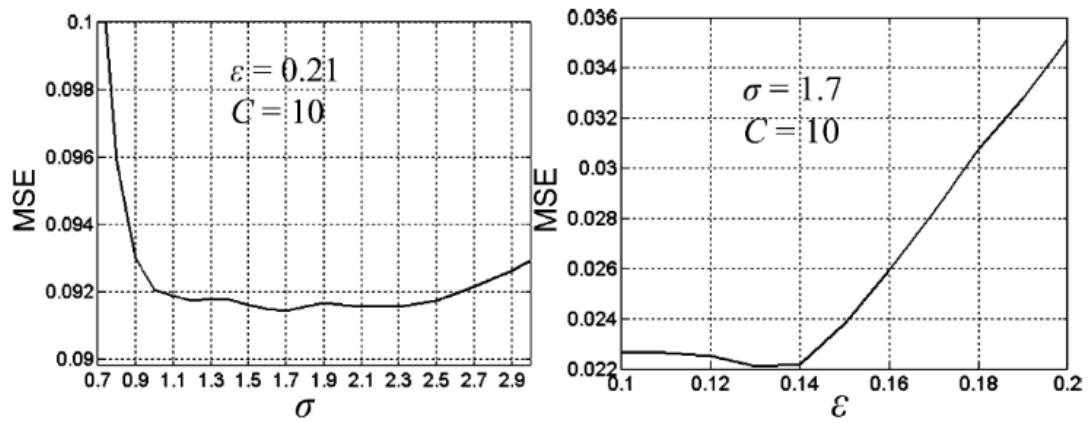
Figure 7.9: Results of LOO procedure in determining kernel parameter σ (a) and parameter ε (b)
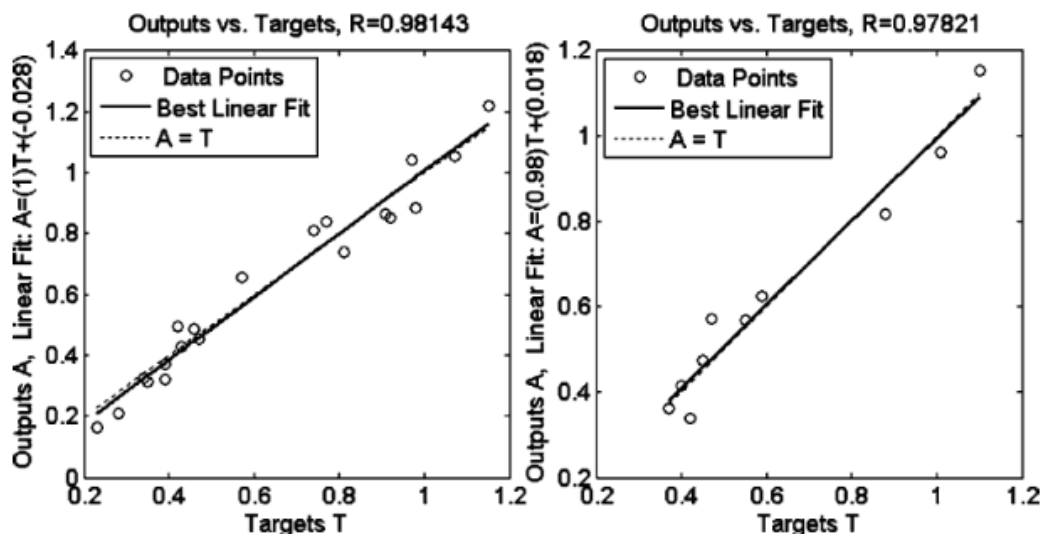
Figure 7.10(a): Results of SVR for training   Figure 7.10(b): Results of SVR for testing

PART B

7.9 SVM-PSO PREDICTION-OPTIMIZED MODEL

Support vector machines (SVMs) are a set of related super-vised learning methods used for classification and regression (Jingchao et al 2020, Gu et al 2020, Hu et al 2019).The SVMs were originally developed for classification and were later generalized to solve regression problems (Dong-Dong et al 2020, Garci et al 2015, Cho et al 2004, Hsueh et al 2008, Wang et al 2014). This last method is called Support Vector Regression (SVR). The model produced by SVR only depends on a subset of the training data, because the cost function for building the model tries to ignore any training data that are close (within a threshold $\in$) to the model prediction. When the regression SVM is applied to nonlinear separable data, it is necessary to use the kernel trick. The reason that this kernel trick is useful is that there are many regression problems that are not linearly regressable in the space of the inputs x, which might be in a higher-dimensionality feature space given a suitable mapping $x \mapsto \psi(x)$ (Kya et al 2014, Gangadhar et al 2014).

The basic idea of SVR is briefly described here. Instead of attempting to classify new unseen variables $\breve{x}$ into one of two categories $\tilde{y}=\pm1$, now to predict a real-valued output y for the observed value t so that our training data is a set of L points of the form $\{x_i, t_i\}$, where $i=1,2,\ldots,L$, $y \in R$, and $x \in R^D$ (Himaanshu et al 2002,Zhang et al 2003, Hong et al 2007, Durgesh et al 2010 and Chen et al 2010).

$$y_i = f(\mathbf{x}_i) = \mathbf{w} \cdot \mathbf{x}_i + b \tag{1}$$

Where "·" denotes the dot product, x_i is the D-dimensional real input vector, w is the normal vector to the maximum-margin hyperplane, and y_i is the predicted output value (equation 1). The parameter $b/\|w\|$ determines the offset of this hyperplane from the origin along the normal vector w. The SVR uses a more sophisticated penalty function: a penalty is not imposed if the predicted value y_i is less than the distance ε away from the actual value ti, i.e., if $|t_i - y_i| < \varepsilon$.

Referring to Figure 7.11, the region bound by $y_i \pm \varepsilon \forall I$ (equation 2), is called the e-insensitive tube. Another modification to the penalty function is that output variables outside the tube are allocated one of two slack variable penalties, depending on whether they lie above ($\xi > 0$ and $\xi +$-)or below($\xi +$) the tube, where $\xi > 0 \forall i$.

$$t_i \leq y_i + \varepsilon + \xi^+$$

$$t_i \geq y_i - \varepsilon - \xi^- \tag{2}$$

The task is then to find a functional form f that can correctly predict new cases that the SVM has not been presented with before. This can be achieved by training the SVM model on a sample set called the training set, a process that involves the sequential optimization of an error function. Depending on the definition of this error function, two types of SVM models can be recognized and the resulting SVM problem can be formulated as follows (Piotr Nazarko 2011, Gupta et al 2011, Anto et al 2011):

(a) Regression SVM type 1 (also known as ε–SVM regression): for this type of SVM, we have to solve an optimization problem, minimizing the following general risk using (equation 3 and 4), function (Piotr Nazarko 2011, Gupta et al 2011,and Kumari et al 2011):

$$R[\mathbf{w}, b, \xi] = \frac{1}{2} \|\mathbf{w}\|^2 + C \sum_{i=1} \left(\xi_i^+ + \xi_i^- \right) \tag{3}$$

Subject to

$$\left\{ \begin{array}{c} \langle \mathbf{w}, \psi(\mathbf{x}_i) \rangle + b - y_i \leq \varepsilon + \xi_i^+ \\ y_i - \langle \mathbf{w}, \psi(\mathbf{x}_i) \rangle - b \leq \varepsilon + \xi_i^- \\ \xi_i^+, \xi_i^- \geq 0 \end{array} \right\} i = 1, \ldots, L \tag{4}$$

(b) Regression SVM type 2 (also known as v–SVM regression): for this SVM model, it is necessary to solve the following optimization problem, minimizing the following general risk function (Piotr Nazarko 2011, Gupta et al 2011, Anto et al 2011, and Garcia et al 2015):

$$R[\mathbf{w}, b, \xi] = \frac{1}{2} \|\mathbf{w}\|^2 - C \left[v\varepsilon + \frac{1}{L} \sum_{i=1}^{L} \left(\xi_i^+ + \xi_i^- \right) \right] \tag{5}$$

Subject to

$$\left\{ \begin{array}{c} \langle \mathbf{w}, \psi(\mathbf{x}_i) \rangle + b - y_i \leq \varepsilon + \xi_i^+ \\ y_i - \langle \mathbf{w}, \psi(\mathbf{x}_i) \rangle - b \leq \varepsilon + \zeta_j^- \\ \xi_j^+, \zeta_j^- \geq 0 \end{array} \right\} i = 1, \dots, L \tag{6}$$

where $\psi : X \rightarrow Z$ is the transformation of the input space into a new space Z, usually a larger dimension space, where we define an inner product by means of a positive definite function k (kernel trick, (equation 6),) (Piotr Nazarko 2011, Gupta et al 2011, Anto et al 2011, and Garcia et al 2015).

$$\langle \psi(\mathbf{x}), \psi(\mathbf{x}') \rangle = \sum_i \psi_i(\mathbf{x}) \psi_i(\mathbf{x}') = k(\mathbf{x}, \mathbf{x}') \tag{7}$$

The above problem is quadratic with linear constraints, and so, the Karush–Kuhn – Tucker (KKT) optimality conditions are necessary and sufficient (equation 7 and 8). The solution, which can be obtained from the dual problem, is a linear combination of a subset of sample point-denominated support vectors (s.v.) (Garcia et al 2015, Kadirgama et al 2012, Lela et al 2009, Shi et al 2007, and Sun et al 2019) as follows:
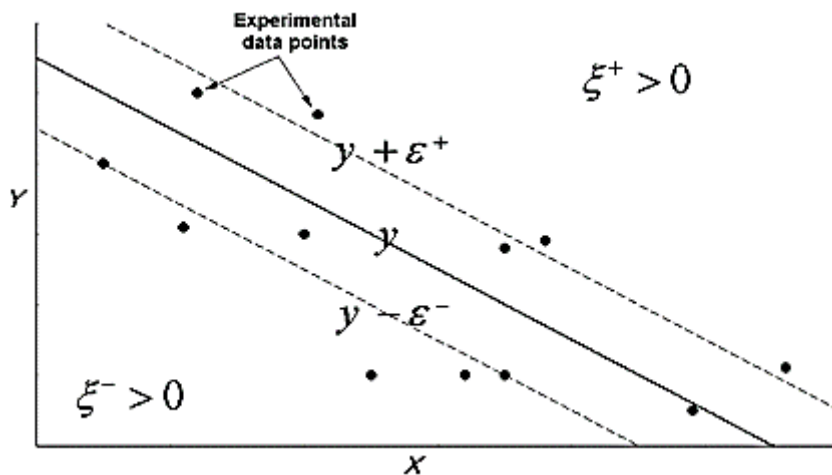
Figure 7.11: SVM Graph

$$\mathbf{w} = \sum_{s.v.} \beta_i \psi(\mathbf{x}_i) \Rightarrow$$

$$f_{\mathbf{w},b}(\mathbf{x}) = \sum_{s.v.} \beta_i \langle \psi(\mathbf{x}_i), \psi(\mathbf{x}) \rangle + b = \sum_{s.v.} \beta_i k(\mathbf{x}_i, \mathbf{x}) + b \tag{8}$$

The reason that this kernel trick is useful is that there are many regression problems that cannot be linearly regressed in the space of the inputs x, which might be in a higher dimensional feature space given a suitable mapping (equation 9). Different kernel functions are described in the bibliography as for example (Himanshu et al 2002, Piotr Nazarko 2011, Gupta et al 2011, Anto et al 2011, Huang et al 2010 and Garcia et al 2015)

Radial basis function

$$k\left(\mathbf{x}_i, \mathbf{x}_j\right) = e^{-\sigma\left\|\mathbf{x}_i - \mathbf{x}_j\right\|^2}$$

(9)

Polynomial Kernel

$$k\left(\mathbf{x}_i, \mathbf{x}_j\right) = \left(\mathbf{x}_i \cdot \mathbf{x}_j + a\right)^b$$

(10)

Where **s, a** and **b (equation 10)** are the parameters defining the kernel's behaviour. To sum up, to use an SVM to solve a regression problem for data that is not linearly separable, we need to first choose a kernel and relevant parameters that can be expected to map the nonlinearly separable data into a feature space where it is linearly separable.

7.10 THE GOODNESS OF FIT OF THIS APPROACH

In this study, an SVR technique in combination with the PSO approach has been implemented in order to predict the milling tool flank wear values using radial basis function (RBF) kernels (Piotr Nazarko 2011). The goodness of fit of a statistical model describes how well it fits a set of observations. Indeed, it is important to select the model that best fits the experimental data. The following criterion was considered here (Gupt et al 2011, Kumari et al 2011, Anto et al 2011):

The coefficient of determination (R): as it is well known, in statistics, the coefficient of determination (R^2) is used in the context of statistical models whose main purpose is the prediction of future outcomes on the basis of other related information (Senthilkumar et al 2016, Shalina et al 2019). If an intercept is included, then R^2 is

simply the square of the sample correlation coefficient between the outcomes and their predicted values. To fix ideas, this ratio indicates the proportion of total variation in the dependent variable explained by the model (milling tool wear in our case). A dataset takes the value "ti", each of which has an associated modelled value "yi"as indicated (equations 11 and 12) (Yamina et al 2020, Shalina et al 2020). The former is called the observed value, and the latter is often referred to as the predicted value. The variability in the dataset is measured through different sums of squares (Piotr Nazarko 2011, Anto et al 2011, Garcia et al 2015, Marco et al 2017)

- $SS_{tot} = \sum_{i=1}^{n} (t_i - \bar{t})^2$: the total sum of squares, proportional to the sample variance.
- $SS_{reg} = \sum_{i=1}^{n} (y_i - \bar{t})^2$: the regression sum of squares, also called the explained sum of squares.
- $SS_{err} = \sum_{i=1}^{n} (t_i - y_i)^2$: the residual sum of squares.

(11)

In the previous sums, $\bar{t}$ is the mean of the n observed data

$$\bar{t} = \frac{1}{n} \sum_{i=1}^{n} t_i$$

(12)

Bearing in mind the above sums, the general definition of the coefficient of determination is

$$R^2 \equiv 1 - \frac{SS_{err}}{SS_{tot}}$$

(13)

The coefficient of determination (equation 13) value of 1.0 indicates that the regression curve fits the data perfectly.

7.11 ANALYSIS OF RESULTS AND DISCUSSION

The predicted output variable is the flank wear (VB) measured in micrometres. Additionally, it is well known that the SVM techniques are strongly dependent on the SVM hyper parameters: the regularization factor C (see Eq. (5), the hyper parameter that defines the e-insensitive tube (allowable error), and s that represents the kernel

199

parameter if an RBF is chosen. There exists a vast body of literature regarding the choice of hyper parameters for SVMs (Piotr Nazarko 2011, Gupta et al 2011, Anto et al 2011, and Garcia et al 2015) Some methods often used to determine suitable hyper parameters are (Gupta et al 2011, Anto et al 2011, Garcia et al 2015, Ali et al 2016) Cross-validation, grid search, random search, Nelder–Mead search, heuristic search, genetic algorithms, pattern search, etc.

In other words, a novel hybrid PSO–SVM-based model was applied to predict the milling tool wear (output variable) from the other three remaining variables (input variables) in a milling process (Piotr Nazarko 2011, Ali et al 2016), studying their influence in order to optimize its calculation through the analysis of the coefficient of determination (R^2) with success Figure 7.12 shows the flowchart of this new hybrid PSO–SVM-based model developed in this study. The PSO-SVM model was tried out by researchers for biomedical field, but the highlight of our study is to implement the PSO-RBF-SVM model for milling with identifying the best kernel and to implement the same for regression that is to carry out prediction and optimization.

The determination coefficient is the statistical measure of how well a regression curve approximates real data points. Furthermore, it is a descriptive measure ranging from zero to one, indicating how good one term is predicted by another one. Thus, $R^2 = 1$ indicates the best approximation and $R^2 = 0$ the worst one.

Table 7.3: Initial ranges of the three hyper-parameters of the PSO–SVM based model with an RBF kernel.

SL.NO	SVR Hyper parameters	Higher Limit	Lower limit
1	c	10^{-3}	10^{-5}
2	ε	10^{-3}	10^{-9}
3	σ	10^{-3}	10^{-5}

Table 7.4: Optimal hyper-parameters of the fitted RBF–SVM-based model found with a PSO technique.

Kernel	Values Of Optimal Hyper parameters
RBF	Regularization Factor $C = 58.726$, $\varepsilon = 0.01631$, $\sigma = 0.5364$
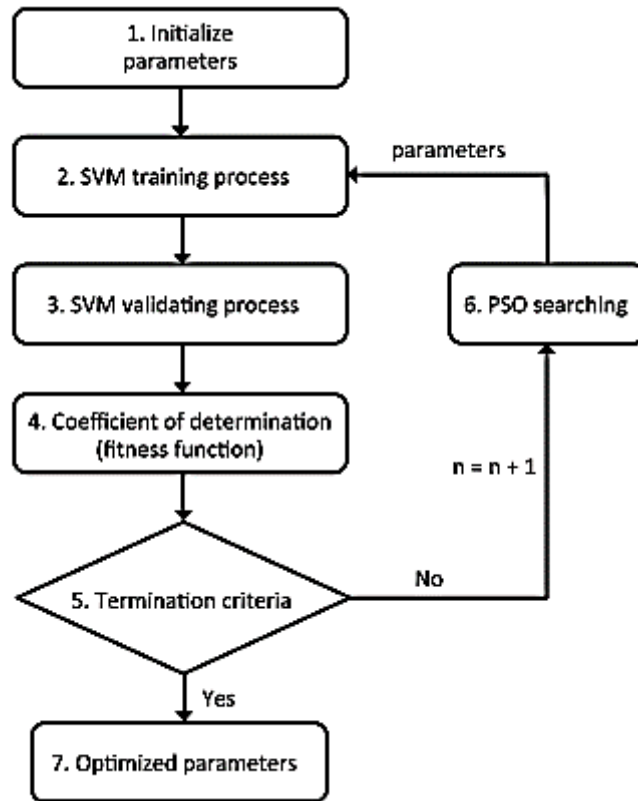
Figure 7.12: Flowchart of the new hybrid PSO–SVM-based model

Cross-validation was the standard technique used here for finding the real coefficient of determination (R^2). The data set is randomly divided into l disjoint subsets of equal size, and each subset is used once as a validation set, whereas the other l-1 subsets are put together to form a training set. In the simplest case, the average accuracy of the l validation sets is used as an estimator for the accuracy of the method (Garcia et al 2015). The combination of the hyper parameters with the best performance is chosen in this way, 10-fold cross-validation was used here.

As it has been previously pointed out, in order to guarantee the prediction ability of the PSO–SVM-based model, an exhaustive 10-fold cross-validation algorithm was used (Wang et al 2014). The referred algorithm consists in splitting the sample into 10 parts and using 9 of them for training and the remaining 1 for testing. This process was performed 10 times using each of the parties of the 10 divisions for testing and calculating the average error. Therefore, all the possible variabilities of PSO–SVM-

based model parameters have been evaluated in order to get the optimum point, looking for those parameters that minimize the average error. With these optimal hyper parameters, the error criterion was calculated from the built model using 90 % of the sample and tested with the remaining 10 %. In this way, we are able to simulate as much as possible the real conditions under which the model would be built in order to later fit it to new observation data unrelated to the construction of the model.

The regression modelling has been performed with SVR–e using the LIBSVM library (Lela et al 2009). The searching in the parameter space has been made, taking into account that the SVM algorithm changes its results significantly when its parameters increase or decrease by a power of 10. The binds (initial ranges) of the space of solutions used in particle swarm optimization (PSO) technique are shown in Table 7.3. The number of particles used has been 20. The stopping criterion is fulfilled if there is no improvement after the 10 iterations, along with the maximum number of iterations equal to 1000.

Table 7.5: Coefficient of determination (R) and correlation coefficient for the hybrid PSO–SVM-based model with an RBF kernel fitted in this study.

Kernel	Coefficients of Determination (R^2)/Correlation Coefficients (r)
RBF	0.94/0.96

Table 7.6: Evaluation of the importance of the variables according to their weights in the fitted PSO–SVM-based model with an RBF kernel.

SL.NO	Input Variable	Weight
1	Spindle Speed	1.9583
2	Depth Of Cut	0.1046
3	Feed Rate	2.3217

To optimize the SVM parameters, the PSO module is used. The PSO searches for the best C, s, and e parameters by comparing the forecasting error of each iteration. Search space is organized in three dimensions, one for each parameter. Main fitness factor is the coefficient of determination (R). Table 7.4 shows the optimal hyper parameters of the fitted RBF–SVM-based model found with the PSO technique. Table

7.5 shows the coefficient of determination and correlation coefficient for the fitted PSO–RBF–SVM-based model from 2006 to 2011. According to this statistic, the SVM with the RBF kernel is the best model for estimating the flank wear in the milling process, since the fitted SVM with the RBF kernel has a coefficient of determination (R2) equal to 0.95 and a correlation coefficient equal to 0.98. These results indicate an important goodness of fit, that is to say, a good agreement is obtained between our model and the observed data.

The importance ranking of the nine input operation variables in order to predict the milling tool wear (output variable) in this high nonlinear complex problem is shown in Table 7.6. Finally, this research work was able to predict the milling tool flank wear in agreement to the actual milling tool wear values observed experimentally using this hybrid PSO–SVM based model with great accuracy and success. Therefore, the use of an SVM model with an RBF kernel is necessary in order to achieve an effective approach to nonlinearities present in the regression problem. Obviously, these results coincide again with the outcome criterion of goodness of fit (R^2) so that the SVM model with an RBF kernel has been the best fitting.

In summary, the PSO–SVM-based model (Wang et al 2020, Hu et al 2019) is a suitable tool in modelling and assessment of singular problems, such as the study of the milling tool wear (flank wear in this case) in an industrial milling process. The most important operation input variables were used to fully characterize the problem. The attained PSO optimal points are represented in Figure 7.13 for LN_2 machining condition. The entire summarized results are shown in Figure 7.14. The Figure 7.14 indicates that SVR technique yields better results compared to that of RSM and BNN techniques in case of LN_2 machining condition.
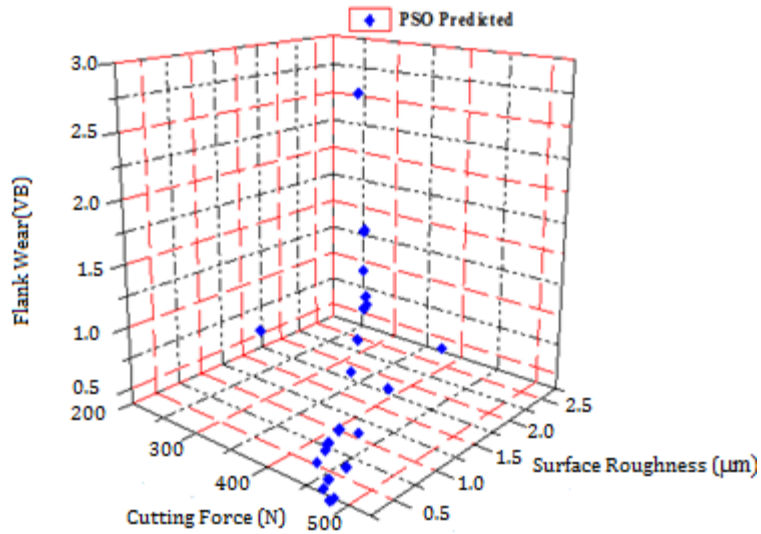
Figure 7.13: PSO Optimal points for SS316 for LN₂ machining condition
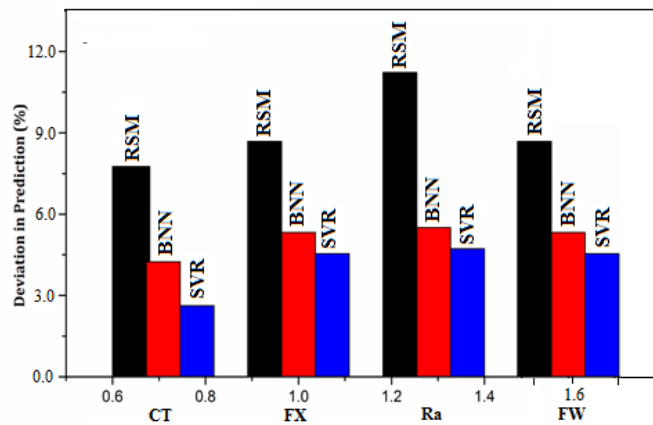
Figure 7.14: Summarized results of RSM, BNN and SVR techniques in terms of % of deviation

Table 7.7: Summary of relative error comparison between RSM, BNN and SVR for output parameters CT, CF, Ra, and FW.

Methods	Relative error (%) CT (°C)	Relative error (%) CF (FX)	Relative error (%) Ra (μm)	Relative error (%) FW (μm)
RSM	8.06 - 10.42	7.48 - 9.78	6.78 - 8.43	8.43 - 10.2
BNN	2.06 - 4.29	2.8 - 4.55	3.39 - 4.35	2.04 - 4.3
SVR	1.61-4.17	1.09-4.28	1.04-3.61	1.99-4.0

Table 7.7 represents the Summary of relative error comparison between RSM, BNN and SVR for output parameters CT, CF, Ra, and FW. Also indicates that SVM prediction approach is much impressive compared to RSM and BNN respectively. Similarly, Table 7.8 shows PSO-RBF-SVR approach is outperformed compared to DFA and PSO optimization tool respectively.

Table 7.8: Summary of optimized process parameters in milling using PSO-RBF-SVR with DFA and PSO approaches respectively.

Optimization Tool	Milling Condition							
	Spindle Speed (rpm)	Feed rate (mm/min)	Depth of cut (mm)	Coolant type	Cutting Temperature (CT, °C)	Cutting Force (Fx, N)	Surface Roughness (Ra, µm)	Flank Wear (VB, µm)
Experiment	3000	350	0.5	1	84	214	0.583	0.142
DFA	3000	350	0.5	1	99.98	225.00	1.14	0.13
PSO	3000	350	0.5	1	97	223	1.10	0.152
PSO-RBF-SVR	3000	350	0.5	1	90	216	0.78	0.149

7.12 CONCLUSIONS

Based on the experimental and numerical results, the main findings of this research work can be summarized as follows:

1. The SVR technique incorporated in this study yields better results as compared to RSM and BNN techniques.
2. RBF kernel function yielded better results compared to other kernel function such as Linear, Polynomial and Sigmoid. So in further study the RBF was incorporated with PSO technique to carry out optimization.
3. The milling responses can be accurately modeled using a hybrid PSO–SVM-based model with an RBF kernel.
4. This hybrid PSO–RBF–SVM-based model to predict the responses and allows to lower costs in the quality's assessment of the milling process.

5. A high coefficient of determination equal to 0.95 was obtained when this hybrid PSO–RBF–SVM-based model was applied to the experimental dataset.

6. The significant order of the input variables involved in the prediction of the milling tool flank wear values was set. Specifically, the input operation variables spindle speed and feed rate could be considered as the most influential parameters, respectively.

7. The influence of the kernel parameter setting of the SVMs on the responses regression performance was established.

8. Finally, the results verify that this hybrid PSO–SVM based regression method significantly improves the generalization capability achievable with only the SVM based regression.

CHAPTER 8

CONCLUSIONS AND SCOPE FOR FUTURE WORK

In the current study, the regression equations are developed on the experimental data collected as per the design of experiments. Generally, the responses are predicted more accurately when the response equation have better fit. This is decided based on R^2, i.e. coefficient of determination value. In this research work, the effort has been to develop input and output relationship in the face milling operation using cryogenic technique.

Later on the model developed has been tested statistically using Analysis of Variance and with the Neural Network (Gradient Descent, Scaled Conjugate Gradient Descent, Levenberg Marquart, and Bayesian Neural Network) approach. From the study, it can be derived that all the models are adequate and effective in making predictions. Later on, the comparison is made among Response Surface Methodology and Neural Network approach via nine test cases in order to check their prediction accuracy and to identify the best suitable back propagation approach predicting model for the current research. From the results, it can be observed that the deviation percentage attained for predicting Ra is found to be less than 10.5% by all the considered models.

Thus neural network method will help to make the prediction of cutting force, surface roughness, cutting temperature, tool wear for opted combination of machine parameters in face milling using cryogenic techniques. The requirement of face milling process using cryogenic technique entirely depends on the required application as requirement of better responses (cutting force, surface roughness, cutting temperature, tool wear) was critical in the current application. Thus the present work will help in minimizing the expensive trial and error methods. Later on, the work can be further implemented in automated numerical based machines in order to control the setting of parameters in web based (online mode) via incremental training of neural network.

8.1 States of Conclusion

The research can be extended towards the various stages. The first stage is by using design of experiments and different combination of parameters to build the database and to identify the significant parameters using Analysis of Variance. The second stage is modelling and comparing the predicted responses (Cutting force, surface roughness, cutting temperature, tool wear) using Response Surface Methodology and neural network (Gradient Descent, Scaled Conjugate Gradient Descent, Levenberg Marquart, and Bayesian Neural Network) approaches. The third stage is formulation of multi objective optimization models to identify the optimum parameters of the desired responses and even to address the performance of Particle Swarm Optimization model with statistical method (Response Surface Methodology). The fourth stage is to elucidate on the concept of machine learning (Support Vector Machine), as in the study Support Vector Machine is applied for the purpose of prediction and optimization. In prediction 4 kernel functions are used for prediction using Support Vector Regression (SVR) technique. Later on, the integration of best attained kernel function (Radial Basis Function) is hybridized to optimization technique forming a hybrid technique PSO-RBF-SVM method to carry out the optimization. The fifth stage is to carry out validation test by conducting 9 experimental test cases to identify the best suitable prediction model in terms of deviation and accuracy.

In the current study, the variation and effects of variables such as spindle speed, feed rate, and doc on cutting force, surface roughness, cutting temperature, tool wear in face milling operation with cryogenic technique is examined. The experiments were conducted on SS316 and the attained results were analysed by incorporating statistical method Regression Analysis, neural network method Bayesian Neural Network and machine learning method Support Vector Regression approaches. All the mentioned three methods were compared with each other in order to identify the best suitable method for the current study.

The best suitable method is chosen based on its attained relative error. The statistical significance of the model is expressed in terms of its performance i.e the error percentage achieved. The deviation attained by the models is as follows:

Response Surface Methodology: 8.43% (Max) - 3.95% (Min)

Bayesian Neural Network: 5.88% (Max) - 2.36% (Min)

Support Vector Regression: 3.61% (Max) - 1.04 % (Min)

It was found that neural network approach Bayesian Neural Network and machine learning model Support Vector Regression prediction correlate well with experimental results. But the best prediction for response surface roughness was attained by Support Vector Regression model with the deviation percentage of 3.61%.

The study also indicated the coolant type and feed rate are more dominant factors on Ra compared to spindle speed and doc, while doc was least influential on response Ra.

1. The investigation was intended to check the acceptability of the cryogenic (LN_2) machining approach for difficult to cut metals like SS316. The supporting inferences were made based on the results obtained from the present study.

LN_2 method of machining was useful in improving the breakability of chips, which is directly due to

> ➢ Reduction of cutting temperature at tool-chip and tool-workpiece junction helping to improve
>
> 1) Tool-life by reducing tool wear.
>
> 2) The surface quality of the product.
>
> 3) Reduction in power consumption in machining due to reduced cutting force.

2. The attained statistical results of the LN_2 method over without-coolant and with-coolant machining concerned to test cases for cutting force Fx (N), cutting temperature CT (ºC), surface roughness Ra (µm) and flank wear FW (µm) are as follows:

- Cutting force - Fx (N) with percentage reduction from 53.21% to 34.20%.

- Cutting temperature (ºC) with percentage reduction from 65.88% to 44.51%.

- Surface roughness (µm) with percentage reduction from 75.43% - 44.27%.

- Flank wear (µm) have minimized from 59.76% to 23.10%.

The machinability of SS316 can be improved in milling by the cryogenic (LN_2) method of machining under the pre-defined range of input process constraints(31).

3. Better performance was attained by Bayesian Neural Network model when compared to Gradient Descent, Scaled Conjugate Gradient Descent, and Levenberg Marquart due to its adoptability and convergence features.

The deviation percentage attained for predicting Ra by the statistical (Response Surface Methodology) and Neural Network based (Gradient Descent, Scaled Conjugate Gradient Descent, Levenberg Marquart and Bayesian regularization or Bayesian Neural Network) approaches lies between as follows: Response Surface Methodology: (8.43% – 6.78%), Gradient Descent: (7.25% – 6.21%), Scaled Conjugate Gradient Descent: (6.52% – 5.08%) , Levenberg Marquart : (5.80% – 4.19%) and Bayesian Neural Network: (4.35% – 3.39%).

4. The outcomes acquired through Particle Swarm Optimization are likewise compared with the customary desirability approach and it was found that Particle Swarm Optimization gives closer values compared to the results obtained with the desirability approach. The Support Vector Regression technique incorporated in this study yields better results as compared to Response Surface Methodology and Bayesian Neural Network techniques.

Radial Basis Function- Kernel function yielded better results compared to other kernel function such as Linear, Polynomial and Sigmoid. So, in further study the Radial Basis Function was incorporated with Particle Swarm Optimization technique to carry out optimization. The output responses can be accurately modelled using a hybrid Particle Swarm Optimization - Support Vector Machine (PSO–SVM) based model with a Radial

Basis Function kernel. This hybrid Particle Swarm Optimization - Radial Basis Function - Support Vector Machine (PSO–RBF–SVM) based model accurately predicts the desired responses and allows optimization leading to quality product economically. The Novelty of the present research work is:

- Implementation of an intelligent prediction and optimization systems through a hybrid model, incorporating Neural Networks, SVR and PSO algorithms.
- The weights generated from among the best of the 4 (GD, SCGD, LM and BNN) approaches, are fed to the desired SVR model.
- Here again the weights generated from among the best of 4 kernels (Linear, polynomial, Radial and Sigmoidal) are interfaced to the PSO model.
- Thus, it can be seen that the weights generated at the initial training phase are further refined in the next stage of SVR training processing and these process lead to best results when used in PSO processing.
- The exhaustiveness interms of different algorithms for neural network and SVR processing as detailed above has not been seen in any of the literature studied in the context of the present work.

8.2 SCOPE FOR FUTURE WORK

The basic purpose of this thesis has been fulfilled by the contributions presented in the preceding chapters of this dissertation. However, there is still scope for future research which facilitates the enhancement of the performance. Among them few possible future research topics have been outlined as follows.

1. Reverse mapping approach can be implemented to predict the responses in various research operations.
2. Classification and clustering of machining type (Cryogenic, dry or wet) with respect to surface roughness value (µm) using image processing technique.
3. Prediction of surface roughness value (µm) of milled samples using machine vision system and image processing technique.

REFERENCES

Ajit, B., Mishra, S.C., Subash, M., and Swain, S.K. (2011). "Cryogenic Technique For Processing Steel Treatment." *National Conference On processing and Characterization of Materials*.

Al-Aomar, Raid, and Al-Okaily (2006). "A GA-Based Parameter Design for Single Machine Turning Process with High-Volume Production." *Computers and Industrial Engineering,* 50 (3), 317–37.

Ameille, J., Wild, P., Choudat, D., Ohl, G., Vaucouler, J., Chanut, J. and Broahard, P. (1969). "Respiratory symptoms, ventilatory impairment, and bronchial reactivity in oil-mist exposed automobile workers." *American Journal of Industrial Medicine.*, 27, 247-256.

Amit, G., Sharath, G., Raghuram, D., and Aditya, B. (2014). "Optimisation of turning parameters by integrating genetic algorithm with support vector regression and artificial neural networks." *The International Journal of Advanced Manufacturing Technology*, 77(1-4), 1-9.

Armarego, E.J.A. and Brown, R.H. (1995). "The Machining of Metals." Prentice Hall, New Jersey.

ASM Specialty Handbook: Tool Materials, 1st Edition, ASM International, USA, ISBN: 0-87170-545-1.

Azlan. Z., Habibollah,H., and Safian, S. (2010). "Prediction of surface roughness in the end milling machining using Artificial Neural Network." *Expert Systems with Applications*, 37(2), 1755-1768.

Azlan. Z., Habibollah,H., Sultan, Q., and Safian. (2012). "Regression and ANN models for estimating minimum value of machining performance." *Applied Mathematical Modelling,* 36(4), 1477-1492.

Bardin, J., Eisen, E.A., Woskie, S.R., Monson, R.R., Smith, T.J., Tolbert, P., Hanmond, K. and Hallock, M. (1997). "Mortality studies of machining fluid exposure in the automobile industry: A case-control study of pancreatic cancer." *American Journal of Industrial Medicine*, 32, 240-247.

Barry, J. and Byrne, G. (2002). "Chip formation, acoustic emission and surface white layers in hard machining." *Annals of CIRP*, 51(1), 65-70.

Baskar, N., Asokan, P., Prabhaharan, G. and Saravanan, R. (2005). "Optimization of Machining Parameters for Milling OperationsUsing Non-Conventional Methods." *The International Journal ofAdvanced Manufacturing Technology*, 25(11-12),1078-1088.

Becze, C.E. and Elbestawi, M.A. (2002). "A chip formation based analytic force model for oblique cutting." *International Journal of Machine Tool and Manufacture*, 42, 529-538.

Benardos, P. G. and Vosniakos, G. C. (2002). "Prediction of Surface Roughness in CNC Face Milling Using Neural Networks and Taguchi's Design of Experiments." *Robotics and Computer-Integrated Manufacturing*, 18(5-6), 343-354.

Bhatia, S.M., Pandey, P.C. and Shaw, H.S. (1978). "Thermal cracking of carbide tools during intermittent cutting." *Wear*, 51, 201-211.

Boothroyd, G. (1985). "Fundamentals of metal machining and machine tools." McGraw-Hill Book Company, New York.

Branimir, L., Drazen, B., and Sonja, J. (2009). "Regression Analysis, Support Vector Machines, and Bayesian Neural Network Approaches to Modeling Surface Roughness in Face Milling." *The international Journal of Advanced manufacturing Technology,* 42, 1082-1088.

Brian, Ripley. (1996). "Pattern recognition and neural networks. Cambridge." UK: Cambridge University Press. Samson.

Brown, C.J. and Hinds, B.K.(1985). "Force and temperature effects when machining titanium." 13th North *American Manufacturing Research Proceedings*, 238-241.

Byrne, G. and Scholta, E. (1993). "Environmentally clean machining processes - a strategic approach." *Annals of CIRP*, 42(1), 471-474.

Cakir, O., Kiyak, M. and Altan, E. (2004). "Comparison of gases application to wet and dry cuttings in turning." *Journal of Materials Processing Technology*, 153-154, 35-41.

Cassin, C. and Boothroyed, G. (1965). "Lubrication action of cutting fluids", *Journal of Mechanical Engineering Science*, 7(1), 67-81.

Chandrasekaram, H. (1985). "Thermal fatigue in tool carbides and its relevance to milling cutters."*Annals of CIRP*, 34, 125-128.

Chandrasekaran, M., Muralidhar, M., Krishna, C. M., and Dixit, U. (2010). "Application of Soft Computing Techniques in Machining Performance Prediction and Optimization: A Literature Review." *The International Journal of Advanced Manufacturing Technology*, 46(5-8), 445-464.

Chattopadhyay, A. B., Bose, A. and Chattopadhyay, A.K. (1985). "Improvements in grinding steels by cryogenic cooling." *Precision Engineering*, 7(2), 93-98.

Chen, Z., Atmadi, A., Stephennon, D.A. and Liang, S.Y. (2000). "Analysis of cutting fluid aerosol generation of environmentally responsible machining." *Annals of CIRP*, 49(1), 53-56.

Choudhury, I.A. and El-Baradie, M.A. (1998). "Machinability of nickel-base super alloys: a general review." *Journal of Materials Processing Technology*,77, 278-284.

Cus, F. and Joze, B. (2003). "Optimization of Cutting Process by GA Approach." *Robotics and Computer Integrated Manufacturing*, 19, 113–21.
Da Silvia, M.B. and Wallbank, J. (1998). "Lubrication and application method in machining." *Industrial Lubrication and Tribology*, 50, 149-152.

Daniel, F., and Bernd, M. (2019). "Tool wear monitoring of a retrofitted CNC milling machine using artificial neural networks." *Manufacturing Letters*, 19, 1-4.

Daniela, D., Mihai, G.C., and Druga, L.N. (2014). "The mathematical modelling of 21NiCrMo2 low alloy steel carburising in less common carburising media." *International Journal of Microstructure and Material Properities,* 9(1), 60-70.

DE Chiffre, L. (1998). "The functions of cutting fluids in machining." *Lubrication Engineering*, 44, 514-518.

Deamly, P.A. and Greason, A.N. (1986). "Evaluation of principal wear mechanisms of cemented carbides and ceramics used for machining titanium alloy IMI 318." *Materials Science and Technology*, 2, 47-58.

Dhananchezian, M. and Pradeep Kumar, M. (2011). "Cryogenic turning of the Ti-6Al-4V alloy with modified cutting tool inserts." *Cryogenics*, 51, 34-40.

Dhananchezian, M. and Pradeep Kumar, M. (2011a). "Cryogenic turning of AISI 304 stainless steel with modified tungsten carbide tool inserts." *Materials and Manufacturing Process,* 26, 781-785.

Dhananchezian, M., and Pradeep Kumar. (2011). "Cryogenic turning of the Ti–6Al–4V alloy with modified cutting tool inserts." *Cryogenics,* 51, 34-40.

Dhar, N.R., Nanda Kishore, S.V., Paul, S. and Chattopadhyay, A.B. (2002). "Effects of cryogenic cooling on chips and cutting forces in turning AISI 1040 and 4320 steel." Proc., *Institution of Mechanical Engineers Part B: Journal of Engineering Manufacture*, 216, 713-724.

Dhar, N.R. and Kamruzzaman, M. (2007). "Cutting temperature, tool wear, surface roughness and dimensional deviation in turning AISI 4037 steel under cryogenic condition." *International Journal of Machine Tool and Manufacture*, 47, 754-759.

Dhar, N.R., Kamruzzaman, M. and Ahmed, M. (2006). "Effect of minimum quantity lubrication (MQL) on tool wear and surface roughness in turning AISI 4340 steel." *Journal of Materials Processing Technology*, 172, 299-304.

Dhar, N.R., Paul, S. and Chattopadhyay, A.B. (2000). "Role of cryogenic cooling on cutting temperature in turning steel." *Journal of Manufacturing Science and Engineering*, 123, 146-154.

Dhar, N.R., Paul, S. and Chattopadhyay, A.B. (2000a). "FEM for determining temperature distribution in machining steel with cryogenic cooling." *Journal of Mechanical Engineers*, The Institution of Engineers, Bangladesh, 28, 68-78.

Dhar, N.R., Paul, S. and Chattopadhyay, A.B. (2000b). "Role of cryogenic cooling in machining AISI 4320 steel." *Proc., International Conference on Competitive Manufacture* (COMA-01), South Africa, 417-425.

Dhar, N.R., Paul, S. and Chattopadhyay, A.B. (2000c). "Improvement in productivity and quality in machining steels by cryo cooling." *Proc., National Conference on Precision Engineering* (COPEN-2000), IIT Madras, India, 247-255.

Dhar, N.R., Paul, S. and Chattopadhyay, A.B. (2000d). "A study of effects of cryogenic cooling on chips and cutting forces in turning NiCr steel." *Proc., Conference* (ICM 2000), Dhaka, Bangladesh, 292-300.

Dhar, N.R., Paul, S. and Chattopadhyay, A.B. (2002a). "Machining of AISI 4140 steel under cryogenic cooling - tool wear, surface roughness and dimensional deviation." *Journal of Materials Processing Technology*, 123, 483-489.

Dhar, N.R., Paul, S. and Chattopadhyay, A.B. (2002b). "The influence of cryogenic cooling on tool wear, dimensional accuracy and surface finish in turning of AISI 1040 and E4340C steels." *Wear*, 249,932-942.

Dikshit, M. K., Puri, A. B. and Maity, A. (2016). "Empirical Modelling of Dynamic Forces and Parameter Optimization Using Teaching-Learning-Based Optimization Algorithm and RSM in High Speed Ball-End Milling." *Journal of Production Engineering*, 19(1),11-21.

Diniz, A.E. and Filho, J.C. (1999). "Influence of the Relative Positions of Tool and Workpiece on Tool Life, Tool Wear and Surface in the Face Milling Process." *Wear*, 232, 67-75.

Diniz, A.E. and Micaroni, R. (2007). "Influence of the direction and flow rate of the cutting fluid on tool life in turning process of AISI 1045 steel." *International Journal of Machine Tool and Manufacture,* 47(2), 247-254.

Eberhart, R., Kennedy, J. (1995). "Particle swarm optimization." *In Proc. of IEEE international conference on neural networks piscataway*, NJ, 1942–1948.

Eisen, E.A., Holcroft, C.A., Greaves, I.A., Wegman, D.H., Woskie, S.R. and Monson, R.R. (1997). "A strategy to reduce healthy worker effect in a cross-sectional study of asthma 46and metalworking fluids." *American Journal of Industrial Medicine*, 31(6), 671-677.

Elbestawi, M.A., Chen, L., Becze, C.E. and EI-Wardany, T.I. (1997). "High speed milling of dies and models in their hardened state." *Annals of CIRP*, 46, 57-62.

Ely, T.S., Pedley, S.F., Hearne, F.T. and Stille, W.T. (1970). "A study of mortality, symptoms and respiratory function in humans occupationally exposed to oil mist." *Journal of Occupational Medicine,* 12, 253-261.

Evans, C. (1991). "Cryogenic Diamond Turning of Stainless Steel." *Annals of CIRP*, 40(1), 571-575.

Ezugwu, E.O. (2005). "Key improvements in the machining of difficult-to-cut aerospace super alloys." *International Journal of Machine Tool and Manufacture*, 45, 1353-1367.

Ezugwu, E.O., Bonney, J., Da Silva, R.B. and Cakir, O. (2007). "Surface integrity of finished turned Ti-6Al-4V alloy with PCD tools using conventional and high pressure coolant supplies." *International Journal of Machine Tool and Manufacture*, 47(6), 884-891.

Fanju, M., Kohsuke, T., Ryo, A., and Hideaki, S. (1994). "Role of Eta-Carbide Precipitations in the Wear Resistance Improvements of Fe-12Cr-MoV-1.4C." *ISIJ International*, 34(2), 205-210.

Farahnakian, Masoud, Mohammad, R. R., Mahdi M. and Mohsen A. (2011). "The Selection of Milling Parameters by the PSO-Based Neural Network Modeling Method." *International Journal of Advanced Manufacturing Technology,* 57 (1–4), 49–60.

Geoffrey Boothroyd. (1975). "Fundamentals of Metal Machining and Machine Tools." Mc Graw Hill.

Ghani, J.A., Choudhury, I.A. and Majuki, H.H.(2004). "Performance of P10 TiN coated carbide tools when end milling AISI H13 tool steel at high cutting speed." *Journal of Material Processing Technology*, 153,1062-1066.

Ghosh, R., Zurecki, Z. and Frey, J.H. (2003)."Cryogenic machining with brittle tools and effects on tool life." *ASME, International Mechanical Engineering Congress*, Washington, 201-209.

Gianni, C., Lorenzo, L., and Antonio, S. (2014). "Optimization of process parameters using a Response Surface Method for minimizing power consumption in the milling of carbon steel." *Journal of cleaner production*, 66, 309-316.

Girish, G., and Kuldip, S. (2015). "Predictive Modelling and Optimization of Machining Parameters to Minimize Surface Roughness using Artificial Neural Network Coupled with Genetic Algorithm." *Procedia CIRP*, 31, 453-458.

Greaves, I.A. (1997). "Respiratory health of automobile workers exposed to metal working fluid aerosols: Respiratory symptoms." *American Journal of Industrial Medicine*, 32(5), 450-459.

Gruman Aircraft Engineering, (1965). "Cryogenic coolants in titanium machining." *Machinery*, 101-102.

Hartung, P.D. and Kramer, B.M. (1982). "Tool wear in titanium machining." *Annals of CIRP*, 31(1), 75-80.

HMT. (2006)."Production Technology." *Tata McGraw-Hill Publishing Company Limited*, New Delhi.

Hollis, W.S. (1961). "The application of controlled atmosphere in machining of metals." *International Journal of Machine Tool Design and Research*, 1, 59-78.

Hong, S.Y. (2001). "Economical and Ecological Cryogenic Machining." *Journal of Manufacturing Science and Engineering*, 123, 331-338.

Hong, S.Y. (2006). "Lubrication mechanism of liquid nitrogen in ecological cryogenic machining." *Machining Science and Technology*, 10(1), 133-155.

Hong, S.Y. and Ding, Y. (2001a). "Cooling Approaches and Cutting Temperatures in Cryogenic Machining of Ti-6Al-4V." *International Journal of Machine Tools and Manufacture*, 41(10), 1417-1437.

Hong, S.Y. and Ding, Y. (2001a). "Micro-temperature manipulation in cryogenic machining of low carbon steel." *Journal of Material Processing and Technology*, 116, 22-30.

Hong, S.Y. and Ding, Y. and Jason Jeong. (2002). "Experimental Evaluation of Friction Coefficient and Liquid Nitrogen Lubrication Effect in Cryogenic Machining." *Machining Science and Technology*, 6(2), 235-250.

Hong, S.Y. and Zhao, Z. (1999). "Thermal aspects, material considerations and cooling strategies in cryogenic machining." *Clean Products and Processes,*1,107-116.

Hong, S.Y., Ding, Y. and Ekkens, R.G. (1999). "Improving Low Carbon Steel Chip Breakability by Cryogenic Chip Cooling." *International Journal of Machine Tools and Manufacture*, 39, 1065-1085.

Hong, S.Y., Ding, Y. and Woo-Cheol Jeong. (2001a). "Friction and Cutting Forces in Cryogenic Machining of Ti-6Al-4V." International Journal of Machine Tools and Manufacture, 41(10),2271-2285.

Hong, S.Y., Irel Markus, and Woo-Cheol Jeong. (2001). "New Cooling Approach and Tool Life Improvement in Cryogenic Machining of Titanium Alloy Ti-6Al-4V." *International Journal of Machine Tools and Manufacture*, 412245-2260.

Howes, T.D., Toenshoff, H.K. and Heuer, W. (1991). "Environmental aspects of grinding fluids."*Annals of CIRP*, 40(2), 623-630.

Huang, Sunan, Kok T., Geok H. and Yoke W. (2007). "Cutting Force Control of

Milling Machine." *Mechatronics,* 17 (10), 533–41.

Hussein. H.F., Druga, L.N., Mihai, G.C., Dumitru, C and Ghinea. A. (2018). "Predicting and monitoring eutectic carbides proportion in cast austenitic cr-ni stainless steels." *UPB Scientific Bulletin, Series B: Chemistry and Materials Science,* 80(4), 169-180.

Jainbajranglal, R. and Chatopadhyay, A.B. (1984). "Role of Cryogenics in metal cutting industry." *Indian Journal of Cryogenics*, 9(1), 42-46.

Jie Gu, Gary Barber, Simon Tung and Ren-Jyh Gu. (1999). "Tool life and wear mechanism of uncoated and coated milling inserts."*Wear*, 225(1),273-284.

Kalpakjian, S. and Schmid, R.S. (2000). "Manufacturing Engineering and Technology." Fourth Edition, *Addison Wesley Longman* (Singapore) Pvt.Ltd.
Kalpakjian, S. and Schmid, R.S. (2003). "Manufacturing Processes for Engineering Materials." Fourth Edition, *Prentice Hall,* New York,181.

Kalyan Kumar, K.V.B.S. and Choudhury, S.K. (2008). "Investigation of tool wear and cutting force in cryogenic machining using design of experiments.*" Journal of Materials Processing Technology*, 20395-101.

Kim, S.W., Lee, C.M., Lee, D.W., Kim, J.S. and Jung, Y.H. (2001). "Evaluation of the thermal characteristics in high speed ball end milling." *Journal of Materials processing Technology*, 113, 406-409.

Kitagawa, T. and Maekawa, K. (1990). "Plasma hot machining for new engineering materials." *Wear*, 139, 251-267.

Kitagawa, T., Kubo, A. and Maekawa, K. (1997). "Temperature and wear of cutting tools in high speed machining of Inconel 718 and Ti-6V-2Sn." *Wear*, 202, 142-148.

Klocke, F. and Eisenblatter, G. (1997). "Dry cutting." *Annals of CIRP*, 106, 68-73.

Kovacevic, R., Cherukuthota, C. and Mzurkiewiez, M. (1995). "High pressurewater jet cooling/lubrication to improve machining efficiency in milling." *International Journal of Machine Tools and manufacture,* 35(10), 1459-1473.

Krabacher, E.J. and Merchant, M.E. (1951). "Basic factors in hot-machining of metals." *American Society of Manufacturing Engineers*, 73(5), 761-776.

Kramar, D., Krajnik, P. and Kopac, J. (2010). "Capability of high pressure cooling in the turning of surface hardened piston rods." *Journal of Materials Processing Technology*, 210, 212-218.

Kuppuswamy, G.(1996). "Principles of Metal Cutting." Universities Press.
Lee, T.S., Lin, Y.J. (2000). " A 3D predictive cutting force model for end milling of parts having sculptured surfaces." *International Journal of Advanced Manufacturing Technology*, 16, 773-783.
Li, J., Yuan, Z. and Zhou, M. (1989). "Cryogenic ultra-precision machining of ferrous metals with natural diamond tools." *Chinese Journal of Mechanical Engineering*, 25, 69-72.

Lincoln, C.B., Reginaldo, T. C., and Alessandro, R.R. (2008). "Experimental and theoretical study of work piece temperature when end milling hardened steels using TiAlN coated & PCBN-tipped tools." *Journal of Materials Processing Technology*, 199, 234-244.

Lio, Y.S., Lin, H.M. and Chen, Y.C. (2007). "Feasibility study of the minimum quantity lubrication in high speed end milling of NAK 80 hardened steel by coated carbide tool." *International Journal of Machine Tool and Manufacture*, 471667-676.

Liu, Z.Q., Ai, X, Zhang, H, Wang, Z.T. and Wan, Y. (2002). "Wear patterns and mechanisms of cutting tools in high speed face milling." *Journal of Materials Processing Technology,* 129, 222-226.

Longbottom, T.M. and Lanham, T.D. (2005) "Cutting temperature measurement while machining – a review." *Aircraft Engineering and Aerospace Technology*, 122-130.

Machado, A.R. and Wallbank, J. (1997). "The effect of extremely low lubricant volumes in machining." *Wear*, 210, 76-82.

Machado, A.R., Wallbank, J., Ezugwu, E.O. and Pashby, I.R. (1998). "Tool performance and chip control when machining Ti-6Al-4V and Inconel 901 using high pressure coolant supply.", *Machining Science and Technology*, 2, 1-12.

Malghan, R. L., Rao, K. M., Shettigar, A. K., Rao, S. S. and D'Souza, R. (2017). "Application of Particle Swarm Optimization and Response Surface Methodology for Machining Parameters Optimization of Aluminium Matrix Composites in Milling Operation." *Journal of the Brazilian Society of Mechanical Sciences and Engineering*, 39(9), 3541-3553.

Malghan, Rashmi L., Karthik, R., Arun, K., Shrikantha, R. and D'Souza (2016). "Application of Particle Swarm Optimization and Response Surface Methodology for Machining Parameters Optimization of Aluminium Matrix Composites in Milling Operation." *Journal of the Brazilian Society of Mechanical Sciences and Engineering*, 39(9), 3541-3553.

Mazurkiewicz, M., Kubala, Z. and Chow, J. (1989). "Metal machining with high pressure jet cooling assistance a new possibility." *Journal of Engineering for Industry*, 111,7-12.

Meddour, I., Mohmed, A.Y., Riad, K., Elbh, M., and Lakhdar, B. (2014). "Investigation and modeling of cutting forces and surface roughness when hard turning of AISI 52100 steel with mixed ceramic tool: cutting conditions optimization." *The International Journal of Advanced Manufacturing Technology*, 77(5-8),1387-1399.

Merchant, M.E. (1958). "The physical chemistry of cutting fluid action." *American Chemical Society Division of Petrol Chemistry*, 3(4), 179-189.

Mirghani, I.A., Ahmed, F.I., Abakr, Y.A. and Nurul Amin, A.K.M. (2007). "Effectiveness of cryogenic machining with modified tool holder." *Journal of Material Processing and Technology*, 185, 91-96.

Mohanraj, T., Shankar, s., Rajsekar, R., Sakthivel, N.R., and Pramanik, A. (2021). "Tool condition monitoring techniques in milling process — a review." *Journal of Materials Research and Technology,* 9(1), 1032-1042.

Montgomery, D. C., (2019). "Design and Analysis of Experiments," 688, 10th Edition, John Wiley & Sons, ISBN: 978-1-119-49244-3.

Mukherjee, Indrajit, and Pradip, K. (2006). "A Review of Optimization Techniques in Metal Cutting Processes." *Computers & Industrial Engineering*, 50 (1-2), 15–34.

Nandy, A.K., Gowrishankar, M.C. and Paul, S. (2009). "Some studies on high – pressure cooling in turning of Ti-6Al-4V." *International Journal of Machine Tool and Manufacture*, 49, 182-198.

Noordin, M.Y., Venkatesh, V.C., Sharif, S., Elting, S. and Abdullah,A. (2004). "Application of response surface methodology in describing the performance of coated carbide tools when turning AISI 1045 steel." *Journal of Materials Processing Technology*, 46-58.

Oppenkowski., A., Weber., S., and Theisen., W. (2010). "Evaluation of factors influencing deep cryogenic treatment that affect the properties of tool steels." *Journal of Materials Processing Technology, 210,* 1949-1955.

Patricia, E., and Paul, G., M. (2010). "Artificial Neural Networks for Surface Roughness Prediction when Face Milling Al 7075-T7351." *Journal of Materials Engineering and Performance,19,185-193.*

Paul, S. and Chattopadhyay, A.B. (1995). "Effects of Cryogenic Cooling by Liquid Nitrogen Jet on Forces, Temperature and Surface Residual Stresses in Grinding Steels." *Cryogenics*, 35, 515-523.

Paul, S. and Chattopadhyay, A.B. (1996a.) "Determination and Control of Grinding Zone Temperature under Cryogenic Cooling." *International Journal of Machine Tools & Manufacture*, 36(4), 491-501.

Paul, S. and Chattopadhyay, A.B. (1996b). "The Effect of Cryogenic Cooling on Grinding Forces."*International Journal of Machine Tools and Manufacture*, 36(1),63-72.

Paul, S., Dhar, N.R. and Chattopadhyay, A.B. (2001). "Beneficial effects of cryogenic cooling over dry and wet machining on tool wear and surface finish in turning AISI 1060 steel." *Journal of Materials Processing Technology*, 116,44-48.

Podgornik., B., Majdic., F., Leskovsek, and Vizintin., J. (2011). "Improving tribological properties of tool steels through combination of deep-cryogenic treatment and plasma nitriding." *Wear*, 288.

Poulachon, G. and Moisan, A.L. (2000). "Hard turning: chip formation mechanisms and metallurgical aspects." *Transactions of ASME*, 122, 406-412.

Prakasvudhisarn, Chakguy, Siwaporn K. and Pisal Y. (2009). "Optimal Cutting Condition Determination for Desired Surface Roughness in End Milling." *International Journal of Advanced Manufacturing Technology,* 41 (5–6), 440–51.

Prashant, B., Makhesana, M.A., Haresh, P. (2021). "Indirect method of tool wear measurement and prediction using ANN network in machining process." *Materials Today: Proceedings*, DOI: 10.1016/j.matpr.2020.11.770

Rahman, M., Seah, W.K. and Teo, T.T. (1997). "The machinability of Inconel 718." *Journal of Materials Processing Technology*, 63, 199-204.

Rahman, M., Senthil Kumar, A. and Choudhury, M.R. (2000). "Identification of effective zones for high pressure coolant in milling." *Annals of CIRP*, 49(1), 47-52.

Rahman, M., Senthil Kumar, A. and Salam, M.U. (2001). "Evaluation of minimal quantities of lubricant in end milling." *International Journal of Advanced Manufacturing Technology*, 18, 235-241.

Rahman, M., Senthil Kumar, A., Salam, M.U. and Ling, M.S. (2003). "Effect of chilled air on machining performance in end milling." *International Journal of Machine Tool and Manufacture,* 2, 787-795.

Raja, S. B. and Baskar, N. (2001). "Application of Particle SwarmOptimization Technique for Achieving Desired Milled SurfaceRoughness in Minimum Machining Time." *Expert Systems withApplications*, 39(5), 5982-5989.

Raja, S. B. and Baskar, N.(2015). "Optimization Techniques for Machining Operations: A Retrospective Research Based on Various Mathematical Models." The *International Journal of Advanced Manufacturing Technology*, 48(9-12), 1075-1090.

Rao, P.N. (2000). "Manufacturing Technology Metal Cutting and Machine Tools." *Tata McGraw Hill*.

Rao, R. V. and Pawar, P. J. (2010). "Parameter Optimization of a Multi-Pass Milling Process Using Non-Traditional Optimization Algorithms." *Applied Soft Computing*, 10(2), 445-456.

Rashid, M. F. F., Hutabarat, W., and Tiwari, A. (2012). "A Review onAssembly Sequence Planning and Assembly Line Balancing Optimisation Using Soft Computing Approaches." *The International Journal of Advanced Manufacturing Technology*, 59(1-4), 335-349.

Razfar, M., Asadnia, M., Haghshenas, M., and Farahnakian, M. (2010). "Optimum Surface Roughness Prediction in Face Milling X20Cr13Using Particle Swarm Optimization Algorithm." *Proc. Institution of Mechanical Engineers*, Part B: Journal of Engineering Manufacture, 224(11), 1645-1653.

Roberts, G.A. and Cary, R.A. (1980). "Tool Steels." 4th Edition, *American Society for Metals*, Ohio, USA, ISBN 0-87170-096-4.Seattle, United States.

Senthil Kumar, A., Rahman, M. and Ng, S.L. (2002). "Effect of High-Pressure Coolant on Machining Performance." *International Journal of Advanced Manufacturing Technology*, 20, 83-91.

Shaw, M.C. (2005). "Metal Cutting Principles." Second Edition, Oxford, New York, Shaw, M.C. Pigott, J.D. and Richardson, L.P. (1951). "Effect of cutting fluid upon chip – tool interface temperature." *American Society of Manufacturing Engineers*, 71, 45-56.

Smart, E.F. and Trent, E.M. (1975). "Temperature distribution in tools used for cutting iron, titanium and nickel." *International Journal of Production Research*, 13(3), 265-290.

Sokovic, M. and Mijanovic, K. (2001). "Ecological aspects of the cutting fluids and its influence on quantifiable parameters of the cutting processes." *Journal of Materials Processing Technology*, 109(1-2), 181-189.

Solntsev., Y.P. (2001). " Modern and promising steels for cryogenic technique".

Sorby, K. and Tonnessen, K. (2006). "High-pressure cooling of face-grooving operations in Ti-Al-4V." *Proc. Mechanical Engineering Part B: Journal of Engineering Manufacturing*, 220, 1621-1627.

Sornakumar, T. and Senthilkumar, A. (2008). "Machinability of Bronze Alumina Composite with tungsten carbide cutting tool insert." *Journal of Materials Processing Technology*, 202, 402-405.

Sreejith, P.S. and Ngoi, B.K.A. (2000). "Dry machining: Machining of the future", *Journal of Materials Processing Technology*, 101(1287-291.

Stanford, M., Lister, P.M., Morgon, C. and Kibble, K.A. (2008). "Investigation into the use of gaseous and liquid nitrogen as a cutting fluid when turning BS 970-080A15 (En 32b) plain carbon steel using WC-Co uncoated tooling." *Journal of Materials Processing Technology*, 209(2), 961-972.

Su, Y., He, N., Li, L. and Li, X.L. (2006). "An experimental investigation of effects of cooling/lubrication conditions on tool wear in high-speed end milling of Ti-6Al-4V." *Wear*, 261,760-766.

Su, Y., He, N., Li, L., Iqbal, A., Xiao, M.H., Xu, S. and Qiu, B.G. (2007). "Refrigerated cooling air cutting of difficult to cut materials." *International Journal of Machine Tool and Manufacture*, 48(6), 927-933.

Suresh, P., Mc Donald, S.D. and Dargusch, M.S. (2009). "Effects of coolant pressure on chip formation while turning Ti-6Al-4V alloy." *International Journal of Machine Tool and Manufacture,* 49, 739-743.

Suresh, R., Styappa, B., Gaitonde, V.N., and Samuel. G.L. (2012) ."Machinability investigations on hardened AISI 4340 steel using coated carbide insert." *International Journal of Refractory Metals and Hard Materials, 33.*

Suresh, Venkateswara, R. and Deshmukh (2002). "A Genetic Algorithmic Approach for Optimization of Surface Roughness Prediction Model." *International Journal of Machine Tools & Manufacture,* 42, 675–80.

Sutherland, J.W., Kulur, V.N. and King, N.C. (2000). "An experimental investigation of air quality in wet and dry turning."*Annals of the CIRP*, 49(1), 61-64.

Takeuchi, Y., Sakamoto, M. and Sata, T. (1982). "Improvement in the working accuracy of an NC lathe by compensating for thermal expansions", *Precision Engineering*, 4(1), 19-24.

Tandon,V., El-Mounayri, H. and Kishawy, H. (2002). "NC End Milling Optimization Using Evolutionary Computation." *International Journal of Machine Tools and Manufacture*, 42(5), 595-605.

Tansel, Ozcelik, Bao, Chen, Rincon, Yang, and Yenilmez (2014). "Selection of Optimal Cutting Conditions by Using GONNS." *Journal of the International Measurement Confederation,* 48, 306-313.

Thepsonthi, T., Hamdi, M. and Mitsui, K. (2009). "Investigation into minimal cutting fluid application in high speed milling hardened steel using carbide mills." *International Journal of Machine Tool and Manufacture,* 49, 156-162.

Thomas Childs, Katsuhiro Maekawa, Toshiyuki Obikawa and Yasuo Yamane. (1999). "Metal Machining." *John Wiley and Sons Inc*.

Thomas, M. and Beauchamp, Y. (2003). "Statistical investigation of modal parameters of cutting tools in dry cutting." *International Journal of Machine Tool and Manufacture*, 43, 1093-1106.

Thomas, R., B. (1989). "Taguchi Techniques for Quality Engineering." Technometrics, 31(2), 253-255.

Trent, E.M. and Wright, P.K. (2000). "Metal Cutting." 4th edition, Butterworth-Heinemann, London, 97-131.

Tsai, H.H. and Hocheng, H. (1998). "Investigation of the transient thermal deflection and stresses of the workpiece in surface grinding with the application of a cryogenic magnetic chuck." *Journal of Materials Processing Technology*, 79, 177-184.

Uehara, K. and Kumagai ,S. (1969a) "Mechanisms of tool wear." *Journal of Japanese Society for Precision Engineering*, 35(9), 43-49.

Uehara, K. and Kumagai, S. (1968). "Chip Formation, Surface Roughness and Cutting Forces in Cryogenic Machining." *Annals of CIRP*, 17(1), 409-416.

Uehara, K. and Kumagai, S. (1969). "Chip formation, surface roughness and cutting force in cryogenic machining." *Annals of CIRP*, 17, 409-416.

Uehara, K. and Kumagai, S. (1970). "Characteristics of tool wear in cryogenic machining." *Annals of CIRP*, 17, 273-277.

Uma, M. P., Harish, D., and Suresh, N. (2018). "Application Of Regression And Artificial Neural Network Analysis In Modelling Of Surface Roughness In Hard Turning Of AISI 52100 Steel." *Materials Today*, 5(2), 4766-4777.

Varadarajan, A.S., Phillip, P.K. and Ramamoorthy, B. (2002). "Investigation on hard turning with minimal cutting fluid application (HTMP) and its comparison with dry and wet turning." *International Journal of Machine Tool and Manufacture*, 42193-200.

Venkata, R. and Pawar (2010). "Parameter Optimization of a Multi-Pass Milling Process Using Non-Traditional Optimization Algorithms." *Applied Soft Computing Journal,* 10 (2), 445–56.

Venkata, R. and Kalyankar (2011). "Parameter Optimization of Machining Processes Using a New Optimization Algorithm." *Materials and Manufacturing Processes,* 27 (9), 978–85.

Venkatesh, M., Suresh, N. (2018)."Optimization of Milling Operations Using Artificial Neural Networks (ANN) and Simulated Annealing Algorithm (SAA)."*Materials Today: Proceedings*, 5(2), 4971-4985.

Venugopal, K.A., Paul, S. and Chattopadhyay, A.B. (2007). "Tool wear in cryogenic turning of Ti-6Al-4V alloy." *Cryogenics*, 47, 12-18.

Venugopal, K.A., Paul, S. and Chattopadhyay, A.B. (2007a). "Growth of tool wear in turning of Ti-6Al-4V alloy under cryogenic cooling." *Wear*, 2621071-1078.

Vieira, J.M., Machado, A.R. and Ezugwu, E.O. (2001). "Performance of cutting fluids during face milling of steels." *Journal of Materials Processing Technology*, 116, 244-252.

Vosough, M. and Svenningsson, I. (2004). "Influence of high pressure water jet assisted Machining on surface residual stresses on the workpiece of Ti-6Al-4V alloy." *Proc. SPIE,* SPIE Singapore, Bellingham.

Wang, Z.Y. and Rajurkar, K.P. (1997). "Wear of CBN tool in turning of silicon nitride with cryogenic cooling." *International Journal of Machine Tool and Manufacture*, 37, 319-326.

Wang, Z.Y. and Rajurkar, K.P. (2000). "Cryogenic machining of hard-to-cut materials." *Wear,* 239, 168-175.

Wang, Z.Y., Rajurkar, K.P. and Murugappan, M. (1996a). "Cryogenic turning of ceramic (Si3N4)." *Wear*, 195, 1-6.

Wang, Z.Y., Rajurkar, K.P., Fan J. and Petrescu, G. (2002). "Cryogenic machining of Tantalum." *Journal of Manufacturing Processes*, 4(2), 122-127.

Wang, Z.Y., Rajurkar, K.P., Fan, J., Lei, S., Shin, Y.C. and Petrescu, G. (2003). "Cryogenic machining of Inconel 718." *International Journal of Machine Tool and Manufacture*, 43, 1391-1396.

Wang, Z.Y., Sahay, C. and Rajurkar, K.P. (1996). "Tool temperatures and crack development in milling cutters." 36(1), 129-140.

Wong, Shaw, V., Wong, and Hamouda (2003). "Machinability Data Representation with Artificial Neural Network." *Journal of Materials Procesisng Technology*, 138, 538-544.

Wright, P.K. and Trent, E.M. (1974). "Metallurgical appraisal of wear mechanisms and processes on high speed steel tools." *Journal of Metals Technology*, 1(3),13-25.

Yakup, Y. and Muammer, N. (2008). "A review of cryogenic cooling in machining process." *International Journal of Machine Tool and Manufacture*, 48, 947-964.

Yalcin, B., Ozgur, A.E. and Koru, M. (2009). "The effects of various cooling strategies on Surface roughness and tool wear during soft materials milling." *Materials and Design*, 30, 896-899.

Yang, W., Yu, G. and Wen-he, L. (2011a). "Optimization of Multi-Pass Face Milling Using a Fuzzy Particle Swarm Optimization Algorithm." *The International Journal of Advanced Manufacturing Technology,* 54 (1–4), 45–57.

Yang, W.-A., Guo, Y., and Liao, W. (2011). "Multi-Objective Optimization of Multi-Pass Face Milling Using Particle Swarm Intelligence." *The International Journal of Advanced Manufacturing Technology*, 56 (5-8),429-443.

Yang, W.-A., Guo, Y., and Liao, W.-H. (2012)."Optimization of Multi-Pass Face Milling Using a Fuzzy Particle Swarm Optimization Algorithm." 54(1-4), 45-57.

Yang, Wen-an, Yu Guo, and Wenhe Liao (2011b). "Multi-Objective Optimization of Multi-Pass Face Milling Using Particle Swarm Intelligence." *The International Journal of Advanced Manufacturing Technology,* 56 (5–8), 429–43.

Yildiz, Y. and Nalbant, M. (2008). "A review of cryogenic cooling in machining processes." *International Journal of Machine Tool and Manufacture*, 48,947-964.

Yoon, Hae, S., Jang, L., Min, S. K. and Sung, A. (2014). "Empirical Power-Consumption Model for Material Removal in Three-Axis Milling." *Journal of Cleaner Production* 78, 54–62.

Yu, C., Xu, T., and Liu, C. (2015). "Design of a Novel UWB Omni directional Antenna Using Particle Swarm Optimization." International Journal of Antennas and Propagation, Article ID: 303195

Yusup, N., Zain, A. M., and Hashim, S. Z. M. (2012). "Overview of PSO for Optimizing Process Parameters of Machining." *Procedia Engineering,* 29, 914-923.

Yusup, Norfadzlan, Azlan, M. Z. and Siti, Z. M. H. (2012a). "Evolutionary Techniques in Optimizing Machining Parameters: Review and Recent Applications (2007-2011)." *Expert Systems with Applications,* 39 (10), 9909–27.

Yuvan Ning, Rahman, M. and Wong, Y.S. (2001)."Investigation of chip formation in high speed end milling." *Journal of Materials Processing Technology*, 133, 360-367.

Zareena, A.R., Rahman, M. and Wang, Y.S. (2001). "High speed machining of aerospace alloy Ti-6Al-4V." *Proc. 33 rd International SAMPE Technical Conference*,

Zarei, Fesanghary, Farshi, Jalili, Saffar, and Razfar (2008). "Optimization of Multi-Pass Face-Milling via Harmony Search Algorithm." *Journal of Materials Processing Technology,* 209, 2386–2392.

Zhang, J. Z., Chen, J. C., and Kirby, E. D. (2000). "Surface Roughness Optimization in an End-Milling Operation Using the Taguchi Design Method". Journal of Materials Processing Technology, 184(1-3), 233-239.

Zhao, Mei, Du, Tao, and Jiang (2012). "Online Evaluation Method of Machining Precision Based on Built in Signal Testing Technology." *Procedia CIRP*. 3 (1), 144–48.

Zheng, L. Y. and Ponnambalam, S. (2010). "Optimization of Multipass Turning Operations Using Particle Swarm Optimization." *Proc. 7th International Symposium on Mechatronics and its Applications (ISMA)*,. 1-6.

Zhirafar, S., Rezaeian, A., and Pug, M. (2007). "Effect of cryogenic treatment on the mechanical properties of 4340 steel." *Journal of Materials Processing Technology,* 186, 298-303.

Zhong, C., Alexander, A., David, A., Stephenson, Steven, Y., Lianga, K. and Venuvinod, P. (2000). "Analysis of cutting fluid aerosol generation for environmentally responsible machining." *CIRP Annals*, 49 (1), 53-56.

Zhou, J., Ren, J., and Yao, C. (2017). "Multi-Objective Optimization of Multi-Axis Ball-End Milling Inconel 718 via Grey Relational Analysis Coupled with RBF Neural Network and PSO Algorithm." *Measurement,* 102, 271-285.

Zuperl, C., and Gecevska (2007). "Optimization of the Characteristic Parameters in Milling Using the PSO Evolution Technique." *Strojniski Vestnik-Journal of Mechanical Engineering,* 53 (6), 354–68.

APPENDIX I
PREDICTION PROGRAM

```
main()
{

        cout << "    Prediction of responses of Milling of SS316" << endl;

        cout << "    Forward Mapping technique through Artificial Neural
            Network " << endl;

        cout << "                        by" << endl;

        cout << "    KARTHIK RAO M C [155078ME15P06]" << endl;

        cout << "    National Institute of Technology Karnataka, Surathkal"
<<endl;

cout << endl;

        cout << endl << "Enter your Network preference" << endl;

        cout << "1. Feed Forward Neural Network" << endl;

        fchoise = getch();

        if (fchoise != '1') { return 0; }

        else  for(;;) {

                char choice;

                cout << endl << "Enter the Training or Prediction preference" <<
        endl;

                cout << "1. load data" << endl;

                cout << "2. learn from data" << endl;

                cout << "3. compute output pattern" << endl;

                cout << "4. make new data file" << endl;

                cout << "5. save data" << endl;

                cout << "6. print data" << endl;

                cout << "7. change learning rate and momentum factor" << endl;
```

```
                cout << "8. exit" << endl << endl;

                cout << "Enter your choice (1-8)";


// HIDDEN1 -> OUTPUT

        for(y=0; y<output_array_size; y++) {

                for(x=0; x<hidden_array_1_size; x++)
                {
                        temp += (hidden1[x] * weight_h_o[x][y]);
                }
                output[pattern][y] = (1.0 / (1.0 + exp(-1.0 * (temp + bias[y +
                hidden_array_1_size]))));

                temp = 0;
         }

        return;
}

void backward_pass(int pattern)
{

         register int x, y;

        register double dweight_h_o = 0.0 , dweight_h_h = 0.0, dweight_i_h = 0.0,
        temp = 0.0;


// COMPUTE ERRORSIGNAL FOR OUTPUT UNITS

for(x=0; x<output_array_size; x++)

{

        errorsignal_output[x] = ((target[pattern][x] - output[pattern][x]) *
        output[pattern][x] * (1- output[pattern][x])) ; }
```

// ADJUST WEIGHTS OF CONNECTIONS FROM HIDDEN LAYER 1 TO OUTPUT UNITS

```
for(x=0; x<hidden_array_1_size; x++) {

        for(y=0; y<output_array_size; y++) {

                dweight_h_o = weight_h_o[x][y] - oldweight_h_o[x][y];

                weight_h_o[x][y] += ((learning_rate * errorsignal_output[y] *
        hidden1[x]) + (momentum * dweight_h_o));

        }

}

        for(x=0; x<hidden_array_1_size; x++)

                for(y=0; y<output_array_size; y++)

                        oldweight_h_o[x][y] = weight_h_o[x][y];
```

// ADJUST BIASES FOR OUTPUT UNITS

```
        for(x=(hidden_array_1_size); x<bias_array_size; x++) {

        bias[x] += (learning_rate * errorsignal_output[x]);
         }
```

// COMPUTE ERRORSIGNAL FOR HIDDEN LAYER 1 UNIT

```
for(x=0; x<hidden_array_1_size; x++) {

        for(y=0; y<output_array_size; y++) {

                temp += (errorsignal_output[y] * weight_h_o[x][y]);
}

errorsignal_hidden[x] = (1-hidden1[x]) * temp;


temp = 0.0;

}
```

// ADJUST BIASES OF HIDDEN LAYER 1 UNIT

```
        for(x=hidden_array_1_size; x<(bias_array_size-hidden_array_1_size); x++)
{

        bias[x] += (learning_rate * errorsignal_hidden1[x]);

}

 // COMPUTE ERRORSIGNAL FOR HIDDEN LAYER 1 UNITS

        for(x=0; x<hidden_array_1_size; x++) {

                temp += (errorsignal_hidden1[y] * weight_h_h[x][y]);
        }

        errorsignal_hidden1[x] = hidden1[x] * (1-hidden1[x]) * temp;

        temp = 0.0;

}
```

******************************* The End ********************************

Particle Swarm Optimization Code

ff = 'Karthik'; % Objective Function

% Initializing variables

popsize = 100; % Size of the swarm

npar = 4; % Dimension of the problem

maxit = 100; % Maximum number of iterations

c1 = 1.7; % cognitive parameter

c2 = 1.8; % social parameter

C=1; % constriction factor

% Initializing swarm and velocities

```matlab
lwb1=26;
lwb2=0.048;
lwb3=0.2;
lwb4=200;
upb1=130;
upb2=0.143;
upb3=0.6;
upb4=600;
par1=rand(popsize,1)*(upb1-lwb1)+lwb1;
par2=rand(popsize,1)*(upb2-lwb2)+lwb2;
par3=rand(popsize,1)*(upb3-lwb3)+lwb3;
par4=rand(popsize,1)*(upb4-lwb4)+lwb4;
%%par2=rand(popsize,1)*0.5;
%par3=rand(popsize,1)*0.2;
par=[par1,par2,par3,par4]; % random population of
% continuous values
vel = rand(popsize,npar); % random velocities
% Evaluate initial population
cost=feval(ff,par); % calculates population cost using
% ff
minc(1)=min(cost); % min cost
meanc(1)=mean(cost); % mean cost
globalmin=minc(1); % initialize global minimum
% Initialize local minimum for each particle
localpar = par; % location of local minima
localcost = cost; % cost of local minima
% Finding best particle in initial population
```

```
[globalcost,indx] = min(cost);

globalpar=par(indx,:);

% Start iterations

iter = 0; % counter

while iter < maxit

iter = iter + 1;

% update velocity = vel

w=(maxit-iter)/maxit; %inertia weiindxht

r1 = rand(popsize,npar); % random numbers

r2 = rand(popsize,npar); % random numbers

vel = C*(w*vel + c1 *r1.*(localpar-par)+c2*r2.*(ones(popsize,1)*globalpar-
par));

% update particle positions

par = par + vel; % updates particle position

overlimit=par<=1;

underlimit=par>=0;

par=par.*overlimit+not(overlimit);

par=par.*underlimit;

% Evaluate the new swarm

cost = feval(ff,par); % evaluates cost of swarm

% Updating the best local position for each particle

bettercost = cost < localcost;

localcost = localcost.*not(bettercost) +cost.*bettercost;

localpar(find(bettercost),:) =par(find(bettercost),:);

% Updating index g

[temp, t] = min(localcost);

if temp<globalcost

globalpar=par(t,:); indx=t; globalcost=temp;
```

end

[iter globalpar globalcost] % print output each

% iteration

minc(iter+1)=min(cost); % min for this

% iteration

globalmin(iter+1)=globalcost; % best min so far

iters=0:length(minc)-1;

plot(iters,minc,iters,meanc,iters,globalmin);

xlabel('generation');ylabel('cost');

****************************** The End ******************************

APPENDIX II - Machine Specifications

DTC- 250/Spark [Drill Tap Machining Center, Vertical]

I. Feed Slide - Z Axis (Vertical)

  a. Type of Feed   : A. C. Servo drive with ball screw and pre-loaded nut.

  b. Feed range   : 1 mm/min. to 10,000 mm/min.

  c. Rapid Traverse   :15000 mm/min.

  d. Motor torque   : 7 Nm.

  e. Max working Stroke : 250 mm.

  f. Axial Thrust   : 350 kg.

II. Feed Slide - X Axis (Horizontal)

  a. Type of Feed   : A. C. Servo drive with ball screw and pre-loaded nut.

  b. Feed range   : 1 mm/min. to 10,000 mm/min.

  c. Rapid Traverse   : 20000 mm/min.

  d. Motor torque   : 3.5 Nm.

  e. Max working Stroke : 300 mm.

  f. Axial Thrust   : 180 kg.

III. Feed Slide - Y Axis (Horizontal)

  a. Type of Feed   : A. C. Servo drive with ball screw and pre-loaded nut.

  b. Feed range   : 1 mm/min. to 10,000 mm/min.

  c. Rapid Traverse   : 20000 mm/min.

  d. Motor torque   : 3.5 Nm.

  e. Max working Stroke : 250 mm.

  f. Axial Thrust   : 180 kg.

IV. Spindle Drive

  a. No. of Spindles   : 1.

  b. Speed Range   : 60 to 6000rpm as std, 80 to 8000 rpm as optional.

  c. Type of Motor   : A.C. Motor with Transistor (PWM) Control.

    d. Constant Power range   : 5.5 kw max at 30 min. of Continuous Running, 3.7 kw

                                 Continuous Running.

    e. Tool Holder Taper   : BT 30.

V. Electrical Supply Condition

    a. Machine   : 415V+ 5%, 5o Cycle/Minute, 3Phase, 4 wire.

    b. Controls   : 24 Volts, DC. Necessary Transformer for Conversion is   provided.

    c. Tool Connected Load : 15 KVA Std.

VI. Automated Tool Changer

    a. Tool Storage   : 6Nos.
         Capacity

    b. Max Tool Weight   : 2.5 kg.

    c. Max Tool Length   : 200mm.

    d. Max Tool Dia   : 80mm.

APPENDIX III

G codes

G00 - Positioning at rapid speed

G01 - Linear interpolation (machining a straight line)

G02 - Circular interpolation clockwise (machining arcs)

G03 - Circular interpolation, counter clockwise

G04 - Dwell

G09 - Exact stop

G10 - Setting offsets in the program

G12 - Circular pocket milling, clockwise

G13 - Circular pocket milling, counter-clockwise

G17 - X-Y plane for arc machining

G18 - Z-X plane for arc machining

G19 - Z-Y plane for arc machining

G20 - Inch units

G21 - Metric units

G27 - Reference return check

G28 - Automatic return through reference point

G29 - Move to location through reference point

G31 - Skip function

G32 - Thread cutting

G33 - Thread cutting

G40 - Cancel diameter offset

G41 - Cutter compensation left

G42 - Cutter compensation right

G43 - Tool length compensation

G44 - Tool length compensation cancel

G50 - Set coordinate system and maximum RPM

G52 - Local coordinate system setting

G53 - Machine coordinate system setting

G54~G59 - Workpiece coordinate system settings

G61 - Exact stop check

G65 - Custom macro call

G70 - Finish cycle

G71 - Rough turning cycle

G72 - Rough facing cycle

G73 - Irregular rough turning cycle

G73 - Chip break drilling cycle

G74 - Left hand tapping

G74 - Face grooving or chip break drilling

G75 - OD groove pecking

G76 - Fine boring cycle

G76 - Threading cycle

G80 - Cancel cycles

G81 - Drill cycle

G82 - Drill cycle with dwell

G83 - Peck drilling cycle

G84 - Tapping cycle

G85 - Bore in, bore out

G86 - Bore in, rapid out

G87 - Back boring cycle

G90 - Absolute programming

G91 - Incremental programming

G92 - Reposition origin point

G92 - Thread cutting cycle

G94 - Per minute feed

G95 - Per revolution feed

G96 - Constant surface speed control

G97 - Constant surface speed cancel

G98 - Per minute feed

G99 - Per revolution feed

M codes

M00 - Program stop

M01 - Optional program stop

M02 - Program end

M03 - Spindle on clockwise

M04 - Spindle on counter-clockwise

M05 - Spindle off

M06 – Tool change

M08 - Coolant on

M09 - Coolant off

M10 - Chuck or rotary table clamp

M11 - Chuck or rotary table clamp off

M19 - Orient spindle

M30 - Program end, return to start

M97 - Local sub-routine call

M98 - Sub-program call

M99 - End of sub program

Details of Publication:
International/National Journals

Sl. No.	Name of Authors	Title of Paper	Journal Name, Year, Volume Number, Issue, Pages)	SCI/SCIE/SCOPUS INDEXED (IMPACT FACTOR)
1	Karthik Rao M C, Rashmi L Malghan, Faut Kara, Arun Kumar Shettigar, Shrikantha S Rao and Mervin A Herbert.	Influence of Support Vector Regression (SVR) on Cryogenic Face Milling	Advances in Material Science and Engineering, **(Hindawi),** August 2021, 9984369. DOI: http://doi.org/10.1155/2021/9984369.	SCI (1.73), 2021
2	Karthik Rao M C, Rashmi L Malghan, Arun Kumar Shettigar, Mervin A Herbert, Shrikantha S Rao	Advantages of cryogenic machining technique over without-coolant and with-coolant machining on SS316	Engineering Research Express, **(IOP),** 3,015040 http://doi.org/10.1088/2631-8695/abecd6	IOP (0.2), 2021
3	Karthik Rao M C, Rashmi L Malghan, Arun Kumar Shettigar, Shrikantha S Rao & Mervin A Herbert	Application of back propagation algorithms in neural network based identification responses of AISI 316 face milling cryogenic machining technique	Australian Journal Of Mechanical Engineering (**Taylor & Francis**), 2020, ISSN: 1448-4846 (Print) 2204-2253 (Online), https://doi.org/10.1080/14484846.2020.1740022	SCOPUS (0.96), 2020
4	Karthik M.C. Rao, Rashmi L Malghan,Mervin A. Herbert & Shrikantha S. Rao	Dataset on flank wear, cutting force and cutting temperature assessment of austenitic stainless steel AISI316 under dry, wet and cryogenic during face milling operation	Data In Brief (**Elsevier**), 2019, 26, 104389, https://doi.org/10.1016/j.dib.2019.104389	SCOPUS (0.97), 2019
5	Karthik Rao M. C,Rashmi L Malghan, S ArunKumar Shrikantha S Rao Mervin A. Herbert	An Efficient Approach to Optimize Wear Behavior of Cryogenic Milling Process of SS316 Using Regression Analysis and Particle Swarm Techniques	Transactions of the Indian Institute of Metals (**Springer**), 2019, 72(1), 191–204 https://doi.org/10.1007/s12666-018-1473-y	SCI (1.3), 2019
6	Karthik Rao M C, Arun Kumar Shettigar Rashmi L Malghan Shrikantha S Rao Mervin A Herbert	Machinability Study of Austenitic Stainless Steel under Wet and Cryogenic Treatment in Face Milling	Journal of Materials Science & Surface Engineering (**JMSSE**) , 2017, 5(6), 653-656 ISSN (Online): 2348-8956 10.jmsse/2348-8956/5-6.3	SCOPUS (1.58), 2017

BIODATA
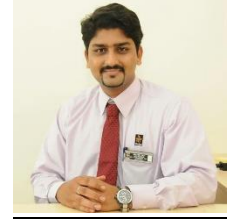
NAME   :   **KARTHIK RAO M C**

DATE OF BIRTH   :   **03/02/1986**

MOBILE NO.   :   **+91 9986087148**

EMAIL ID   :   **karthikmvit@gmail.com**

ADDRESS   :   **C-401, Sharanya Enclave, Shanthi Nagara, Manipal 576104**

Educational Qualification:

Examination/Degree	Board/Institute	Academic Year	Percentage/CGPA
PhD (Mechanical)	NITK, Surathkal	2015-2021	9.5
M.Tech (Mechatronics Engg.)	NITK, Surathkal	2008-2010	8.04
B.E (Mechanical Engineering)	SirMVIT, Bangalore	2003-2007	60%

Industrial/Academic Experience:

Sl.No.	Name of the Institute/ Company	Designation	Period
1	Debre Markos University, Ethiopia	Assistant Professor	Oct 2017-Jan 2021
2	Manipal Institute of Technology, MAHE,Manipal	Assistant Professor	Aug 2016-Sep 2017 July 2012-July 2015
3	NITK,Surathkal	Assistant Lecturer	Dec 2011-May 2012
4	CTPL, Bangalore	Application Engineer	Mar 2011-Dec 2011
5	SEMAC Pvt. Ltd, Bangalore	Design Engineer	Dec 2007-June 2008

Declaration:

I hereby declare that the above-written particulars are true to the best of my knowledge.

Place: NITK, Surathkal

Date: KARTHIK RAO M C